



Renewable Energy Research Conference 2010

June 7th – 8th, 2010

Zero Emission Buildings

**Editors: Associate Professor Matthias Haase and
Professor Anne Grete Hestnes**

© Renewable Energy Conference & Tapir Academic Press, 2010

ISBN 978-82-519-2623-2

This publication may not be reproduced, stored in a retrieval system or transmitted in any form or by any means; electronic, electrostatic, magnetic tape, mechanical, photo-copying, recording or otherwise, without permission.

Layout: Tapir Uttrykk

Editors:

Matthias Haase and Anne Grete Hestnes

NTNU, Department of Architectural Design, History, and Technology

Alfred Getz vei 3

7491 TRONDHEIM

matthias.haase@sintef.no

Tapir Academic Press publishes textbooks and academic literature for universities and university colleges, as well as for vocational and professional education. We also publish high quality literature of a more general nature. Our main product lines are:

- *Textbooks for higher education*
- *Research and reference literature*
- *Non-fiction*

We only use environmentally certified printing houses.

Tapir Academic Press

NO-7005 Trondheim, Norway

Tel.: + 47 73 59 32 10

Email: forlag@tapir.no

www.tapirforlag.no

Publishing Editor: lasse.postmyr@tapir.no

Renewable Energy Research Conference 2010

June 7th – 8th, 2010

Zero Emission Buildings

Organisation:

SFFE, Centre for Renewable Energy

<http://www.sffe.no>

NTNU, Department of Architectural Design, History and Technology, Trondheim, Norway
Alfred Getz vei 3
7491 Trondheim
Norway
<http://www.ntnu.no>

SINTEF Building and Infrastructure, Department Buildings
Alfred Getz vei 3
7465 Trondheim
Norway
<http://www.sintef.no>

Organizing committee:

Associate professor Matthias Haase, NTNU/SINTEF

Professor II Inger Andresen, NTNU/SINTEF

Professor Anne Grete Hestnes, NTNU

Scientific committee:

Professor Anne Grete Hestnes, ZEB Centre director, NTNU, Department of Architectural Design, History and Technology

Professor Arild Gustavsen, NTNU, Department of Architectural Design, History and Technology

Professor II Inger Andresen, NTNU, Department of Architectural Design, History and Technology

Senior researcher Berit Time, SINTEF Building and Infrastructure

Professor Vojislav Novakovic, NTNU, Department of Process Engineering

Associate professor Thomas Berker, NTNU, Department of interdisciplinary studies of culture

Senior researcher Tor Helge Dokka, SINTEF Building and Infrastructure

The Research Centre on Zero Emission Buildings - ZEB

The vision of The Research Centre on Zero Emission Buildings, ZEB, is to eliminate the greenhouse gas emissions caused by buildings. This conference parallel presents the latest developments in research, innovation, and implementation within the field of energy efficient zero-emission buildings.

Invited key-note speakers

- Per Heiselberg, Head of Zero Emissions Buildings research center, Professor at Aalborg University, Hybrid ventilation Center, Denmark
- Prof. Marco Perino, Dipartimento di Energetica, Politecnico di Torino, Italy

Sessions and program

- Advanced materials technologies
- Climate-adapted low-energy envelope technologies
- Energy supply systems and services
- Energy efficient use and operation
- Concepts and strategies for zero emission buildings

Renewable Energy Research Conference 2010

June 7th – 8th, 2010

Program - Zero Emission Buildings

Monday 7 th , 14:30 - 16:00	Concepts and strategies for zero emission buildings	page
Chairman:	<i>Inger Andresen, SINTEF Building and Infrastructure</i>	
14:30 – 15:00	Invited lecture: Zero Emission Buildings – A solution for sustainable development in the building sector? <i>Per Heiselberg, Aalborg (Dk)</i>	-
15:00 – 15:20	Proposal of a Norwegian ZEB definition: Storylines and Criteria <i>Igor Sartori, Ingeborg Graabak and Tor Helge Dokka, SINTEF Building and Infrastructure</i>	179
15:20 – 15:40	North European Understanding of Zero Energy/Emission Buildings <i>Anna Joanna Marszal, Julien S. Bourrelle, Björn Karlsson, Jyri Nieminen, Arild Gustavsen and, Per Heiselberg, Aalborg (Dk)</i>	167
15:40 – 16:00	ZEB Definition: Assessing the Implications for Design <i>Igor Sartori, Inger Andresen and Tor Helge Dokka, SINTEF Building and Infrastructure</i>	191

Renewable Energy Research Conference 2010

June 7th – 8th, 2010

Program - Zero Emission Buildings

Monday 7 th , 16:30 - 18:00	Energy supply systems and services	page
Chairman:	<i>Hans-Martin Mathiesen, NTNU</i>	
16:30 – 16:50	Renewable energy applications in zero emission buildings – a case study <i>Matthias Haase and Vojislav Novakovic, NTNU</i>	109
16:50 – 17:10	A life cycle cost analysis of large-scale thermal energy storage technologies for buildings using combined heat and power <i>K. Gaine and A. Duffy, Dublin Institute of Technology (Ie)</i>	49
17:10 – 17:30	The impact of domestic load profiles on the grid-interaction of building integrated photovoltaic systems in extremely low-energy dwellings <i>Ruben Baetens, Roel De Coninck, Lieve Helsen, and Dirk Saelens, K.U.Leuven (Be)</i>	3
17:30 – 18:00	Presentation of Posters (see at the end of the program for details)	

Renewable Energy Research Conference 2010

June 7th – 8th, 2010

Program - Zero Emission Buildings

Tuesday 8 th , 08:30 - 10:00	Climate-adapted low-energy envelope technologies	page
Chairman:	<i>Berit Time, SINTEF Building and Infrastructure</i>	
08:30 – 09:00	Invited lecture: The building enclosure - from the envelope to the skin <i>by Marco Perino, Turin (It)</i>	-
09:00 – 09:20	Towards an active, responsive and solar building envelope <i>Francesco Goia, Marco Perino, Valentina Serra, Fabio Zanghirella, Politecnico di Torino (It)</i>	73
09:20 – 09:40	Accelerated Ageing of Vacuum Insulation Panels <i>Erlend Wegger, Bjørn Petter Jelle, Erlend Sveipe, Steinar Grynning, Arild Gustavsen and Jan Vincent Thue, NTNU</i>	227
09:40 – 10:00	Application of Vacuum Insulation Panels in Retrofitting of Timber Frame Walls – An Experimental Investigation <i>Erlend Sveipe, Bjørn Petter Jelle, Erlend Wegger, Sivert Uvsløkk, Jan Vincent Thue, Steinar Grynning, Ole Aunrønning, Egil Rognvik, and Arild Gustavsen, NTNU</i>	203

Renewable Energy Research Conference 2010

June 7th – 8th, 2010

Program - Zero Emission Buildings

Tuesday 8 th , 10:30 - 12:00	Energy efficient use and operation	
		page

Chairman:	<i>Thomas Berker, NTNU</i>	
10:30 – 10:55	User Evaluations of Energy Efficient Buildings – Literature Review and Further Research <i>Åshild L. Hauge, Judith Thomsen and Thomas Berker, SINTEF Building and Infrastructure</i>	97
10:55 – 11:20	Potential of passive cooling, natural ventilation and solar control in cold climates office buildings <i>Luca Finocchiaro, Tore Wigenstad, Anne Grete Hestnes, NTNU</i>	39
11:20 – 11:45	Efficient Building Operation as a Tool to Achieve Zero Emission Buildings <i>Natasa Djuric and Vojislav Novakovic, NTNU</i>	27
11:45 – 12:00	Discussion	

Renewable Energy Research Conference 2010

June 7th – 8th, 2010

Program - Zero Emission Buildings

Tuesday 8th, 13:00 - 14:30

Advanced materials technologies

page

Chairman:	<i>Arild Gustavsen, NTNU</i>	
13:00 – 13:20	Nano Technology and Possibilities for the Thermal Building Insulation Materials of Tomorrow <i>Bjørn Petter Jelle, Arild Gustavsen, Steinar Grynning, Erlend Wegger, Erland Sveipe and Ruben Baetens, NTNU</i>	121
13:20 – 13:40	Nanoelectrochromics with Applied Materials and Methodologies <i>Tao Gao, Arild Gustavsen and Bjørn Petter Jelle, NTNU</i>	61
13:40 – 14:00	Dynamic Solar Radiation Control in Buildings by Applying Electrochromic Materials <i>Bjørn Petter Jelle and Arild Gustavsen, NTNU</i>	133
14:00 – 14:20	The Effect of Wall-Integrated Phase Change Material Panels on the Indoor Air and Wall Temperature – Hot-box Experiments <i>Sunliang Cao, Arild Gustavsen, Sivert Uvsløkk, Bjørn Petter Jelle and Jussi Maunuksela, NTNU / University of Jyväskylä (Fi)</i>	15
14:20 – 14:30	Discussion	

Renewable Energy Research Conference 2010

June 7th – 8th, 2010

Program - Zero Emission Buildings

Presentation of Posters	page
An Efficient Numerical Method for Simulation of Long-term Operation of Horizontal Ground Heat Exchangers with Parallel Shallow Pipes <i>Michael Greene, Laurentiu Dimache, Niall Bruke, John Lohan and Ray Clarke</i>	85
Rock core samples cannot replace thermal response tests - A statistical comparison based on thermal conductivity data from the Oslo region (Norway) <i>Heiko Liebel, Kilian Huber, Bjørn Frengstad, Randi Kalskin Ramstad and Bjørge Brattli, NTNU</i>	145
Utilisation of Geothermal Heat Pumps within Permeable Pavements for Sustainable Energy and Water Practices <i>Kiran Tota-Maharaj, Miklas Scholz and Stephen J. Coupe, University of Edinburgh (Gb)</i>	215
Thermosyphon Heated Thermal Store, the Influences of Valve Opening on flow, an Experimental Analysis <i>John Macbeth, John Currie, Dr. Mohamed Imbaby and Dr. Neil Finlayson, Greenspace Research (Gb)</i>	155
Towards a zero emission built environment – M.Sc. programme in Sustainable Architecture <i>Annemie Wyckmans, NTNU</i>	239

Table of contents

The impact of domestic load profiles on the grid-interaction of building integrated photovoltaic (BIPV) systems in extremely low-energy dwellings	3
R. Baetens, R. De Coninck, L. Helsen and D. Saelens	
The Effect of Wall-Integrated Phase Change Material Panels on the Indoor Air and Wall Temperature – Hot box Experiments	15
Sunliang Cao, Arild Gustavsen, Sivert Uvsløkk, Bjørn Petter Jelle, Jacques Gilbert and Jussi Maunuksela	
Efficient Building Operation as a Tool to Achieve Zero Emission Building.....	27
N. Djuric and V. Novakovic	
Potential of passive cooling, natural ventilation and solar control in cold climates office buildings	39
Luca Finocchiaro, Tore Wigennstad and Anne Grete Hestnes	
A life cycle cost analysis of large-scale thermal energy storage technologies for buildings using combined heat and power	49
Kenneth Gaine and Aidan Duffy	
Nanoelectrochromics with Applied Materials and Methodologies.....	61
Tao Gao, Arild Gustavsen and Bjørn Petter Jelle	
Towards an active, responsive and solar building envelope.....	73
F. Goia, M. Perino, V. Serra and F. Zanghirella	
An Efficient Numerical Method for Simulation of Long-term Operation of Horizontal Ground Heat Exchangers with Parallel Shallow Pipes	85
M. Greene, J. Lohan, N. Burke, L. Dimache and R. Clarke	
User Evaluations of Energy Efficient Buildings – Literature Review and Further Research	97
Å. L. Hauge, J. Thomsen and T. Berker	
Renewable energy application in zero emission buildings – a case study.....	109
M. Haase and V. Novakovic	
Nanotechnology and Possibilities for the Thermal Building Insulation Materials of Tomorrow	121
Bjørn Petter Jelle, Arild Gustavsen, Steinar Grynning, Erlend Wegger, Erland Sveipe and Ruben Baetens	
Dynamic Solar Radiation Control in Buildings by Applying Electrochromic Materials	133
Bjørn Petter Jelle and Arild Gustavsen	
Rock Core Samples Cannot Replace Thermal Response Tests - A Statistical Comparison Based On Thermal Conductivity Data From The Oslo Region (Norway) ..	145
H.T. Liebel, K. Huber, B.S. Frengstad, R. Kalskin Ramstad and B. Brattli	

Thermosyphon Heated Thermal Store, the Influences of Valve Opening on flow, an Experimental Analysis.....	155
J. N. Macbeth, H. Smith, Dr. J. Currie, Dr. N. Finlayson	
North European Understanding of Zero Energy/Emission Buildings.....	167
Anna Joanna Marszal, Julien S. Bourrelle, Jyri Nieminen, Björn Berggren, Arild Gustavsen, Per Heiselberg and Maria Wall	
Proposal of a Norwegian ZEB definition: Storylines and Criteria.....	179
I. Sartori, I. Graabak and T. H. Dokka	
ZEB Definition: Assessing the Implications for Design	191
Igor Sartori, Inger Andresen and Tor Helge Dokka	
Application of Vacuum Insulation Panels in Retrofitting of Timber Frame Walls – An Experimental Investigation	203
Erland Sveipe, Bjørn Petter Jelle, Erlend Wegger, Sivert Uvsløkk, Jan Vincent Thue, Steinar Grynning, Ole Aunrønning, Egil Rognvik and Arild Gustavsen	
Utilisation of Geothermal Heat Pumps within Permeable Pavements for Sustainable Energy and Water Practices	215
Kiran Tota-Maharaja, Miklas Scholza and Stephen J. Coupeb	
Accelerated Ageing of Vacuum Insulation Panels (VIPs).....	227
Erlend Wegger, Bjørn Petter Jelle, Erland Sveipe, Steinar Grynning, Arild Gustavsen and Jan Vincent Thue	
Towards a zero emission built environment – M.Sc. programme in sustainable architecture	239
A. Wyckmans	

The impact of domestic load profiles on the grid-interaction of building integrated photovoltaic (BIPV) systems in extremely low-energy dwellings

R. Baetens ^a, R. De Coninck ^{b,c}, L. Helsen ^b & D. Saelens ^a

^a Division of building physics, Department of civil engineering, K.U.Leuven,
BE-3000 Leuven, Belgium

^b Division of applied mechanics and energy conversion, Department of mechanical
engineering, K.U.Leuven, BE-3000 Leuven, Belgium

^c 3E, BE-1000 Brussels, Belgium

ABSTRACT

A BIPV system may produce the same amount of electricity as consumed in the building on a yearly base, however the simultaneity of production and consumption needs to be evaluated. The present paper aims at quantifying the impact of domestic load profiles on the integration of building-integrated photovoltaic (BIPV) electricity generation in a Belgian climate.

In this work, a multi-zone TRNSYS model for a dwelling with compression heat pump for both space heating and domestic hot water (DHW), domestic consumers and on-site photovoltaic generation is set-up. As a consequence of the dynamics of the electricity demand and supply, it is necessary to use small time-steps. The model is used to assess the influence of the user behaviour, the influence of the dimensioning of the heating installation and grid-interactions on the auto-consumption of BIPV systems. Furthermore, bottle-necks for possible large-scale implementation of on-site photovoltaic generation are illustrated.

The electricity consumption of a dwelling typically peaks when the habitants wake up and arrive back home, whereas the BIPV system shows a profile depending on the local weather and system characteristics. By putting the results of the requested and delivered power within the same model, it is shown that the domestic load profiles due to human behaviour do not coincide with the output of photovoltaic systems.

A dwelling with a classic gas-fired heating system is compared by a dwelling equipped with a electricity-driven heat pump for space heating and DHW. Therefore, the cover factor is defined, i.e. the ratio of domestic demand that is covered by the BIPV, for a BIPV installation with a yearly electricity production that equals the yearly domestic demand. If no attempt is made to bring the electricity demand and supply into balance on instant basis, a cover factor of 0.42 is found if a classic heating system is installed, denoting that more than half of the produced electricity will be passed on to the grid and withdrawn on another moment. If a heat pump is used for space heating and DHW, the cover factor decreases to 0.29.

If one aims to drastically decrease the domestic electricity demands from the main distribution grid, the installation of a BIPV might not be sufficient due to the imbalance of domestic electricity demand on the production by the BIPV system. An integrated approach including the current practice, the domestic installation, the mixture of loads and the grid is necessary.

Keywords: Domestic load profile, photovoltaic, BIPV, cover factor, smart grid

1. INTRODUCTION

Due to a favorable subsidy system in the Flemish region since the year 2006, the market of photovoltaic (PV) installations grew exponentially. By the end of year 2009, the total installed capacity grew to a cumulated capacity of 312 MWp in Belgium making it the fifth largest market for PV systems in Europe (Neyens 2009, VREG 2009). From the currently total installed capacity, nearly eighteen thousand installations with a size between 2 and 4 kWp are positioned on the sloped roofs of private houses in Flanders, practically all privately financed by the owners of the dwellings and the government subsidies (Neyens 2009) and - so far - all grid-connected (EurObserv'ER 2009). Although the total installed capacity is high, however, the total electricity production of all PV installations together remains relatively low due to low solar radiation levels in the moderate Belgian climate.

For a business-as-usual model where no further attempt is made towards optimizing the energetic advantage of the BIPV installation - as in most of the current dwellings where the PV installation is installed on existing buildings - the reduction of the grid electricity demand of the dwelling is expected to remain rather low as the PV power output peaks around 12h whereas an average domestic load profile is expected to peak around 8h and after 18h (see Fig.1). On the other hand, the challenges for the distribution grid become high in quarters with a high penetration of BIPV. The grid is seen as a virtual storage unit for electricity and, as a high share of the produced PV power will be directed to the grid, instability of the grid may form a major drawback.

For quantifying the reduction of the grid electricity demand by a BIPV installation in a business-as-usual model and illustrating the auto-consumption and grid injection of such a PV installation, a multi-zone TRNSYS model for a dwelling with an electricity-driven, air-to-water compression heat pump for both space heating and domestic hot water (DHW), domestic consumers and on-site photovoltaic generation is set-up. In order to simulate correctly the dynamics of the system, a small time-step of 1 minute is chosen. The model is used to visualize grid-interactions, the influence of the user behaviour and the influence of the heating system on the auto-consumption and grid-injection of BIPV, and to visualize bottle-necks for possible large-scale implementation of BIPV generation.

2. BOTTOM-UP DOMESTIC POWER DEMAND

An extremely low-energy detached house is modeled in detail for simulating the profile of electricity demand. The dwelling is modeled as a multi-parameter multi-zone building in TRNSYS (Solar Energy Laboratory 2009) where each single room is a zone. It has a usable area of 210 m², a roof area of 270 m² and U-values of 0.17, 0.20 and 1.17 W/(m²K) respectively for the façade, roof and window panes. The total extract air flow is 175 m³/h and the air tightness n₅₀ is 4 h⁻¹. Furthermore, internal gains of 8 W/m² are taken into account for both the day zone and night zone. Within the model, 4 major groups of domestic electricity consumption are taken into account:

1. standby power and domestic cooling appliances,
2. non-shiftable occupancy and behaviour based power demand (i.e. lighting, ventilation, cooking and the use of media),
3. shiftable power demand (i.e. washing machines, tumble dryers and dishwashers) and
4. heat production for space heating and domestic hot water by means of an electricity-driven, air-to-water compression heat pump.

The use of the washing machine and tumble dryer are not modeled in detail as their current use is determined by the day and night regime of electricity. Also small electric appliances which show a higher power demand but are used for a very short period are not modeled.

Some groups such as the cooling appliances (1), lighting and ventilation (2), as well as for space heating and domestic hot water (4) have a high potential for optimisation towards a higher system efficiency with BIPV systems because they can be shifted in time or influenced by design. The power demand for most appliances is hard to shift as it strongly depends on human behaviour and the appliance characteristics. Washing machines, tumble dryers and dishwashers (3) form an exception on these domestic appliances as they are not strongly connected to human behaviour. Here, some improvements may be achieved by means of a domestic energy control system.

In the current Belgian building stock, it is not common to use electricity to produce space heating and domestic hot water (DHW). However, heat pumps are currently gaining high interest in low-energy or passive dwellings for both space heating and DHW. As such, two different situations are considered: A dwelling (i) without electricity demand for space heating and DHW and (ii) with a heat pump for both space heating and DHW.

Modelling of each of the electricity demands in a business-as-usual setting is described in the following sections.

2.1 Standby and cooling appliances

In order to define the base line for power demand, distinction is made between the standby power of appliances and the electricity consumption of the cooling appliances. Based on the work of Almeida et al. (2008) a standby power of 40 W is considered as an average based on standby power and ownership rates. The distinction between two categories within the continuous power demand is necessary due to the small simulation time step of 1 minute: whereas the standby power demand of electric appliances is constant through time while domestic cold appliances will permanently switch between an on and off state within a certain time interval (Firth et al. 2008, Liu et al. 2004). The effective power profile depends on the used model of cold appliance, whereas a 120 W appliance with a 40' interval is taken into account. The impact of the room temperature or opening of doors on the power demand of cold appliances (Meier 1995, Saidur et al. 2002) is not taken into account.

2.2 Occupancy-based electricity demand

Within this work, both occupancy and lighting demand profiles are generated with the available model tool *Domestic Lighting Model 1.0c* (Richardson & Thomson 2008) provided by Richardson and Thomson (Richardson et al. 2008, 2009). The occupancy model for energy demand simulations generates ten-minute domestic building occupancy profiles with the Markov-Chain Monte Carlo technique. Here, the transition probability matrices are derived from a large time-use survey conducted in the United Kingdom in the year 2000 (Office For National Statistics 2003). The governing parameters in the model are (i) the number of residents of the dwelling and (ii) the day of the week. From the resulting occupancy profile, the lighting demand is derived based on the model by Stokes et al. (Stokes et al. 2004). For the purpose of detailed energy prediction and simulation, the original tool (Richardson & Thomson 2008) has been coupled to minute global irradiance data derived from Meteonorm 6.1 (Meteotest 2008) for Uccle, Belgium. This results in a daily variation of the climate and - as only a single building is simulated - the installed lighting power is

defined instead of statistically chosen for each day. Here, 1 461 W is taken into account as the average installed lighting power in Stokes et al. (2004).

A balanced mechanical ventilation is supposed to be installed in the dwelling.. The nominal electric power for operating of the fans of the mechanical ventilation needs to be defined based on the exact design of the ventilation network in the dwelling. For generalisation, the required electric power for mechanical balance ventilation may be defined as $\Phi = 0.235 V_{sec}$ (W) (Flemish Region 2006) where V_{sec} (m^3) is the volume that is ventilated. As such, the required power is 95 W for the modelled dwelling. The required electric power for ventilation has been correlated to the occupancy pattern of the habitants, i.e. ventilation will be switched on when persons are present in the building.

Domestic cooking results in short but high peaks in the domestic electricity demand. The probability matrices for cooking are derived based on a time-use survey conducted in Belgium in the year 1999 (Glorieux & Vandeweyer 2002). The parameters are (i) the domestic occupancy pattern and (ii) the day of the week. During the week, cooking is concentrated sharply around 12h20 and 18h20, whereas the peaks in the weekend may be found more distributed and later on the day. The installed total power for cooking in dwellings may peak up to 10 kW (Wood & Newborough 2003) whereas 7 kW is taken into account in the model.

The use of television and the use of computer is modelled through probability matrices derived based on the same time-use survey (Glorieux & Vandeweyer 2002). Also here, the parameters are (i) the domestic occupancy pattern and (ii) whether it is a weekday or weekend. On average, habitants watch 2.5 h/day television and work 1h on the computer at home. The required power for a television ranges from 50 W to 340 W, with 150 W as an average. For personal computers, a power demand of 200 W is depicted (TPDCB 2010).

2.3 Heat generation by means of a heat pump

Because of the limited heat demand and the resulting possibilities for low-temperature heat emission systems in low energy dwellings, a heat pump is often used for space heating. The same heat pump is also used for the production of DHW.

The modeled extremely-low energy dwelling is equipped with classic hydronic low-temperature (i.e. with a supply temperature of 45°) radiators and an electricity-driven, air-to-water compression heat pump. The required electricity demand is closely related to the occupancy pattern of the habitants: comfort has to be met whenever persons are present in the building. In the model, 21°C is used as set-point temperature for the central room-thermostat during occupation periods at which the space heating system is allowed to be switched off, while the room temperature may never drop below 16°C.

DHW profiles are generated based on (i) the occupancy profiles and (ii) the daily probability distributions in Jordan & Vijen (Spur et al. 2006, Jordan & Vajen 2001) for both small and medium loads, bathing and showering. For the use of ‘alternative’ sources of energy, a DHW temperature of 45°C is accepted in general (Spur et al. 2006) whereas a seasonal cold water temperature of $10 \pm 3^\circ C$ is assumed.

The installation consists of a storage tank for heating with an integrated domestic hot water heat exchanger coupled to the pump with a nominal power of 10.0 kW and a COP of 4.26 at nominal conditions (i.e. 2/35°C). A seasonal energy efficiency ratio (SEER) of 3.0 is found by simulation. The total electricity demand by the heat pump in the model is 6 MWh/a of which 2.8 MWh/a for DHW. This results in an electricity demand for space heating of 15 kWh/(m²a).

2.4 Results and limits of the model

The resulting electricity demand profiles of the dwelling can be found in Figure 1. For the situation with a classic heating system, the profile shows an increased electricity demand typically between 6h and 10h in the morning and between 18h and 23h in the evening. During the weekend, a higher demand may be found during the complete day. Due to the combination of appliances, the demand fluctuates between 0.1 kW and 0.9 kW within these periods. Short but high peaks up to 5 kW may be found on average around 12h and 18h30 due to the use of cooking appliances. For the situation including space heating and DHW, more peak consumption between 3 kW and 4 kW can be denoted due to the electricity demand of the heat pump. During heating season, this high demand coincides in general with the occupancy pattern due to the impact of space heating. In summer, only DHW results in short but lower (i.e. due to the higher outdoor temperature) peaks in electricity demand.

The average yearly electricity consumption for the modeled situation is 8.4 MWh/a including space heating and DHW, and 2.4 MWh/a without heat production. For Belgium, the average domestic electricity consumption for a similar dwelling is 3.5 MWh/a. The difference may be explained as follows:

- Shiftable load profiles such as the washing machine and tumble dryer are not modeled. Their current times of use are highly determined by the current day and night regime of the electricity supply, but are not bound to a moment of the day based on human behavior. Based on the number of cycles, the average electricity consumption per cycle and the ownership rates (Danish Energy Agency 1995), these appliances count for an average annual electricity consumption of 0.7 MWh/a.
- The remaining difference might be explained by small electric appliances which might show a higher power demand but are used for a very short period.

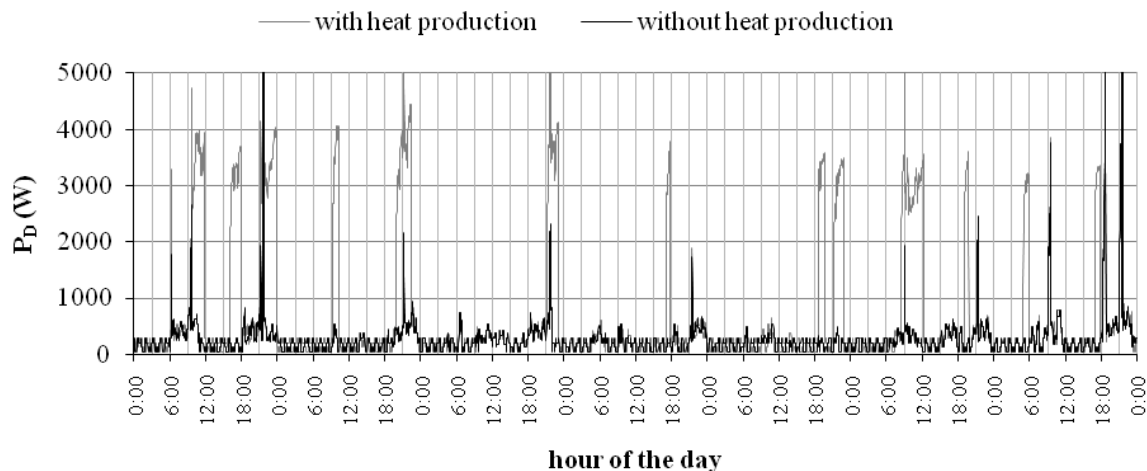


Fig.1. Example week profile for a typical mid-season week of the modelled electricity demand P_D (W) for a dwelling without (black) and with (grey) electricity-based heat generation for space heating and DHW.

3. PV POWER SUPPLY

The photovoltaic power output P_{PV} (W) is modelled with the available TRNSYS Type 194 implementing the basic 5-parameter model developed by the research group of Beckman (Duffie & Beckman 1991)

$$P_{PV} = I_{PV}V \text{ where } I_{PV} = I_L - I_0 \left[\exp\left(\frac{V + I_{PV}R_s}{a_{ref}}\right) - 1 \right] - \frac{V + I_{PV}R_s}{R_{sh}} \quad (1)$$

where I_L (A) is the light generated current, I_0 is the reverse saturation current of the diode, R_s (Ω) is the series resistance of the cells, R_{sh} (Ω) is the shunt resistance of the cells and a_{ref} is the modified ideality factor for compensation of second-order effects depending on the cell, the number of cells in series within a module and the cell temperature.

The method for determining the necessary parameters in Eq.1 is based on the model described by De Soto et al. (2006). Here, the five parameters a_{ref} , I_0 , I_L , R_s and R_{sh} are defined for reference conditions based on manufacturer data, whereafter these values are used to calculate the parameters at any other operating conditions. The necessary manufacturer data are the short circuit current I_{sc} (A), the open circuit voltage V_{oc} , the current at maximum power point I_{pm} (A) and the temperature coefficient β_{Voc} of the open circuit voltage. The five parameters depend on the operating conditions by means of the operating cell temperature, the incidence angle and the mass of air the beam radiation has to traverse.

The positioning of the PV panels has been chosen to maximize the total power output over an entire year for the climate data of Uccle (Belgium), i.e. they have an inclination of 34° and are oriented directly to the South (Huld & Suri 2010). No effects of elevated horizons or possible shadow of the environment on the tilted surface of the PV module are taken into account. For retrieving a high-resolution power output of the photovoltaic system, minute values for the sky diffuse and beam radiation on the tilted surface of the PV cells and the solar zenith angle are generated from Meteonorm 6.1 (Meteotest 2008) for Uccle (Belgium). An example resulting PV output is shown in Fig.2. The PV installation is dimensioned for each situation in such way that a zero energy building is achieved, i.e. the total yearly delivered energy equals the total electricity consumption, resulting in a 4 kWp to 12 kWp installation in a Belgian climate. As such, an attempt is made to exclude the effect of the PV installation size on the results. As a single climate file is used instead of a stochastic weather generator, the power output of a modeled installation is predictable and the yearly balance can be achieved by running each simulation twice.

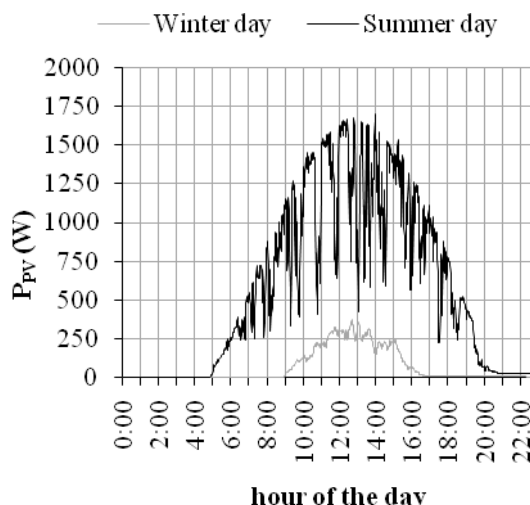


Fig.2. Example day-profile of modeled minute-values for the photovoltaic power supply P_{PV} (W) for a random winter (grey) and summer (black) day.

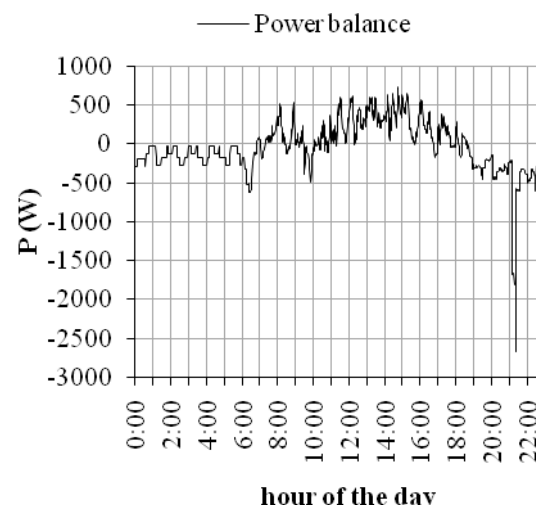


Fig.3. Example day-profile of modeled minute-values for the power balance of the dwelling. Positive values indicate supply to the grid.

4. RESULTS

4.1 Cover factors γ_D and γ_{PV}

In this paper, the effectiveness of the building integrated photovoltaic system for reducing the electricity demand from the main distribution grid is expressed by quantifying the cover factor. In general, a cover factor γ (-) is a number that indicates to what extent a set of threads is covered by another set of threads. Within this context, the cover factors γ_D and γ_{PV} provide efficiency-like information and are defined as ‘the ratio to which the power demand is covered by the BIPV supply’ and ‘the ratio to which the BIPV supply is covered by the power demand’ respectively

$$\gamma_D^{[t_1, t_2]} = \frac{\int_{t_1}^{t_2} \min\{P_{PV}, P_D\}}{\int_{t_1}^{t_2} P_D} \text{ and } \gamma_{PV}^{[t_1, t_2]} = \frac{\int_{t_1}^{t_2} \min\{P_{PV}, P_D\}}{\int_{t_1}^{t_2} P_{PV}} \quad (2)$$

where P_{PV} (W) is the BIPV supply power i.e. here from the photovoltaic system and P_D (W) the power demand. The term $\min\{P_{PV}, P_D\}$ represents the part of the power demand covered by the supply power or the part of the supply power covered by the power demand equalling the minimum of P_{PV} and P_D .

In a business-as-usual model where no attempt is made towards power load matching and thus increasing γ_D and γ_{PV} , a maximum value $\gamma_{D,max}$ for the cover factor γ_D on daily basis can be defined based on the length of daytime and the resulting maximum daily period during which power output of the PV array is possible as function of the locations latitude. This $\gamma_{D,max}$ expresses the ratio of the electricity demand during sunshine to the total electricity demand, independently of the PV installation. Within this context, the cover efficiency ϵ_{γ_D} is as ‘the ratio of the effective cover factor to the maximum cover factor for a certain time interval’

$$\epsilon_{\gamma_D}^{[t_1, t_2]} = \frac{\gamma_D^{[t_1, t_2]}}{\gamma_{D,max}^{[t_1, t_2]}} \text{ where } \gamma_{D,max}^{[t_1, t_2]} = \frac{\int_{t_1}^{sunrise} P_D}{\int_{t_1}^{sunset} P_D} \quad (3)$$

4.2 Results

For the modelled dwelling without heat pump, a γ^{year} of 0.42 for a γ_{max}^{year} of 0.48 is found. These values change to a γ^{year} of 0.29 for a γ_{max}^{year} of 0.63 if heat is generated by the heat pump. Even if a zero energy building is aimed determining the PV system, this results in low cover factors in a Belgian climate and the need for the main distribution grid to act as a virtual storage (see Fig.3).

Both γ_D and γ_{PV} (see Fig.4-5) show a seasonal pattern for both situations. The seasonal pattern of γ_D and $\gamma_{D,max}$ may be explained by the length of the day. As the electricity demand peaks in the morning and evening, the higher demands fall out of the day during winter. The seasonal pattern of γ_S can be explained by a higher solar radiation on the BIPV system due to a higher solar zenith and longer days.

From the point of view that grid demand reductions of the building is aimed at, several findings can be made based on the derived cover factors γ , γ_{\max} (see Fig.4-5) and cover efficiencies ε (see Fig.6):

- The cover factor γ_{PV}^{day} does not reach unity in the winter while on the same time also $\varepsilon_{\gamma D}$ does not reach unity for both situations. Even when only limited power supply of the BIPV system is available, a substantial part of the PV power is put on the grid.
- The finding is more pronounced for the situation including the heat pump: whereas the average γ_{PV}^{day} is 0.74 and $\varepsilon_{\gamma D}^{day}$ is 0.67 during winter for the situation without heat pump, the average γ_{PV}^{day} is only 0.65 however $\varepsilon_{\gamma D}^{day}$ is 0.43 if heat production is included. The reason may be found in the high power demand during relatively short periods of time (see Fig.1), e.g. for cooking but mainly for the heat production - although here dimensioning of the storage tank, the heat pump nominal power and its control plays an important role.
- For both modelled situations, the cover efficiency $\varepsilon_{\gamma D}^{day}$ does not reach unity in summer while on the same time also γ_{PV}^{day} does not reach unity. Even when a high power supply of the BIPV system is available, a substantial part of the domestic load during the day is not covered by the PV system.

Also here, the finding is more pronounced for the situation including the heat pump: whereas the average $\varepsilon_{\gamma D}^{day}$ is 0.95 and γ_{PV}^{day} is 0.37 during winter for the situation without heat pump, the average $\varepsilon_{\gamma D}^{day}$ is only 0.88 however γ_{PV}^{day} is 0.22 if heat production is included. The reason is probably the same as mentioned earlier.

Both in winter and summer, the BIPV systems use the main distribution grid for 'storage' of electricity to cover electricity demand on another moment of the day when BIPV power supply is expected. Possible consequence of using the grid as virtual storage plant is the local instability of this grid which might be avoided by limiting the required storage capacity of the grid and using or storing more energy in the building itself.

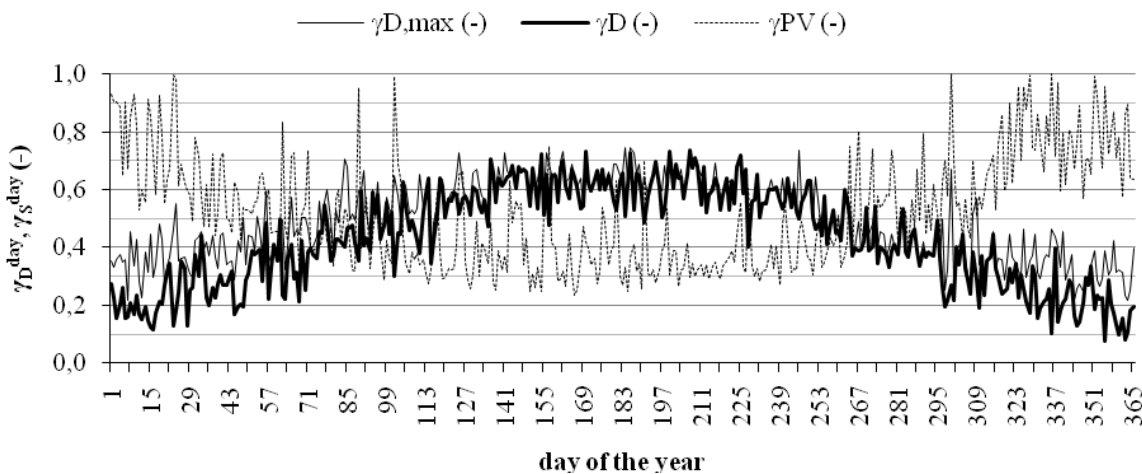


Fig.4. γ_D^{day} (bold), $\gamma_{D,max}^{day}$ (black) and γ_{PV}^{day} (dashed) through the year for a modelled dwelling without space heating and domestic hot water by means of a heat pump. A resulting γ^{year} of 0.42 and a value $\varepsilon_{\gamma D}^{year}$ of 0.87 is found.

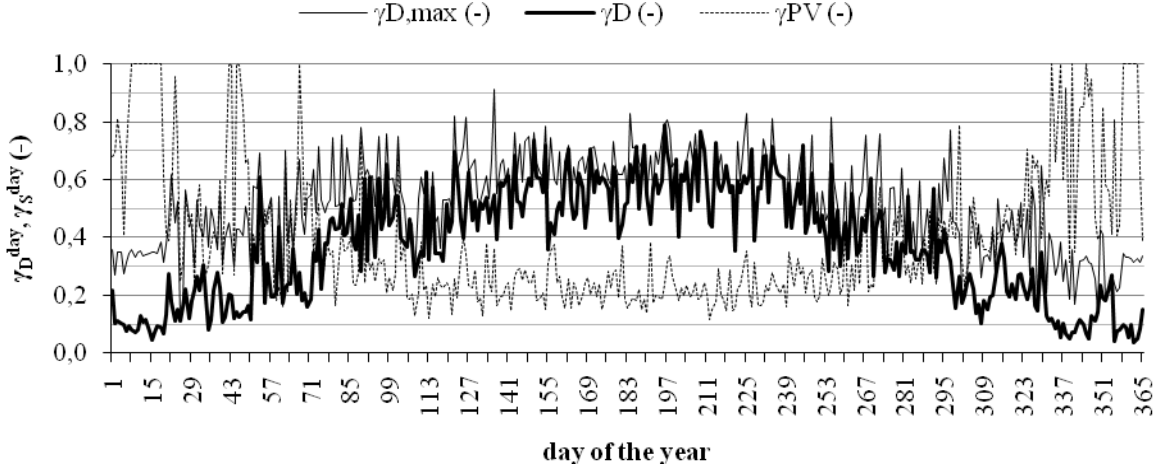


Fig.5. γ_D^{day} (bold), $\gamma_{D,\text{max}}^{\text{day}}$ (black) and $\gamma_{\text{PV}}^{\text{day}}$ (dashed) through the year for a modelled dwelling with space heating but without domestic hot water by means of a heat pump. A resulting γ^{year} of 0.29 and a value $\varepsilon_{\gamma D}^{\text{year}}$ of 0.46 is found.

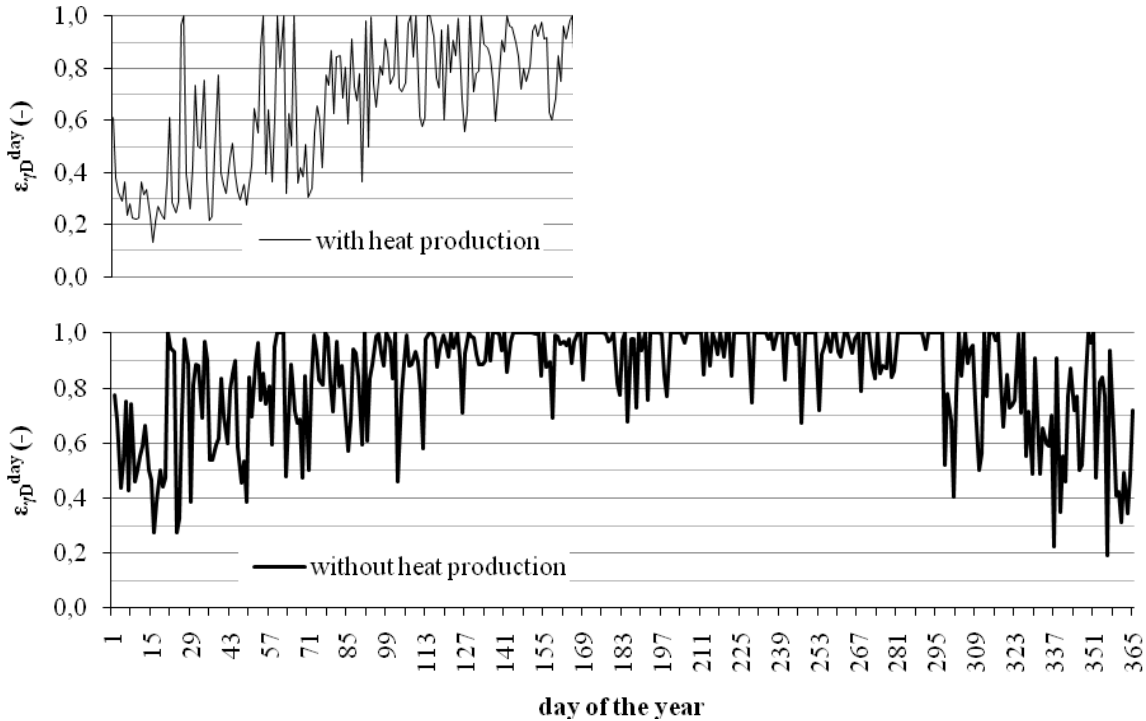


Fig.6. $\varepsilon_{\gamma D}^{\text{day}}$ through the year for a modelled dwelling with (upper graph) and without (lower graph) space heating and domestic hot water (DHW) by means of a heat pump.

5. DISCUSSION

The simulations show that only a fraction of the electricity demand of the dwelling is covered by the BIPV system, implying that somehow the excess of produced energy should be stored or used by other consumers. In this section, some options at different scales to overcome the injection of electricity in the main distribution grid are discussed.

5.1 Single dwelling

When studied at the building level only, the BIPV installation is generally seen from the objective to maximize the total output on a yearly basis in order to compensate the total consumption of the dwelling or from an economic perspective: when on yearly basis a total energy production is achieved that equals the total consumption, this dwelling or building might be depicted as a zero energy building. However - as shown above - the dwelling remains strongly dependent on the electricity grid as virtual storage as only a limited ratio of the energy consumption is covered by its own production, and a zero emission building is far from achieved intrinsically due to the domestic load profile. Electricity with zero marginal greenhouse gas emission is injected into the grid and again extracted from the grid when necessary (e.g. during the night). If no distribution problems occur, the input of BIPV generated electricity may result in a reduction of greenhouse gas emission at district level.

If only studied at the scale of a single building, the cover factor γ_S could be influenced based on several possibilities such as:

- Raising $\gamma_{D,max}$ by controlling time-shiftable loads such as washing machines, dryers and dishwashers. Based on the electricity consumption per cycle (Danish Energy Agency 1995) for the mentioned wet appliances, an increased $\gamma_{D,max}^{year}$ is retrieved from 0.49 to 0.61 if the complete electricity demand of these appliances is considered to lie completely in the day regime. However, increasing $\gamma_{D,max}$ by shifting these appliances does not automatically result in a raised γ_D due to possible high peak loads and attention should be paid to the demand profile of these appliances cycles.
- Influencing the domestic electricity demand profile of space heating and domestic hot water. Due to the differences in results (see Ch.4.2) between the modeled situation with and without heat generation by means of a heat pump and storage tank, it becomes clear that the choice and sizing of the installation have a high potential to increase the cover factor. As an example - instead of basing the control on the heat demand - controlling heat supply based on the BIPV power supply and limiting peak power demands might raise de cover factors, the maximum cover factor and cover efficiency significantly.
- Influencing the PV energy supply profile by orienting the PV arrays so that a high power supply is achieved at the same time as a high power demand of the dwelling.

5.2 Buildings at district scale

Due to the unbalanced profiles of electricity consumption and production of a single dwelling with BIPV, the dwelling will act as a net electricity provider on many moments (see Fig.3). When studied at the level of the building stock at district scale, different aspects are to be taken into account such as the variety of load profiles and the grid connecting individual buildings.

Due to the varied mixture of different load profiles at district scale, a higher cover factor γ of the PV installation could be achieved if the factor is not determined for a single dwelling but for a group of dwellings or buildings in general. As such, (i) peak demands are flattened out in the calculations and (ii) the possibility of a BIPV system on one dwelling delivering electric power to another dwelling can be considered. The exchange of PV power between different buildings in the same district could be one of the major advantages of distributed electricity generations by BIPV systems: due to the large variety of load profiles, the reduction of green house gas emission at district level might be easier to achieve, eg. by implementing a smart grid, as a major part of the electric power extracted from the grid by the individual dwellings might be PV generated. However, if the electricity exchange between different buildings is simulated by the model additional phenomena such as

transportation losses, the possibility for two-way transport on the grid and additional power and inefficiencies due to control devices should be accounted for.

5.3 Integrated point of view

Improvements achieved at the building scale might not scope with the potential of possible adaptations made on the district level and vice versa. To evaluate the potential of BIPV systems and the impact of the domestic load profile on this potential, an integrated approach from different levels is necessary. If not, each optimum found at a single level will remain a sub-optimum if not all different levels are considered.

6. CONCLUSIONS

A one-minute multi-zone TRNSYS model for a dwelling with classic heating on one hand and with heat pump for both space heating and domestic hot water on the other hand, electricity consumption by domestic consumers and BIPV generation has been set-up for a typical Belgian climate. The model is used to illustrate the influence of the user behaviour, the influence of the domestic heat installation and grid-interactions on the possibilities of BIPV systems. By coupling the electricity demand and production within the same model, it is shown by means of a cover factor that the domestic load profiles due to human behaviour do not coincide with the output of photovoltaic systems. The BIPV system is sized to cover the electricity demand of the dwelling on a yearly basis but no attempt is made to balance the electricity demand and supply. For the traditional heating installation and boiler, a cover factor of 0.42 is found indicating that more than half of the produced electricity will be passed on to the grid and withdrawn on another moment. If a heat pump is used for space heating and DHW, the cover factor decreases to 0.29 due to the increased consumption in the morning and evening periods and high peak power demands caused by the heat pump.

Large-scale implementation of BIPV systems require energy storage within the same or another energy vector at building level or the implementation of smart grids in which not the energy supply of a single dwelling is considered but a cluster of buildings with different load profiles.

ACKNOWLEDGEMENTS

The authors gratefully acknowledge the K.U.Leuven Energy Institute (EI) for granting a research project, entitled *Optimized energy networks for Buildings*, for funding this research.

REFERENCES

- Almeida, A. et al., 2008. REMODECE - Residential monitoring to decrease energy use and carbon emissions in Europe - Final report. , 96.
- Danish Energy Agency, 1995. Washing machines, Driers and Dishwashers - Final Report. , 76.
- De Soto, W., Klein, S.A. & Beckman, W.A., 2006. Improvement and validation of a model for photovoltaic array performance. *Solar Energy*, 80, 78-88.
- Duffie, J.A. & Beckman, W.A., 1991. *Solar Engineering of Thermal Processes*, 2nd ed. 2nd., Wiley.

- EurObserv'ER, 2009. Baromètre photovoltaïque / Photovoltaic barometer : 9 533,3 MWc dans l'UE / in the EU. *Systèmes solaires - Le journal du photovoltaïque*, 1, 72-103. Available at: <http://www.eurobserv-er.org/pdf/baro190.pdf>.
- Firth, S. et al., 2008. Identifying trends in the use of domestic appliances from household electricity consumption measurements. *Energy and Buildings*, 40(5), 926-936.
- Flemish Region, 2006. Bijlage I - Bepalingsmethode van het peil van primair energieverbruik van woongebouwen.
- Glorieux, I. & Vandeweyer, J., 2002. Statistische studie nr110 - 24 uur ... Belgische tijd, een onderzoek naar de tijdsbesteding van de Belgen.
- Huld, T. & Suri, M., 2010. PVGIS, PV Estimation Utility. Available at: <http://re.jrc.ec.europa.eu/pvgis/apps/pvest.php?lang=en&map=europe>.
- Jordan, U. & Vajen, K., 2001. Realistic domestic hot-water profiles in different time scales - Final report. , 18.
- Liu, D., Chang, W.R. & Lin, J.Y., 2004. Performance comparison with effect of door opening on variable and fixed frequency refrigerators/freezers. *Applied Thermal Engineering*, 24, 2281-2292.
- Meier, A., 1995. Refrigerator energy use in the laboratory and in the field. *Energy and Buildings*, 22(3), 233-243.
- Meteotest, 2008. METEONORM Version 6.1 - Edition 2009.
- Neyens, J., 2009. The PV market in the Flemish region - Status May 2009. , (May 2009), 1-4.
- Office For National Statistics, 2003. The United Kingdom 2000 Time Use Survey. Available at: www.statistics.gov.uk.
- Richardson, I. & Thomson, M., 2008. Domestic lighting demand model 1.0. *Loughborough University*. Available at: <http://hdl.handle.net/2134/4065> .
- Richardson, I. et al., 2009. Domestic lighting: A high-resolution energy demand model. *Energy and Buildings*, 41(7), 781-789.
- Richardson, I., Thomson, M. & Infield, D., 2008. A high-resolution domestic building occupancy model for energy demand simulations. *Energy and Buildings*, 40(8), 1560-1566.
- Saidur, R., Masjuk, H.H. & Choudhury, I.A., 2002. Role of ambient temperature, door opening, thermostat setting position and their combined effect on refrigerator-freezer energy consumption. *Energy Conversion and Management*, 43(6), 845-854.
- Solar Energy Laboratory, 2009. TRNSYS 16 - A transient system simulation program.
- Spur, R. et al., 2006. Influence of the domestic hot-water daily draw-off profile on the performance of a hot-water store. *Applied Energy*, 83(7), 749-773. Available at: <http://linkinghub.elsevier.com/retrieve/pii/S0306261905001066>.
- Stokes, M., Rylatt, M. & Lomas, K., 2004. A simple model of domestic lighting demand. *Energy and Buildings*, 36(2), 103-116.
- TPDCB, 2010. The power consumption database. Available at: www.tpcdb.com.
- VREG, 2009. Marktmonitor 2009. , 82. Available at: <http://www.vreg.be/vreg/documenten/rapporten/RAPP-2009-10.pdf>.
- Wood, G. & Newborough, M., 2003. Dynamic energy-consumption indicators for domestic appliances: environment, behaviour and design. *Energy and Buildings*, 35(8), 821-841.

The Effect of Wall-Integrated Phase Change Material Panels on the Indoor Air and Wall Temperature – Hot box Experiments

Sunliang Cao^{1,2,3}, Arild Gustavsen^{2,*}, Sivert Uvsløkk³,
Bjørn Petter Jelle^{3,4}, Jacques Gilbert⁵ and Jussi Maunuksela¹

¹ Renewable Energy Program, Department of Physics,
P.O. Box 35 (YFL), FI-40014 University of Jyväskylä, Finland.

² Department of Architectural Design, History and Technology, Norwegian University of Science and Technology (NTNU), Alfred Getz vei 3, NO-7491 Trondheim, Norway.

³ Department of Materials and Structures, SINTEF Building and Infrastructure,
Høgskoleringen 7B, NO-7465 Trondheim, Norway.

⁴ Department of Civil and Transport Engineering, Norwegian University of Science and Technology (NTNU), Høgskoleringen 7A, NO-7491 Trondheim, Norway.

⁵ DuPont de Nemours (Luxembourg) S.à r.l., Société à responsabilité limitée, au capital de 74.370.250 Euro, Rue Général Patton, L-2984 Luxembourg, R.C.S. Luxembourg B 9529.

ABSTRACT

Phase change materials (PCMs) have opened a new door towards the renewable energy future due to their effective thermal energy storage capabilities. Several products have recently found their way to the market, using various types of PCMs. This paper focuses on one particular wall-board product, integrated in a well-insulated wall constructed of an interior gypsum board, PCM layer, vapor barrier, mineral wool, and a wind barrier. The wall is tested with and without the PCM layer in order to get comparative results.

Experiments are conducted in a traditional guarded hot box. The hot box is composed of two full-scale test chambers, where the tested wall is located between those two chambers. There are two heaters inside the metering box: heater 1 functions as a thermostat which is used to maintain a constant air temperature (of about 20 °C) in the metering box, while heater 2 is a normal electrical heater that provides a constant heating power when turned on. The cold chamber has a fixed temperature equal to -20 °C. The experiments are arranged in a comparative way, i.e. comparing walls with and without a PCM layer. Temperature, heat flux, air velocity, and electrical power are recorded during testing. By applying well-distributed thermocouples, the influences of the PCM layer on the interior temperatures can be shown. Furthermore, with attached heat flux meters, the energy storage effect and convective heat flows can be determined. Finally, with the electrical power meter, the energy saving effect can also be calculated.

In this paper, initial experimental results are presented, showing the indoor air and surface wall temperatures. The experiments show that inclusion of the PCM layer in the wall reduces the interior air and wall temperatures by a maximum of about 2 °C compared to a wall without PCM. The results also show that increasing the air velocity over the interior surface during the heating period lowers the maximum air and surface temperatures by the end of the heating period.

Keywords: Phase Change Materials, PCM, Wall-integrated PCM, Energy Storage, Experimental, Hot box.

* * Corresponding author's email: Arild.Gustavsen@ntnu.no

1. INTRODUCTION

Nowadays, as global warming becomes one of the most urgent problems in the world, there is a need to find better ways to utilize energy: not only in the field of energy production, transmission, distribution, and consumption, but also in the area of energy storage. With energy storage technologies, it is possible to overcome the contradiction between the energy production and consumption, alleviate the tense production load of power plants at peak hours, and reduce consumers' electricity costs by avoiding higher peak hour tariffs. Moreover, energy storage technologies are badly needed to aid in the utilization of renewable energy sources. Currently, most of the renewable energy sources, especially wind energy and solar energy, are time-constrained energy sources, whose available energy densities are variable and unevenly distributed during different daily hours. Therefore, energy storage systems can be used to store the excess renewable energy in high production hours, make up for the low production valleys, and better integrate renewable energy generation into the local electricity grids.

Energy storage solutions are usually classified into thermal and electrical storage solutions, although they are not so strictly divided due to the theoretically possible conversions between each other. In this paper the focus is put on one thermal energy storage solution, Phase Change Materials (PCMs). PCMs, which again often are categorized as a latent heat storage solution, have a high enthalpy change during the phase change process, and can thus be used to store and release a large amount of thermal energy, usually at a specified temperature or within a temperature range. Several systems have been designed where PCMs are used to store energy in buildings. Baetens et al. (2010) list several examples. Applications include "immersion" of PCMs into construction materials like concrete (e.g. Bentz and Turpin 2007), insulation materials (e.g. Kosny et al. 2007), and windows (e.g. Ismail et al. 2008). Besides the method of "immersion", "attachment" of PCM integrated products to the building envelopes is currently widely used in the commercial market, such as PCM integrated gypsum boards and PCM integrated composite panels. In this case the PCM product is a separate material layer that can be added to a typical building assembly to increase the energy storage capability. Such products have also been studied in several recent publications, like e.g. Kuznik and Virgone (2009a and 2009b) and Ahmad et al. (2006).

In this paper a well-insulated wall with and without PCM layer is studied experimentally in a hot box with respect to different interior conditions (generated heat and air velocity along the interior surface of the tested wall). Emphasis is put on the fluctuations in the interior air and wall surface temperatures.

2. EXPERIMENTAL INVESTIGATIONS

2.1 Description of the Hot box

The hot box used in the experiments is in accordance with ISO 8990 (1994) and ISO 12567-1 (2000). A brief schematic of the hot box with the tested specimen is shown in Figure 1. The test rig is mainly composed of two boxes: box 1 and box 2. Box 2 is normally called the "cold box" or "climatic chamber" and has cooling units with fans to provide the required low temperature. During the testing, the temperature in the cold box was kept at a constant value of about -20 °C.

Box 1 is normally called the "hot box" which comprises a metering box and a thermal guard. The metering box functions as the main test cell, inside which two heaters (labeled as Heater 1 and Heater 2) and a fan (labeled as Fan 1) have been equipped (see Figure 1). Heater 1 is

used as an automatic thermostat to guarantee that the temperature inside the metering box will not be lower than 20 °C; whereas heater 2 is a normal electrical heater that provides an additional heating power when turned on. Fan 1 can be used to generate air circulations inside the metering box. The electrical power of the fan and the corresponding air velocities over the tested wall is shown in Table 1. Since Fan 1 is completely placed inside the metering box, it can be considered that all of the electrical power driving the fan will be converted to heat.

A thermal guard is surrounding the metering box. The heating element in the thermal guard is controlled by a feedback system to maintain the air temperature in the thermal guard (marked as T1 in Figure 1) identical to that of the air in the metering box (marked as T2 in Figure 1). This ensures that no or only limited heat flux will pass through the metering box walls. In this way, according to the energy balance, during the steady-state condition, the heat generated from the heat sources inside the metering box will be equal to the heat flowing through the tested wall.

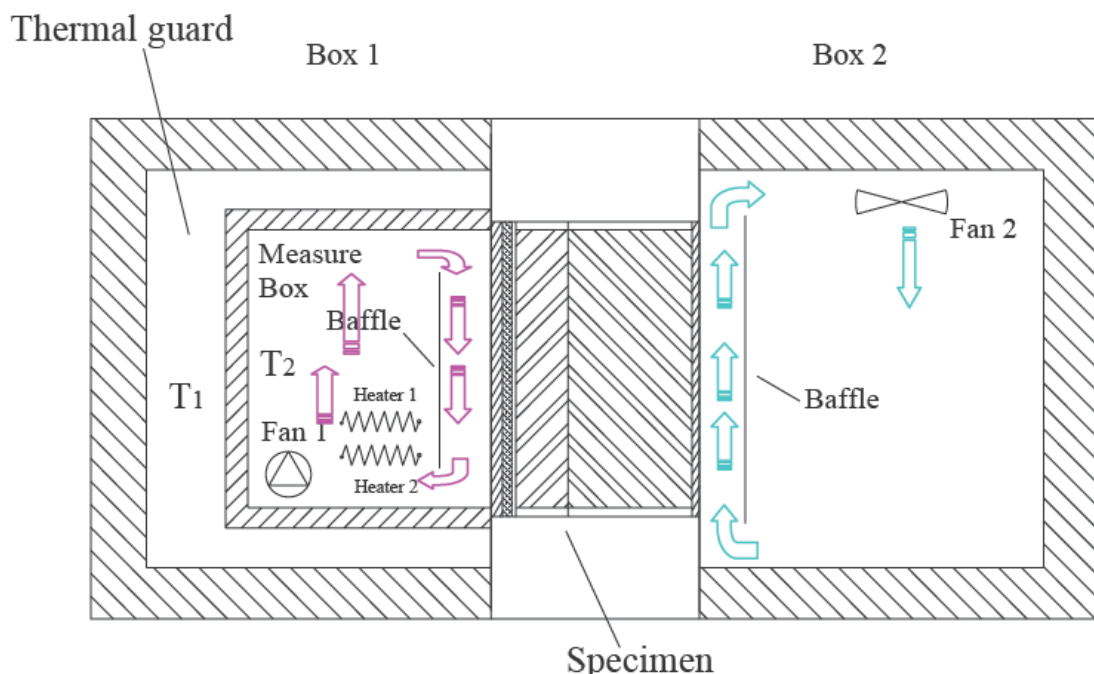


Figure 1. Schematic of the hot box with the tested specimen.

Table 1. The air velocities of the fan and the corresponding electrical powers.

Air velocity (m/s)	Electrical power (W)
0	0
0.1	9.5-10.0
0.2	29.5-30.5
0.3	66.6-67.6
0.4	90.0-91.0

As shown in Figure 1, baffles are used to achieve a more evenly distributed air flow over the tested wall, better control the convective heat transfer over the interior or exterior surfaces, and shield the radiative thermal effects from most of the other surfaces in the corresponding chamber. The dimensions of the metering box and cold box are shown in Figure 2 and Figure 3.

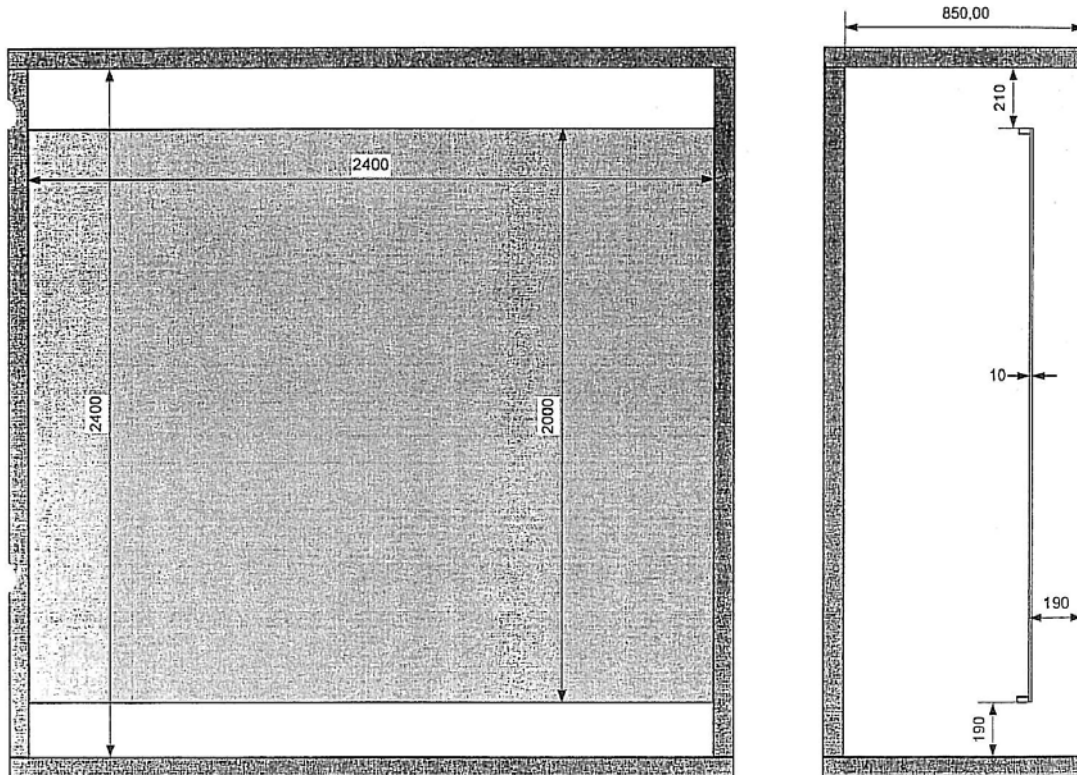


Figure 2. Dimensions of the metering box.

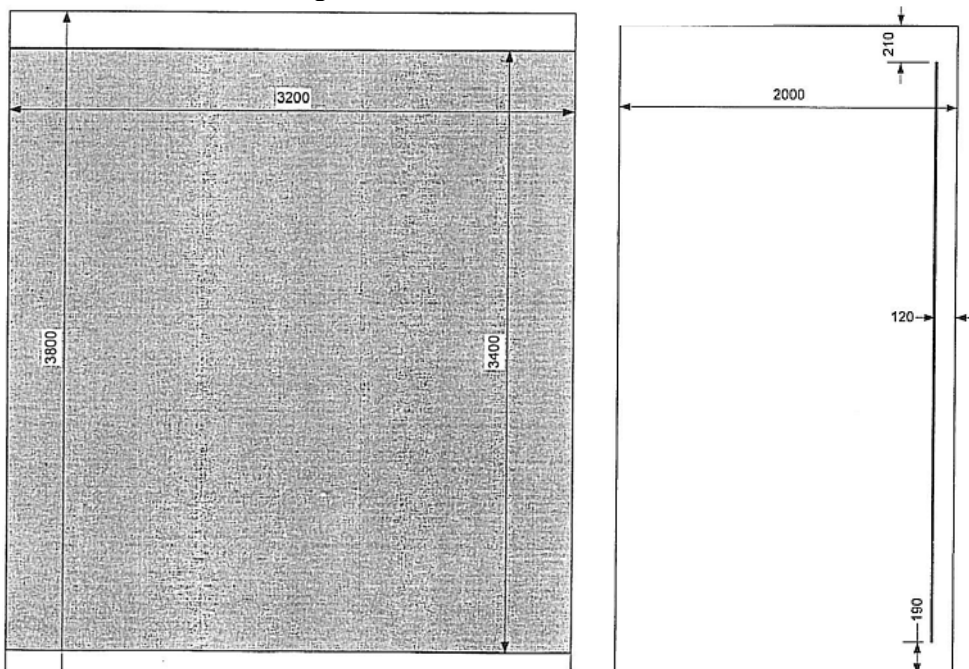


Figure 3. Dimensions of the cold box.

2.2 The configurations of the tested wall

The commercial PCM product used in the experiment is Dupont™ Energain® PCM panel (Dupont Energain, 2010). The main component of this product is 60% molecularly encapsulated paraffin wax within a copolymer (Dupont Energain, 2010). The most important thermophysical properties are listed in Table 2. The specific heat capacity (c_p) – temperature (T) curve of this product is shown in Figure 4. In this paper the hysteresis effect (Kuznik and Virgone 2009b) during the heating and cooling processes is neglected, and the $c_p(T)$ curve is

based on a DSC measurements with a heating rate of 0.05 °C/min (Sallee 2008). The corresponding specific enthalpy (h) – temperature (T) curve based on the $c_p(T)$ curve is depicted in Figure 5. The width and length of the Dupont™ Energain® PCM panel are 1000 mm and 1198 mm, respectively, while the thickness is 5.26 mm (Dupont Energain, 2010). A photo taken after the PCM panels being mounted in the wall is shown in Figure 6.

Table 2. Table showing some of the most important thermal parameters of the Dupont™ Energain® PCM panel (based on data in Dupont Energain (2010) and personal communication with DuPont).

Thermal parameter	Value
Melting point	21.7 °C
Latent heat storage capacity	>70 kJ/kg
Total heat storage capacity (from 14 °C to 30 °C)	>170 kJ/kg
Thermal conductivity	0.18 W/m·K

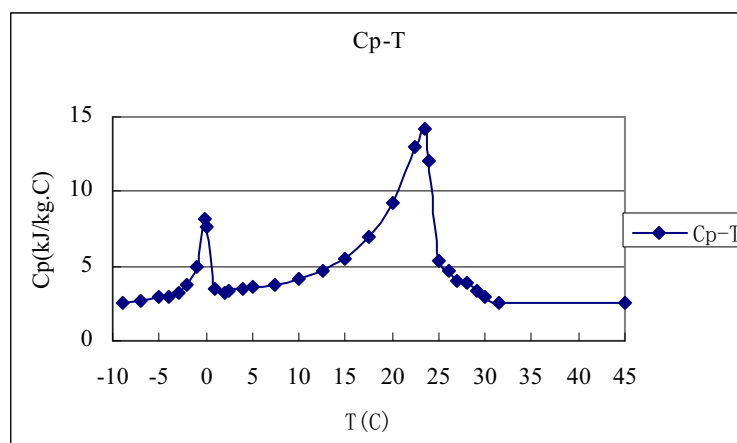


Figure 4. The $c_p(T)$ curve of Dupont™ Energain® PCM panel (Sallee, 2008).

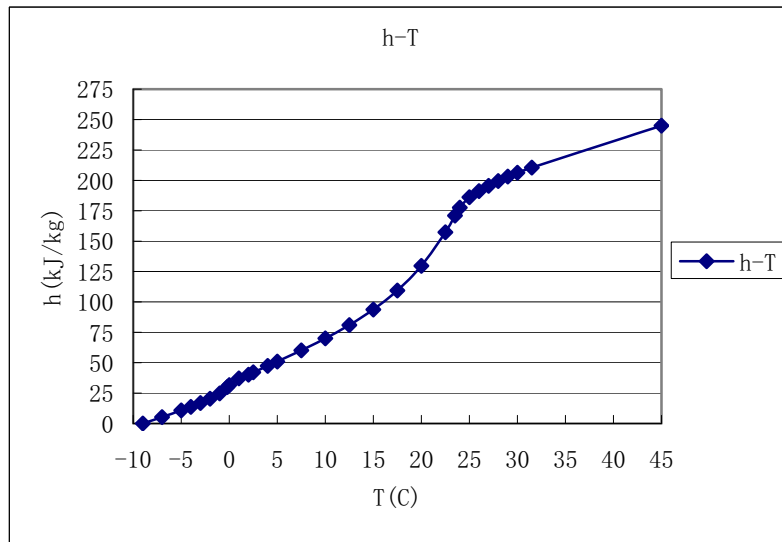


Figure 5. The corresponding h(T) curve of Dupont™ Energain® PCM panel.



Figure 6. Photo of test wall with the Dupont™ Energain® PCM panels. In addition a gypsum board was mounted on the interior side, covering the PCM panels.

As the experiments were arranged in a comparative way, two groups of tests were conducted, under the conditions with and without a PCM layer. Brief schematics of the tested walls are shown in Figure 7. From the side of metering box to the side of the climatic chamber, the configurations of the tested wall with PCM are arranged in such a way as follow: 13 mm thick interior gypsum board, 5.26 mm thick PCM layer, 0.15 mm thick vapor barrier, two layers of 148 mm thick mineral wool, 9 mm thick exterior gypsum board. The configuration of the tested wall without PCM is similar but lacks the PCM layer, i.e. the interior gypsum board is directly attached to the vapor barrier. The dashed line marked in Figure 7 represents the interfaces of two wooden studs, the interior stud with a thickness of 98 mm and the exterior one with a thickness of 198 mm. The detailed framework and dimensions of the two studs (as well as the top and bottom sleepers) are shown in Figure 8.

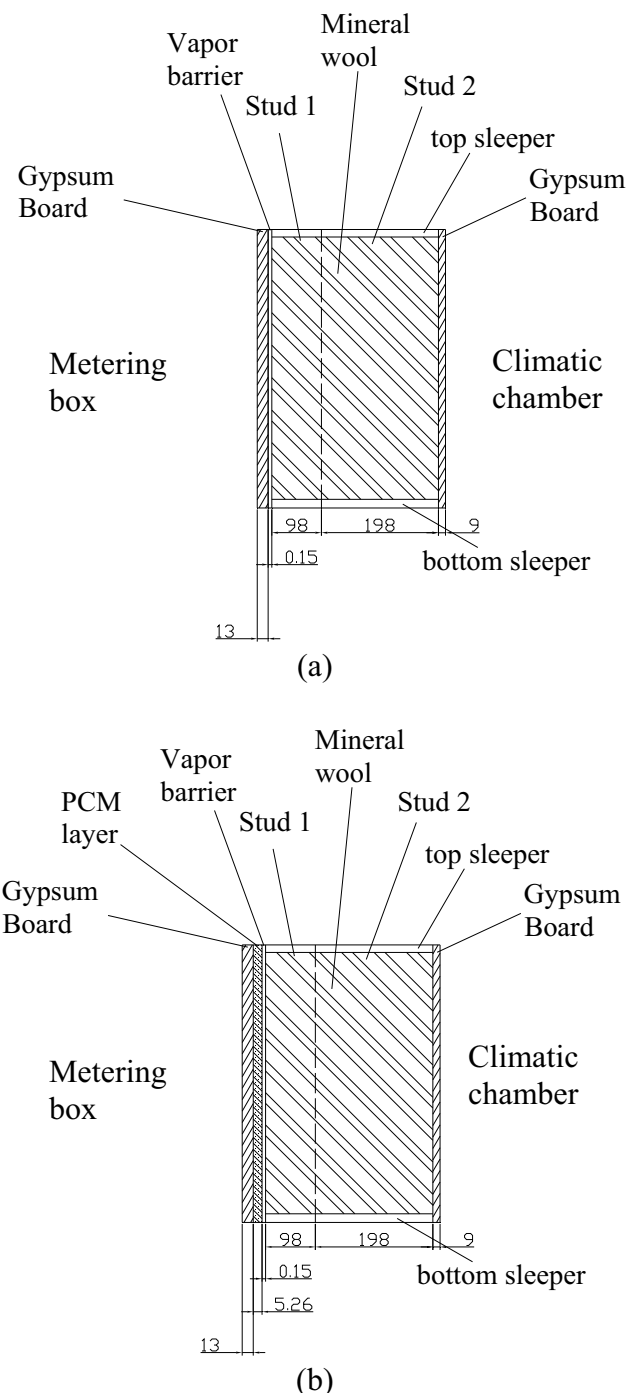


Figure 7. Configurations of (a) the tested wall without PCM and (b) the tested wall with PCM. (The units are in mm.)

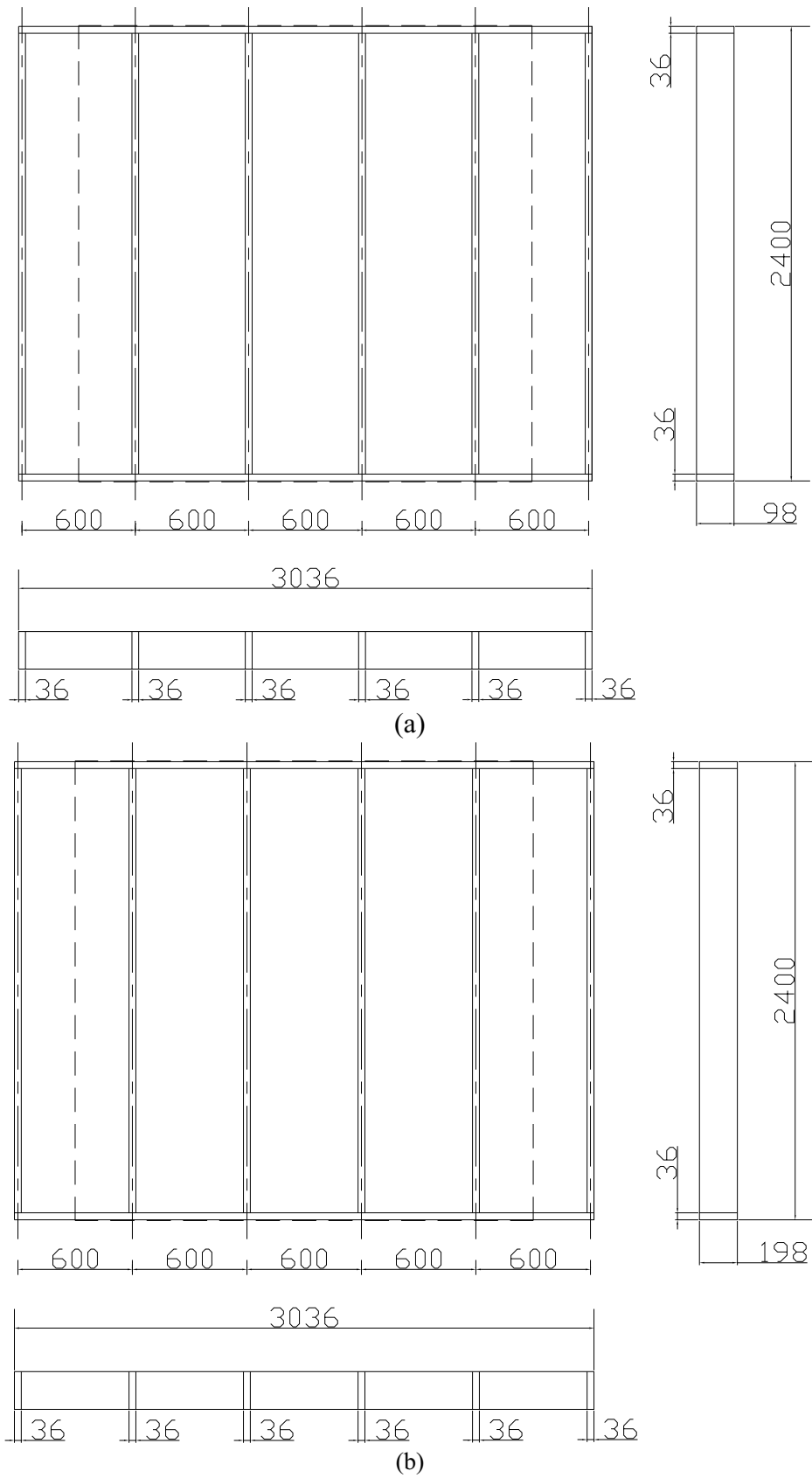


Figure 8. Figures of wood framework of (a) stud 1 and (b) stud 2 with the sleepers. The dashed line in the figures denotes the area of the metering chamber. (The units are in mm.)

2.3 Measurement Devices

A lot of data was logged during the experiments, i.e. various temperature data (e.g. on the wall surfaces and inside the wall), local heat fluxes, air velocities over the interior surface of the tested wall, and powers of heater 1, heater 2 and fan 1. The thermocouples used are of the type T30/2/506 made by Gordon with an accuracy of about ± 0.1 °C, while the heat flux meters are type PU_43T made by Hukseflux with an accuracy of about $\pm 5\%$. The data logging system Orchestrator was used to monitor and collect the temperature, heat flux and electrical power data per 10 minutes. The thermocouples and heat flux meters were well distributed in different layers of the tested wall and the hot boxes (Cao, 2010). Moreover, in order to measure the air velocity over the interior surface of the tested wall, an air velocity sensor of the type AVM501TC made by Prosser Scientific Instruments Ltd. was used.

2.4 Experimental Procedure

As mentioned above, this experiment was arranged in a comparative way. Two groups of tests have been conducted: wall with PCM and wall without PCM. Under both test groups the hot box was operated in an almost identical way, so that the effects and influences due to the PCM layer could be measured and compared. The heating and cooling methods in the metering box have been listed below:

- During the heating period heater 2 and/or fan 1 were turned on; while they were controlled in such a way that the total heating powers of heater 2 and fan 1 were almost the same in each test, see Table 3. The total heating power during each heating period has a value of about 91.36 W with a slight deviation of ± 0.77 W.
- During the cooling period: heater 2 and fan 1 were both turned off, so that the cooling period in the metering box was only influenced by the natural convection.

Each test cycle was composed of two successive periods: heating for 7 hours (from 10:00 to 17:00), and then cooling for the remaining 17 hours (from 17:00 to 10:00 the next day). The reason for arranging the heating and cooling periods in this way was to assure that the metering box had enough time for returning to the initial steady-state condition.

Table 3. Test procedure.

The air velocity during the heating procedure (m/s)	With or without PCM layer	Power of heater 2 (W)	Power of fan 1 (W)	The total heating powers of heater 2 and fan 1
0.4	without	0.00	90.59	90.59
0.3	without	24.62	66.65	91.27
0.2	without	61.86	29.55	91.41
0.1	without	80.90	9.86	90.76
0.0	without	91.16	0.00	91.16
0.4	with	0.00	90.59	90.59
0.3	with	24.52	67.54	92.06
0.2	with	61.79	30.33	92.12
0.1	with	80.90	9.79	90.69
0.0	with	91.22	0.00	91.22

3. RESULTS AND DISCUSSIONS

In this section some initial experimental results will be presented and discussed, focusing on temperature data on the warm side of the hot box. Later studies will also look into the heat fluxes through the walls and also compare experimental results with numerical simulations.

Figure 9 shows the weighted mean temperature (vertical axis in the figure) of the metering box air and the interior surface of the tested wall, as a function of time (horizontal axis in the figure). The weighted mean temperature is based on methods described in ISO 8990, basically area-weighting the respective temperatures. Further the figure includes temperature data for various air velocities on the warm side for the hot box, ranging from 0.4 m/s to about 0 m/s (natural convection).

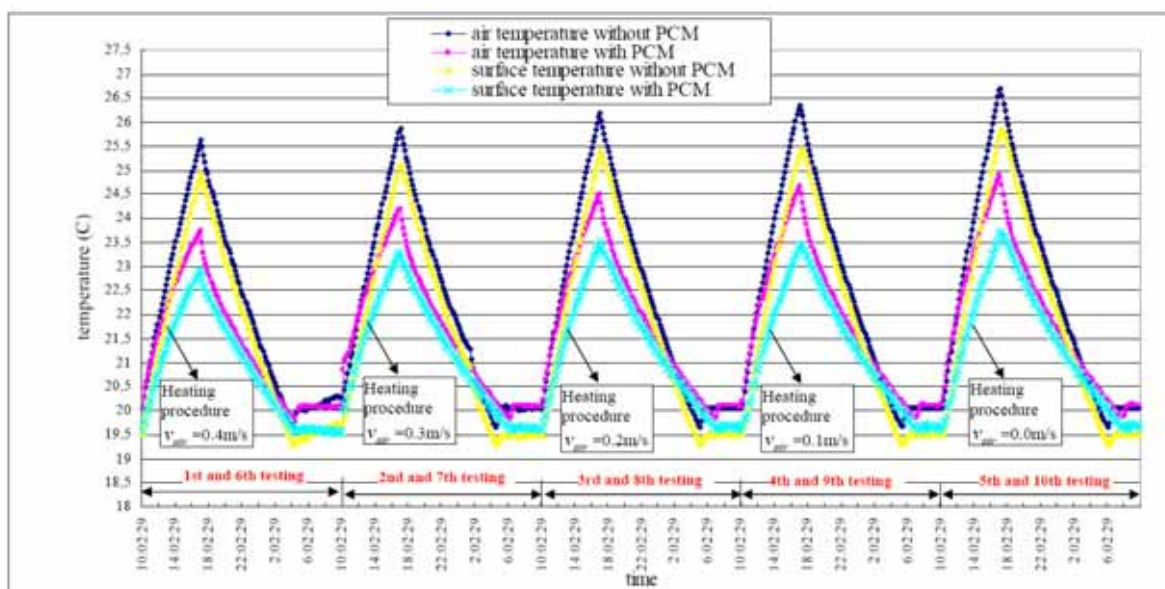


Figure 9. The (weighted) mean temperature evolutions of the metering box air and the interior surface of the tested wall with and without PCM layer during the experiments.

From the figure it is quite easy to see the attenuation effect of the mean air and interior surface temperatures by attachment of PCM layer. By comparing the results of the comparative tests, the maximum temperatures of air and wall surface are decreased by almost 2 °C by attachment of PCM layer. Further, it can be seen and concluded that the higher the air velocities over the interior surface during the heating period, the lower the maximum air and surface temperatures would be by the end of each heating period. This is because that a higher air velocity increases the heat exchange process between the air and the wall.

Furthermore, from Figure 9 it can also be seen that the air temperature presents a quasi linear increasing profile during the heating period when there is no PCM layer in the wall. However, for the PCM case the increase rate of the air temperature was continuously decreasing during the heating period, especially after the air temperature reached 22 °C (which is the melting point for the PCM). Similarly, during the cooling period, the air temperature presents a quasi linear decrease profile under the condition without PCM, while the decrease rate was slowed down under the condition with PCM. The reason of these phenomena is mainly due to the phase change processes of the PCM layer.

In addition, Figure 9 shows that the temperature difference between the metering box air and wall surface under the condition with PCM layer was larger than the case without PCM, especially during the heating period. The reason for this phenomenon is that the wall surface temperature during the phase change processes of the PCM panel increased at a lower rate than the air temperature in the metering box. For the case without a PCM layer, the gypsum board is directly attached to the vapor barrier and the mineral wool. Thus, the lack of phase change processes in the traditional insulation materials and the lower heat flow rate through the gypsum board made the temperature increase rate of the interior wall surface similar to that of the air.

4. CONCLUSIONS AND FUTURE WORK

The attenuation effect of the mean air and interior surface temperatures by attachment of PCM layer is very obvious, and the time lag effect during the cooling period for the air temperature to return to 20 °C could be noticed in each testing. Furthermore, the higher the air velocity over the interior surface during the heating period, the lower the maximum air and surface temperatures would be by the end of the heating period. The increase or decrease rate of the air temperature in the metering box slowed down due to the enhanced heat exchange between the interior air and tested wall during the phase change processes of the PCM layer. Moreover, the temperature difference between the metering box air and surface temperature of the tested wall with PCM layer was larger than that of the case without PCM, especially during the heating period.

Future studies will be performed on the effect of the PCM layer on the energy flow through the wall. Further, the experimental results will be compared to numerical simulations and more detailed studies will be conducted related to the temperature and heat flow variation inside the wall.

5. ACKNOWLEDGEMENTS

This work has been supported by the Research Council of Norway and several partners through the NTNU and SINTEF research project "*The Research Centre on Zero Emission Buildings*" (ZEB).

REFERENCES

- Ahmad, M., Bontemps, A., Sallee, H. and Quenard, D. 2006. Experimental investigation and computer simulation of thermal behaviour of wallboards containing a phase change material, *Energy and Buildings*, Vol. 38, pp. 357-366
- Baetens, R., Jelle, B.P., and Gustavsen, A. 2010. Phase change materials for building applications: A state-of-the-art review. *Energy and Buildings*, Vol. 42, pp. 1361-1368.
- Bentz, D.P. and Turpin, R. 2007. Potential application of phase change materials in concrete technology, *Cement & Concrete Composites*, Vol. 29, pp. 527–532.
- Cao, S. 2010. *State-of-the-art thermal energy storage solutions for high performance buildings*. Master's thesis in Renewable Energy Programme, Department of Physics, University of Jyväskylä, Finland / The Research Centre on Zero Emission Buildings (ZEB), Norwegian University of Science and Technology (NTNU) / SINTEF Building and Infrastructure.

Dupont Energain, *DupontTM Energain® Energy-Saving Thermal Mass Systems, Data Sheet-Measured Properties*, DupontTM Energain®, 2007. [Online]. Available: http://energain.co.uk/Energain/en_GB/assets/downloads/tech_info/dupont_energain_datasheet.pdf. [Accessed: April 23, 2010].

Ismail, K.A.R., Salinas, C.T., and Henriquez, J.R. 2008. Comparison between PCM filled glass windows and absorbing gas filled windows, *Energy and Buildings*, Vol. 40, pp. 710-719.

ISO 8990. 1994. *ISO 8990: 1994 – Thermal insulation – Determination of steady-state thermal transmission properties - Calibrated and guarded hot box*. International Organization for Standardization, Geneva.

ISO 12567-1. 2000. *ISO 12567-1: 2000 – Thermal performance of windows and doors – Determination of thermal transmittance by hot box method – Part 1: Complete windows and doors*. International Organization for Standardization, Geneva.

Kosny, J., Yarbrough, D.W., Miller, W., Petrie, T., Childs, P., Syed, A.M. and Leuthold D. 2007. Thermal performance of PCM-enhanced building envelope systems, *Thermal Performance of the Exterior Envelopes of Whole Buildings X, Proceedings of the ASHRAE/DOE/BTECC Conference*, Clear Water Beach, FL, December 2–7 (2007), pp. 1–8.

Kuznik, F., and Virgone, J. 2009a. Experimental assessment of a phase change material for wall building use, *Applied Energy*, Vol. 86, pp. 2038-2046.

Kuznik, F. and Virgone, J. 2009b. Experimental investigation of wallboard containing phase change material: Data for validation of numerical modeling, *Energy and Building*, Vol. 41, pp. 561-570.

Sallee, H. 2008. *Thermal characterization, before and after aging of DupontTM Energain® Panels*, CSTB, Saint Martin d'Hères, N/Réf. CPM/09-035/HS/MLE/, February 13, 2008.

Efficient Building Operation as a Tool to Achieve Zero Emission Building

N. Djuric, V. Novakovic

Norwegian University of Science and Technology,

Department of Energy and Process Engineering, NO-7491 Trondheim, Norway

ABSTRACT

Quality control of the complete energy system is essential if CO₂ targets are to be met. Building energy management systems (BEMS) provide information and means to monitor building energy performance efficiently. Therefore, strategies and tools for ensuring that the technical goal of zero emission buildings (ZEB) is robustly realized are necessary. Lifetime commissioning (LTC) has been recognized as a tool that can perform quality control of buildings. The aim of our study was to present LTC procedures and three assessment tools that can be used for quality control of ZEB energy supply in operation phase. LTC procedures were introduced using a generic framework on building performance. The three developed assessment tools were: mass balance inspection algorithm for consumer substation, regression model for predicting heating load based on outdoor temperature and building use, and advanced method for improved measurement of heat pump performance based on data integration. LTC procedures and tools were tested on two case studies. The results showed that 20% of all the defined building performance data can be monitored by BEMS. Using the mass balance inspection algorithm, it was found that fault in mass balance prevented implantation of desired temperature control for floor heating system. The regression models based on sequential quadratic programming algorithm are very robust because they can be extended with many parameters and functions. For heat pump performance, measurement of differential water temperature can have random errors, and the use of compressor electrical signal can give more precise data on heat pump performance.

Keywords: lifetime commissioning, building performance, BEMS, data analysis

1. INTRODUCTION

The ambitious targets of ZEB can only be achieved if advanced energy efficiency technologies match expectations. If not, CO₂ can be even increased compared to designed one. In the work of Firth et al. (2010), it was shown that the building CO₂ emissions are the most sensitive on changing in energy efficiency measures. Therefore, quality control of the complete energy system is essential if CO₂ targets are to be met as pointed in (Firth 2010). To perform a proper quality control of a building, it is necessary to have enough data on building performance. For example, in the study of Parker (2009), it was shown that to evaluate real-world potential of Zero energy homes in North America, most of the buildings needed to be highly instrumented and monitored. One building was even instrumented with dynamic feedback on building performance to occupants.

Buildings are becoming more complex systems with many elements, while building energy management system (BEMS) provides much data about the building systems. There are, however, many faults and issues in building performance, but there are legislative and cost-benefit forces induced by energy savings (Djuric 2008). To overcome these problems and challenges, it is necessary to have a tool that can help provide quality control on building energy performances, to

perform fault detection and diagnosis, and overcome poor functional integration induced by information loss. Lifetime commissioning (LTC) has been recognized as a tool that can perform these given tasks (Visier 2004; Djuric and Novakovic 2009; Xiao and Want 2009). In this study we have adopted commissioning (Cx) as the process of ensuring that systems are designed, installed, functionally tested, and capable of being operated and maintained to perform in conformity with the design intent as defined in ASHRAE Guideline 1–1996 (1996). Actually, in the study, LTC is treated as performance verification. Also, LTC is described as performance verification in the work of Kjellman et al. (1996). The first aim of this study is to present the Norwegian LTC procedures. These procedures are presented using suggested generic framework for the building energy performances.

Since a building process is typically split into fragments with different participants, information loss appears with performance degradation as a consequence (Djuric and Novakovic 2010). In the construction industry, experience can be re-applied and shared among engineers and participants to enhance construction processes and minimize costs and problem-solving time (Lin 2008). In the work of Lee and Akin (2008), it was found that there is a 12% potential for maintenance improvement by providing proper information support. Therefore, the purpose of the Norwegian LTC procedures is to be a knowledge-based tool that can enhance collection of building performance data for efficient operation.

Among different technologies to provide energy saving opportunities in buildings, energy analysis and building performance evaluation are also taken into consideration (Ma and Wang 2009). LTC implies use of these tools. Availability of BEMS and additional measurements are necessary for proper building performance estimation. Further, integration of these measurements and mathematical methods encourage building performance estimation. For example, heating system performance can be analyzed using BEMS data and sequential quadratic programming (SQP) (Djuric et al. 2008). Since measurement data can be corrupted by errors, use of data fusion technique can help to estimate real performance data as shown in (Huang et al. 2009).

This paper consists of two parts. The first part presents the Norwegian LTC procedures together with three developed tools for assessment of building energy performance in operation. The second part introduces two case studies and presents findings in them discovered using the developed tools.

2. METHOD

2.1 Norwegian LTC Procedures

The Norwegian LTC procedures for improving building performance were developed based on international commissioning experience and national practical experience. The procedures are a manual and consist of nine parts. The aim of the procedures is to create a good information system between all the participants during the building lifetime. The focus is on ensuring the owner's project requirements so that the performance quality control is enabled. The method has been reported in (Djuric and Novakovic 2010).

As a building lifetime is going, activities described in a certain document have to be fulfilled. These procedures consist of the following parts: Part 1: Performance requirements for the LTC; Part 2: Performance requirements for Cx in the design phase; Part 3: Performance requirements for Cx in the construction phase; Part 4: Performance requirements for Cx in the operation phase; Part 5: Plan for the Cx in the design phase; Part 6: Plan for the Cx in the construction phase; Part 7: Plan for the Cx in the operation phase; Part 8: Requirements list for the Cx; Part 9:

Performance description. Based on the building owner requirements, a supervision plan has to be established by using Part 1. Based on valid standards and the owner requirements, a list of requirements should be developed according to Part 2. The performance description enables monitoring and quality control of the building performances through the building lifetime, and therefore this documentation is extending through the entire lifetime.

Practically, the necessary information for fulfillment of the LTC procedures can be collected in different ways. In our study, a generic framework on building performance is suggested. This framework describes building performance data as a data model (Djuric and Novakovic 2010). A building performance is a function of a building element, which can be defined by a few performance data as shown in Figure 1.

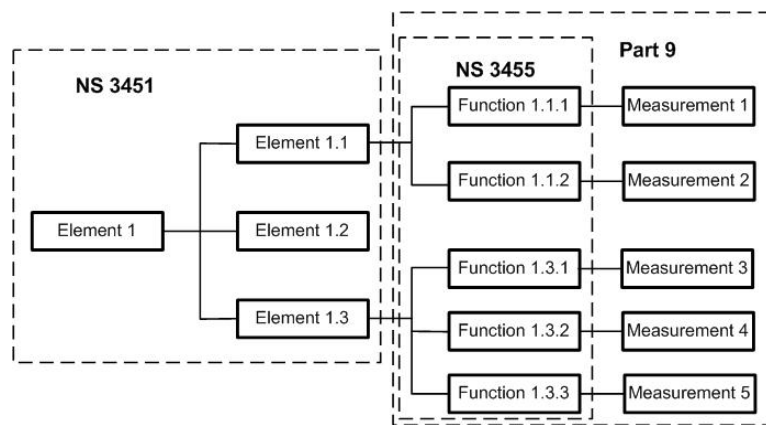


Figure 1. Relationship between building elements and functions

A building element can consist of a few sub-elements (in Figure 1 three elements), which can be defined by a few functions. The function numbers of an element depends on the element specification and which performance data are necessary for performance estimation. To follow-up each desired function, it is necessary to define measurement of that function. Therefore, measurement of desired performance data should be defined as soon as an element performance is involved in a building project. This suggested framework on building performance enables generic definition of performance data and their requirements. In that way, different manipulation of performance data is enabled for different purposes.

2.2 Mass Balance Inspection Algorithm

For example, in the design and balancing phase, it is possible to meet a problem that water flow balance is not fulfilled in consumer substation. Since branches in consumer substation influence each other, such problem contributes to that the desired water flow is not achieved in separate branches. Further, if the water flow is different from the designed one, a desired temperature control cannot be achieved. Consequently, energy consumption can be very different than the designed one. Use of mass balance equation permits detection of flow measurement errors and evaluation of system performance as shown in the work of Menendez et al. (1998). They suggested a method that integrated measurement uncertainty data and the maximum likelihood least-square estimation to estimate true water flow in the branches.

In our study, after data was obtained from LTC procedures, it was possible to perform different manipulations on water flow data in the consumer substation. The suggested algorithm

consists of three steps: 1. Estimating real water flow; 2. Estimating error; 3. Defining inspection rules. To explain the algorithm for mass balance inspection, simplified supply side branches in the consumer substation are used as shown in Figure 2.

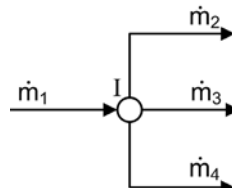


Figure 2 . Simplified supply branch

Mass balance equation for the system with one node in Figure 2 can be written as

$$\sum_{j=1} a_j \cdot m_j^* = 0 \quad (1)$$

where m^* is mass flow rate and a_j is the entry/exit coefficient to the node I. Coefficient a_j is 1 if flow is entering node I and -1 if flow is exiting the node. Eq. (1) should be fulfilled in each phase: design, construction, and operation. Due to poor estimation or faults, it can occur that water flows do not fulfill Eq. (1). Regardless of faults, the system naturally finds balance. The achieved balance represents real water flow. The real water flows were estimated by calibrating the model in Eq. (1) to the data from the LTC procedures. The model calibration was done using optimization method as shown in (Djuric 2008; Djuric et al. 2008), and the objective function was

$$\min 100 \cdot \sum_{i=1} (M_i - M_{D_i}/M_i)^2 \quad (2)$$

where $M = [m_1^*, m_2^*, \dots, m_j^*, \dots, m_n^*]$ is a vector consisting of all the real estimated branch water flows, M_D are water flows in documentations, and $i=1,2,3$ is the number of measurement. In our case, 1 for the data in the design phase, 2 for the construction phase, and 3 for balancing phase. To solve the optimization problem in Eq. (2), the SQP algorithm was used.

After estimated flow rates were obtained, errors between estimated and flow rates in documents at each building phase were calculated. Finally, mean error μ , and standard deviation of error σ , for each measurement were used to define inspection rules for mass balance algorithm. The developed inspection rules were the following:

1. If $\mu \leq -10\%$, the water flow rate at the branch is always higher than in the documents.
2. If $\mu \geq 10\%$, the water flow rate at the branch is always lower than in the documents.
3. If $\sigma \geq 10\%$, the branch is wrongly integrated. This means that data in each phase have been chosen arbitrarily without any correlation with previous phases.

2.3 Improved Heat Pump Performance Estimation

Data fusion implies the use of techniques that combine data from multiple sources and gather information in order to achieve more efficient and more accurate conclusions than if a single

source was used. Use of LTC procedures provided data on HVAC systems and access to BEMS gave the possibility to measure HVAC system performance in operation phase. Consequently, it was beneficial to combine these data with the aim to give a more accurate estimation on the system performance. Data from manufacturer technical guide and BEMS measurement were combined to estimate heat pump performance in an office building in Trondheim, Norway. Analyzed heat pump is shown in Figure 3.

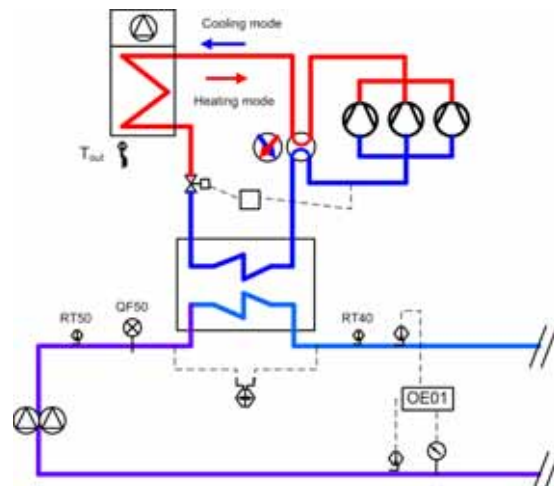


Figure 3. Heat pump in Trondheim office building

The heat pump in Figure 3 is a water/air heat pump and supplies eight heating/cooling coils in air handling units. Depending on evaporation and condensation temperatures, maximal heating capacity of the condenser can be 550 kW, and maximal compressor power can be 150 kW. During winter the heat pump supplies heating, while during the summer it supplies cooling to the coils. The heat pump has three compressors, which are step-wise controlled. The heating capacity of the condenser could be measured based on the temperature difference between supply temperature RT 40 and return temperature RT 50, and water flow rate, in Figure 3. Beside to these temperatures, BEMS gives possibility to monitor electric compressor signals. Figure 4 displays measurements of the sensors RT 40 and RT 50 shown in Figure 3.

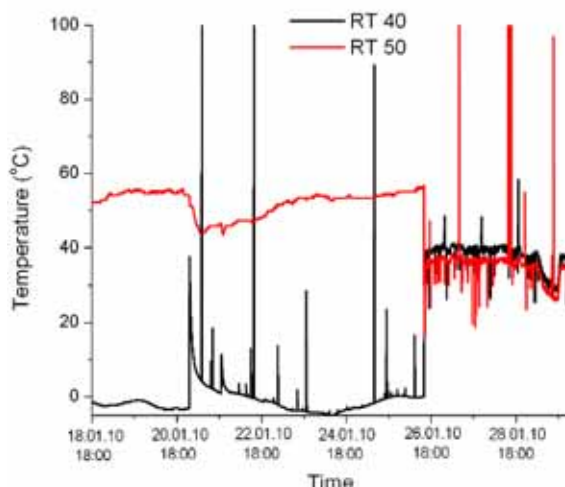


Figure 4. Measurement of the supply/return temperature to condenser

In practice, temperature sensors mostly cannot measure the water temperature directly, and therefore measurements easily suffer from noise, outliers, systematic errors, and uncertainty as noticed in (Huang et al. 2009). An example of water temperature measurement of the supply and return temperatures of the heat pump condenser is shown in Figure 4.

In the winter period when the heat pump is used to heat the supply water, temperature RT 40 should be higher than RT 50. Due to mentioned difficulties in the temperature measurement, it is possible that measurements such as in Figure 4 are obtained. Such measurements cannot be used for further performance analysis of the heat pump. The additional data for the heat pump estimation were the heat pump performance from the manufacturer technical guide and the electrical compressor signal. The manufacturer of the heat pump provided compressor power, and condenser and evaporator load based on the evaporation and condensation temperatures. Therefore, based on the manufacturer technical data and the electrical signal, it is possible to indirectly estimate: the compressor power P , and the heat pump condenser load \dot{Q}_{con} as

$$P = p \cdot f_1(T_{ev}, T_{con}) \quad (3)$$

$$\dot{Q}_{con} = p \cdot f_2(T_{ev}, T_{con}) \quad (4)$$

where T_{ev} is the evaporation temperature, T_{con} is the condensation temperature, and p is compressor partial load obtained by summing electric compressor signals. Since the heat pump in Figure 3 is step-wise controlled, it usually works at part load. The electrical signal from the compressors gives information which part of the compressor is in use. Finally, using the electrical signal from the compressors and provided performances, it was possible to obtain the compressor power at part load.

2.4 Regression Model

In order to inspect and predict building performance, it is beneficial to develop reference performance models. These performance models can be developed as regression models with different driving variables as shown in the work of Wang et al. (2010), where different performance indices of HVAC system were developed as regression models. Driving variables can be variables that are possible to monitor in BEMS. Heating load is a metric of building energy performance. Driving variables for heating load can be outdoor temperature T_{out} , and mass flow rate $m\dot{v}$. The heating load \dot{Q} can be defined as:

$$\dot{Q} = \sum_{j=0}^2 \sum_{k=0}^2 b_{jk} \cdot T_{out} \cdot m\dot{v}. \quad (5)$$

The regression model parameters, b_{jk} were obtained using optimization method as shown in (Djuric 2008; Djuric et al. 2008). The regression model in Eq. (5) can be developed by using 1) only outdoor temperature, or 2) using both outdoor temperature and mass flow rate in the substation. The difference in these models is that the second model is considering building users. The mass flow rate is changing based on the building energy demand, which is determined by building users. If there are more users in a building, the mass flow rate is higher because a large

part of the equipment is in use. In that way, it is possible to consider that the building users define the water flow rate.

3. TEST OF THE LTC PROCEDURES

3.1. Description of the Case Studies

The Norwegian LTC procedures were tested on two office buildings in Stavanger and Trondheim, Norway. The case buildings are displayed in Figure 5 and 6. The first case building, in Figure 5, with $19\ 623\ m^2$ of heated area, is located in Stavanger. This case building has been in use since June 2008. The second case building, in Figure 6, with $16\ 200\ m^2$ of heated area, is located in Trondheim. This case building has been in use since September 2009. Both case buildings are rented as office buildings.



Figure 5. Office building in Stavanger



Figure 6. Office building in Trondheim

The ventilation system concept is different in these buildings, while energy supply systems are similar. Heating energy for ventilation, space heating, and domestic hot water is supplied by district heating and heat pumps. Cooling energy is supplied by two cooling plants. Heat realized from the cooling plant condensers is used as additional energy for heating. In that way, these cooling devices are at the same time heat pumps.

3.2. Assessment of Available Data

ZEB would require large amounts of data to build a good knowledge for efficient operation. Here current situation on available building information is represented. Reported case buildings are modern and new office buildings. In this study, data were collected using generic framework, and assessment of available data was possible. Data assessment showed that the ventilation systems were presented with more performance data than the other systems in both case buildings. In the second case building, it was possible to find 65% of the defined functions by comparing the installed functions, which were found in the manufacturer technical guides, and the defined LTC functions. There was a similar situation in the first case building, where there were 60% installed functions for the ventilation system.

The situation was opposite for the hydronic systems like the domestic hot tap water system, hydronic heating system, fan-coil system, and cooling systems. For example, the amount of installed functions were 20% of defined functions in the first case, while in the second case

building there were 40% of the defined functions. This means that energy audit, inspection, and testing of these systems could be difficult.

In total, about 20% of all the defined building performance data can be monitored by BEMS. Among these monitored performance data, almost half belonged to the ventilation systems. There are only 10% of common performance data among different documents and building levels. This means that there is no generic framework among different building documents. This can discourage any attempt to track building performance during the building lifetime.

3.3. Results on Substation Mass Flow Inspection

The algorithm for the mass balance inspection was tested on the case building in Trondheim. The inspection was performed for the consumer substation shown in Figure 7. Labeling in Figure 7 is according to NS 3451 (2006) and the multidisciplinary labeling system established by the Norwegian Public Construction and Property Management (Statsbygg).

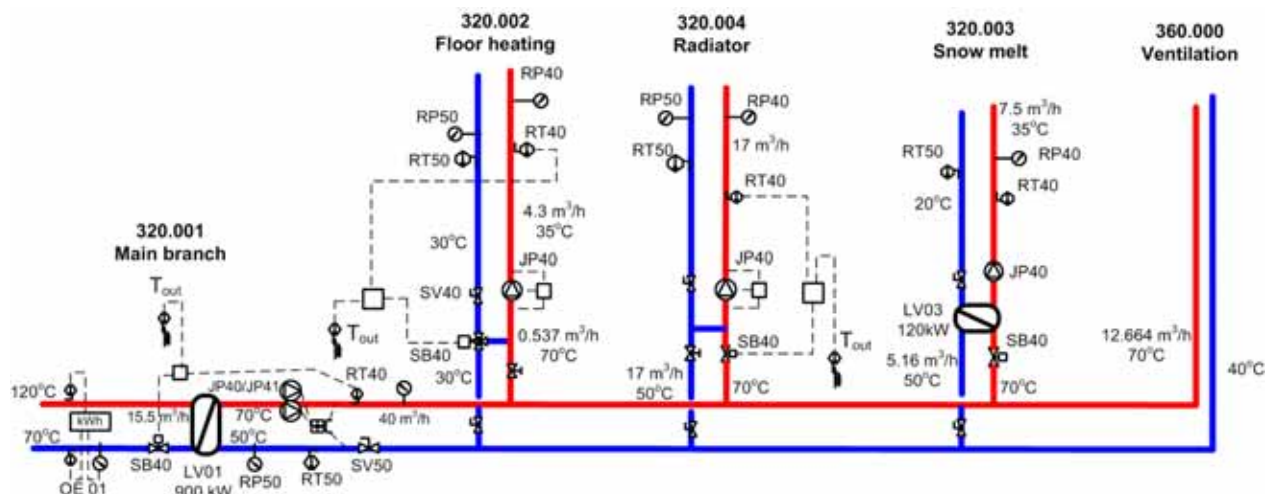


Figure 7. Schematic of consumer substation

The main branch, 320.001, supplies four branches for floor heating, radiators, snow melting, and ventilation system. Volumetric flow rates and temperatures in Figure 7 are from design drawings.

Date from the LTC procedures that were used for the mass balance inspection are given in Table 1. Date on the water flow rate in the design phase were found in the assembling drawings. Data from the construction phase are based on delivered equipment size and manufacturer technical guides. Data from balancing were provided from balancing reports.

Table 1. Documented water flow rates in kg/s

Branch Phase	320.001	320.002	320.003	320.004	36.000
Design	10.92	0.15	1.41	4.64	3.46
Construction	13.16	0.15	1.44	4.64	3.84
Balancing	12.12	0.16	1.47	5.24	4.19

If mass balance has to be established in the substation, data in Table 3 have to satisfy Eq. (1). If we check data in Table 1, it is obvious that sum of mass flows in the branches 320.002,

320.003, 320.004, and 36.000 is not equal to the mass flow in the branch 320.001. Therefore, it was necessary to estimate mass flow using Eqs. (1) and (2). Estimated flow rates are given in Table 2.

Table 2. Estimated flow rates in kg/s

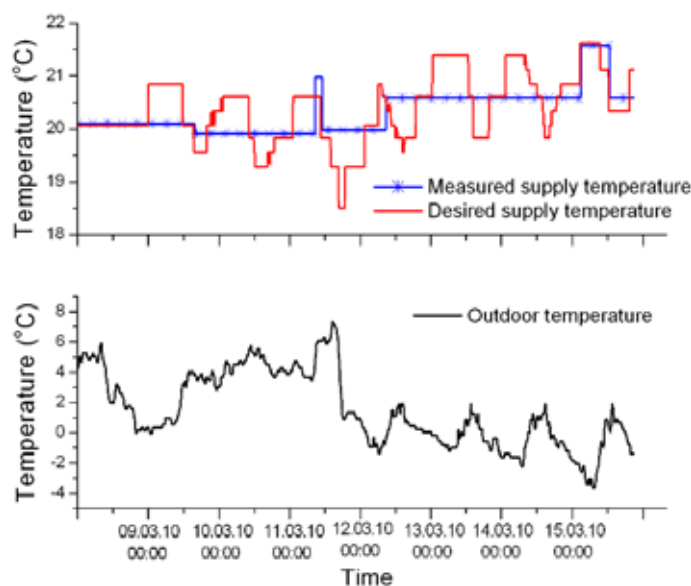
Branch \ Phase	320.001	320.002	320.003	320.004	36.000
Design	10.62	0.42	1.61	4.89	3.70
Construction	10.79	0.42	1.62	4.89	3.86
Balancing	10.95	0.27	1.53	5.06	4.09

In contrast to Table 1, data in Table 2 are satisfying mass balance, Eq. (1). Overview of the calculated errors for each branch in Figure 7 is given in Table 3. Finally, use of error can help to detect where possible faults can appear in the system during the operation phase.

Table 3. Errors, mean error, and standard error deviation on the flow rate

Branch \ Phase	320.001	320.002	320.003	320.004	36.000
Design	2.72	-64.94	-12.71	-5.14	-6.52
Construction	21.62	-64.94	-11.42	-5.14	-0.38
Balancing	11.46	-41.29	-3.40	3.59	2.48
μ	11.93	-57.05	-9.18	-2.23	-1.47
σ	9.46	13.67	5.05	5.04	4.60

Using the established rules for the mass balance inspection, it was found that in the branch for floor heating, 320.002, the water flow would always be higher than was found in the documentation. Such difference in the mass flow implies difficulties in the control of the supply water temperature to the branch 320.002. BEMS data were used to analyze this issue. Measurement on the supply water temperature for the floor heating is shown in Figure 8.

**Figure 8. Biased supply water temperature at the floor heating branch**

In Figure 8, it is noticeable that supply water temperature to the floor heating is most of the time different from the desired value. This bias could be up to ± 1.5 K, when outdoor temperature was in the range of $-3.5 - 7.5$ °C. Since the floor heating is a low temperature heating system, with temperature difference on the supply/return side of 5 K, such large bias in the supply temperature could induce an increase of approximately 20% in energy consumption for the floor heating.

3.4. Estimated Performance of Heat Pump Based on Data Integration

Using introduced method for heat pump performance estimation, the compressor power and condenser load were estimated. The condenser load was also estimated using the temperature difference between supply and return water temperature. The estimation results are shown in Figure 9.

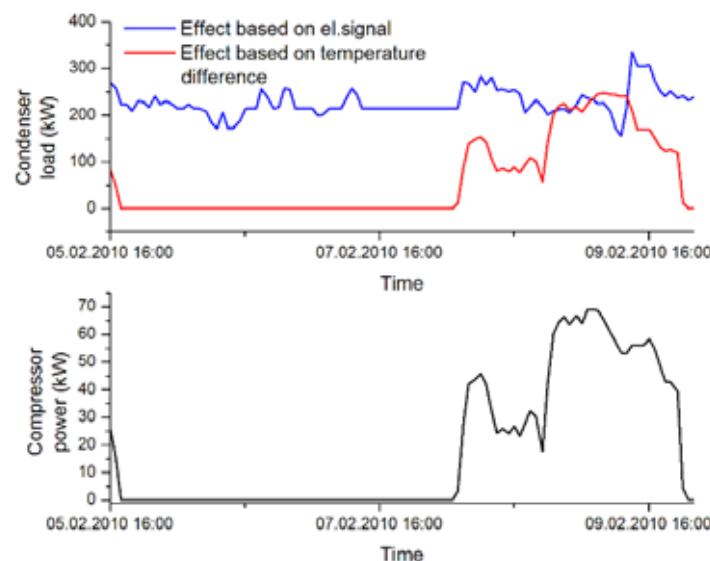


Figure 9. Compressor power and condenser load for heat pump

February 5th – 7th was a weekend and the heat pump was not in use. Estimation of the compressor power, as shown in the lower part of Figure 9, shows that the heat pump was not in use. Estimation of the condenser effect based on the electrical signal, the red line in the upper part of Figure 9, shows no heating load of the condenser. However, estimation of the condenser load based on the temperature difference, the blue line in the upper part of Figure 9, shows a certain heating load on the condenser. This difference happened because the circulation pump is always on as a measure for freezing protection, and therefore a small temperature difference can give a certain heating load. Results in Figure 9 show that use of only temperature difference to estimate the heat pump performance can mislead us to treat that heat pump is running even when it is off.

3.5. Regression Model for Heating Load

Heating load model was calibrated against heating load data in the office building in Stavanger. Models are declared to be calibrated if they produce mean bias error (MBE) within $\pm 10\%$ and coefficient of variation of the root mean squared error (CV(RMSE)) within $\pm 30\%$

when using hourly data (ASHRAE 2002). For the heating load models introduced in Eq. 5, these model errors are given in Table 4.

Table 4. Heating effect model errors

Model	MBE (%)	CV(RMSE) (%)
Outdoor temperature	-30.7	56.8
Outdoor temperature and users	-9.2	21.8

Results in Table 4 clearly show that model with two parameters is more accurate than the model based on the outdoor temperatures only. Comparison of these two models is given in Figure 10.

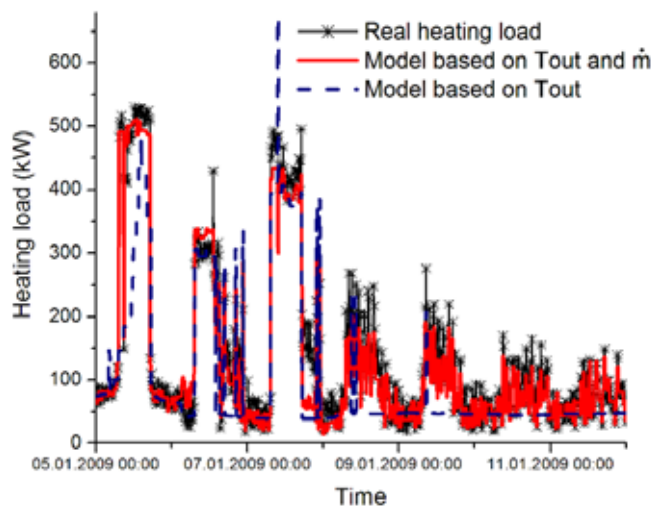


Figure 10. Regression models of heating load

The model in Eq. 5 which uses the outdoor temperature and water flow as driving variables, fits better to the real heating effect. This example shows that availability of several measurement data encourages model development for performance estimation in operation phase.

4. CONCLUSION

The paper presents some of the reasons for integrating building operation encouraged with LTC as an inherent part of ZEB's solution development, where energy-efficiency is important to be met. As reasons to integrate life-time commissioning into ZEB development, the following were emphasized: building information collection, building performance monitoring and analysis, and energy consumption analysis. For each of these reasons, tools and examples were given in the paper.

Since building information loss induces performance degradation, LTC procedures are necessary to be a knowledge-based tool that can enhance collection, tracking, and quality control of the building performance data during the building lifetime. Current situation in the case buildings showed that 20% of all the defined building performance data can be monitored by BEMS, while about 60% of all the defined performance data can be found in the different documents. For efficient operation of ZEB, it would be necessary to have a higher monitoring level than current situation, especially on the energy supply side. This need for enhanced measurement in the hydronic system and on the energy supply side was shown on the

measurement of the heat pump and the consumer substation. Heat pump performance estimation can be more accurate using data integration, where data from construction and operation phase were combined. Example with regression model showed that energy consumption cannot be related only to the outdoor temperature, and additional variables give more accurate models. Low temperature systems can be relevant for ZEB's solutions. Combining data from design, construction and operation phase, it was shown that a fault in the mass balance induced fault in the temperature control for the floor heating regardless of the good intention.

ACKNOWLEDGEMENTS

This work was financially supported by the Research Council of Norway and the other members of the project: Life-Time Commissioning for Energy Efficient Operation of Buildings (project number 178450/s30).

REFERENCE:

- NS 3451, Table of building elements, Standards Norway, 2006,
- ASHRAE, 1996, *ASHRAE Guideline 1-1996: The HVAC Commissioning Process*, The American Society of Heating, Refrigerating and Air-Conditioning Engineers, Atlanta, US.
- ASHRAE, 2002, *ASHRAE Guideline 14: Measurement of Energy and Demand Savings*, The American Society of Heating, Refrigerating and Air-Conditioning Engineers, Atlanta, US.
- Djuric, N., 2008, Real-time supervision of building HVAC system performance. Department of Energy and Process Technology. Trondheim, Norwegian University of Science and Technology. PhD thesis: 224.
- Djuric, N., Novakovic, V., 2009, Review of possibilities and necessities for building lifetime commissioning, *Renewable and Sustainable Energy Reviews*, 13: 486-492.
- Djuric, N., Novakovic, V., 2010, Correlation between standards and the lifetime commissioning, *Energy and Buildings*, 42(4): 510-521.
- Djuric, N., Novakovic, V., Frydenlund, F., 2008, Heating system performance estimation using optimization tool and BEMS data, *Energy and Buildings*, 40(8): 1367-1376.
- Firth, S. K., Lomes, K.J., Wright, A.J., 2010, Targeting household energy-efficiency measures using sensitivity analysis, *Building Research & Information*, 38(1): 25-41.
- Huang, G., Wang S.W., Xiao, F., Sun Y., 2009, A data fusion scheme for building automation systems of building central chilling plants, *Automation in Construction*, 18(3): 302-309.
- Kjellman, C. R., Haasl, R.G., Chappell, C.A., 1996, Evaluating commissioning as an energy-saving measure, *ASHRAE Transaction*, 102: 492-501.
- Lee, S., Akin, O., 2008, Shadowing tradespeople: Inefficiency in maintenance fieldwork, *Automation in Construction*, 18: 536-546.
- Lin, Y. C., 2008, Developing construction assistant experience management system using people-based maps, *Automation in Construction*, 17: 975-982.
- Ma, Z., Wang, S.W., 2009, Building energy research in Hong Kong: A review, *Renewable and Sustainable Energy Reviews*, 13(8): 1870-1883.
- Menéndez, A., Biscarri, F., Gómez, A., 1998, Balance equations estimation with bad measurements detection in a water supply net, *Flow Measurement and Instrumentation*, 9(3): 193-198.
- Parker, D. S., 2009, Very low energy homes in the United States: Perspectives on performance from measured data, *Energy and Buildings*, 41(5): 512-520.
- Statsbygg, viewed on Jun 8 2009, Multidisciplinary labeling system, http://www.statsbygg.no/FilSystem/files/Dokumenter/prosjekteringsanvisninger/0GenerellePA/PA0802_TFM/TFM_Start.pdf.
- Visier, J. C. (Eds.), 2004, Commissioning for improved energy performance, Results of IEA ECBCS Annex 40, IEA Annex 40.
- Wang, S. W., Zhou Q., Xiao, F., 2010, A system-level fault detection and diagnosis strategy for HVAC systems involving sensor faults, *Energy and Buildings*, 42(4): 477-490.
- Xiao, F., Wang, S.W., 2009, Progress and methodologies of lifecycle commissioning of HVAC systems to enhance building sustainability, *Renewable and Sustainable Energy Reviews*, 13: 1144-1149.

Potential of passive cooling, natural ventilation and solar control in cold climates office buildings

Luca Finocchiaro^a (luca.finocchiaro@ntnu.no),

Tore Wigenstad^b (tore.wigenstad@sintef.no)

Anne Grete Hestnes^a (annegrete.hestnes@ntnu.no)

^a Department of Architectural Design, History and Technology, NTNU, 7491 Trondheim

^b Sintef Building and Infrastructure, 7465 Trondheim

ABSTRACT

The comparison between the exterior and the desired internal comfort conditions is not only fundamental to understand which strategies might be adopted in a certain climatic context but also determines the grade of complexity in the architectural design. If two different passive strategies are usually necessary in temperate climates for overheated and underheated periods, a simpler approach, aiming at maximizing the solar heat gain and minimize thermal losses during the whole year, traditionally characterizes architectural design in cold climates¹. Today the use of extremely air tight and insulating envelopes, in combination with the high internal gains due to occupancy and equipment, is not only questioning the convenience of designing compact shapes in cold climates but also determining the need of adopting strategies for natural cooling, ventilation, and solar control in such climates². Most of those strategies are commonly adopted in temperate or even hot climate contexts and, in order to work properly, require external conditions sometimes not available in cold countries. These contradictions are leading architectural design of cold climates office buildings into a new complexity.

In this study the results of an analysis conducted on the comparison between the thermal comfort zone and cold climates is presented. The impact of both climate change and technological development of new architectural components and materials on the definition of the most appropriate passive strategy was investigated. Results showed that the spontaneous thermal correction due to the heat production of internal loads has to be taken in account in the preliminary analysis of the architectural design in order to define an efficient low energy strategy.

Keywords: Climate, comfort, strategy, internal gains.

1. INTRODUCTION

The comparison between the exterior and the desired internal comfort conditions is not only fundamental to understand which strategies should be adopted in a certain climatic context but also determines the resulting grade of complexity in the architectural design. In order to ensure proper comfort conditions, a relatively simple approach, aiming at maximizing the solar heat gain and minimize thermal losses during the whole year, traditionally characterized architectural design in cold climates. Today new regulations aiming at reducing energy use in buildings are implying the use of extremely airtight and insulating envelopes. If these last ones are able to significantly reduce the heating demand, when combined with high internal loads, they might on the other hand lead to overheating problems during hot seasons. The use of cooling equipment in office buildings has for this reason become a “must” even in extremely cold climates, dramatically increasing the energy use. This is not simply

questioning the convenience of indiscriminately using such hermetic envelopes but also leading the architectural design of cold climates office buildings into a new complexity. A certain grade of uncertainty has also arisen by climate change predictions that forecast an increase in mean temperatures and precipitation within the next decades. Environmental sensitivity and adaptability to changing external conditions then becomes the most efficient way to ensure energy efficiency. Inside this scenario, which one is the real impact of climate change and technological development on the architectural design process of low energy buildings? In this study the results of an analysis conducted on the comparison between the environmental requirements of office buildings and cold climates is presented. The impact of both climate change and technological development of the skin on the architectural design in combination with different internal loads was investigated. The use of a weather analysis tool, based on monitored data, has been combined with a simulation software able to evaluate the robustness of the different variables considered in the analysis.

2. THE CLIMATE-COMFORT COMPARISON

The comparison between climate and architecture, that leads the architectural design of low energy buildings, is based on the physical dimension of the environment and has three main protagonists: the external thermal conditions – determined by the climatic factors - the environmental requirements of interior spaces and the envelope, that act as climatic moderator between the first two ones. The strategies and the consequent corrections that can be adopted play on the interaction between the first two protagonists and lead to an architectural design of the third one that should be able to create internal conditions as close as possible to the thermal comfort requirements.

The main focus of this study was the architectural design of office buildings³ and the definition and potential of the different low energy strategies that could be adopted in a specific climatic context (Oslo, 59°55'N 10°45'E). The hypothesis is that the elevated internal loads that characterize office buildings, in combination with the new regulations in force, are affecting the traditional approach for the definition of the most appropriate strategy, based on the comparison between the comfort zone and the climatic conditions. The deviations calculated inside the Psychrometric chart (reference tool for the definition of the strategy to be adopted and the quantification of its potential), assume a fundamental role in the comprehension also of the architectural implications of this shift.

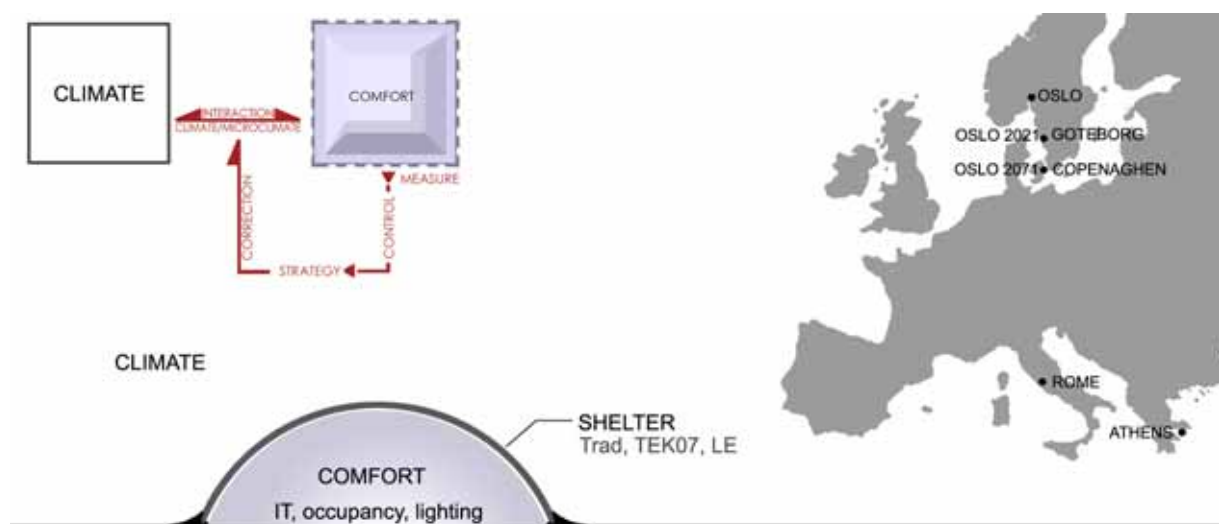


Fig. 1 – Climate, comfort and the shelter - Relation diagram. Climate change forecast.

2. CLIMATE CHANGE AND POTENTIAL OF STRATEGIES FOR COOLING AND NATURAL VENTILATION

On the basis of a study conducted by the RegClim authority in Norway, a significant increase in the mean temperature and precipitation is going to affect the country within the next decades⁴. This will be even more evident in the western coast where it might lead to hot and humid summer periods. According to this study the climate of Oslo will get close to the present Goteborg one within the next 10 years and to the Copenhagen one within the next 60 years. This shift in temperatures will extend the overheating problems over a longer period than today.

Compared to Oslo, Copenhagen is characterized by less rigid winters and a longer warm season – from May to August temperatures normally exceed the comfort zone (Fig. 2).

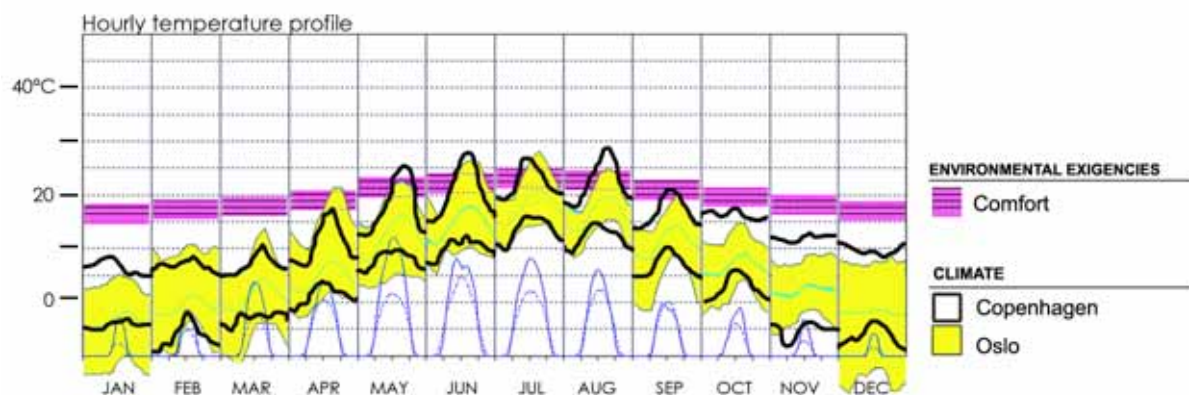


Fig. 2 – Comparison between Oslo and Copenhagen hourly temperature profiles.

This increase in temperatures, although small, would result in a significant increase in the potential of the strategies for natural ventilation and cooling in the overheated months. The effect of each system is shown as an increase in the number of hours spent within the comfort zone each month, which is defined using the monthly thermal neutrality range (Fig.3).

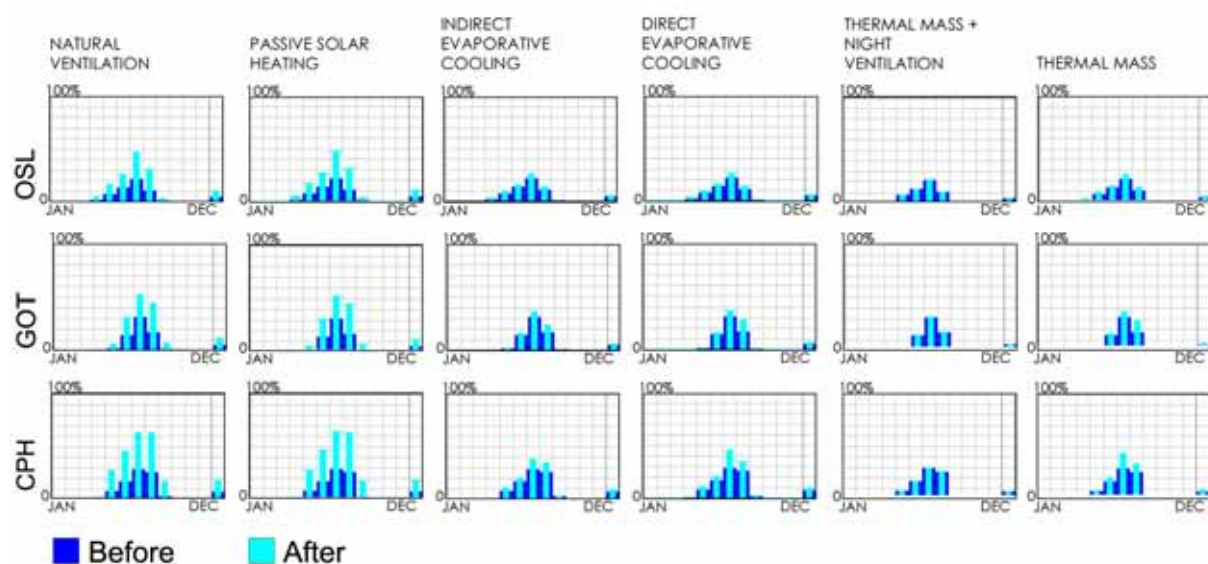


Fig.3 – Potential of low energy strategies for Oslo, Goteborg and Copenhagen.

The deviation between the comfort zone and the distribution of the climatic conditions during the year determines the number of heating and cooling degree-hours. A comparison between Oslo, Goteborg, and Copenhagen⁵ (Fig. 4) shows how the forecasted increase in temperatures would result in a significantly lower number of heating degree-hours in the colder months but not in the cooling degree-hours in the warmer ones. This means that, although strategies for cooling and natural ventilation present a higher potential, their use is not yet required for a much larger number of hours.

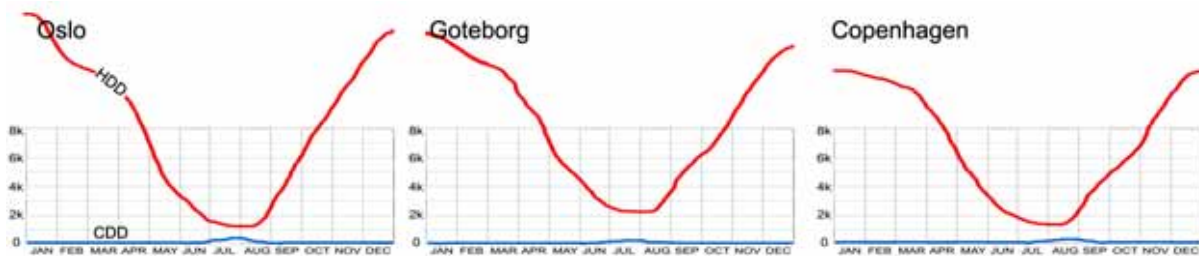


Fig 4 – Heating and Cooling degree-hours for Oslo, Goteborg and Copenhagen

The use of the psychrometric chart also suggests the same low energy strategies - passive solar heating and thermal mass for most of the months - for both Oslo and Copenhagen. The eventual increase in temperatures during the year (from OSL to CPH conditions) does not then imply a different architecture of the building but just affect, to a small extent, its environmental behaviour and efficiency (Fig. 5).

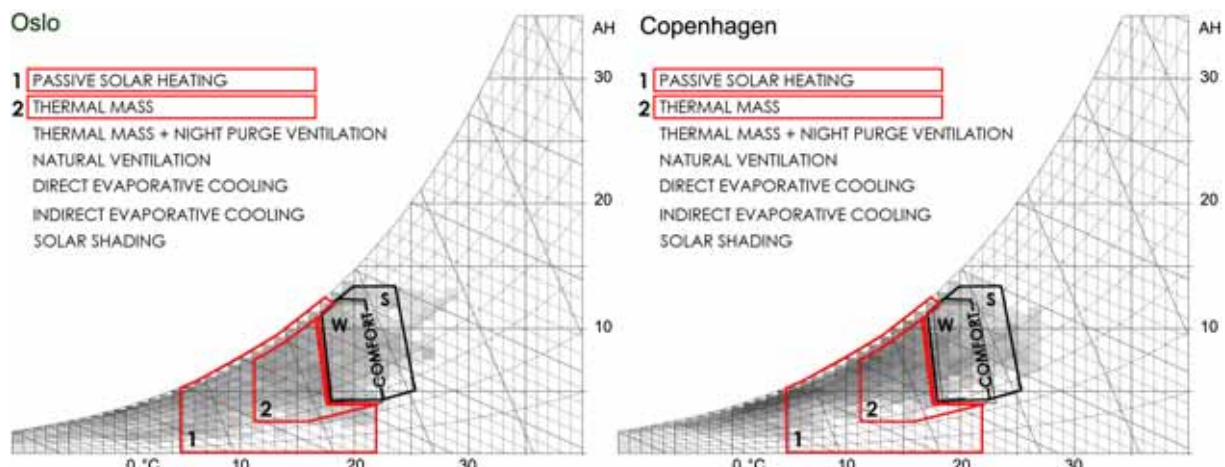


Fig.5 – Psychrometric chart analysis of Oslo and Copenhagen climates.

This result seems to clash with empirical experience about the increased need for cooling coming out from the combination of hermetically sealed envelopes and elevated internal loads. The psychrometric chart is apparently inadequate to define an efficient strategy for coping with the high internal loads of office buildings. This is clearly due to the natural tendency of this functional typology to overheat through the thermal loads produced by occupancy and technical equipment for lighting and IT. The main issue is then that of translating this natural tendency in a correction inside the psychrometric chart, quantifying the shift due to specific characteristics of the envelope and internal loads, comprehending the architectural implications.

3. METHODOLOGY

Different simulations have been performed on a virtual office building with the following characteristics⁶ (traditional systems, TEK07, LE):

Tab. 1 – Coefficients used for the simulations correspond to different standards⁷.

	Unit	Trad.syst.	TEK07	LE
U-value external wall	$W/m^2/K$	1.2	0.18	0.18
U-value roof	$W/m^2/K$	0.60	0.13	0.13
U-value floor on ground	$W/m^2/K$	0.50	0.15	0.15
U-value windows, glazed walls and roofs	$W/m^2/K$	2.4	1.2	1.2
Air-tightness	ach	3.0	1.5	0.6
Heat recovery system efficiency	-	0.7	0.7	0.85
Occupancy	$persons/m^2$	0.1	0.1	0.1
Cooling set point temperature	$^{\circ}C$	26	26	26
Heating set back temperature	$^{\circ}C$	18	18	18
Lighting load	W/m^2	8	8	8
Equipment load	W/m^2	11	11	11

All the simulations have been performed assuming the building working every day - from 8 a.m. to 8 p.m. - without any sort of HVAC system for environmental control. This has been done in order to quantify the spontaneous air temperature increase in the interior spaces.

4. RESULTS

The results, presentd in figures 6 and 7, show how the spontaneous temperature increase due to the internal gains is related to the specific characteristics of the envelope (u-value and air-tightness). Internal gains due to IT equipment and lighting have been assumed, in a first time, equal to $25 W/m^2$ ($19 W/m^2$ sensible + $6 W/m^2$ latent gain).

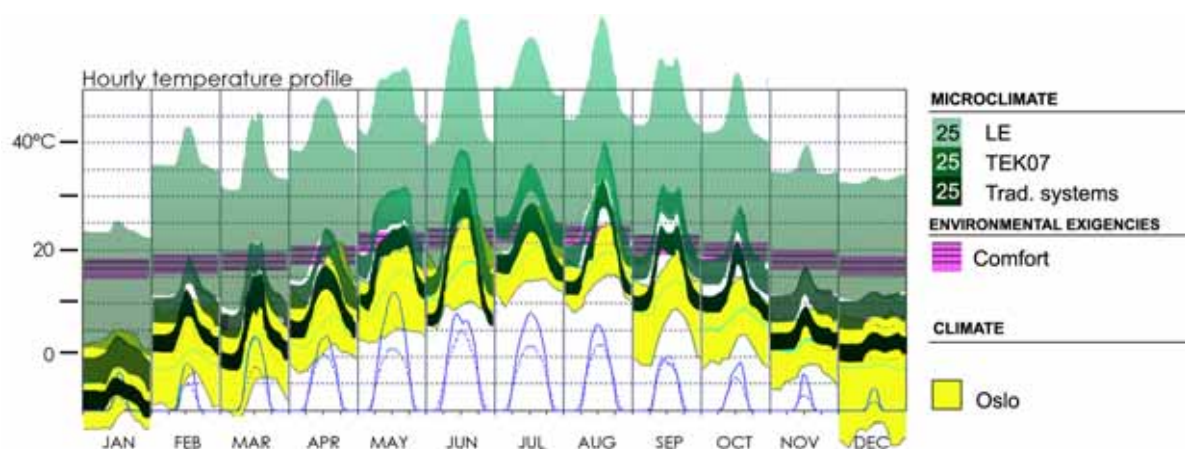


Fig. 6 – The spontaneous increase in hourly temperature profiles due to a thermal load of $25 W/m^2$ for IT equipment and lighting related to the specific characteristics of the envelope.

Then the simulations have been performed again but with much lower internal gains due to IT equipment and lighting, $14 W/m^2$, corresponding to the best practice⁸ ($12 W/m^2$ sensible + $2 W/m^2$ latent gain). Occupancy has always been assumed being $10 m^2/person$ for both groups of simulations.

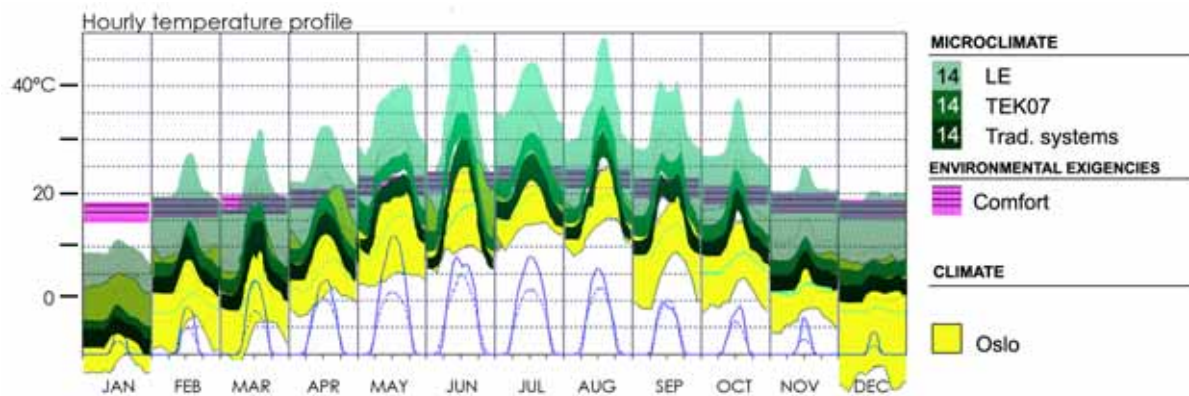


Fig. 7 – The spontaneous increase in hourly temperature profiles due to a thermal load of 14 W/m² for IT equipment and lighting related to the specific characteristics of the envelope.

Once the deviation has been calculated it have been reported inside the psychrometric chart and compared with both the external climate and the thermal comfort zone.

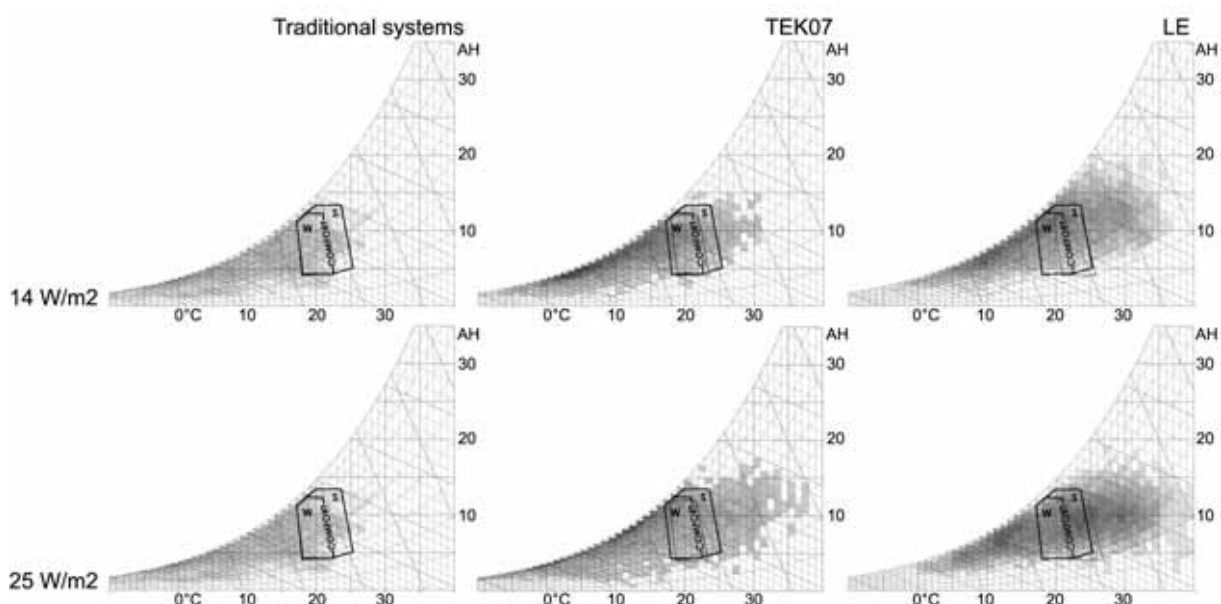


Fig. 8 – Psychrometric chart – comparison of the different deviations due to thermal load in relation to the specific characteristics of the envelope.

The results presented in fig. 8 show the microclimate that would be spontaneously generated inside a more or less airtight and insulated envelope (Traditional construction Systems, TEK07, LE) by two different internal gains (14 and 25 W/m² corresponding to best and good practice) inside an office with occupancy of 10 m²/person. The diagrams show that the thermal loads imply a thermal correction that is larger the more airtight the external envelope is. The strategy suggested by the direct climate-comfort comparison (Fig.5) would not be sufficient when respecting the regulations in force TEK07 or the even higher standard LE. These thermal corrections due to the internal loads have then to be taken into account in order to avoid overheating problems.

5. CONCLUSION

On the basis of the analysis conducted the direct comparison between the climate and the thermal comfort zone, commonly assumed as the basis for a correct bioclimatic architectural design, might suggest inefficient strategies. If the thermal comfort zone needs to be adjusted according to the activity, subjectivity and clothes, the spontaneous deviation due to the internal gains also has to be taken into account. This deviation, as seen, is strongly related to the specific characteristics of the envelope and implies a significant increase in the number of cooling degree hours in the warmer months (Fig.9).

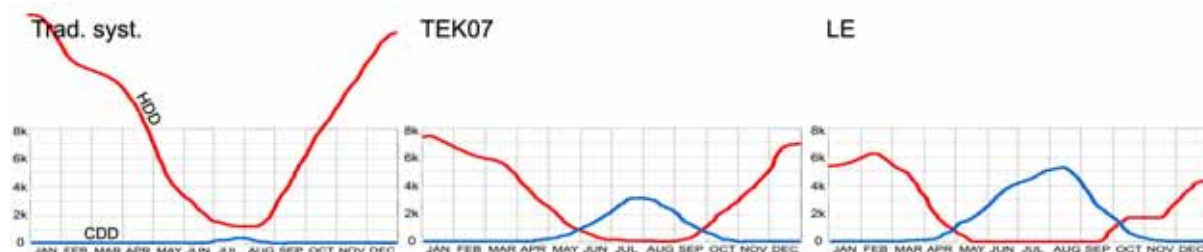


Fig.9 – Heating and cooling degree hours calculated for the thermal conditions inside the envelope.

This consequently makes even more important the use of strategies for cooling and ventilation that present a remarkably increased potential (Fig. 10).

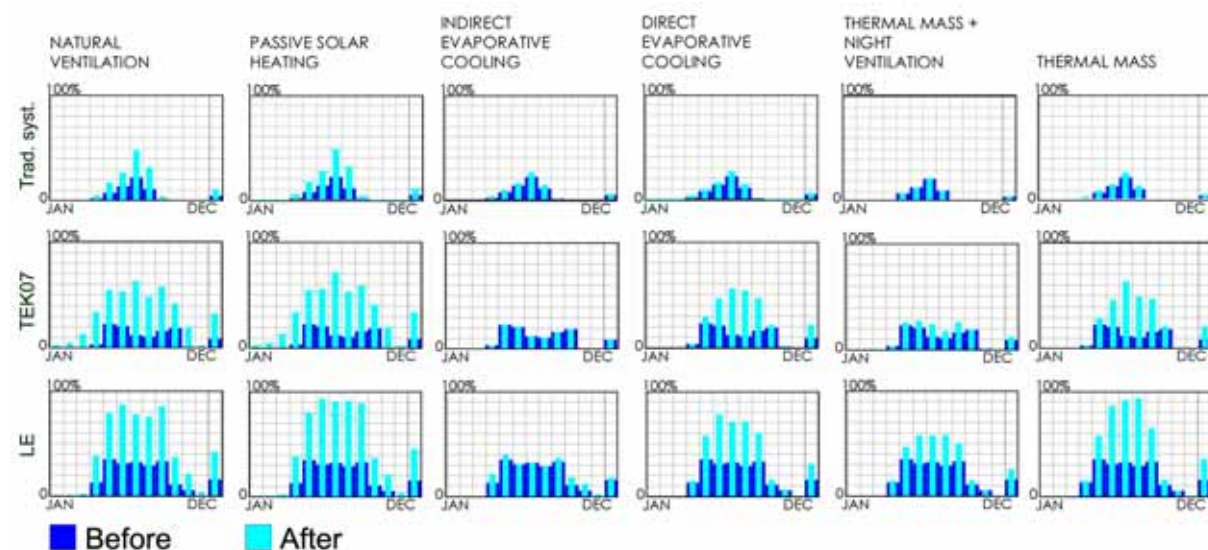


Fig.10 – Potential of low energy strategy in relation to the new thermal conditions spontaneously generated inside the envelope by the thermal loads.

6. ARCHITECTURAL IMPLICATIONS

The study conducted has implication both for the process and the product. Implications for the process pertain to the need of quantifying the potential thermal deviation coming from the internal thermal loads and include it in the preliminary climate-comfort comparison. In the case of office buildings this deviation represents a force strong enough to completely upset the whole architectural concept of the building. The increased potential of strategies for passive cooling and natural ventilation, together with the larger number of cooling degree

hours, suggest and justify a new approach in architectural design of low energy office buildings in cold climates. The permeability of the envelope, required by the use of strategies for cooling and natural ventilation, is not in contrast with the tendency of adopting even higher low energy standards and is not calling TEK07 or LE standards into question. Control of the thermal exchanges happening through the envelope is essential for reducing heating in the winter. The new fundamental requirement is, instead, environmental adaptability to changing conditions, not only of the envelope itself but of the whole architectural concept.

Most energy efficient office buildings today take advantage of the free heat produced inside the interior spaces by the thermal loads. Heat is usually used for partial heating of the outside air before letting it inside the building by means of a heat exchanger. This results in significant energy savings. But a different approach is also possible through the use of intermediate spaces that give the architecture a deeper environmental sensitivity. Flexibility and adaptability is in this case obtained translating the potential microclimate generated by the interior heat production in an intermediate space between the interior and the exterior. This type of space is usually controlled by different kinds of phenomena, like the greenhouse effect or thermal air stratification, and in most cases is possible to naturally ventilate it.

The spontaneous and free shift of temperatures due to internal gains has a large potential for heating during the colder months but it is also the reason for overheating during an extended period of the year. On a conceptual level, the microclimate generated inside the envelope by the elevated internal thermal loads will be comparable to the Rome climate in case of the adoption of TEK07 standards and to the Athens climate in case of the even higher LE standards (fig. 11 and 12).

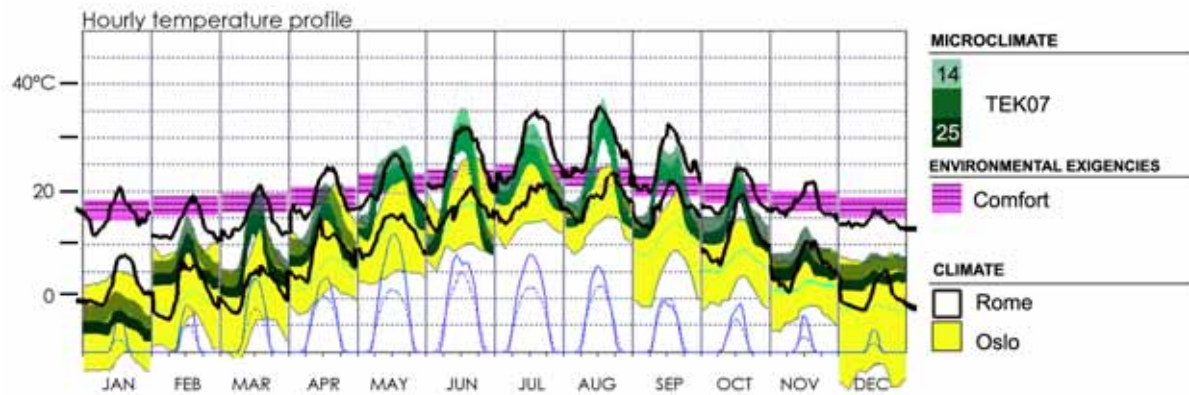


Fig. 11 - Microclimate generated inside a ventilated intermediate space - TEK07.

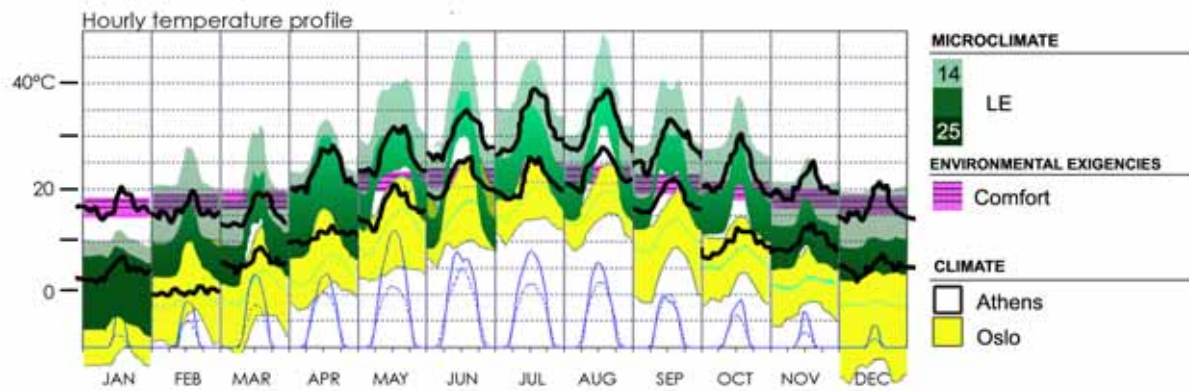


Fig. 12 - Microclimate generated inside a ventilated intermediate space – LE.

The intermediate space can have several forms: it can be as thin as a blade – double skin facades - or as thick as a livable plaza - atriums. What is more important for the definition of

the low energy strategy, is that the perimeter of the building takes possession of small fragments of exterior spaces that by passive means can have thermal conditions close to the internal comfort requirements. Intervening in the interaction between climate and architecture is now possible in two different steps (Fig. 13); firstly acting in the interface between the climate and the microclimate and secondly in the interface between the microclimatic one and the office spaces.

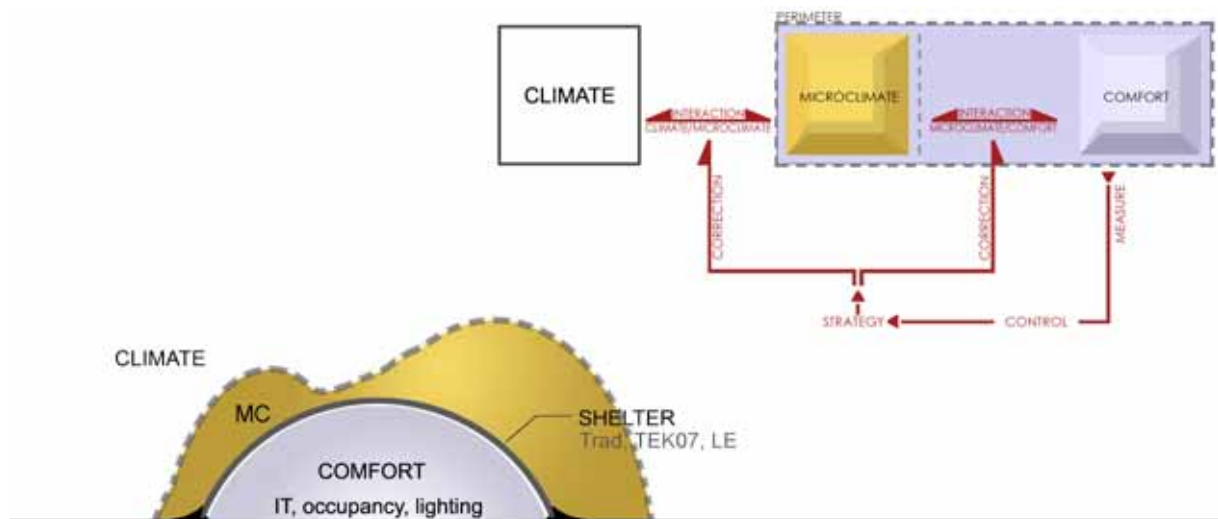


Fig. 13 – The microclimate and the in-between space. Conceptual diagram.

The microclimate generated inside the gap is usually controlled through different passive strategies, and can, given its geometrical and specific characteristics, have completely different environmental behaviours. Its thermal conditions are not simply the translation of the one spontaneously generated inside the skin but can also be controlled through different other phenomena coming from the direct dialogue with the exterior climate.

The thermal comparison is also split in two different steps. An advantage of such an approach is that, when required, the contribution of the first skin can be canceled reestablishing a microclimate equal to the exterior thermal conditions.

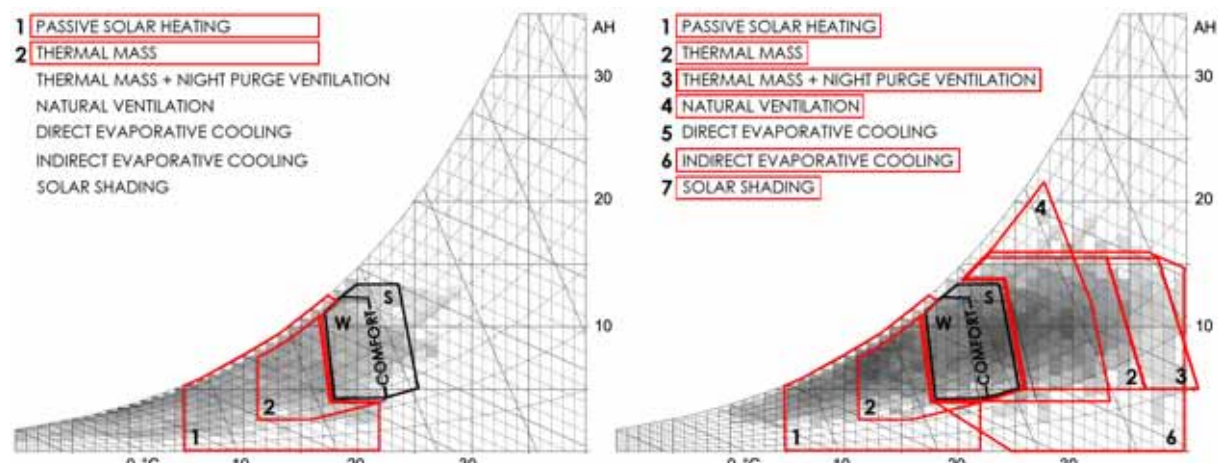


Fig. 14 – Thermal comparison between the external climate and the comfort zone on the left. Thermal comparison between the microclimate and the comfort zone on the right. The second one suggests a more appropriate strategy to cope with the internal loads.

ACKNOWLEDGEMENT

This paper has been written within the ongoing SINTEF project “LECO” on low energy commercial buildings. The authors gratefully acknowledge the Research Council of Norway.

REFERENCES

1. Olgay, V., 1963. Design with climate: bioclimatic approach to architectural regionalism. Princeton University Press, Princeton, N.J.
2. Haase M., Andersen I., The role of passive cooling strategies for Norway. The international journal of climate change. Impacts and responses. Volume 1, Number 3, Common ground publishing, 2009.
3. A.E.Kohn & P. Katz, Building type basics for office buildings, John Wiley and sons Inc., New York, 2002
4. Trond Iversen et all. RegClim. Norges Klima om 100 år. Usikkerheter og risiko. 2005.
5. Steven V Szokolay, Introduction to Architectural Science. The basis of Sustainable Design, Architectural Press, 2008
6. Haase M., Andresen I, Berit Time and Anne Grete Hestnes. Design and future of energy-efficient office buildings in Norway, Building Simulation conference (BS09), Strathclyde 2009
7. TEK, 2007. Energi – Te,aveiledning, in: Statens BygningstekniskeEtat (Ed.). Norsk Byggjenestes Forlag.
8. Marton Varga, Keep Cool. Internal heat loads, Österreichische Energiagentur – Austrian Energy Agency

A life cycle cost analysis of large-scale thermal energy storage technologies for buildings using combined heat and power

Kenneth Gaine* and Aidan Duffy*

*School of Civil and Building Services engineering,

Dublin Institute of Technology, Bolton Street, Dublin 1.

ABSTRACT

Buildings account for approximately 40% of energy consumption and greenhouse gas (GHG) emissions in developed economies, of which approximately 55% of building energy is used for heating and cooling. The reduction of building-related GHG emissions is a high international policy priority. For this reason and because there are many technical solutions for this, these policies should involve significant improvements in the uptake of small-scale energy efficient (EE) systems.

However the widespread deployment of many technologies, must overcome a number of barriers, one of which is a temporal (diurnal or seasonal) mismatch between supply and demand. Cost-effective thermal storage solutions have the potential to improve financial performance, while simultaneously reducing associated GHG emissions.

The aim of this paper is to identify existing thermal energy storage (TES) technologies and to present and assess the economic and technical performance of each for a typical large scale mixed development. Technologies identified include: Borehole Thermal Energy Storage (BTES) and Aquifer Thermal Energy Storage (ATES). A Heat transfer analyses and system simulations of a variety of BTES systems are carried out using a Finite Element Analysis package (ANSYS) and energy balance simulation software (TRNSYS) to determine the optimal system design. Financial models for each system are developed, including capital, installation, running and maintenance costs. Using this information the unit costs of energy recovered from the storage area are estimated. It was found that a deep BTES was the least economically attractive solution for daily storage and that a medium depth in the region of 50 meters was the most feasible with running costs of approximately €0.055 per kWh.

Keywords: Thermal energy storage; Combined heat and power; Life cycle cost; Borehole;

1 INTRODUCTION

A reduction in carbon emissions and lower running costs for buildings are a worldwide concern with many government policies implementing schemes to bring emissions and costs to a lower level. The development of Energy Efficient (EE) and renewable energy supply technologies are central to these policies. However, due to the intermittent and/or unreliable nature of Renewable

Energy Supply (RES), energy storage technologies will be critical to effective emissions abatement policies. One such technology is known as Thermal Energy Storage (TES). This technology solves a problem, common to most other RES systems whereby it acts as a buffer between the mismatch in supply and demand of energy.

One of the disadvantages to any EE system is that it increases the initial capital cost of the building. However by increasing the energy efficient technologies in a building, the running costs over the life of the system are expected to decrease when compared to a more conventional non EE system thus justifying a higher initial cost. Capital costs can be decreased by integrating the building design and EE system to lower the loads of the system, hence reducing the capacity of the building services system.

The aim of this paper is to assess the technical and financial performance of the most appropriate TES system technology for a large scale commercial mixed use building using CHP. Site conditions are estimated and the TES system is examined under a number of designs and loads.

2 LITERATURE REVIEW

A TES system stores thermal energy which can be used at a later time; the thermal energy may be either be in the form of heat (at a higher temperature than the surrounding environment) or as coolth (at a lower temperature). The most common types of TES are diurnal systems which are used to store heat usually during the night - so that it can be used during the day. An example of such system is a hot water cylinder in the home. This system takes one day to complete a cycle. The TES system can be designed to work on an annual or seasonal cycle also. However in order to store the energy needed to meet a seasonal load, a large volume is required. In a Seasonal Thermal Energy system (STES), waste heat from the building or, waste heat from industrial process and/or energy from solar gains during the summer are sent to the storage facility via a heat exchange system and stored there to be released in the winter. Also, after the heat is removed from the storage volume, it is now cooled and can be used for cooling during the summer. STES systems are usually underground, so that they can store the large amount of energy needed for heating or cooling for the year. These are known as Underground Thermal Energy Storage (UTES) systems.

2.1 TES Technologies

For large scale TES systems for buildings, UTES systems are preferred for a number of reasons:

- Valuable floor area is not needed;
- The ground is able to hold energy relatively constant all year round compared to other systems such as above ground tanks; and
- They are usually unobtrusive.

UTES systems can be classified into two types depending on the site conditions: Aquifer thermal energy storage (ATES); or Borehole thermal energy storage (BTES) system.

2.1.1 Aquifer Thermal Energy Storage (ATES)

An aquifer is a porous rock, clay or gravel that is usually deep below the surface, can hold or store water and allow water to be abstracted from it (Boyle 2004). An ATES system transfers heat to and from the aquifer by means of manmade wells. The system uses two wells, an injection and extraction, or hot and cold well. The heat stored in the groundwater is extracted from the aquifer through the well and passed through a heat exchanger, for use in the building. The extracted groundwater is cooled during the process and is then sent back to the aquifer via the other well. This is known as an open loop or ‘pump and dump’ system. The excess heat from the building can be stored in the aquifer for the desired time. This raises the groundwater temperature of the aquifer and hence means less energy and fuels are used in the production of the heat in the winter.(David W.Bridger and Diana M.Allen 2005). Aquifers are typically 25% water and the larger the storage area, the larger the capacity and more economical it becomes. ATES systems have been used for projects ranging in thermal power from 50kW to 10,000kW and usually store at temperatures ranging from 10 °C – 40 °C. When storing higher temperatures, thermal losses through the bedrock, the sides and the top soil become significant. For high temperature storage, above 100°C, deeper wells of over 200 meters are needed in order to reduce heat losses. This has a significant impact on the cost of the project and needs to be examined closely.

An example of an ATES system used for heating and cooling is used in Malmo, Sweden. The purpose of this system is to deliver free cooling for a district cooling system at a temperature of 6 °C. The system uses 5 warm and 5 cold wells at a depth of 70 to 80 meters. In the aquifer, cold from the nearby sea and waste cold produced from the heat pump is stored from the winter to the summer. The system was installed in 2000 and has been successful, delivering 1,300kW and a total of 3,900 MWh per year(Dincer).

2.1.2 Borehole Thermal Energy Storage (BTES)

A BTES system is a closed loop type where many closely spaced vertical boreholes are placed usually 50-200 meters below the ground. The storage medium in this method is the ground itself, as opposed to the aquifer where it uses the flowing groundwater. A single U-Shape pipe in each borehole is installed in the ground and a fluid is pumped through the pipe to absorb or realise its energy to/from the ground. The pipes act as a large heat exchanger with the earth. (Pahud 2002). By having numerous boreholes over a large area, significant thermal energy storage is possible, however when one borehole is used, it is only suitable for heating or cooling on a small scale. Once the borehole is complete and the pipe is installed, the hole is then backfilled with a suitable high thermal conductivity grouting material such as water, sand or clay. This helps the heat transfer between the pipe and the earth.

The desirable ground characteristics for BTES are:

- a high specific heat and thermal conductivity value; and
- a low ground water flow rate

An example of a BTES is used for a district heating and cooling system in Canada. The Drake landing borehole field uses 144 boreholes of 150mm in diameter and 35 meters deep where installed as part of a district heating and cooling system. This BTES system is used to store heat at temperatures of up to 80°C from solar(Bernier 2009).

3 METHODOLOGY

The uptake in EE systems are often hampered by a high capital cost but offer the user the potential of lower operating costs. To show whether these lower operating costs offset the high upfront costs sufficiently to make storage cost-competitive with conventional generation, a life cycle cost analysis is undertaken. A thermal energy model was established to identify the associated costs. Many different technologies have been identified and a BTES system used to store waste heat from a CHP machine on a daily basis has been chosen initially. Further work is being carried out on other designs. The model comprised of two parts: the first to determine the heat transfer rate to the storage area under specific site conditions; and the second to simulate the thermal storage model over a number of years. The results from these tests were used to build a financial model showing the capital needed and estimate the running costs of each system.

3.1 Operating conditions/building services design

Large scale-mixed developments often have a simultaneous heating and cooling load as well as a 24hr electrical load. For the purposes of this study, it is assumed that this electrical load is met by CHP. During day-time operation of the system, waste heat from the CHP is used to power an absorption chiller to provide the cooling load directly to the building via a ‘chilled beam’ circuit (despite its name, this is used for both heating and cooling). During the night, waste heat is sent to the BTES area and a heat pump is used to control the temperature and compensate for losses. Operating conditions were obtained from case studies presented by (Gao 2008) and Pre-design guide (Hellstrom 2004). A building integrated CHP cooling circuit typically works on a 90°C/70°C circuit. The outlet 90°C water from the CHP is sent to the storage area every night from 8PM until the 8AM the following morning. This heat raises the ground temperature where it can be recovered on a daily or seasonal basis for heating. This model focuses on a daily storage design. The heating is met by using a ‘chilled beam’ circuit which operates at on a 40°C/60°C. Cool water enters the BTES system at a temperature of 40°C during the day where it absorbs the energy that was sent there the night previously by the CHP. The water returns close to 60°C to be used in the heating circuit. The heat pump is used to raise the temperature to the 60°C needed.

3.2 Numerical analyses

The first analysis determined the average heat transfer rate using a FEA (Finite Element Analysis) package ANSYS.(Lee and Lam 2008) have presented a number of FEA models specifically tailored to BTES systems and these have been adopted in this methodology. A single borehole with a single U-tube pipe was modeled using three dimensional implicit finite difference method under the site conditions and using operating conditions from design guides. Figures 1 and 2 below are images of the FEA model. Figure 1 is a close up view of the inlet and outlet from the borehole pipe and Figure 2 shows the entire mesh of the borehole. The soil conditions used in the analysis are shown in Table 1. Case studies (Paksoy 2007) show that the average depth used in BTES range from 20 to 250 meters. Three models were made using borehole depths of 20, 50 and 200 meters. Three Dimensional (3D) grids measuring 5 meters by 5 meters were made with single borehole drilled in the centre to the required depth. Depths of 30, 70 and 220 metres were modelled - the additional space below the borehole was allowed to model heat flow downwards from the pipe. Specific inlet temperatures and flow rates shown in Table 1 were inputted into the analyses to simulate a 14 hour period. This is the night time charging period of when the waste heat is available. The outlet temperature and average soil temperature were recorded. The analysis estimated the heat transfer rate to the storage volume under the site conditions. Details of the analysis are shown in Table 1.

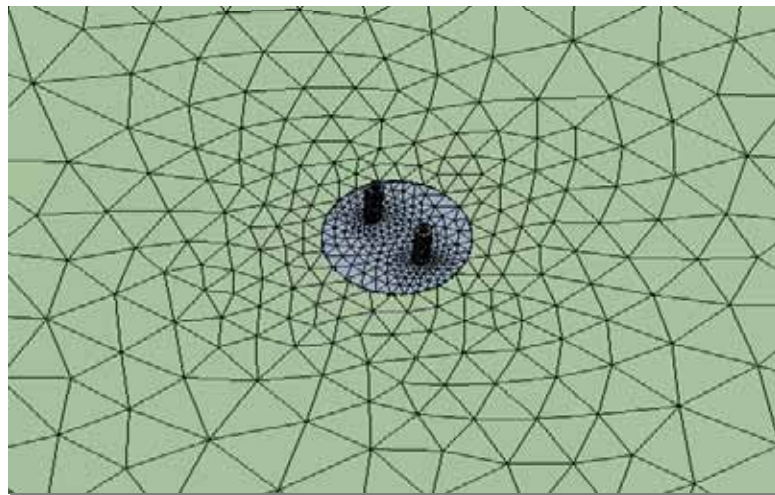


Figure 1: Close up view of the inlet and outlet of the borehole pipe

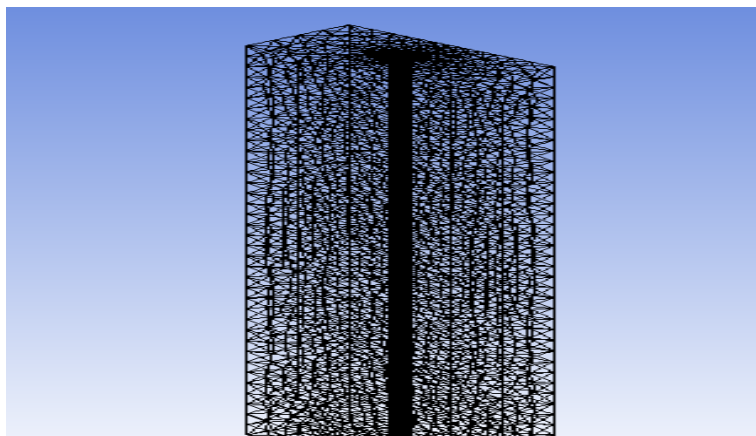


Figure 2: Total view of FEA Mesh

3.3 Thermal energy balance

A second simulation was carried out for a number of different borehole quantities, depths, capacities and times. This was undertaken using the Duct Storage Model (DST) on TRNSYS version 16 as recommended in the Pre-Design Guide for Thermal Energy Storage (Hellstrom 2004). This is a transient simulation package which has been developed over the last 35 years and has been presented in the Pre-Design Guide for Thermal Energy Storage. Flow rates and temperatures entering the system are assumed constant. The model is used to show the outlet temperature of the borehole field and the average ground temperature. Initial conditions of the ground are shown in Table 1 and the following assumptions were made:

- The Soil mixture within the TES area is homogeneous and isotropic;

- The Specific heat and thermal conductivity of the storage medium are constant; and
- Groundwater flow is neglected

Each system was modeled in 1,000kWh increments of storing 1,000 kWh to 10,000kWh under the same operating conditions. The numbers of boreholes needed to store the given quantities of energy were determined numerically based on the average heat transfer rate from the results of the FEA analyses above.

Table 1: Analyses settings

Parameters	Values	Parameters	Values
Borehole diameter	0.08m	Average Heat transfer rate	109 wm^{-2}
Outer radius of Pipe	0.03m	Soil temperature end of year 1	59.75°C
Inner radius of Pipe	0.025m	Soil temperature end of year 5	61.2°C
Inlet temperature - charging	90°C	Soil temperature end of year 10	61.3°C
Inlet temperature – discharging	40°C	Soil temperature end of year 20	61.3°C
Inlet flow rate	0.3 $\text{m}^{-3}\text{hr}^{-1}$	Outlet temperature charging	57.3°C
Storage volume	Various	Outlet temperature discharging	54.2°C
Time period	14 hours	Soil Thermal Conductivity	1.8W $\text{m}^{-1}\text{K}^{-1}$
Time step	0.02s	Soil Density	1600 kg m^{-3}
		Soil Specific Heat Capacity	2200 J $\text{kg}^{-1}\text{K}^{-1}$
Convergence - max/min iterations	100 / 20	Node qty	220,000

3.4 Financial model

A Life cycle cost (LCC) analyses of a project is used to determine if future operational savings will justify the initial capital costs.(Kneifel 2009). The capital and operating costs of a number of different BTES systems were therefore estimated for a large-scale mixed development, cash flows estimated and net present values (NPV) determined. Costing data was gathered from Irish boring and groundwork contractors for the installation.

3.4.1 Capital costs:

These are costs that are incurred at the initial stages of the project. They are the highest and biggest barrier to almost any EE system. For a BTES the capital costs include some of the following:

- Site investigation and testing;
- Design;
- Site preparation and set up;
- Drilling;
- Pipe work installation;
- Backfilling the borehole;
- Header and piping to energy supply centre; and
- Commissioning.

The total of these add up to give the capital costs associated with the BTES system. Industry quotations, rates and estimates were obtained and were applied to each system analysed. Piping from the borehole headers to the energy centre has been accounted for based on an average pipe length of 75 meters.

3.4.2 Running costs.

These are the costs that are associated with the day to day operation of the plant. For the BTES system, electrical energy is needed for pumping power to deliver and recover energy from the storage area. The pumping power required was calculated by obtaining the total equivalent length of pipe and calculated the pressure drops in each system(Douglas). An average industrial tariff for electricity of €0.12 per kWh in Ireland has been used to calculate the total running costs for the pumps. The fixed costs for maintaining the system include repairs, cleaning and controls. The controls of these systems are the highest cost associated with maintenance as they can chance on a daily basis.

4 RESULTS AND DISCUSSION

The thermal energy model was simulated for different system configurations. It was observed that the average ground temperature rises from an initial value of 12°C to approximately 60°C after 18 months of operation for the 20 and 50 meter system. The ground temperature using deeper 200 meter system had risen to approximately 55°C. The outlet temperature from the day time operation was raised to approximately 60°C in the shallow systems. Additional heating was required for the deep system. From using the waste heat available, nearly 100% of the daily heating load was achieved. Based on a 20 year life span, the heating load can be achieved for approximately €0.055 per kWh.

4.1 Thermal energy balance results

Figure 3 shows the outlet temperature in red from the borehole field and the average soil temperature over a 20 year period in blue. The outlet temperature ranges from 57°C to 63°C daily as the inlet temperature changes from the 90°C input from the waste heat output from the CHP to 40C input from the chilled beam heating circuit.

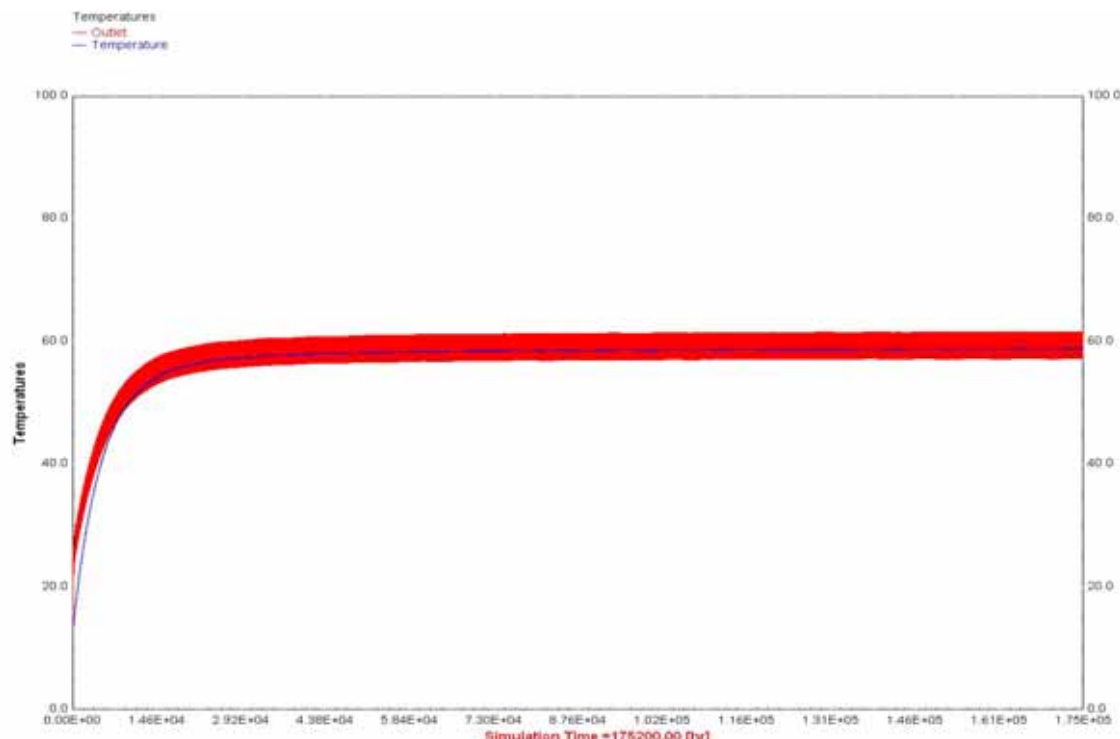


Figure 3: 20 year operation of 100no. 20 meter boreholes

Figure 4 and 5 shows the ground temperature and the outlet temperature of the 200 and 50 meter deep borehole configuration. It can be seen that the ground temperature has not risen to the 60°C needed for the heating circuit in the 200 meter system. Additional ‘top up’ boilers are therefore required resulting in extra heating costs. The shallow (20m) and medium (50m) systems display similar results.

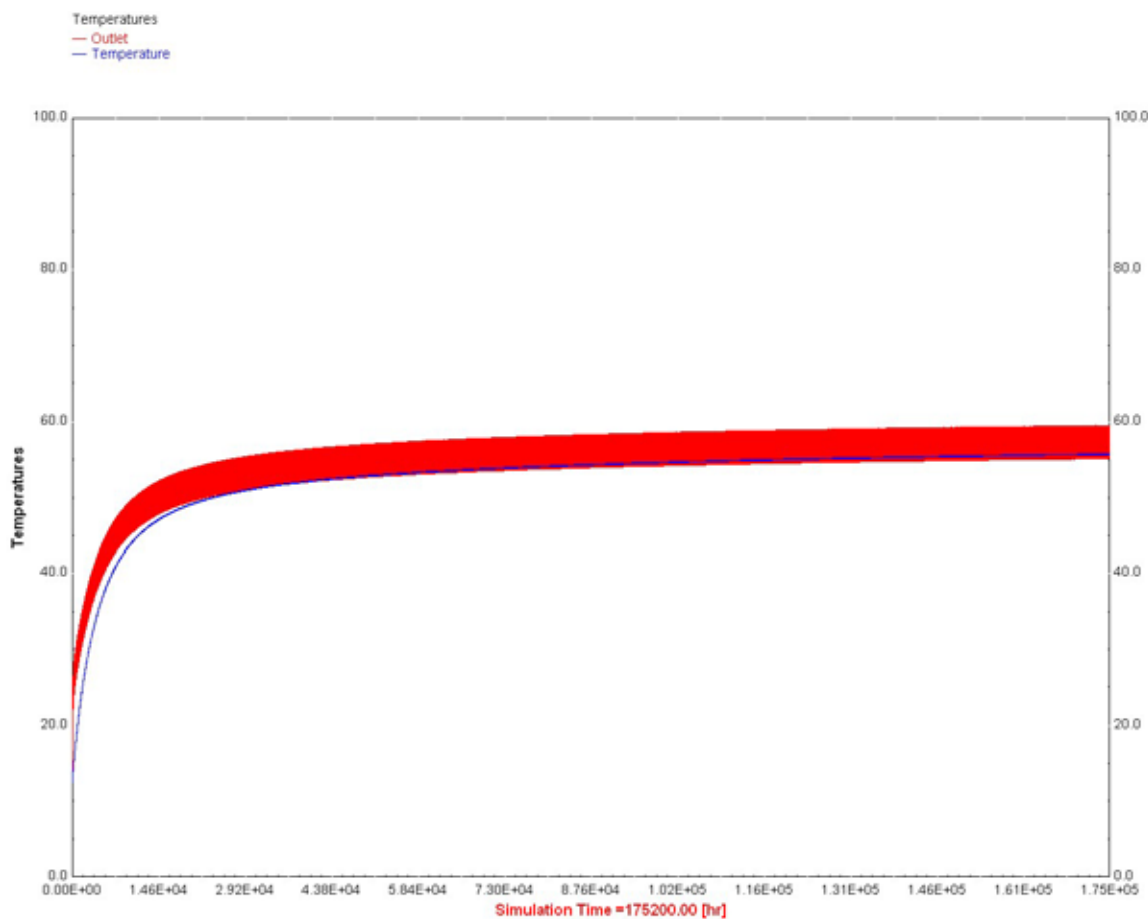


Figure 4: 20 year operation of 10no. 200 meter deep boreholes

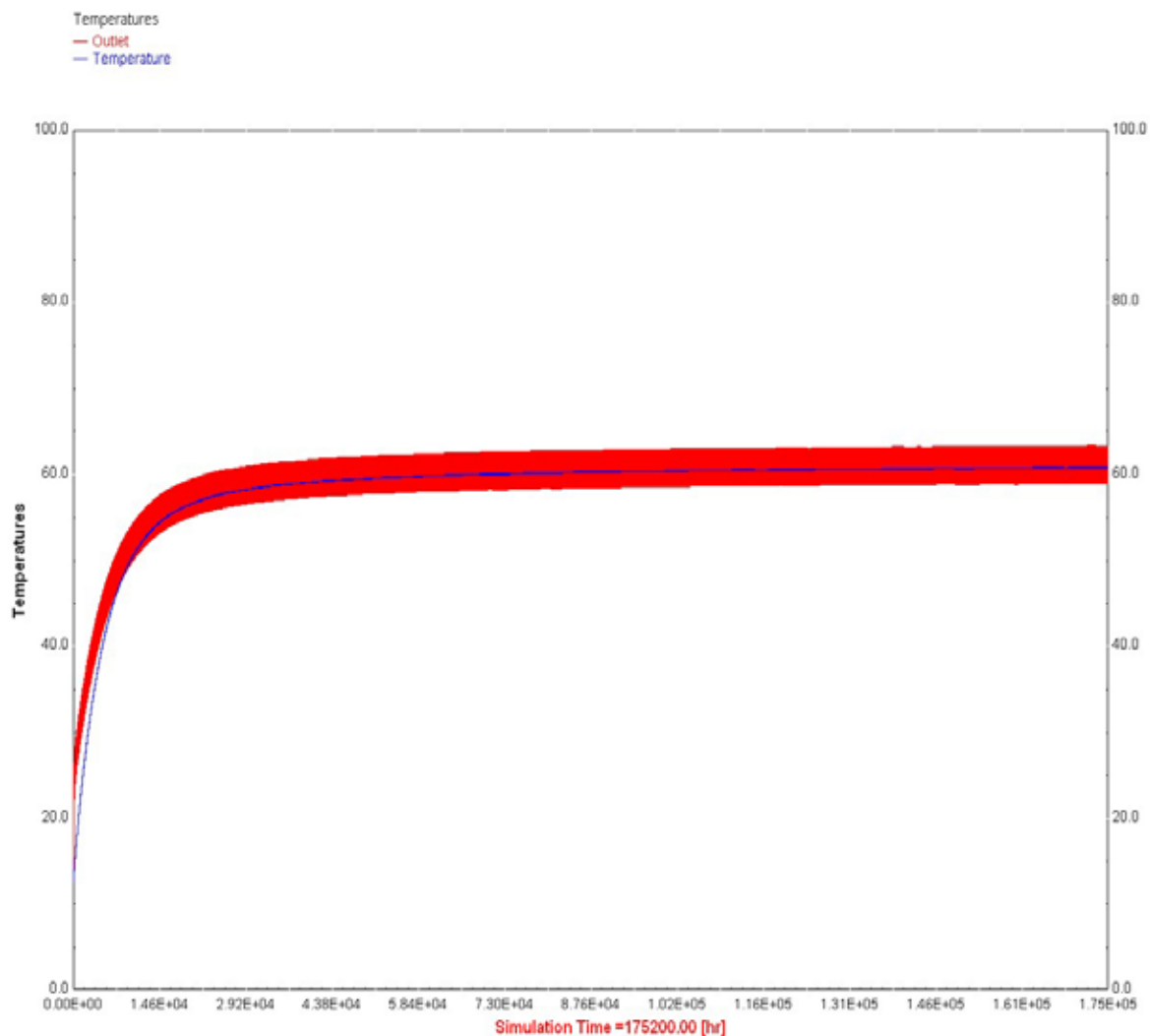


Figure 5: 20 year operation of 40no. 50 meter deep boreholes

4.2 LCC costs

Figure 6 is showing three different cost curves (€/kWh of stored energy) recovered from the storage area. It shows that for low quantities of energy stored, deep borehole systems are considerably more expensive than shallow systems. This is due to its thermal performance: it is not able to reach the needed ground temperature resulting in additional heating costs. But, above 4,000kWh, 200 meter becomes preferable than the shallow system. Due to economies of scale, the capital costs are a higher percentage of the LCC for smaller size systems. This can be seen in figure 6 as the curve increases in cost as the quantity of energy stored decrease.

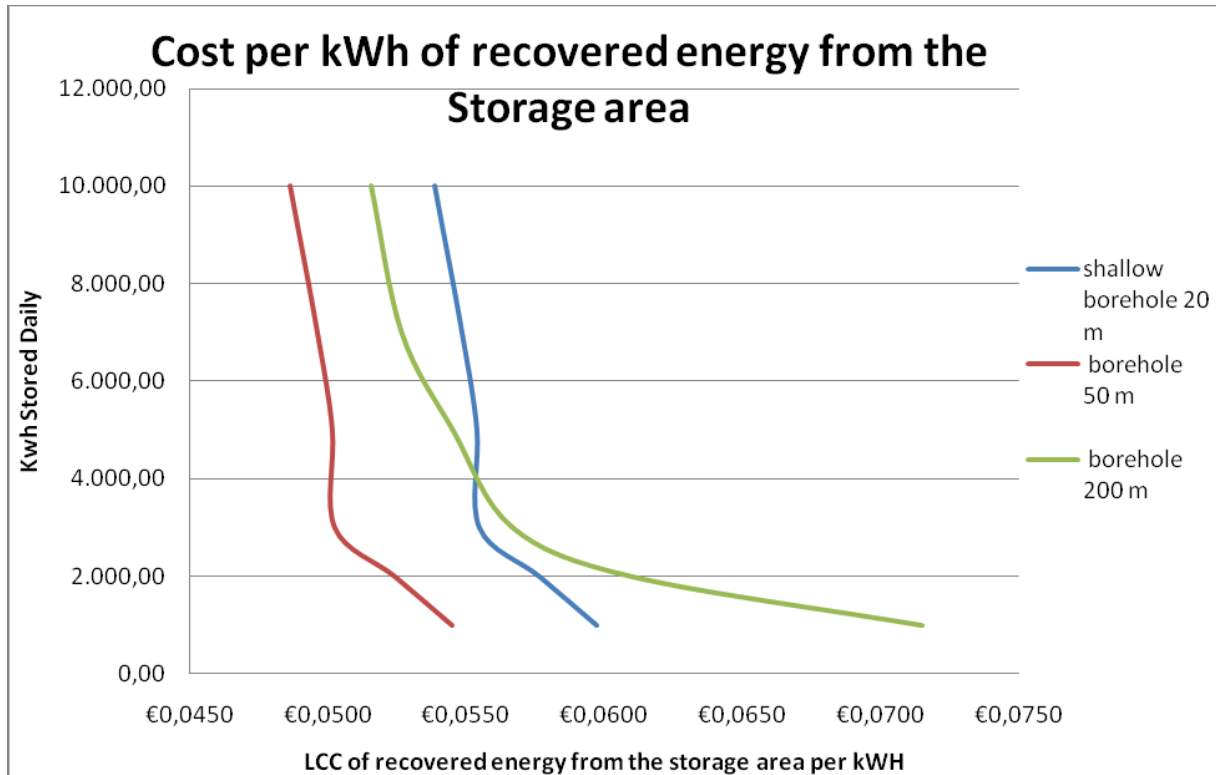


Figure 6: LCC of 20 year period per kWh of recovered energy from the storage area

5 CONCLUSION

Three different configurations of a BTES system have been examined to determine the LCC of recovering stored energy. Initial findings show that the deep BTES system has the highest LCC for small systems and becomes more favorable when storing large amounts. This was due to higher losses, a lower rate of heat transfer which resulted in additional costs to further raise water temperature. The medium system had the lowest LCC in all cases. The shallow system had higher installation costs mainly due to more pipe work installation to and from the energy centre and a larger ground area required.

This paper deals with various arrangements of the BTES system. Further analysis is being carried out to include ATES and energy piles. In addition to the extra systems, a seasonal analysis is being carried out on all systems. Worldwide costing data is also being gathered.

6 REFERENCES

- Bernier, S. C. a. M. (2009). "Seasonal Storage of solar Energy In Borehole Heat Exchangers." Building Simulation.
- Boyle, G. (2004). "Renewable Energy: Power for a sustainable Future." second edition: 351.
- David W.Bridger and Diana M.Allen, P. D. (2005). "Designing Aquifer Thermal Energy Storage Systems."

- Dincer, i. "Thermal Energy storage systems and applications." p414.
- Douglas, J. F. "Fluid Mechanics." (Fifth Edition): 856-857.
- Gao, e. a. (2008). "Thermal performance and ground temperature of vertical pile-foundation heat exchangers: A case study." *Applied Thermal Engineering* 28(17-18): 2295-2304.
- Hellstrom, T. S. G. (2004). "Pre Design Guide for Ground Source cooling systems with energy storage." EU Commission SAVE programme & Nordic Energy Research.
- Kneifel, J. (2009). "Life-cycle carbon and cost analysis of energy efficiency measures in new commercial buildings." *Energy and Buildings* 42(3): 333-340.
- Lee, C. K. and H. N. Lam (2008). "Computer simulation of borehole ground heat exchangers for geothermal heat pump systems." *Renewable Energy* 33(6): 1286-1296.
- Pahud, D. (2002). "Ground heat storage." 66/133.
- Paksoy, H. O. (2007). "Thermal Energy Storage for sustainable energy consumption: fundamentals, case studies and designs." 155.

Nanoelectrochromics with Applied Materials and Methodologies

Tao Gao^{a,*}, Arild Gustavsen,^a and Bjørn Petter Jelle^{b,c}

^a Department of Architectural Design, History and Technology, Norwegian University of Science and Technology (NTNU), Trondheim, Norway.

^b Department of Materials and Structures, SINTEF Building and Infrastructure, Trondheim, Norway.

^c Department of Civil and Transport Engineering, Norwegian University of Science and Technology (NTNU), Trondheim, Norway.

* Corresponding author: E-mail: tao.gao@ntnu.no

ABSTRACT

Electrochromic (EC) materials that change their optical transmittance under an external electrical field may form the basis of “smart windows”, which are of great interest in forthcoming building technologies. Nanostructured EC materials or assemblies have revealed remarkable improvement on colouration efficiency and switching time due to their small featured sizes and large surface areas. Here, the recent progress of nanoelectrochromics is reviewed; the scientific and technical issues related to material preparation and device assembly for large-area and large-scale window applications are discussed.

Keywords: Nanoelectrochromics, Electrochromism, Nanomaterials, Smart Windows

1. INTRODUCTION

Over the past two decades there has been a dramatic increase in dynamic glazing technologies (i.e. smart windows) for architectural and automotive applications (Lampert 1998, Granqvist 2008). The primary advantage of smart windows is their capability to control radiant energy (both light and heat) transfer through the window aperture, providing opportunities to maximize building energy efficiency by reducing a certain amount of heating, cooling, and lighting loads.

A smart window is in principle an optical switching device integrated in or attached to a window glazing and offers adjustable control of radiant energy (Lampert 1984). Apparently, the key to smart windows is a material/system that can change reversibly its optical properties (transmission, reflection, etc) in a controllable way. Electrochromic (EC) materials that exhibit a persistent and reversible colour change induced by an externally applied electric field have attracted great attention (Granqvist 2008). EC materials have several distinguished advantages when considering window glazing applications: (1) they only require a small voltage (typically 1–3V) during/for switching; (2) they exhibit good open circuit memory in either bleached or coloured state, and (3) they can respond in a controllable way to the ambient environment. Moreover, EC smart windows can incorporate other window innovations such as low-E coating, gas-filling, and vacuum insulation to achieve the ultimate energy efficiency (Deb *et al.* 2001).

It is not surprising that EC smart windows are experiencing a pronounced market pull (Beatens *et al.* 2010); though relatively few products are yet commercially available. Most EC smart windows on the market are still rather small in size compared to most glazing requirements and are relatively expensive. Increasing the size and reducing the cost but not sacrificing too much

the performance are difficult and involve a combination of many different research areas which are all interdependent.

Thanks to the rapid development of nanotechnology, the possibility of designing advanced EC devices by using nanostructured EC materials or nanoassemblies (denoted hereafter as nanoelectrochromics) has attracted great attention. It has been demonstrated that the application of nanoelectrochromics can lead to high colouration efficiency, high colour contrast, and fast switching (Vidotti and Cordoba de Torresi 2008). However, only minor attention has been paid to large-scale window applications. For many EC nanomaterials, even the most popular WO_3 -based systems, insufficient data are available for a conclusive evaluation. In this paper, we review recent progresses on nanoelectrochromics, in particular those involving transition metal oxides. A number of excellent review articles highlighting the EC materials and smart window technology have been reported so far, though few of them specially emphasize the challenge and opportunity of nanoelectrochromics for large-area and large-scale window applications (Vidotti and Cordoba de Torresi 2008).

2. NANOELECTROCHROMICS

Electrochromism has been demonstrated in a number of compounds, both inorganic and organic materials (Granqvist 1995, Monk *et al.* 2007). The most studied inorganic EC materials appear to be mixed-valence transition metal oxides (e.g., WO_3 , MoO_3 , Nb_2O_5 , V_2O_5 , TiO_2 , and NiO); the most popular organic materials showing electrochromism include viologens, pyridines, conductive organic polymers, and some organometallic compounds. Within each class, there are differences in morphology, crystal structure, degree of order, and stoichiometry for each EC compound. There are also differences in device configurations and whether a solid or liquid ion conductor is used.

Figure 1 illustrates schematically the most studied EC smart window architecture. The optical switching part consists of some five functional components: two transparent electrical conductor layers to inject charge, an active EC layer, an electrolyte, and an ion storage layer, which may in some cases be another EC layer. This sandwich configuration allows a reversible electrochemical reaction to cycle between the EC layer and the ion storage media, with simultaneous injection of electrons/holes and cations/anions. The overall transparency of the EC layer is changed due to the formation of colour centers (or defect complexes) or to an electrochemical reaction that produces a coloured compound; a voltage pulse with opposite polarity makes the device regain its original properties. Taking the most popular WO_3 material as an example, the involved electrochromism can briefly be interpreted in terms of a double-charge-injection model that describes the formation of tungsten bronze (M_xWO_3) as a consequence of injection of electrons and positively charged ions ($\text{M} = \text{H}^+$, Li^+ , Na^+ , etc.) into the transparent WO_3 (Bange 1999):

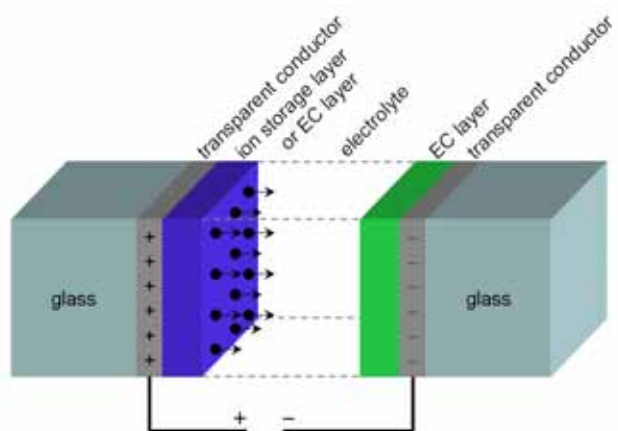
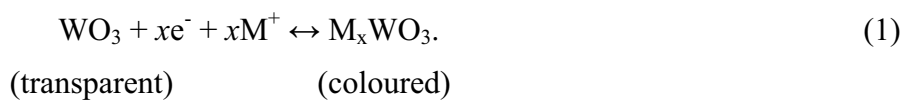


Figure 1 Architecture of an EC smart window, showing the transport of cations under an external electrical field.

62



The ion insertion is limited both by the diffusion coefficient and by the length of the diffusion path: the former depends primarily on the chemical structure and crystal structure of the material; while the latter is determined by material microstructures (Lee *et al.* 2005). In case of nanomaterials, the diffusion path length is represented by the smallest dimension of the particles. Thus, designing a nanomaterial with the proper composition and crystal structure is important to achieve fast kinetics. However, one must also consider the surface phenomenon as the particle size decreases, such as surface defects, stability and reactivity, which also affect the overall performance.

Table 1 Electrochromic properties of some WO_3 nanomaterials

shape ^a	size (nm)	electrochromic property			reference
		insertion ion	switching time (s) colouring/bleaching	colouration efficiency (cm ² C ⁻¹)	
NPs	10–20	H ⁺ / aq.	- ^b	42	Lee <i>et al.</i> 2005
NRs	D: ^c 3 L: ^d ~ 50	H ⁺ / aq.	6.4 / 3.0	132	Park <i>et al.</i> 2009
NRs	D: ~ 100 L: ~ 2 μm	H ⁺ / aq.	25 / 18	37.6	Wang <i>et al.</i> 2009
NWs	D: 30–70 L: ~ 5 μm	Li ⁺ / aq.	3.0 / 1.5	61.3	Liao <i>et al.</i> 2007
NWs	D: ~ 7 L: ~ 800	H ⁺ / aq.	-	47.5	Yoo <i>et al.</i> 2008
MWs	D: ~ 60 L: tens of micron	H ⁺ / aq.	4.2 / 1.0	56	Shim <i>et al.</i> 2009
MPs	pore: 5–10	Li ⁺ / aq.	3 / 2	70	Deepa <i>et al.</i> 2006
MPs	pore: 12–13	Li ⁺ / aq.	~ 30	~ 26	Sallard <i>et al.</i> 2007

^a: NPs = nanoparticles, NRs = nanorods, NWs = nanowires, MPs = mesoporous.

^b: data not available.

^c: D ≡ diameter

d. L = length

2.1 Electrochromic Nanomaterials

A number of EC nanomaterials have been reported in literature. As mentioned before, WO_3 represents probably the most widely studied compound (Deb 2008). Table 1 reports some of the recent progress on WO_3 nanomaterials. In general, the EC performance may be improved by nanotechnology, though an improved understanding of the thermodynamics and kinetics of

electrochromism at nanometer scale is still necessary. Other transition metal oxide nanomaterials showing interesting EC properties include MoO_3 , Nb_2O_5 , V_2O_5 , TiO_2 , NiO , and so on, which follow similar principles as those for the WO_3 -based materials.

Normally, crystalline WO_3 films exhibit good structural stability but poor electrochromism, while the best EC performance is usually obtained in amorphous films with poor stability. Note that the amorphous and crystalline WO_3 films are solar absorbing and reflecting films, respectively. Lee *et al.* (2005) reported an interesting approach to combine the EC performance and cycling stability by using WO_3 nanomaterials. They prepared WO_3 nanoparticle films with high porosity by electrophoresis. By comparing EC properties of the WO_3 nanoparticle films with those of the amorphous and crystalline ones, they concluded that WO_3 nanoparticles enabled a higher charge insertion density, indicating faster kinetics. For example, the cathodic charge spent for WO_3 nanoparticles was about $32 \text{ mC cm}^{-2} \text{ mg}^{-1}$, compared with *ca.* $3 \text{ mC cm}^{-2} \text{ mg}^{-1}$ and $9 \text{ mC cm}^{-2} \text{ mg}^{-1}$ for crystalline and amorphous WO_3 films, respectively. Such improvement can be attributed to large active surface area and low density of the nanoparticle films, which provide direct and sufficient contact between electrolyte and electrodes. The WO_3 nanoparticle films showed also excellent cycling stability, probably due to the improved crystallinity. For example, the WO_3 nanoparticle films had no obvious changes over 3000 cycles in acidic electrolyte, whereas the amorphous WO_3 films degraded significantly after only 500 cycles, as shown in Figure 2.

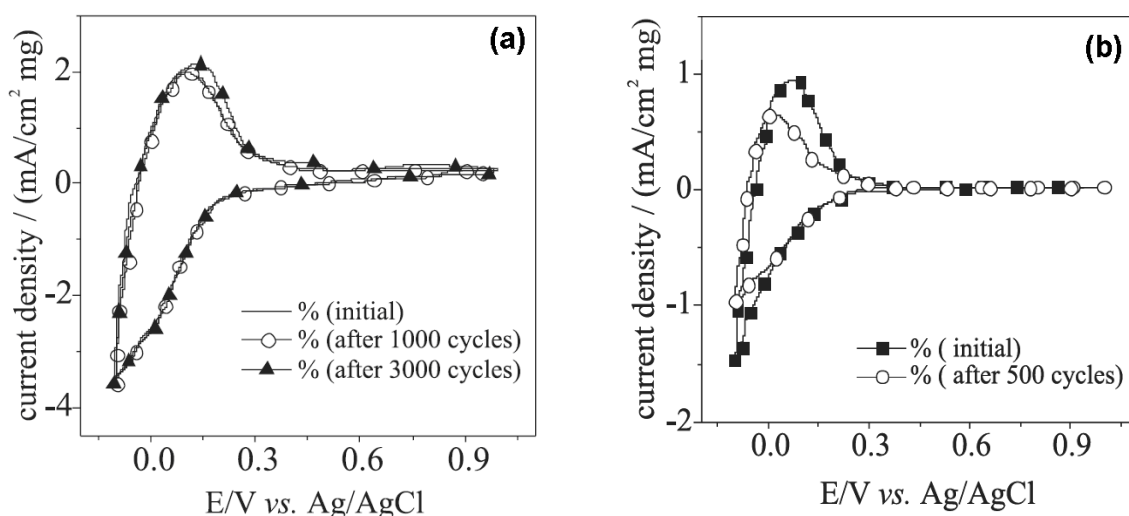


Figure 2 Cyclic voltammograms of (a) nanoparticle WO_3 films and (b) amorphous WO_3 films after a single cycle (initial) and after different cycles in 1 M H_2SO_4 . Reproduced from Lee *et al.* (2005).

Park *et al.* (2009) reported EC performance of WO_3 nanorod-based films and found a highly improved response time. The initial WO_3 nanorod film (12 wt%; rod diameter $\sim 3 \text{ nm}$) had a typical colouring and bleaching time of about 6.4 s and 3.0 s, respectively, which were significantly prolonged as the WO_3 particle size increased. For example, the crystalline WO_3 films (particle size: $61 \pm 11 \text{ nm}$) had a typical response time of about 159 s and 1267 s for colouring and bleaching, respectively. It is known that the response time of an EC material is dependent on the length of the diffusion path and the diffusion coefficient of anions or cations; therefore the size control of the EC materials is very critical to achieve fast response times.

It is worth pointing out that the primary interest in nanoelectrochromics is still for exploration of new EC nanomaterials and systems, so they are in principle case studies. More efforts towards thermodynamic and kinetic details of nanoelectrochromics are still important and necessary.

2.2 Nanoparticle-Incorporated Electrochromic Materials

An ideal EC material should have high conductivity, both ionic and electronic (Bange 1999), which is unfortunately not the case for many transition metal oxides. For example, WO_3 has relatively high electrical resistance, which usually results in nonuniform potential distribution when an external voltage is applied across it, leading to nonuniform colouration (Shen *et al.* 1991). Doping represents probably the most promising method to improve the electrical conductivity of transition metal oxides; though selecting the right dopants remains difficult.

Alternatively, metallic nanoparticle modified EC materials have been widely studied. Haranahalli and Holloway (1981) studied the influence of metal overlayers on EC performance of WO_3 films. They found that the resistance effects in WO_3 were reduced by the metallic overlayers; consequently, the colouration and bleaching rate and the proton transfer rate at the WO_3 -electrolyte interface were greatly increased. This technology has been followed by subsequent researches, where the metallic overlayers have been replaced by, in some cases, noble metal nanoparticles such as Ag, Au, and Pt. For example, He *et al.* (2001a) found that the addition of Au nanoparticle overlayers on a WO_3 thin film resulted in an increased film conductivity and a better EC performance in an aqueous acid system. Similar phenomena were also observed in Au nanoparticle coated MoO_3 thin films (Yao *et al.* 1998, He *et al.* 2001b), Ag nanoparticle modified WO_3 films (Pang *et al.* 2010), and Au nanoparticle incorporated NiO films (Ferreira *et al.* 2003).

Park (2005) reported some different results for co-sputtered Au- WO_3 nanocomposite films containing a high gold concentration (60 mol% Au), where a shorter response time (typically 3 ~ 5 s) relative to the pure WO_3 thin films was observed. Surprisingly, the obtained Au- WO_3 nanocomposite films showed a reverse optical modulation with respect to applied potential compared to that of the pure WO_3 films, as shown in Figure 3. The reversal colouration was attributed by the author to forced ionic insertion due to the presence of metal phases. The same reversal colouration was also observed in co-sputtered Pt- WO_3 nanocomposite films (Park *et al.* 2006). Apparently, when comparing with the previous results on Au- WO_3 systems (Sichel *et al.* 1977), more efforts are still necessary for details.

Metallic nanoparticle incorporated EC materials usually exhibit strong characteristic absorptions, i.e., surface plasmon resonances, related to metallic nanoparticles in the dielectric matrix (Sichel *et al.* 1977). A combination of optical modulation by the EC matrix with the selective absorption by metallic nanoparticles opens a possibility to achieve new EC materials with improved properties. Considering the fact that a number of elements may be used to modify

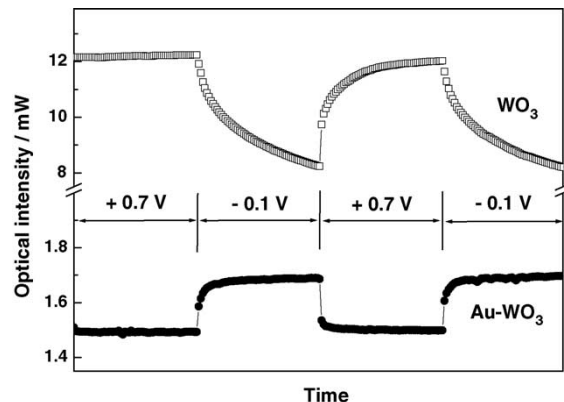


Figure 3 Optical intensity modulation curves of the WO_3 and $\text{Au}-\text{WO}_3$ electrodes as a function of pulse potential in 0.5 M H_2SO_4 . Reproduced from Park (2005).

the EC materials, it is the viewpoint of the authors that some theoretical approaches might be necessary to guide and interpret the experimental results.

2.3 Organic-Inorganic Electrochromic Nanoassemblies

An interesting EC design for an electronic display device has been proposed by Cummins *et al.* (2000). As shown in Figure 4 (Grätzel 2001), the device consists of two porous metal oxide nanoparticle films sandwiched between glass electrodes; the negative electrode is coated with a layer of TiO_2 , with viologen molecules (they turn blue when injected with charge) anchored to the surface of the nanoparticles (Figure 4a); the positive electrode consists of $\text{SnO}_2:\text{Sb}$, which is linked to phenothiazine molecules that turn red when oxidized (Figure 4b). When the electrochromic cell is filled with an electrolyte and a voltage is applied, the colour can be switched on and off in 250 ms. The common principle in this device lies on fast interfacial electron transfer between the nanoparticles and the adsorbed modifier as well as on the high surface area of the substrate that amplifies optical phenomena.

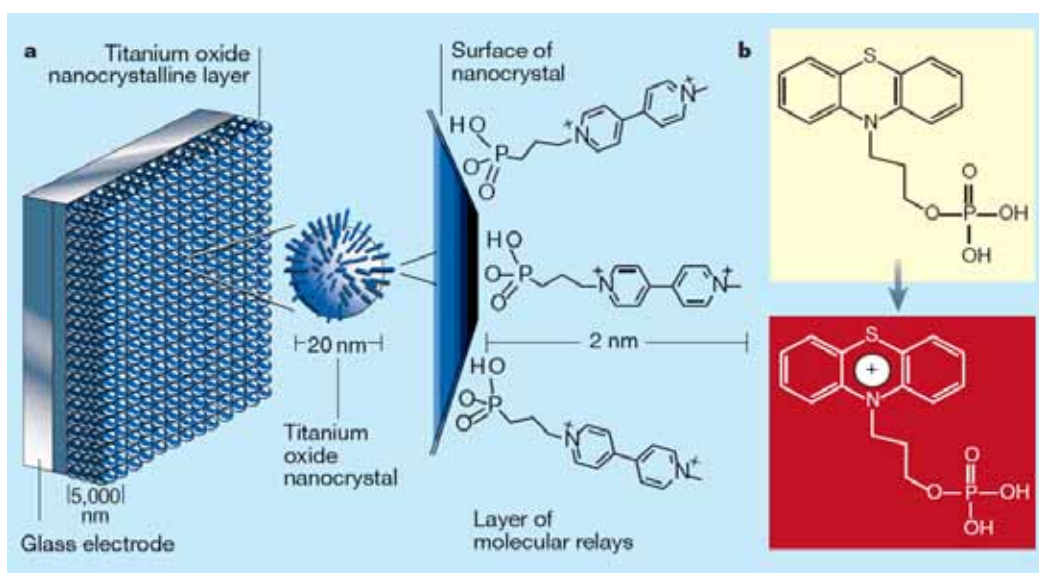


Figure 4 Ingredients for making a dynamic colour display. Reproduced from Grätzel (2001).

As shown in Figure 4, the EC process or colour change is basically due to the absorbed EC organic molecules; therefore, oxides which may not necessarily have electrochromism can also be employed. For example, Sun and Wang (2008) assembled an electrochemical cell using a viologen-modified ZnO nanowire array as the EC electrode. The ZnO nanowire array was grown directly on an $\text{In}_2\text{O}_3:\text{Sn}$ glass and then modified with viologen molecules. The ZnO nanowire EC device showed fast switching time (170 and 142 ms for colouration and bleaching, respectively), high colouration efficiency ($196 \text{ cm}^2/\text{C}$), and good stability. These improved performances were attributed to the large surface area, high crystallinity, and good electron transport properties of the ZnO nanowire arrays.

Though the device configuration of an EC display device is slightly different from that of the smart window (note that a transparent state is a restrictive requirement for EC transmission devices), considering the variety of organic molecules that show interesting electrochromism

(Argun *et al.* 2004), it is no doubt that there will be plenty of opportunities for organic-inorganic hybrid nanoassemblies for smart window applications. However, the disadvantage of this design is that the long-term stability of the EC organics, especially when exposed to UV light, must be considered. The possible photodecomposition of organics by metal oxide nanoparticles need to be evaluated (Fox 1983).

2.4 Self-Powered Electrochromic Systems

An EC smart window consumes, even though not too much, electricity when operating. Nevertheless, ideally this is not a desirable feature when considering energy efficiency. The idea of combining a photovoltaic (PV) device with an EC device then becomes very compelling as the PV systems are being increasingly used in building facades. Moreover, the operational characteristics of both PV and EC technologies are mutually compatible.

Deb *et al.* (2001) reported a monolithic, tandem PV-EC device, which consisted of a wide band gap a-SiC/H PV cell as a semitransparent power supply and a $\text{Li}_y\text{WO}_3/\text{LiAlF}_4/\text{V}_2\text{O}_5$ EC device as an optical transmittance modulator. A prototype 16 cm² device, as reported by Gao *et al.* (1999), could modulate the transmittance by more than 60% over a large portion of the visible spectrum. The device changed colour from pale yellow in the bleached state to dark blue in the coloured state. The colouring and bleaching times of the device were approximately 2 min under normal operating conditions (~ 1 V). The main technical challenge lies in reducing the thickness of the PV cell to less than 100 nm for semitransparency. However, when the PV device becomes very thin, the top contact may short-circuit the PV cell more easily and render the PV-EC stack useless.

There were also interesting approaches to integrate the EC and PV devices into a single electrochemical cell, with the EC and PV layer being one of the electrodes (Bechinger *et al.* 1996). The resulting system usually featured photochromism, i.e., colour changes upon light illumination, but unlike conventional photochromic films, the light absorption and colouration processes were separated and could therefore be optimized individually. For example, Wu *et al.* (2009) reported an electrochemical cell composed of a patterned WO_3/Pt EC electrode and a dye-sensitized TiO_2 nanoparticle photoanode. Under light illumination, the cell was coloured at short-circuit with tunable transmittance and it was bleached exceedingly fast by simply opening the circuit. This performance resulted from the crucial charge transfer pathways provided by the patterned WO_3/Pt EC electrode.

These proposed PV-EC cells may establish a scheme for constructing a self-powering, fast-response, transmittance tunable smart window. However, it may also be interesting to consider the possibility of storing electricity from the PV cells. An integrated Li-battery would be an obvious choice. This possibility will be discussed in subsequent work.

2.5 Layer-By-Layer Self-Assembly

An important advantage of nanoelectrochromics is their capability for large-scale production of EC smart windows. Unlike the traditional EC thin films made by physical methods such as sputtering and chemical vapor deposition, EC nanomaterials can be prepared as well as assembled by wet chemical methods that are usually cheap and scalable.

There are several methods for assembly of EC nanomaterials into large-scale devices, such as spin coating, dip coating, and spray. Note that a typical five-layered EC smart window is about one micron in thickness; therefore, it is necessary and important to achieve a structurally uniform

and thin EC film containing tiny nanoparticles. Layer-by-layer (LBL) self-assembly in this regard has obvious advantages, as shown in Figure 5 (Cassagneau and Fendler 2001). In a classical LBL process, a charged substrate is exposed alternately to dilute aqueous solutions of polycations and polyanions, enabling the deposition of a polyelectrolyte complex as a thin film with controlled thickness and composition. This approach can be extended to immobilize EC nanoparticles. For example, DeLongchamp and Hammond (2004) assembled Prussian blue nanoparticle films by using linear poly(ethylene imine) as polycations (DeLongchamp and Hammond 2004).

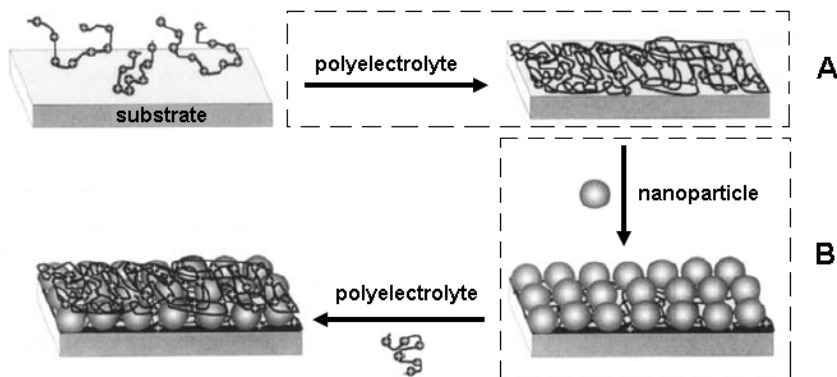


Figure 5 Schematic representation of the principle of electrostatic LBL self-assembly. The process consists of treating substrate and nanoparticle with oppositely charged polyelectrolytes and then depositing them alternately. Repeating the A and B process gives a nanoparticle film with controlled thickness. Reproduced from Cassagneau and Fendler (2001).

The LBL technique also allows a combination of different materials, which is ideal for assembly of EC devices if considering the fact that the most appropriate configuration of an EC smart window is essentially a multilayered thin film (e.g., as depicted in Figure 1). Obviously, the LBL self-assembly approach opens the possibility of immobilizing different EC compounds synthesized as nanoparticles, which may result in multicoloured window glazing.

3. FINAL REMARKS

Nanomaterials usually exhibit some specific properties that are correlated to their small featured sizes and a large fraction of surface atoms or ions; both are important for advanced EC devices with fast kinetics and improved thermodynamics. At this point, the development of new EC nanomaterials with new or improved EC performance will still be the focus of the research.

Wet chemical approaches can result in high-quality EC nanomaterials with controlled size, shape, surface and stoichiometry. The wet chemical methods are favourable with respect to reduced material and manufacturing costs and for large-scale production. Moreover, the surface of EC nanomaterials may readily be modified with organic surfactants, forming colloidal materials that are ideal for layer-by-layer self-assembly. This means that cheap EC smart windows with a large-area may be developed at a large-scale by employing mainly the wet chemical approaches.

New architectures, such as all-solid, self-powered EC smart windows, represent another important research area; though the complexity of these electrochemical cells suggests much more scientific and technical efforts during the progress.

ACKNOWLEDGEMENTS

This work has been supported by the Research Council of Norway and several partners through the SINTEF and NTNU research projects “*Robust Envelope Construction Details for Buildings of the 21st Century*” (ROBUST) and “*The Research Centre on Zero Emission Buildings*” (ZEB).

REFERENCES

- Argun, A. A., Aubert, P. H., Thompson, B. C., Schwendeman, I., Gaupp, C. L., Hwang, J., Pinto, N. J., Tanner, D. B., MacDiarmid, A. G., Reynolds, J. R., 2004, Multicoloured electrochromism in polymers: Structures and devices, *Chem. Mater.*, 16:4401-4412.
- Baetens, R., Jelle, B. P., Gustavsen, A., 2010, Properties, requirements and possibilities of smart windows for dynamic daylight and solar energy control in buildings: A state-of-the-art review, *Sol. Energy Mater. Sol. Cells*, 94:87-105.
- Bange, K., 1999, Colouration of tungsten oxide films: A model for optically active coatings, *Sol. Energy Mater. Sol. Cells*, 58:1-131.
- Bechinger, C., Ferrere, S., Zaban, A., Sprague, J., Gregg, B. A., 1996, Photoelectrochromic windows and displays, *Nature*, 383(17):608-610.
- Cassagneau, T. P., Fendler, J. H., 2001, Electron transfer and charge storage in ultrathin films layer-by-layer self-assembled from polyelectrolytes, nanoparticles, and nanoplates, In: Hodes, G., *Electrochemistry of nanomaterials*, Wiley-VCH, Mörrenbach:247-286.
- Cummins, D., Boschloo, G., Ryan, M., Corr, D., Rao, S. N., Fitzmaurice, D., 2000, Ultrafast electrochromic windows based on redox-chromophore modified nanostructured semiconducting and conducting films, *J. Phys. Chem. B*, 104:11449-11459.
- Deb, S. K., Lee, S. H., Edwin Tracy, C., Roland Pitts, J., Gregg, B. A., Branz, H. M., 2001, Stand-alone photovoltaic-powered electrochromic smart window, *Electrochim. Acta*, 46:2125-2130.
- Deb, S. K., 2008, Opportunities and challenges in science and technology for WO_3 for electrochromic and related applications, *Sol. Energy Mater. Sol. Cells*, 92:245-258.
- DeLongchamp, D. M., Hammond, P. T., 2004, High-contrast electrochromicsm and controlled dissolution of assembled Prussian blue/polymer nanocomposites, *Adv. Funct. Mater.*, 14(3):224-232.
- Deepa, M., Srivastava, A. K., Sood, K. N., Agnihotry, S. A., 2006, Nanostructured mesoporous tungsten oxide films with fast kinetics for electrochromic smart windows, *Nanotechnology*, 17:2625-2630.
- Ferreira, F. F., Haddad, P. S., Fantini, M. C. A., Brito, G. E. S., 2003, Composite Au-NiO films, *Solid State Ionics*, 165:161-168.
- Fox, M. A., 1983, Organic heterogeneous photocatalysis: chemical conversions sensitized by irradiated semiconductors, *Chem. Rev.*, 16(9):314-321.
- Gao, W., Lee, S. H., Bullock, J., Xu, Y., Benson, D. K., Morrison, S., Branz, H. M., 1999, First a-SiC:H photovoltaic-powered monolithic tandem electrochromic smart window device, *Sol. Energy Mater. Sol. Cells*, 59:243-254.

- Ghicov, A., Albu, S. P., Macak, J. M., Schmuki, P., 2007, High-contrast electrochromic switching using transparent lift-off layers of self-organized TiO₂ nanotubes, *Small*, 4:1063-1066.
- Granqvist, C. G., 1995, *Handbook of Inorganic Electrochromic Materials*, Elsevier, Amsterdam, 633 p.
- Granqvist, C. G., 2008, Oxide electrochromics: Why, how, and whither, *Sol. Energy Mater. Sol. Cells*, 92:203-208.
- Grätzel, M., 2001, Ultrafast colour displays, *Nature*, 409(1):575-576.
- Haranahalli, A. R., Holloway, P. H., 1981, The influence of metal overlayers on electrochromic behavior of WO₃ films, *J. Electron. Mater.*, 10(1):141-172.
- He, T., Ma, Y., Cao, Y., Yang, W., Yao, J., 2001, Enhanced electrochromism of WO₃ thin films by gold nanoparticles, *J. Electroanal. Chem.*, 514:129-132.
- He, T., Ma, Y., Cao, Y., Yin, Y., Yang, W., Yao, J., 2001, Enhanced visible-light coloration and its mechanism of MoO₃ thin films by Au nanoparticles, *Appl. Surf. Sci.*, 180:336-340.
- Lampert, C. M., 1984, Electrochromic materials and devices for energy efficient windows, *Sol. Energy Mater.*, 11:1-27.
- Lampert, C. M., 1998, Smart switchable glazing for solar energy and daylight control, *Sol. Energy Mater. Sol. Cells*, 52:207-221.
- Lee, S. H., Deshpande, E., Parilla, P. A., Jones, K. M., To, B., Mahan, A. H., Dillon, A. C., 2005, Crystalline WO₃ nanoparticles for highly improved electrochromic applications, *Adv. Mater.*, 18:763-766.
- Liao, C. C., Chen, F. R., Kai, J. J., 2007, Annealing effect on electrochromic properties of tungsten oxide nanowires, *Sol. Energy Mater. Sol. Cells*, 91:1258-1266.
- Monk, P. M. S., Mortimer, R. J., Rosseinsky, D. R., 2007, *Electrochromism and electrochromic devices*, Cambridge University Press, New York, 483 p.
- Pang, Y., Chen, Q., Shen, X., Tang, L., Qian, H., 2010, Size-controlled Ag nanoparticle modified WO₃ composite films for adjustment of electrochromic properties, *Thin Solid Films*, 518:1920-1924.
- Park, K. W., 2005, Electrochromic properties of Au-WO₃ nanocomposite thin-film electrode, *Electrochim. Acta*, 50:4690-4693.
- Park, K. W., Shim, H. S., Seong, T. Y., Sung, Y. E., 2006, Modified electrochromism of tungsten oxide via platinum nanophases, *Appl. Phys. Lett.*, 88:211107.
- Park, S. Y., Lee, J. M., Noh, C., Son, S. U., 2009, Colloidal approach for tungsten oxide nanorod-based electrochromic systems with highly improved response times and color efficiencies, *J. Mater. Chem.*, 19:7959-7964.
- Shen, P. K., Syed-Bokhari, J., Tseung, A. C. C., 1991, The performance of electrochromic tungsten trioxide films doped with cobalt or nickel, *J. Electrochem. Soc.*, 138(9):2778-2783.
- Shim, H. S., Kim, J. W., Sung, Y. E., Kim, W. B., 2009, Electrochromic properties of tungsten oxide nanowires fabricated by electrospinning method, *Sol. Energy Mater. Sol. Cells*, 93:2062-2068.
- Sichel, E. K., Gittleman, J. I., Zelez, J., 1977, Electrochromism in the composite material Au-WO₃, *Appl. Phys. Lett.*, 31(2):109-111.

- Sun, X. W., Wang, J. X., 2008, Fast switching electrochromic display using a viologen-modified ZnO nanowire array electrode, *Nano Lett.*, 8(7):1884-1889.
- Vidotti, M., Cordoba de Torresi, S. I., 2008, Nanochromics: Old materials, new structures and architectures for high performance devices, *J. Braz. Chem. Soc.*, 19:1284-1257.
- Wang, J., Khoo, E., Lee, P. S., Ma, J., 2009, Controlled synthesis of WO_3 nanorods and their electrochromic properties in H_2SO_4 electrolyte, *J. Phys. Chem. C*, 113:9655-9658.
- Wu, J. J., Hsieh, M. D., Liao, W. P., Wu, W. T., Chen, J. S., 2009, Fast-switching photovoltaic chromic cells with tunable transmittance, *ACS Nano*, 3(8):2297-2303.
- Yao, J. N., Yang, Y. A., Loo, B. H., 1998, Enhancement of photochromism and electrochromism in MoO_3/Au and MoO_3/Pt thin films, *J. Phys. Chem. B*, 102:1856-1860.
- Yoo, S. J., Jung, Y. H., Lim, J. W., Choi, H. G., Kim, D. K., Sung, Y. E., 2008, Electrochromic properties of one-dimensional tungsten oxide nanobundles, *Sol. Energy Mater. Sol. Cells*, 92: 179-183.

Towards an active, responsive and solar building envelope

F. Goia, M. Perino, V. Serra, F. Zanghirella
TEBE Research Group, Department of Energetics, Politecnico di Torino, Italy

ABSTRACT

The building envelope plays a key role in achieving building energy efficiency and indoor comfort for the occupants. The most promising (and innovative) strategy for the building envelope of tomorrow is based on a dynamic, active and integrated solution, able to optimize the thermal performance, integrating active elements and systems, exploiting energy from renewable source. Considerable efforts in research and development are necessary to achieve a sustainable and effective building envelope with a dynamic behaviour. Within the field of the light and transparent building envelope, a general trend in research can be drawn: along with the innovation of the façade's subsystems, researchers and producers are moving from the *double skin façade* concept towards a more complex façade, where the functional strategies are improved and the integration with active elements and the HVAC system is deeper. The most relevant results of a decade-long research activity carried out at the TEBE Research Group at Politecnico di Torino, on active and integrated building envelope, are here presented. The analysis provides useful information about the contribution of each subsystem (e.g. glazing, sun-shading devices, natural and mechanical ventilation...) to the achieved energy efficiency and user thermal comfort. Furthermore, the paper also presents the concept for an innovative façade module – which prototype is currently under construction – conceived in the frame of a National Research Project. The ActResS module (Active, Responsive and Solar module) is a dynamic building envelope element, capable of changing its thermo-physical behaviour in order to maximize the energy efficiency and the environmental comfort of buildings occupants.

Keywords: Double Skin Façades, Advanced Integrated Façades, Adaptive building envelope technologies, Solar energy, Low energy architecture.

1. INTRODUCTION

Present-day façade technologies are, of course, the result of a long process developed over thousands of years, but a radical change in the building envelope technologies occurred in the past century. From the Ancient architecture to the early Contemporary architecture, people living in Western countries have always preferred massive wall constructions, which provide in only one element the thermal insulation and the energy storage (along with the load transfer). Over the centuries, indeed, the materials and construction details have changed and have been improved, but no radical innovations have occurred. On the contrary, at the beginning of the XXth century, Modernism's theories deeply modified the form and the technology of the building enclosure, proposing the dissolution of the massive envelope. In particular, thanks to the separation of the vertical load transfer from the other task of the building enclosure, it was possible to dissolve the massive wall into a light, glazed façade and to introduce the *curtain-wall*. As result of this fact, fully transparent façades have been vastly realized since the Fifties and industrialized glass curtain-walls have become very popular.

During the first decades of the Modernism, designers were more interested in the formal aspects of the new architecture rather than in its energy performance and climate behaviour, looking for an *International style* which totally ignored the local climate conditions. As result of this attitude, building usually showed unacceptable indoor comfort conditions (due to the high energy loss in winter, the excessive thermal gain in summer, the poor natural ventilation, the visual discomfort caused by the absence of shading devices...) and relevant energy consumption (related to the HVAC systems, which were absolutely necessary to provide suitable indoor conditions). The consciousness of the environmental costs of the constructions and the evidences of the relation between inefficient façades and energy consumption determined another step forward in the innovation of the building envelope. *Double skin façades* (DSFs) were realized by adding an external layer of glass and providing the façade with a certain *dynamicity*, which allow to lower the heat loss during winter (thanks to the thermal buffer in the façade gap) and to reduce the thermal gain in summer (because of the ventilated cavity). Actually, the dynamic envelope is not a new concept, since Le Corbusier's "*mur neutralizant*" (1929), the first concept of a ventilated wall, composed by two membranes and a gap with warm/cold air flow.

DSFs became very popular in the Nineties (Oesterle 2001) and were usually associate to high-tech architecture, although the drawbacks of such technology were sometime larger than the benefits and its potentials were not completely exploited. *Advanced Integrated Façades* (AIFs) (Annex 44, IEA) are the natural evolution of the DSF concept and represent the state of the art of innovative building envelope technologies. Through the more complex integration between the building envelope and building services, AIFs enhance the dynamic features and the active behaviour partially introduced by DSFs, toward the development of a multifunctional building envelope, which will be able to continuously change its characteristic and function, in order to suit the occupant demand and to reduce the energy consumption. Mike Davies' "*polyvalent wall*" (1981) may be considered the basic (and first) concept of a building enclosure where several incorporated functional layers are required to perform different task (e.g. sun and heat protection, energy flow regulation according to needs and boundary conditions, exploitation of solar energy...). However, due to technological and economical aspects, *multi-functional façade modules* (MFM) are not an easy task and considerable efforts in research and development are still necessary.

2. OVERVIEW OF THE RESEARCH ACTIVITY

The research about active and integrated building envelopes, carried out by the TEBE Research Group at the Politecnico di Torino, started in 2000. During the decade-long activity, several typologies of advanced transparent façades have been evaluated by means of experimental campaigns and numerical analysis.

As far as the experimental activity is concerned, the measurements have been performed on field or by means of the TWINS test facility, in Northern Italy (Humid Subtropical Climate, according to the Köppen climate classification). The TWINS is a test rig developed to test responsive building envelope elements integrated with HVAC systems, and consisting of two identical test cells, one used for reference purposes (Serra et al. 2010). The façade typologies (Annex 44 – IEA) which have been tested, so far, are: *Double Skin Façade*, *Climate Façade*, "*Highly Integrated*" *Façade*, *Hybrid Ventilated Double Skin Façade*. The analysis of the performance of the façades, in terms of energy efficiency and thermal comfort, have been performed considering the following physical quantities and parameters:

- the pre-heating efficiency η (as defined by Di Maio and van Passen 2001);
- the dynamic insulation efficiency ε (as defined by Cognati et al. 2007);
- the “long-wave”¹ and the “total”² heat fluxes through the façade;
- the normalized “long-wave” and “total” heat fluxes ϕ_x and daily energies Σ_x (from 08:00 to 20:00) through the façade (Serra et al. 2007)
- the temperature and the normalized temperature θ of the inner glazing

A summary of the adopted performance parameters is reported in Table 1³.

Table 1: Adopted performance parameters.

Pre-heating efficiency	Dynamic insulation efficiency	Normalized heat fluxes	Normalized daily energy through the façade	Normalized surface temperatures
$\eta = \frac{T_{exh} - T_{inlet}}{T_i - T_o}$	$\varepsilon = \frac{\dot{Q}_R}{\dot{Q}_{IN}}$	$\phi_x = \frac{\dot{Q}_{x,fac} - \dot{Q}_{x,ref}}{\dot{Q}_{x,ref}}$	$\Sigma_x = \frac{E_{x,fac} - E_{x,ref}}{E_{x,ref}}$	$\theta = \frac{T_{gi,fac} - T_{gi,ref}}{T_{gi,ref}}$

3. DOUBLE SKIN FAÇADES

The *Double Skin Façade*⁴, tested by means of the TWINS facility, was equipped with operable lamellas at the inlet and at the outlet openings of the ventilated cavity. It is mandatory to notice that, although the tested DSF adopted the same functional strategies of a “traditional” DSF, its design and construction materials reflected the current state of the art of the technology (i.e. low-e glass, high performance roller screen...).

In winter time, the concept of the DSF is based on the exploitation of the solar energy to provide the façade with a thermal buffer. The air contained in the space between the layers of glass is heated up by the solar radiation impinging on the shading devices contained in the cavity. Therefore the façade behaves as an air solar collector, increasing the temperature of the air enclosed in the gap. The resulting “long-wave” heat flux entering the indoor environment through the façade is always far higher with respect to a single skin façade. On the contrary, if the façade is naturally ventilated, the profile of the “long-wave” heat flux is very similar to the one of the reference façade (Fig. 1a). Lower heat loss in night time can be explained considering highly performance low-e glass of the DSF (the reference façade had a conventional double glazed unit). If the thermal buffer configuration is adopted, the surface temperature of the indoor glazing is also increased, with a peak value of about 3 °C higher than the reference façade (Fig. 1c). This fact has a positive effect on the thermal comfort of the occupants, reducing the risk discomfort caused by radiant temperature asymmetry. If the façade gap is ventilated, the positive effect does not occur, as the DSF presents higher energy loss and lower surface temperature.

In summer and mid-season, when a stack driven ventilation occurs through the façade cavity, both the “long-wave” and the “total” heat flux are reduced if compared to a conventional

¹ The term “long-wave” indicates the heat flux exchanged at the indoor surface of the glazing with the indoor environment. It includes the convective heat flux and the long-wave radiative heat flux.

² Convective heat flux plus short-wave and long-wave radiative heat fluxes.

³ In the normalized parameters, the sub-script “x” are replaced by “lw” when considering “long-wave” fluxes and “long-wave” energies and are replaced by “t” when considering “total” fluxes and total energies.

⁴ Façade layers: external clear single glazing, 160 mm naturally ventilated cavity with venetian blind or reflective roller screen, internal clear double glazing with low-e coating.

single skin façade (Fig. 1b). The temperature of the air and of the shading devices in the façade gap may reach critical values (Fig. 1d) during the central hours of the day (respectively more than 40 °C and 50 °C) and dedicated strategies must be adopted in order to avoid the overheating risk (e.g. low-e glass, increased natural ventilation...).

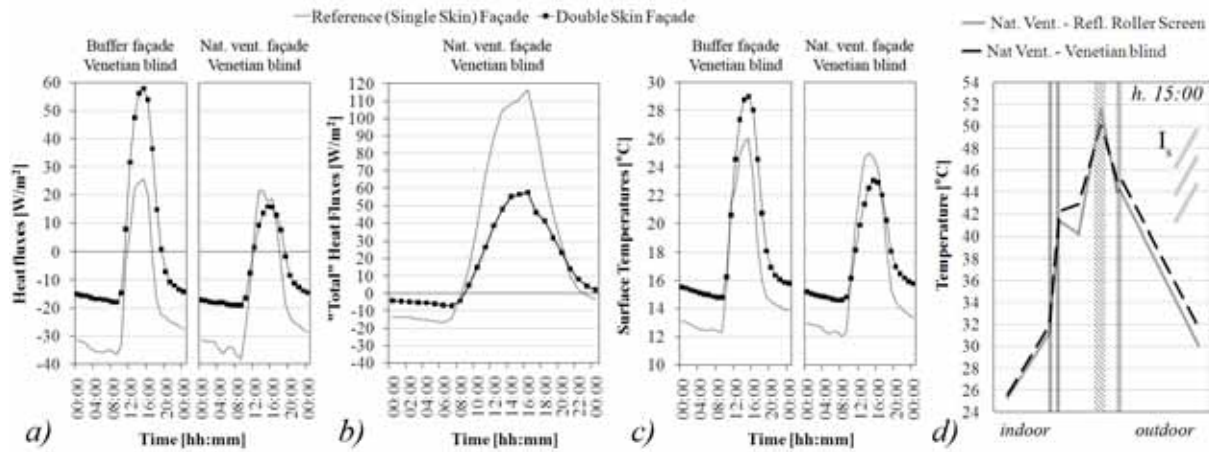


Figure 1: Double skin façade – (a) “long-wave” heat fluxes in winter conditions; (b) “total” heat fluxes in summer conditions; (c) surface temperatures of the inner glass in winter conditions; (d) temperature profiles with different shading devices in summer conditions.

DSF is a “simple” adaptive building envelope technology, showing poor integration with the HVAC. Critical issues of the design and implementation of such technology are mostly based on the adoption of highly performance subsystems (glass and shading device) and on increasing the stack effect. Problems of overheating must be correctly addressed and carefully considered during the design phase.

4. FAÇADES INTEGRATED WITH THE BUILDING SERVICES

4.1 Climate façades

The *climate façade* typology⁵ was studied in two different experimental campaigns, one performed on field (Corgnati *et al.* 2007) and the second at the TWINS facility (Serra *et al.* 2010). This type of façade can be considered as a part of the HVAC system, operating as an exhaust for the ventilation air. The air coming from the indoor environment flows in the cavity of the façade, which is mechanically ventilated. The exploitation of the solar radiation is obtained by the interaction between the solar shield, which adsorbs most of the irradiance, and the air flowing in the cavity, which is heated by the solar shield. During winter this creates a warm dynamic buffer between the indoor environment and the outdoor. Furthermore, the heat flux absorbed by the air can be used, through a heat recovery unit, to pre-heat the outdoor ventilation air flow (Fig. 2b).

In winter time and in sunny days, the presence of the warm buffer results in “long wave” heat flux entering the indoor environment. The air flow and the ‘long-wave’ heat gains are inversely proportional: increasing the air flow leads to a reduction in the entering heat flux (Fig. 3a). The dynamic buffer also affects the temperature of the inner glazing: in the climate

⁵ Façade layers: external clear double glazing, 140 mm mechanically ventilated cavity with venetian blind or reflective roller screen, internal single clear glazing.

façade the temperature is always higher with respect to a single skin façade. As for the heat fluxes, also for the temperatures a higher air flow rate worsens the performance of the façade, and, therefore, in winter conditions its value must be set according to the needs for ventilation purposes (Serra *et al.* 2010). The pre-heating efficiency (Figure 4b), shows that the façade cools the air flowing through the gap, instead of heating it, for at least 50% of the operative time. This means that an energy efficient use of the façade as a ventilation system exhaust is possible, but it is important to control the temperature of the air exhausted by the façade, and to choose whether to use it in a heat exchanger or not. A shading device with a high solar absorption (an aluminum venetian blind instead of a PVC reflecting roller screen), provides a higher pre-heating efficiency, as a low air flow rate does.

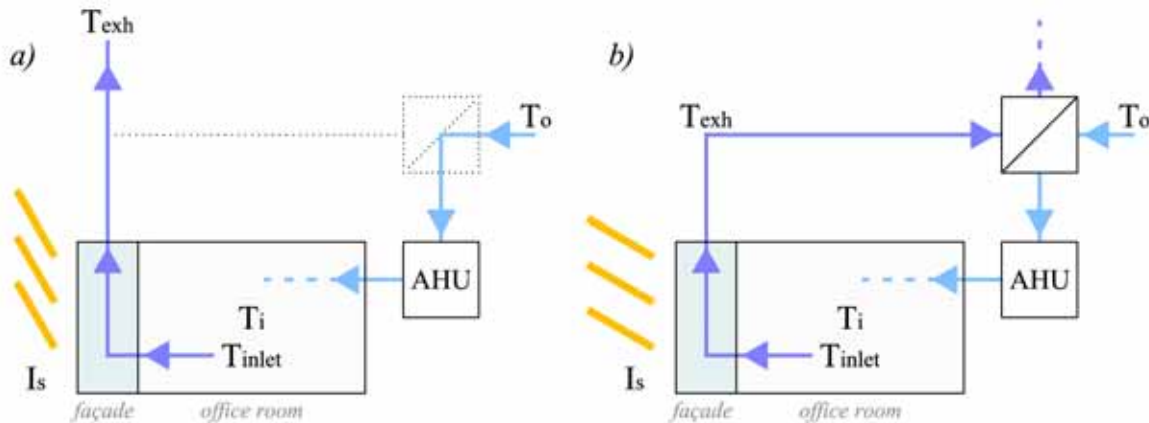


Figure 2: Operating strategy of the climate façade - (a) summer and midseason; (b) winter.

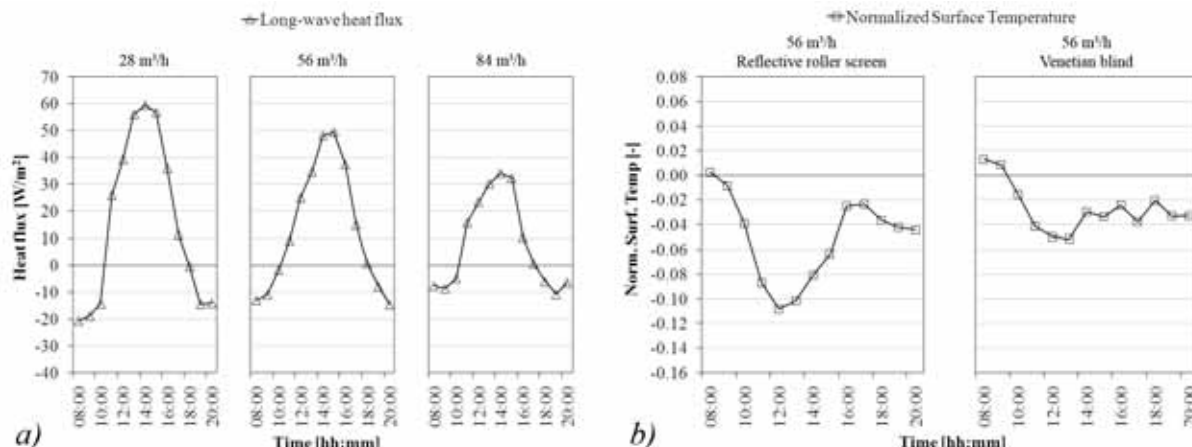


Figure 3: Climate façade – (a) “long wave” heat fluxes in winter conditions, configuration with venetian blind, and different air flow rates; (b) normalized surface temperature of the inner glass in summer conditions, configuration at 56 m³/h with different shading devices.

In summer conditions the aim of the climate façade is to collect most of the solar radiation in the ventilated cavity and to remove part of this heat loads through the exhaust air, which by-passes the heat recovery system and is discharged directly into the outdoor environment (Fig. 2a). The ability of the façade to remove part of the solar loads, represented by the dynamic insulation efficiency (Fig. 4a), improves with the air flow. If the air flow rate varies from 28 m³/h to 84 m³/h, the reduction in the entering load varies from 37% to 58%, for at least 50% of the time. The corresponding dynamic insulation efficiency is proportional for intermediate air flow rate values. The adoption of a reflecting and continuous shading device (a PVC reflecting roller screen instead of an aluminum venetian blind) affects the fluid

dynamic phenomena occurring in the cavity, improving the performance of the façade. With the same boundary conditions, the energy heat loads entering through the climate façade are about 37–46% lower than those entering through a single skin façade, depending to the configuration adopted for the climate.

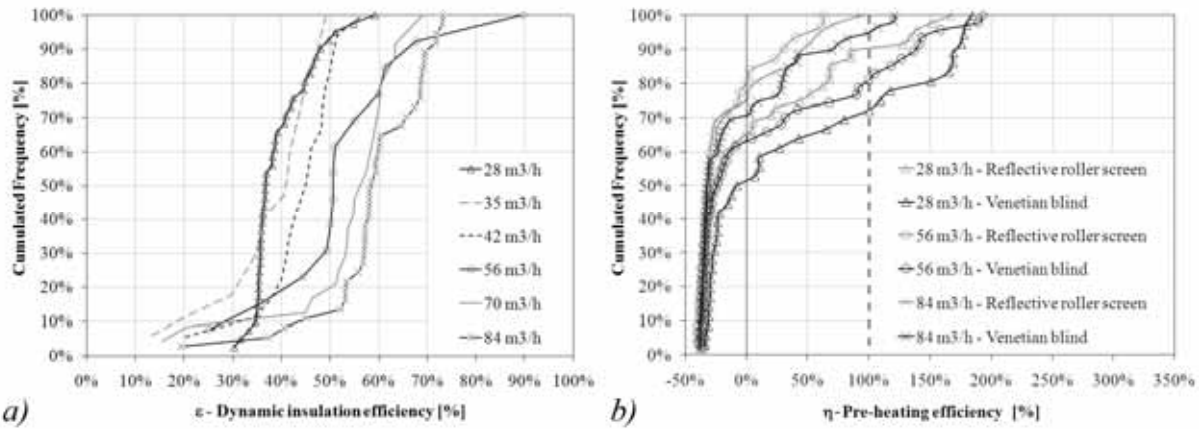


Figure 4: Climate façade – (a) dynamic insulation efficiency in summer conditions at different air flow rates; (b) pre-heating efficiency in winter conditions at different air flow rates and with different shading devices.

A possible problem related to this typology is the overheating of the cavity, leading to a possible overheating of the inner glass and to problems of radiant asymmetry. In presence of high solar radiation, the inner glass temperatures reaches values up to 39°C. These values can represent a discomfort problem for occupants. The performance of the climate façade is still better than the one provided by a single skin (Figure 3b), with a reduction in the temperature values between 2% and 10%. A higher reduction and thus a better performance is obtained at high air flow rates and adopting a continuous and less absorbing shading device (a PVC reflecting roller screen instead of an aluminum venetian blind).

4.2 “Highly integrated” façades

A façade⁶ with a higher integration with the building services have been monitored in field (Zanghirella *et al.* 2010). The exploitation of the solar radiation is similar to the one typical of climate façades: the ventilation cavity is meant to be a solar collector, creating a dynamic warm buffer in winter and removing part of the solar loads in summer. In this case, though, the façade is not directly an exhaust for the ventilation air: the exhaust air from the indoor environment is sent to a heat exchanger (air-air) to pre-heat (in winter) or to pre-cool (in summer) the fresh air. In winter time (Fig. 5b) the air is then sent to the plenum placed in the lower part of the façade. The air, after flowing along the façade, is extracted in the upper part of the cavity and is exhausted to the outdoor. In summer and in midseason (Fig. 5a), a second heat exchanger (air-water) may be activated and the air is pre-cooled before entering the ventilated cavity of the façade. The suitable heat exchanger makes use of well water, at 14°C. This heat exchange can be activated when the temperature of the air at the exhaust of the façade exceeds a value, set according to the season. In each operational strategy, the air exhausted in the upper part of the façade could potentially be sent to an additional heat exchanger, to exploit the related enthalpy flux.

⁶ Façade layers: external clear single glazing, 720 mm mechanically ventilated cavity with reflective, low-e roller screen, internal clear double glazing with low-e coating.

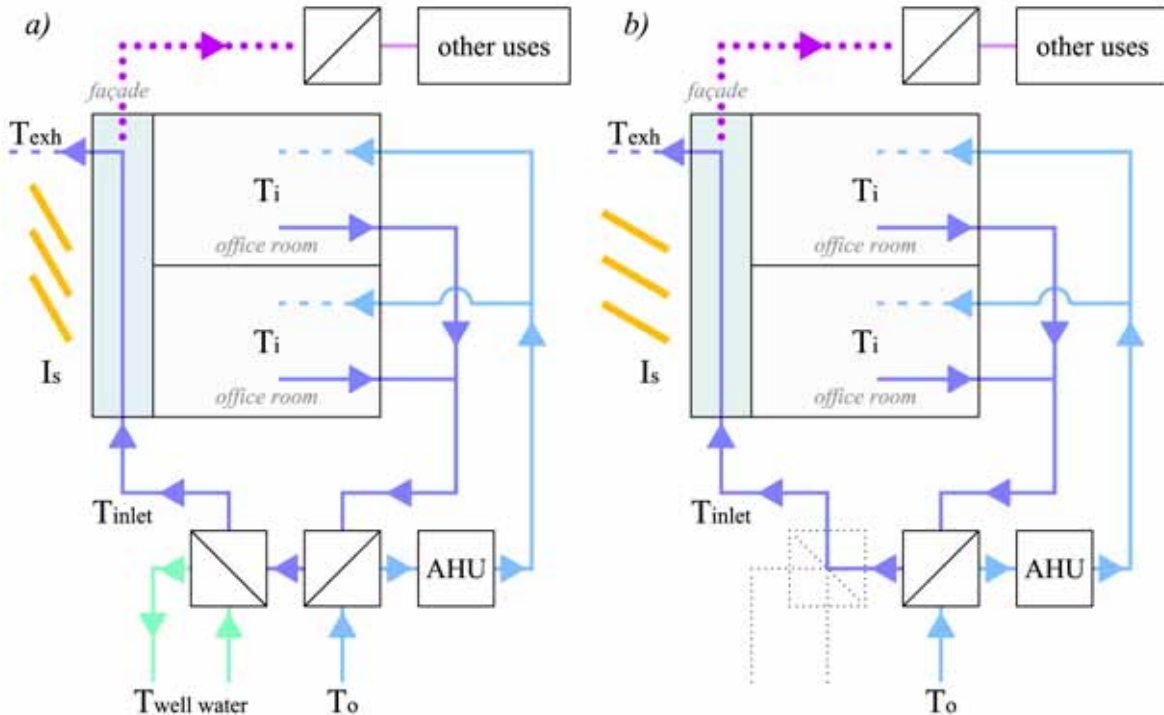


Figure 5: Operating strategy of the highly integrated façade - (a) summer and midseason; (b) winter season.

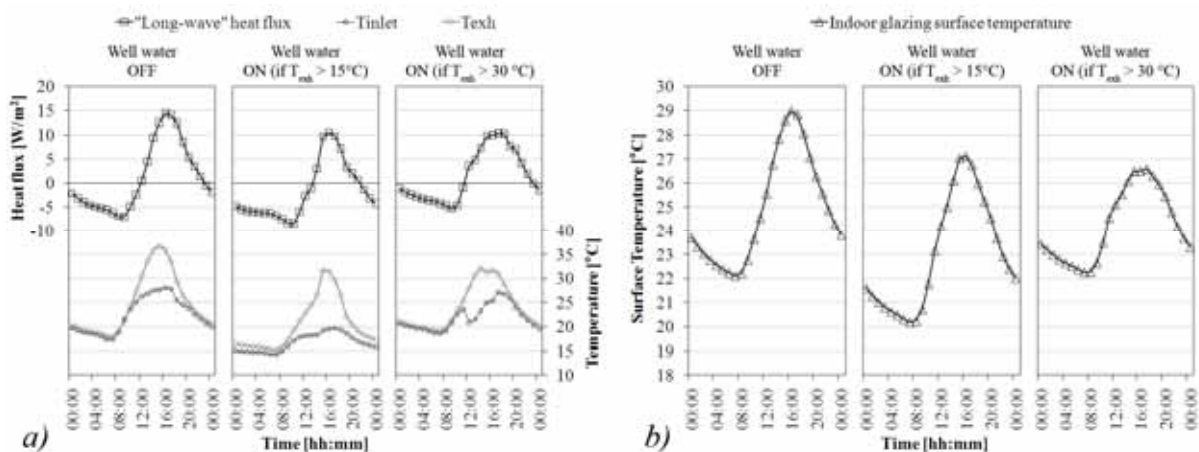


Figure 6: Highly integrated façade, midseason conditions - (a) "long-wave" heat fluxes, inlet and exhaust temperature; (b) temperature of the inner glass surface.

The façade shows a good thermal and comfort performance if compared to a single skin façade, with lower heat losses in winter and lower cooling loads in summer. This good performance is related to the high performance level of the various components (low-e double glazing, roller screen with a low-e coating) of the façade, to the air flow in the cavity and, in summer, to the ability to lower the temperature of the air entering the ventilated cavity. The highly integrated façade presents a lower warm dynamic buffer in winter and a lower ability to remove part of the solar loads in summer, with respect to the climate façade (as the heat recover occurs before the entrance of the air in the ventilated cavity). In these cases, the façade presents a very good behaviour, and the overall energy performance of the HVAC-façade integrated system seems to be better than the climate façade's one.

The integration between the façade and the well water cooling system leads to lower temperature values in the ventilated cavity, and this increases the ability of the façade to

remove part of the solar loads. In midseason conditions, the pre-cooling effect is useful to lower the entering cooling loads in the afternoon. However, if it is activated during the morning hours, it may increase the heat losses (Figure 6a). A correct choice of the value for the control temperature is therefore essential. A set-point value of 25°C (similar to the indoor air temperature) demonstrated to be a good compromise. In summer conditions, the pre-cooling lowers the temperature of the air flowing in the gap of about 5°C, and this allows to reduce the “long-wave” and the total cooling loads entering the indoor environment of about 19% and 6%, respectively. In summer conditions, thus, the interaction with the well water is always advisable during daytime.

Table 2: “Long-wave”, total daily cooling loads and peak temperatures of the inner glass in summer conditions.

Configuration	“Long-wave” cooling loads [Wh/m ²]	Total cooling loads [Wh/m ²]	Peak temperature of the inner glass [°C]
Pre-cooling at 25°C	87	254	29.3
No pre-cooling	107	271	28.5

As far as the thermal comfort issues are concerned, the high performance level of the components leads to temperatures of the inner glazing higher than 16°C in winter and lower than 30°C in summer, even when the pre-cooling system is not activated. The effect of the activation of the well water is to lower the glazing temperature (up to 1.5°C in summer and 2.5°C in midseason) and to further improve the performance of the façade (Fig. 6b, Tab. 2).

Considering the highly integrated façade, it is probably more appropriate to evaluate the performance of the complex system represented by the façade and the HVAC system, rather than the performance of the façade itself. This system has the potentiality to be very efficient and to provide good performances, but a very good and precise regulation of each part of the system is essential to its good functioning. A lack in the regulation system may cause undesirable effects.

5. FAÇADES EXPLOITING RENEWABLE ENERGY SOURCES

The experimental campaign on the so-called *Hybrid Ventilated DSF*⁷ was performed by means of a test cell apparatus and the performances of the façade were compared with the ones of a traditional single skin façade (Serra *et al.* 2009). Similarly to a “traditional” DSF, the HV-DSF operates as an outdoor air curtain in summer season in order to reduce the cooling loads. An integrated PV panel powers up to 6 fans, which enhance the ventilation through the façade cavity (Fig. 7a).

In winter time, the façade acts as a thermal buffer (Fig.7b), the behaviour of the HV-DSF is comparable with the one of the tested DSF, with increased “long-wave” heat flux and energy entering the indoor environment, as well as a more comfortable surface temperature of the inner glazing. Considering the supply-air configuration (Fig. 7c), it is interesting to investigate the ability of the HV-DSF to heat the air flowing in the cavity and subsequently released to the indoor environment. The façade is able to heat the air flow for almost 100% of the time (despite the fact that both days with high and low solar radiation were used to evaluate the pre-heating efficiency). Almost independently from the shading devices (venetian blind and roller screen), a value $\eta > 1$ is obtained for a large period of time (35-

⁷ Façade layers: external clear single glazing, 160 mm hybrid (fan assisted) ventilated cavity with venetian blind or reflective roller screen, internal clear double glazing with low-e coating.

40% of the time), which means that the façade is able to heat the incoming fresh air to a higher temperature than the indoor air temperature. Therefore, under this circumstance, the heat loss due to the natural ventilation of the indoor environment are fully compensated.

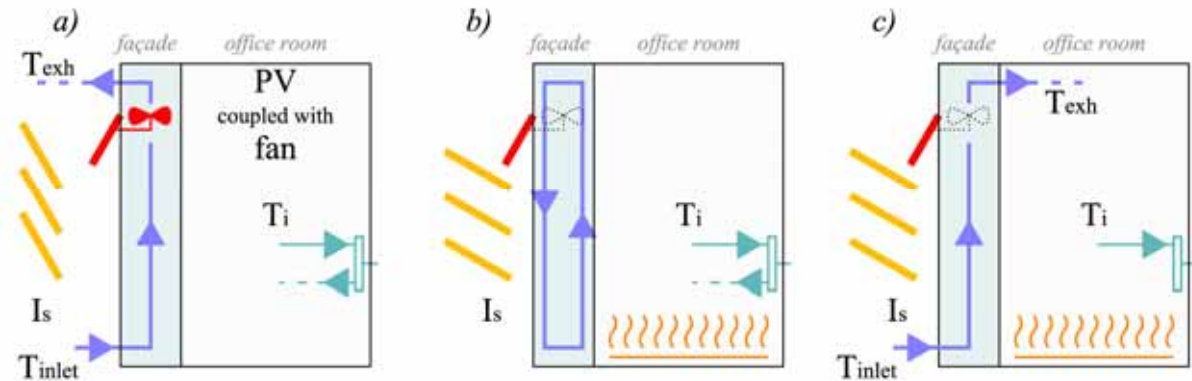


Figure 7: Operating strategy of the hybrid ventilated DSF - (a) summer season; (b) winter season; (c) air supply in winter and midseason.

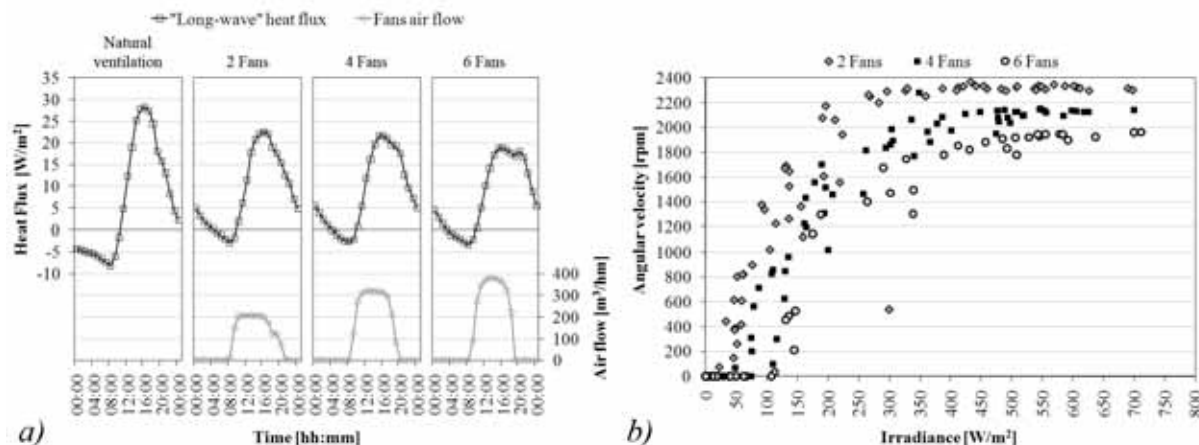


Figure 8: Hybrid ventilated DSF – (a) “long-wave” heat fluxes with different ventilation strategies, in summer conditions; (b) relation between fans angular velocity and irradiance.

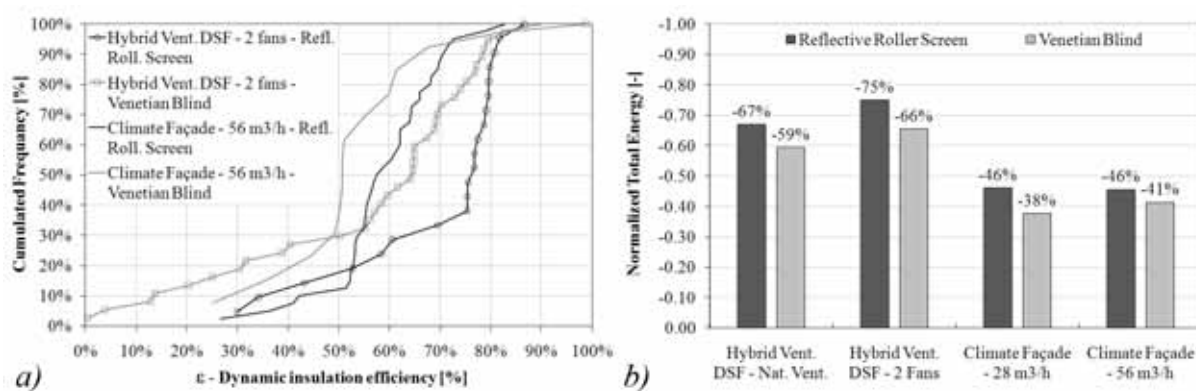


Figure 9: Hybrid ventilated DSF and climate façade, in summer conditions - (a) dynamic insulation efficiency; (b) normalized total daily energy.

In order to evaluate the energy efficiency of the façade in summer season, the dynamic insulation efficiency of the HV-DSF was compared with the one of the climate façade. For more than the 60% of the time, the HV-DSF is able to remove (thanks to the air flow) more than 75% (if equipped with a reflective roller screen) and 60% (if equipped with a venetian

blind) of the total heat flux reaching the façade (Fig. 9a). When considering the normalized total daily energy (Fig. 9b), it can be noticed that the HV-DSF with 2 fans reduces to about one-quarter the energy gain with respect to a conventional single skin façade. Additionally, it is more efficient than the DSF (total energy gain about -10%) and than the climate façade (total energy gain about -60%). It must be stated that, while the better performance with respect to the DSF can be explained mostly considering the increased ventilation, the comparison with the climate façade is deeply affected by the technologies of the two façades (different glazed layer and positions, different integration with the HVAC system...).

The HV-DSF is slightly more complex than a conventional DSF, allowing a certain integration with the building services. Additionally, the incorporation of a technology (PV panel) for the direct solar energy conversion allows to provide the façade with a fair electric power which can be used directly by the façade itself. In this configuration, the power is used to increase the ventilation during the hot season, reducing the overheating risk (which may occur in a conventional DSF) and increasing the façade's efficiency in removing potential cooling loads.

6. FURTHER DEVELOPMENT: THE ACTRESS FAÇADE CONCEPT

Starting from first-hand experiences and literature survey, a new façade module has been conceived, named *ActResS – Active, Responsive and Solar – façade module*. The weak spots of today AIF have been considered during the design phase, in order to develop a new module which may represent a step forward in the field of adaptive and dynamic building envelope. Among the other, the following critical issues were considered:

- the poor thermal inertia of the current light-weight and transparent façade, which negatively influences the passive control of the heat fluxes crossing the façade;
- the disproportion between the transparent and the opaque surface in AIF, which heavily affects the behaviour of the façade (e.g. glazing still present lower thermal resistances with respect to opaque materials).
- the possibility to incorporate technologies (PV and solar panels) to increase the direct exploitation of solar energy.

With respect to the “traditional” configurations of DSF and AIF, the façade module presents a balance (50-50) between the transparent and the opaque surface (which is not usual in DSF) in order to increase the heat capacity of the building envelope and to reduce the heat loss due to the low thermal resistance of the glazed layers. The non-transparent sub-module performs as an Opaque Ventilated Façade (OVF), with fan-forced ventilation. Additionally, the opaque surface allows to incorporate a fair amount of PV devices for direct solar energy conversion. Behind the cavity, a highly insulating VIP layer is placed, coupled with a PCM panel (facing the indoor environment), for thermal energy storage and the moderation of the indoor microclimate. The transparent sub-model is similar to a conventional single skin façade, with double glazed unit with low-e coating (indoor) filled with inert gas. A low-e coated roller screen is placed in the glazing cavity, to control the solar and light transmission.

As far as the natural and forced ventilation is concerned, the prototype allows to test the potential of the façade module according to different functional strategies (e.g. exhaust air façade, supply air façade, outdoor air curtain...), corresponding to different integration levels

with the HVAC systems. Among the others, the following functional strategies will be evaluated by means of experimental analysis.

- In summer, the ActResS module is expected to work as an outdoor air curtain façade or as an exhaust air façade. After being heated up within the cavity, the air is released to the outdoor environment or to a duct for following use (e.g. heat exchanger...).
- In winter, the ActResS module is expected to work as a supply air façade or to provide a thermal buffer to reduce the heat loss. Different configuration may be also tested (e.g. exhaust air façade to be coupled with centralized heat recovery device).

As far as the direct conversion of solar energy thorough PV panel is concerned, the following behaviour is expected.

- In summer, the PV panel provides the power to activate the ventilation fans and to control the shading devices (that have a direct relationship with the amount of solar radiation); the exceeding current is released to the electric system.
- In winter, the current generated by the PV panel is expected to heat up a PCM layer, contained in the OVF sub-module, by means of an heated carpet.

An experimental campaign is planned to start in July 2010, in order to assess the potentials of the ActResS façade module. The thermo-physical behaviour, the energy efficiency and the thermal and visual comfort performances of the ActResS façade module prototype will be compared to a conventional single skin façade by means of the continuous measurement of transmitted irradiances, heat fluxes and temperatures.

7. CONCLUSIONS

Although the dynamic and active building envelope concept has been established since time, the research and innovation necessary to reach the polyvalent and multifunctional building skin, still require considerable efforts. The technological evolution of the DSF and AIF may represent a possible trajectory towards the multifunctional façade concept. The lesson learned both from first-hand experiences and from literature review allows to assess the influence of each subsystems and the role of the strategies of integration between the building skin and the building services, in order to achieve the best performance both in terms of energy efficiency and indoor environmental comfort. Considerable improvements have occurred since the first DSF appeared, both concerning each subsystem components and the interaction among these elements. Such advancements have increased the performances of the transparent dynamic façades, but few innovations have appeared as far as the functional strategies are concerned. A deeper exploitation of solar energy (direct conversion via PV devices) represents an interesting perspective, which may allow to increase the efficiency of the façade and to explore new building skin concepts, based on the direct use of the electrical power within the façade itself.

Negative aspects of AIF also need to be considered for the advancement of these building skins. “Conventional” AIF are usually conceived for a worldwide application, while different climate regions claim for individual and dedicated solutions, based on local climate conditions. An exhaustive example of this attitude is represented by the poor thermal inertia of AIF, which is a crucial feature for the building envelope in warm and hot climates and reduces the energy efficiency of these technologies in the Mediterranean region. The integration between the AIF and the building services is probably the hottest topic in the field of the dynamic skin. Several experiences reveal that a deep fusion between the building

services and the active building enclosure can enhance the features and the efficiency of the responsive building envelope. However, the higher is the façade integration with the HVAC system, the more complex are the design, the construction and the management of the building. In this case, it is mandatory that the planning of the integrated façade is realized together with the environmental services: the façade can be seen as a part of the HVAC system or it can be even considered the link between the building and the mechanical plant. Additionally, it must be observed that a deep integration between the building skin and services can be realized only when economy of scale is reached and especially for some building types, such as offices, retails, hotels... On the contrary, a stand-alone façade, based on an advanced module, integrating different functions, can be seen as a promising solution, suitable also for smaller scale buildings.

Alongside with the research activity on “*highly integrated*” façade, a new investigation is about to start at the TEBE Research Group at the Politecnico di Torino, based on a stand-alone façade technology. An innovative prototype (ActResS façade module) has been conceived in the frame of a national research project, with the aim to improve the current technology of active and dynamic building envelopes. The main features of the façade module concern, along with the responsive behaviour, an increased the thermal inertia of the component, the reduction of the disproportion between the transparent and the opaque surfaces and the exploitation of the solar energy.

ACKNOWLEDGMENTS

Financial supports were provided by: Italian Ministry of Education, Universities and Research (PRIN 2007 – RES2: Responsive by Renewable) and Somec Marine & Architectural Envelopes s.r.l. The research projects were one of the Italian activities in IEA – Annex 44.

REFERENCES

- Annex 44 – IEA – ECBCS Report, EXPERT GUIDE – PART 2: RBE, editors: Øyvind Aschehoug: Norwegian University of Science and Technology (NTNU), Trondheim, Norway, Marco Perino, Politecnico di Torino, Dipartimento di Energetica (DENER) Torino, Italy, 2010. (In press)
- Corgnati, S.P., Perino, M. and Serra, V., 2007, Experimental assessment of the performance of an Active Transparent Façade during actual operating conditions, *Solar Energy*, vol. 81, no. 8: p. 993-1013.
- DiMaio, F. & Van Paassen, A.H.C. 2001. Modelling the air infiltrations in the second skin façade. In *Proceedings of IAQVEC Conference*: p. 873 - 880. Changsha, China.
- Oesterle, E., Lieb, R.D., Lutz, M. and Heusler, W., 2001, *Double-Skin Façades-Integrated Planning*. Prestel, Munich.
- Serra V., Zanghirella F., Perino M., 2009, Experimental energy efficiency assessment of a hybrid ventilated transparent façade, In: *Energy Efficiency and new approaches, Proceedings of the 4th International Building Physics Conference*: Vol. 1. p. 247- 254.
- Serra V., Zanghirella F. and Perino M., 2010, Experimental evaluation of a climate façade: Energy efficiency and thermal comfort performance, *Energy and Buildings*, vol. 42, no. 1: p. 993-1013.
- Zanghirella F., Serra V., Perino M. and Sossai C., 2010, Active transparent façade integrated with a well water cooling system: an experimental analysis. In *Proceedings of CLIMA 2010 Conference*. Antalya, Turkey. (In press)

An Efficient Numerical Method for Simulation of Long-term Operation of Horizontal Ground Heat Exchangers with Parallel Shallow Pipes

M. Greene, J. Lohan, N. Burke, L. Dimache and R. Clarke

Centre for the Integration of Sustainable Energy Technologies (CiSET),
Galway-Mayo Institute of Technology (GMIT), Dublin Road, Galway, Ireland.

ABSTRACT

As part of the HP-IRL study a horizontal ground heat exchanger in winter mode was simulated using the finite difference method in Cartesian coordinates. The authors have found that while a finite difference liquid energy balance simulation of the heat exchanger is accurate; fully transient and mimics real life, it is best suited for simulation of shorter system on-times of hours or days, as it becomes cumbersome to simulate every meter of the heat exchange fluid along with ground temperature distribution over long system on-times of months. This paper demonstrates a simulation based on estimating the heat exchanger's local heat flux at the exit of the pipe in order to determine the fluid's return temperature. For a 150m pipe this makes the calculation domain 150 times smaller than the liquid energy balance domain meaning the method is more efficient to use when a ground source heat pump system is to be simulated over long time periods such as months. It works best when the heat pump system is running in an approximate steady state condition, meaning turned on for all or a part of each day. Validation shows that the maximum error in hour average return temperature prediction is 1°C. This method along with the more common liquid energy balance method, both in Cartesian coordinates, are currently in use as part the HP-IRL study to simulate new heat exchanger designs in order to optimize system efficiency in Ireland's maritime climate.

Keywords: Horizontal, Ground, Heat Exchanger, Numerical, Climate

1. INTRODUCTION

HP-IRL is a study of Ground Source Heat Pump (GSHP) performance in Irish maritime conditions carried out at the Galway-Mayo Institute of Technology (GMIT) which aims to set out methods for optimized, location specific heat exchanger design and heat pump system control. Horizontal ground heat exchangers are deployed in GSHPs to absorb thermal energy stored within the grounds surface layer. Thermal energy absorbed by the heat exchanger is replenished through a combination of solar energy stored underground, the climate above the surface and in some locations the geothermal gradient. During winter operation the Coefficient of Performance (COP) of heat pump systems drops as the difference between the evaporating and the condensing temperatures, the temperature lift, increases. The condensing temperature is controlled by the user and for building applications remains relatively constant. The evaporating temperature however is variable and reduces with continued duty and with unfavorable climatic influences on the ground, resulting in higher 'lift' and a lower COP. The desired result of this mathematical analysis of the ground heat exchanger is to calculate the variation in the return temperature from the ground with time, given the heat exchanger's dimensions, the ground thermal properties and the variation in both the duty cycle and weather patterns with time. Such information would allow the optimum collector design to emerge given the climate conditions and application.

2. MODEL DEVELOPMENT

Using the liquid energy balance method involves simulating every meter of the heat exchange pipe; the authors have found that this consumes a huge amount of processing time and memory for long duration simulations. If a heat exchanger local heat flux method was used then individual segments of the heat exchanger could be simulated independently. There are two problems encountered, the first is that the local heat flux varies along the length of a heat exchange pipe; it is above average at the pipe entrance and below average at the pipe exit. The second problem is that this variation in local heat flux along the pipe length changes with time as the heat pump system is run and the far-field distance increases. A steady-state analysis will give further insight into this problem. Figure 1 defines the domain to be analyzed including the ground, the heat exchanger pipes and the relevant dimensions.

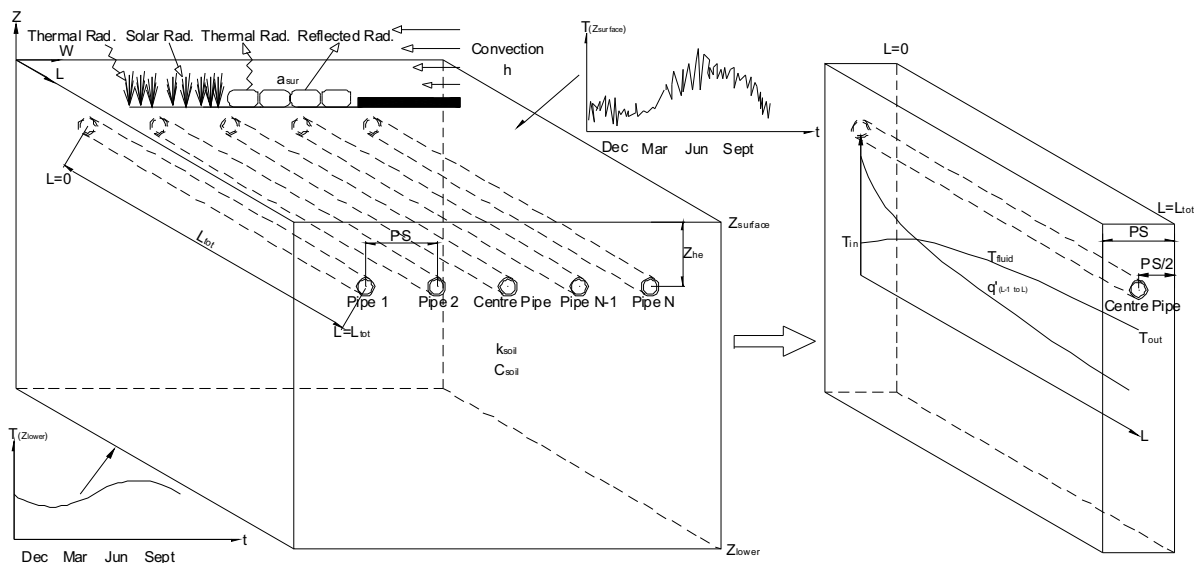


Figure 1: Selecting a pipe for study from a parallel pipe ground heat exchanger

The ground heat exchanger consists of a flow and return manifold connected by N pipes, each of internal and external diameters D_i and D_o respectively and total length L_{tot} . These pipes are buried at a depth Z_{he} beneath the surface in a parallel configuration with a pipe-spacing PS . The flow rate of liquid to and from the manifold \dot{V}_{man} is divided equally among these N pipes and the resulting volumetric flow \dot{V}_{pipe} enters the pipes at a flow temperature T_{in} and exits at a return temperature T_{out} . The returning liquid then passes through a heat pump of known nominal capacity and operational characteristics with an associated duty, before re-entering the flow manifold and entering the N pipes. The ground in which the pipes are buried is subject to temperature fluctuations induced by energy fluxes from above and below and has a far-field temperature at the heat exchangers depth (Z_{he}) of T_f that is measured in a control area outside the heat exchangers region of influence. The distance to this far-field temperature is a radius r_f with a corresponding diameter D_f , when $D_f=PS$ then no thermal interference will take place between parallel pipes.

2.1 Heat Transfer for Fluid in a Pipe

Incorpora and DeWitt (2002) present a form of eq. 1 as a solution for the return temperature of a fluid travelling through a single pipe buried in a uniform medium, where T_f is the far-field temperature $T_{out(L)}$ is the return temperature, a function of pipe length and T_{in} is the flow

temperature. Using a standard resistance in series summation eq. 2 represents the total resistance that exists between the fluid and the far-field location.

$$\frac{T_f - T_{out(L)}}{T_f - T_{in}} = \exp\left(\frac{-1}{\pi k_p R_{(L)}}\right) = \varphi_{(L)} \quad (1)$$

$$R_{(L)} = R_{conv(L)} + R_{cond,pipe(L)} + R_{cont(L)} + R_{cond,soil(L)} \quad (2)$$

Based on the work in Ireland of O'Connell and Cassidy (2004) the thermal contact resistance can be dropped for winter mode operation, however it may be significant in summer operation. Accordingly since a winter mode analysis is being carried out the contact resistance term is dropped from eq. 2. The soil's conductive resistance however presents a problem, since it changes with system on-time as the distance to far field grows. Hart and Couvillion (1986) propose that $r_f = 4\sqrt{\alpha t}$, for calculating the distance to far-field (r_f) with system on-time (t). For parallel pipes the authors have proposed eq. 3 when $D_f < PS$ and eq. 4 which includes linear resistance terms when $D_f > PS$ after thermal interference has taken place. The two ΔZ terms in eq. 4 can be calculated based on $(r_f - PS/2)$, where r_f is limited above the heat exchanger by the ground surface. Figure 2 presents eq. 1 used along with recorded data during steady-state operation of the HP-IRL system. In this analysis r_f is taken as 4m throughout, resistance for a single pipe is found using eq. 3 while the resistance of the HP-IRL average pipe spacing of 0.29m is found using eq. 4.

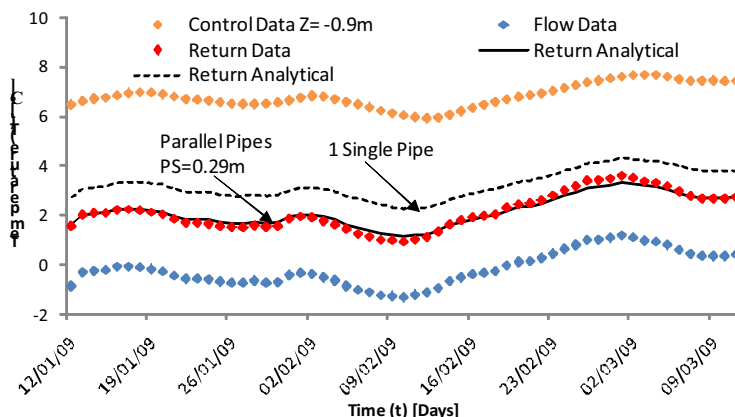


Figure 2: Data for T_f , T_{in} and T_{out} along with calculated T_{out} for a single pipe and parallel pipes between January and March 2009.

$$R_{(L)} = \frac{1}{\pi D_i h_{(L)} L} + \frac{\ln(D_o / D_i)}{2\pi k_{pipe} L} + \frac{\ln(D_f / D_o)}{2\pi k_{soil} L} \quad (3)$$

$$R_{(L)} = \frac{1}{\pi D_i h_{(L)} L} + \frac{\ln(D_o / D_i)}{2\pi k_{pipe} L} + \frac{\ln(PS / D_o)}{2\pi k_{soil} L} + \frac{1}{(k(PS)L)/(\Delta Z_{above}) + (k(PS)L)/(\Delta Z_{below})} \quad (4)$$

2.2 The Local Heat Extraction per Meter

Further study of the simple analytical equation presented in section 2.1 leads to a better understanding of how the heat exchange process takes place along the length of the pipes. Firstly the rate of heat extraction from the ground by a pipe of length L is found with eq. 5 and the average heat extraction per meter of pipe is found using eq. 6. The local heat

extraction rate per meter for a segment is found using eq. 7 and this differs from the average rate along the pipes length.

$$q_{(L)} = n\kappa c_p (T_{out(L)} - T_{in(L=0)}) \quad (5)$$

$$\bar{q}_{(L)} = q_{(L)} / L \quad (6)$$

$$\dot{q}_{(L-1 \text{ to } L)} = n\kappa c_p (T_{out(L)} - T_{out(L-1)}) \quad (7)$$

The local heat extraction rate per meter at the pipe entrance is above the average rate but at the pipes exit below the average rate. If a function was used to express this, called in this instance β in eq. 8, it could be used to convert a nominal heat extraction per meter value supplied by an installer into a local heat extraction at any meter segment. Such a function would allow a transient heat flux simulation to be carried out on a single segment of the ground to access the drawdown in that area, or a simulation at the start and end of the collector would yield the approximate transient flow and return temperatures. The β function can be found by returning to eq. 1 and evaluating the right hand side of that equation at the required pipe lengths as expressed in eq. 9.

$$\dot{q}_{(L-1 \text{ to } L)} = \beta_{(L-1 \text{ to } L)} (\bar{q}_{(L_{tot})}) \quad (8)$$

$$\beta_{(L-1 \text{ to } L)} = [L_{tot}(\varphi_{(L-1)})] / (1 - \varphi_{(L_{tot})}) \quad (9)$$

The resulting function is plotted in Figure 3 for the HP-IRL heat exchanger as it was analyzed in section 2.1, $r_f=4m$, at 2 different volume flow rates. The β function is dependent on r_f and varies from the start to the finish of a long system run-time. Initially a large portion of the heat is extracted at the start of the heat exchanger and the β function is most extreme, high at the pipe inlet and low at the pipe exit. However as the ground at the start is depleted with time the resistance grows and more heat is extracted further along the pipe. As this process continues the β function flattens. For this reason the β function is dependent on the soil resistance which changes with time and therefore in order to carry out a heat flux based ground simulation β must be calculated for the system on-time in question. For shorter simulations of a few hours on-time each day then a lower soil resistance is calculated and the result is a more extreme β function. For the HP-IRL experiment to be simulated a long on-time was used and therefore the β values shown in Figure 3, calculated at $r_f=4m$ are used. While this decision and calculation process adds complexity to the simulation initial set-up for the heat flux method and is not required for the liquid energy balance method it reduces the calculation domain and hence the processing time for the former by 150 times when compared with the latter.

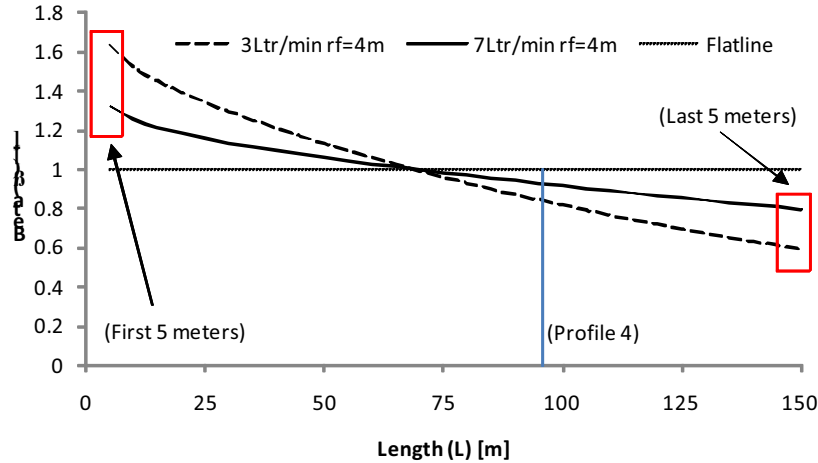


Figure 3: The β function for flow rates of 3 and 7 Ltr/min, $r_f=4\text{m}$ along a 150m pipe

2.3 Transient Numerical Model

It is impractical to attempt to simulate the entire volume of ground plus the N pipes and the fluid within. Instead one pipe and the surrounding ground volume are chosen for numerical analysis and the analysis is segmented so that 1 meter sections of this chosen volume are analyzed. This is similar to a method used in many simulations such as Demir (2009), Piechowski (1995) and Mei (1986). In this study however, the heat flux method is chosen; it will mean that based on the accuracy of the β function any segment of the collector can be simulated individually. However the accuracy of this method is unknown and will be assessed as part of the aims of this paper. Figure 4 shows the dimensions and layout of the proposed simulation method and presents in graphical form the logic involved in creating the simulation matrix.

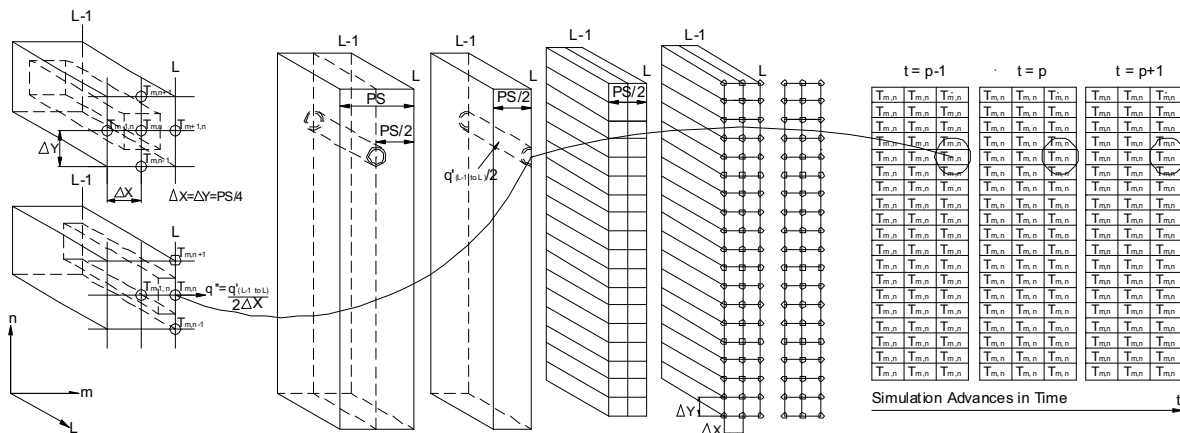


Figure 4: A graphical representation of the simulation method, showing dimensions and positions along with the logic of the method

2.3.1 Ground-Climate Boundary Condition

The explicit finite difference equation for the surface boundary node is derived by applying the energy balance principle to the half volume surrounding the surface node, the result is eq. 10. In implementing the energy balance equation using an explicit finite difference method, some restrictions apply. In order to ensure a stable forward difference model eq. 11 must be

satisfied at all time steps, this means that Δt needs to be selected suitably. The convection coefficient correlations in eq. 13 and 14 are presented in Palyvos (2008).

$$T_{m,n}^{p+1} = Fo(2T_{m,n-1}^p + T_{m-1,n}^p + T_{m+1,n}^p + 2BiT_{amb}) + (1 - 4Fo - 2BiF0)T_{m,n}^p + 2Fo(q_{rad,net}'' \Delta x / k) \quad (10)$$

$$Fo(2 + Bi) \leq \frac{1}{2} \quad (11)$$

$$q_{rad,net}'' = (1 - a_{sur})q_{solar}'' + q_{thermal,in}'' - q_{thermal,out}'' \quad (12)$$

$$h = 3.95u_{wind} + 5.8 \quad (u_{wind} \leq 5m/s) \quad (13)$$

$$h = 7.1(u_{wind}) + 5.36e^{-0.6u_{wind}} \quad (u_{wind} \leq 5m/s) \quad (14)$$

2.3.2 Internal Nodes

The finite difference form of the heat equations for internal nodes is presented in Incopera and De Witt (2002) and is displayed in eq. 15. This equation is easily modified to cater for adiabatic nodes located on boundaries of zero heat flux.

$$T_{m,n}^{p+1} = Fo(T_{m-1,n}^p + T_{m+1,n}^p + T_{m,n-1}^p + T_{m,n+1}^p) + (1 - 4Fo)T_{m,n}^p \quad (15)$$

2.3.3 Heat Exchanger Interface Node

The finite difference equation for the node at which the heat exchangers local heat flux acts is derived using the energy balance for a half volume node and is expressed in eq. 16. The local heat flux of the heat exchanger is expressed as positive in eq. 17 for summer mode and negative for winter mode. In eq. 17 the nominal heat exchanger rate in Watts is multiplied by the percentage on-time (duty) for the time-step (Δt) then it is divided by the number of pipes on the manifold (N) and the total length of the pipes (L_{tot}) to convert it to an average heat extract rate per meter of pipe. It is multiplied by β to convert it to a local heat extract rate per meter for the segment of interest then divided by 2 since the adiabatic line of the model segment bisects the heat exchanger pipe, finally it is divided by Δx to convert it to a local heat flux for the heat exchanger node of the segment. For greater accuracy the nominal extract rate can be written as a function of the return temperature in accordance with the manufacturer's performance data. This is expressed in eq. 18, where the calculated heat exchanger node temperature at the pipe exit is used to estimate the heat exchange rate for the next time-step.

$$T_{m,n}^{p+1} = Fo(T_{m-1,n}^p + T_{m,n-1}^p + T_{m,n+1}^p) + (1 - 4Fo)T_{m,n}^p + 2Fo(q_{he(L-1 to L)}'' \Delta x / k) \quad (16)$$

$$q_{he(L-1 to L)}'' = \frac{\beta_{(L-1 to L)} (\%On-time) q_{nom}}{(NL_{tot} 2\Delta x)} \quad (17)$$

$$q_{nom}^{p+1} = f(T_{he,L_{tot}}^p) \quad (18)$$

2.3.4 Lower Boundary Nodes and Initial Condition for all Nodes

The expression given in eq. 19 is used at the lower boundary of the simulated section; it is also used as the initial condition for all nodes of the simulation. It can be seen in Figure 5 that eq. 19 becomes visibly more accurate at greater depths, this means the deeper the lower boundary is set the greater the accuracy, the authors have found that a boundary at $-10 > Z_{\text{lower}} < -5 \text{m}$ is suitable.

$$T_{z,t} = T_{\text{ave}} + \frac{\text{Amp}}{2} \left\{ e^{\left(z \sqrt{\frac{\omega}{2\alpha}} \right)} \sin \left(\omega(t + t_0) + z \sqrt{\frac{\omega}{2\alpha}} \right) \right\} \quad (19)$$

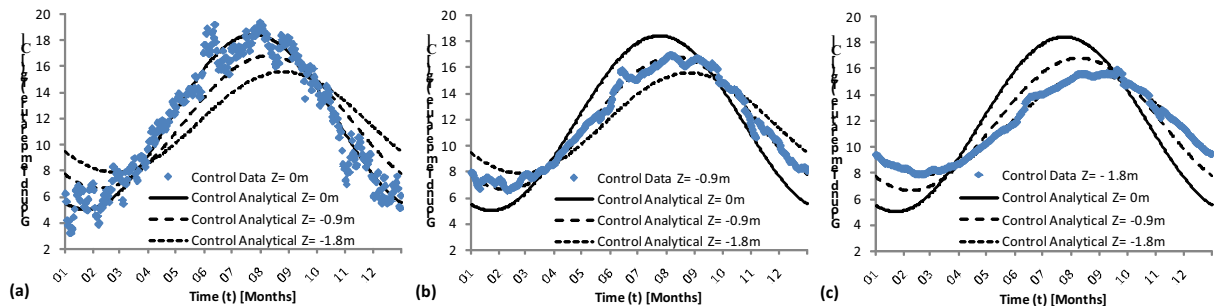


Figure 5: Eq. 19 compared with a 3-year average (2007-2009) of mean daily ground temperatures measured at 3 depths (a) $Z=0$, (b) $Z= -0.9$ and (c) $Z= -1.8\text{m}$

3. EXPERIMENTAL VALIDATION

Validation of the numerical method was carried out using the HP-IRL test facility. This test facility complete with data acquisition, continuously monitors: climate, soil, heat exchanger and heat pump parameters as described in Lohan *et. al* (2006) and Greene *et. al* (2007) and (2008). Simulated results are compared to ground temperature data recorded in 2008, 2009 and 2010 and ground heat exchanger fluid temperatures recorded in 2009 and 2010. Recorded weather data and duty cycle data are used in both ground temperature and fluid temperature simulations. The heat pump to manifold flow rates were 70Ltr/min and 30Ltr/min in 2009 and 2010 respectively, meaning 7Ltr/min and 3Ltr/min in each pipe of the 10 pipes. The nominal heat sink extraction rates for 2009 are taken from the heat pump installers guides and are confirmed by measured data (10.8kW), the nominal value for 2010 is taken from measured data (7.8kW) since the unit was running outside normal operating conditions for study purposes.

3.1 Undisturbed Ground Temperature Simulation Control Location January to December 2008

In Figure 6 the data recorded at 0.15m below the solid soil surface is compared with the simulation results from 0.25m below the model surface since in the time after the PT100

sensors were buried; significant organic material, roots and grass have developed above it. While the grass is part of a landscaped area and is kept trimmed regularly it is fair to estimate that 0.1m or more of organic material, some well compacted exists above the vertical profile of sensors.

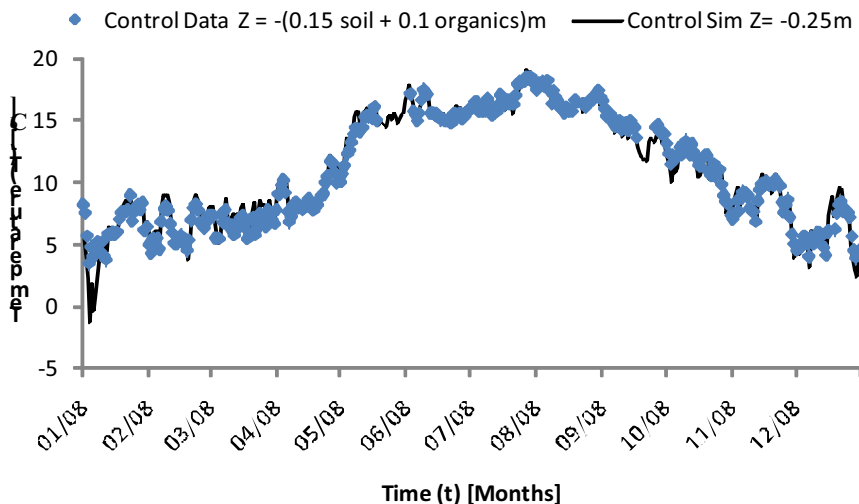


Figure 6: 12 months of mean hourly simulated results $Z=-0.25$ compared with mean hourly data $Z= -0.15\text{m}$ (0.1m allowed for organics and grass cover)

The lower boundary comprising eq. 19 is set at 7.5m below the surface which is more than sufficient for accurate simulation and can be set at a shallower level such as $-3 < Z_{\text{lower}} < -4\text{m}$ to save time and memory. The Δx is set at 0.0625m so this 3×120 matrix of equations is then marched forward in time with weather data provided to the upper boundary equations at each Δt , 12 minutes apart. A lower boundary at $Z_{\text{lower}} = -3\text{m}$ would mean a 3×48 matrix and a 1-dimensional analysis can be done with a larger Δx of 0.25m meaning a 1×12 matrix can be used at a Δt of 1 hour if a heat exchanger is not being modeled.

3.2 Flow and Return Fluid Temperature Simulation

It was also of interest to assess the usefulness and accuracy of a heat flux based simulation of ground heat exchanger operation as opposed to a fluid energy balance method. The fluid energy balance method is more commonly used however with the inclusion of the β function from the steady-state analysis the heat flux method can be used to access drawdown in the ground heat source at different points along L . Also the expected flow and return temperatures can be approximated as the heat exchanger node temperature simulated using $\beta_{(L=0)}$ and $\beta_{(L=L_{\text{tot}})}$ respectively. Most importantly from the $\beta_{(L=L_{\text{tot}})}$ simulation, the temperature difference ΔT between T_f and $T_{\text{out}(L)}$ when steady-state is reached for a particular nominal extract rate and fluid flow rate is found. Figure 7 and 8 display comparisons between simulated and measured results.

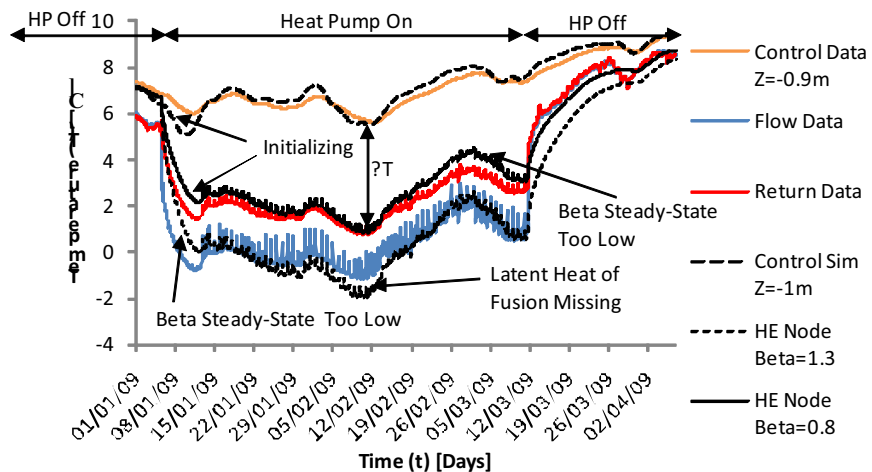


Figure 7: Simulated results of the control profile and the collector node in the flow and return segments displayed alongside control data and measured flow and return temperatures over a 14 week period in 2009, $q_{\text{source,nom}}$ was 10.8 kW with a ρ_{pipe} of 7 Ltr/min

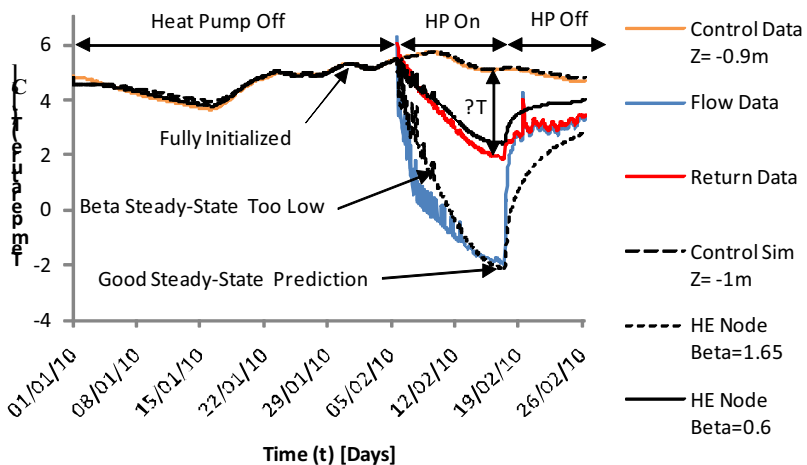


Figure 8: Simulated results of the control profile and the collector node in the flow and return segments displayed alongside control data and measured flow and return temperatures over an 8 week period in 2010, $q_{\text{source,nom}}$ was 7.8 kW with a ρ_{pipe} of 3 Ltr/min

3.3 Ground Temperature Drawdown by Heat Exchanger Node

As identified in section 3.2, the finite difference simulation can be used to investigate the thermal drawdown in the ground around the heat exchanger. This allows insight into the effect of extreme or relaxed duty cycles and positive or negative weather effects at the surface. By altering parameters of the simulation related to the heat exchanger such as: depth, pipe-spacing, ground backfill, surface cover and surface solar inclination or parameters related to the heat pump such as: the duty cycle, the flow rate or the nominal extract rate, many new system designs can be studied for system optimization in a unique climate situation. Figure 9 displays simulated and measured results against both time and depth at 90m ($\beta=0.87$) along one of the centre heat exchanger buried pipes.

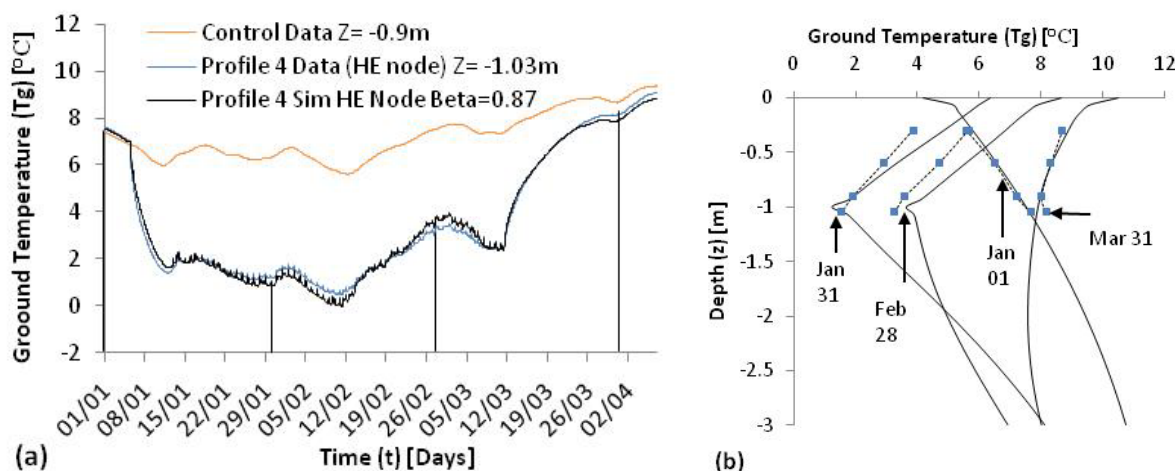


Figure 9: From 2009 (a) Simulated collector node temperature compared with measured pipe-soil interface temperature for profile 4 located at $L=90m$ along one of the centre pipes of the heat exchanger (b) simulated temperature gradients and measured temperature gradients in profile 4

4. CONCLUSIONS

In conclusion the authors have offered a heat flux based simulation of a ground heat exchanger pipe and the surrounding soil. The simulation was carried out in Cartesian coordinates to allow full inclusion of thermal interference between parallel pipes and climatic effects on the surface. Since a long system on-time of 14 weeks was simulated the decision was made to seek an alternative to the liquid energy balance method in order to reduce the calculation domain. For this reason a local heat flux method was used. This method allows simulation of individual 1 meter segments of the ground as opposed to the liquid energy balance method which requires every meter of pipe to be simulated. Simulating the heat exchanger node at the pipes exit over time gives a good approximation of the transient fluid return temperature, the results show a maximum error of 1°C when compared with experimental results recorded in the HP-IRL study. However this method requires that the user estimate the soils thermal resistance to heat flow which varies with the length of system on-time being simulated. This resistance is needed in order to calculate β which is the ratio of local heat extraction rate for a meter segment to the average heat extraction rate per meter for the entire pipe. This requirement aside this method presents an efficient alternative to a liquid

energy balance simulation and also includes full climate and thermal interference effects, allowing accurate simulation of long system on-times. This method will be further refined and used along with the liquid energy balance method and neural networks to optimize heat exchanger design and heat pump control strategies for the Irish maritime climate.

ACKNOWLEDGEMENTS

The authors wish to acknowledge the support of Enterprise Ireland, Dunstar Ltd., the Irish Research Council for Science Engineering and Technology, the Irish Department of Education and Science and the Galway-Mayo Institute of Technology.

REFERENCES

- Demir, H., Koyun, A and Temir, G., 2009, Heat Transfer of Horizontal Parallel Pipe Ground Heat Exchanger and Experimental Verification, *Applied Thermal Engineering*, Vol. 29, p. 224-233.
- Greene, M., Burke, N., Lohan, J. and Clarke, R., 2008, Ground Temperature and Moisture Content Surrounding Horizontal Heat Pump Collectors in a Maritime Climate Region, *9th International IEA Heat Pump Conference*, International Energy Agency
- Greene, M., Burke, N., Lohan, J and Clarke, R., 2007, Ground Temperature Gradients Surrounding Horizontal Heat Pump Collectors in a Maritime Climate Region, *Energy and Sustainability*, WIT Transactions on Ecology and the Environment, WIT Press, Vol 105, p. 309-319.
- Hart, D.P., and R. Couvillion, 1986, Earth Coupled Heat Transfer, *Publication of the National Water Well Association*
- Incorpera, F., DeWitt, D., 2002, *Fundamentals of Heat and Mass Transfer 5th Edition*, John Wiley & Sons Inc., Hoboken, New Jersey.
- Lohan, J., Burke, N., Greene, M., 2006, The Development of a Ground Source Heat Pump Characterization Facility for the Irish Maritime Climate, *Renewable Energy in Maritime Island Climates*, International Solar Energy Society UK, Issue 85, p. 119-124.
- Mei, V. C., 1986, Theoretical Heat Pump Ground Coil Analysis with Variable Ground Far-field Boundary Conditions, *AICHE*, Vol 32, No 7.
- O'Connel, S., Cassidy, S.F., 2004, Soil-Collector Thermal Contact Resistance for a Ground-Source Heat Pump, *Technical Papers*, Society of Manufacturing Engineers-All Series
- Palyvos, J.A., 2008, A survey of wind convection coefficient correlations for building envelope energy systems modeling, *Applied Thermal Engineering*, Vol 28, p. 801-808.
- Piechowski, M., 1999, Heat and mass transfer model of a Ground Heat Exchanger: theoretical development, *Int. J. Energy Research*, Volume 23, p. 571-588.

NOMENCLATURE

Table 1: Nomenclature of all symbols including superscripts and subscripts

Symbol	Meaning	Units	Value	Symbol	Meaning	Units	Value
COP	Coefficient of Performance	-	-	Δx	FD Increment (m direction)	m	PS/4
N	Number of Pipes on the Manifold	-	10	Δy	FD Increment (n direction)	m	PS/4
D _i	Inner Pipe Diameter	m	0.026	Δt	Finite Difference Timestep	s	720
D _o	Outer Pipe Diameter	m	0.032	T _{m,n}	Centre Node	-	-
D _f	Far-field Diameter	m	8	T _{m-1,n}	East Node	-	-
r _f	Far-field Radius	m	4	T _{m+1,n}	West Node	-	-
L	Length Dimension of Pipe	m	-	T _{m,n-1}	South Node	-	-
L _{tot}	Total Pipe Length	m	150	T _{m,n+1}	North Node	-	-
Z	Height Dimension above Surface	m	-	T _{m,n} ^p	Node in Previous Timestep	-	-
Z _{he}	Heat Exchanger Height	m	-1	T _{m,n} ^{p+1}	Node in Current Timestep	-	-
Z _{lower}	Lower Boundary Height	m	-7.5	q _{rad,net}	Net Radiation Energy Transfer Rate	W	-
PS	Pipe Spacing	m	0.25 to 0.4	q _{conv}	Convection Energy Transfer Rate	W	-
\dot{V}_{man}	Heat Exchanger Manifold Flow Rate	Ltr/min	30 to 70	q _{cond}	Conduction Energy Transfer Rate	W	-
\dot{V}_{pipe}	Heat Exchanger Pipe Flow Rate	Ltr/min	3 to 7	q _{st}	Rate of Change of Stored Energy	W	-
T _{in}	Flow Temperature	°C	-	Fo	Fourier Number	-	-
T _{out(L)}	Return Temperature Lm of Pipe	°C	-	Bi	Biot Number	-	-
T _f	Farfield Temperature	°C	-	k	Ground Thermal Conductivity	W/mK	2.3
γ_{int}	Thermal Interference Factor	-	2	α	Ground Thermal Diffusivity	m ² /s	1.05E-06
\dot{m}	Pipe Mass Flow Rate	kg/s	0.05 to 0.12	ρ	Ground Density	kg/m ³	1600
c _p	Fluid Specific Heat Capacity	J/kgK	3748	c	Ground Specific Heat Capacity	J/kgK	1370
R _(L)	Total Resistance of Lm of Pipe	K/W	-	h	Surface Convection Coefficient	W/m ² K	-
R _{conv(L)}	Convection Resistance	K/W	-	q'' _{rad,net}	Net Radiation Flux	W/m ²	-
R _{cond,pipe(L)}	Conduction Resistance	K/W	-	q'' _{solar}	Solar Radiation Flux	W/m ²	-
R _{cont(L)}	Soil Contact Resistance	K/W	-	a _{sur}	Surface Solar Albedo	-	0.2 to 0.4
R _{cond,soil(L)}	Soil Conduction Resistance	K/W	-	q'' _{thermal,in}	Incoming Thermal Radiation Flux	W/m ²	-
$h_{(L)}$	Fluid Convection Coefficient	W/m ² K	-	q'' _{thermal,out}	Outgoing Thermal Radiation Flux	W/m ²	-
k _{pipe}	Thermal Conductivity of Pipe	W/mK	0.41	u _{wind}	Wind Speed	m/s	-
k _{soil}	Thermal Conductivity of Soil	W/mK	2.3	q _{source,nom}	Nominal Extraction Rate	W	1.08 x 10 ⁴
k _{fluid}	Thermal Conductivity of Fluid	W/mK	0.577	q _{sink,nom}	Nominal Rejection Rate	W	-
Nu _{D(L)}	Nusselt Number for Lm Pipe	-	-	%on-time	Percentage Duty	-	-
Re _D	Reynolds Number Internal Flow	-	-	q'' _{he(L-1 to L)}	Local Heat Exchanger Flux	W/m ²	-
Pr	Prandtl Number of Fluid	-	25	T _{ave}	Mean Annual Ground Temperature	°C	11.7
q _(L)	Heat Extraction Rate of Lm Pipe	W	-	Amp	Amplitude of Surface Fluctuations	°C	7.2
$\bar{q}'_{(L)}$	Average Extraction Rate per Meter	W/m	-	T _{max,ave}	Average Summer Maximum	°C	18.9
q' _(L-1 to L)	Local Extraction Rate per Meter	W/m	-	T _{min,ave}	Average Winter Minimum	°C	4.5
$\beta_{(L-1 to L)}$	Beta (Ratio of Local to Average q')	-	-	t ₀	Celestial vs Calendar Time	s	2.18 x 10 ⁷
$\phi_{(L)}$	Steady State Calculation ΔT Factor	-	-	ω	Angular Velocity of Earth's Orbit	rad/s	1.99 x 10 ⁻⁷

User Evaluations of Energy Efficient Buildings – Literature Review and Further Research

Å. L. Hauge*, J. Thomsen** & T. Berker***

* SINTEF Building and Infrastructure, P.O.Box 124 Blindern, 0314 Oslo, Norway

**SINTEF Building and Infrastructure, Alfred Getz vei 3, 7465 Trondheim, Norway

***Centre for society and technology, dep. of interdisciplinary studies of culture, Norwegian university of science and technology, NTNU, 7491 Trondheim, Norway

ABSTRACT

This paper is based on a review of research that describes user experiences with different types of energy efficient buildings, focusing on indoor climate, technical operation, user attitudes, and general satisfaction. Energy efficient buildings are often rated better than conventional buildings on indoor climate, but when investigating more thoroughly, the users have different concerns. The varying results from the user evaluations reflect that the quality of the buildings differs. However, user concerns may also be a result of inappropriate use. Perceived personal control and sufficient information on operation and use is crucial for an overall positive experience of the building. Three areas for further research could be identified: There is a shortage of research that takes into account the social context for evaluation. The social environment, the process of moving into an energy efficient building, and prior knowledge on environmental issues, influences the evaluation of the building. Energy efficient buildings may also require specific architectural solutions, and further research should consider architectural and aesthetic aspects in the evaluation. Research on use and operation of energy efficient buildings is increasing, but there is still a need to give more detailed attention to different ways of providing information and training in operation and use.

Keywords: User evaluations, POE, energy efficient buildings, passive houses

INTRODUCTION

In the end, the performance of buildings depends on the users. Therefore, it is important to focus on users' experiences with different types of energy efficient buildings. There exists a well-known gap between predicted and actual performance of energy efficient buildings. In some cases, actual performance is quite different from predicted performance, especially for the first years (Hinge *et al.* 2008). A study by the New Building Institute (2008) found that 30% of LEED¹-rated buildings (Leadership in Energy and Environmental Design) perform better than expected, 25% perform worse than expected, and a handful of LEED buildings have serious energy consumption problems. These problems may be caused by technical failures, too high expectations, or by inappropriate operation and use.

Bordass *et al.* (2004) suggest that the gap between a building's expected and actual energy consumption “*not so much arise because predictive techniques are wrong, but because the assumptions often used are not well enough informed by what really happens in practice because so few people who design buildings go on monitor their performance*” (Bordass *et al.* 2004:1).

Hinge *et al.* (2008) do also point to the use of the buildings, and the meaning of the role and active involvement of building operators and facility management to explain this gap. In order to reach a building stock that has zero emission of greenhouse gases related to them, it is not only crucial that the building operation is comprehensible, and that people get the information they need to operate it, but also that they will want to live and work in zero emission buildings. Therefore, it is essential to take into consideration the use and implementation of these buildings.

Concerning usability, there are many aspects in common for all types of energy efficient buildings. The evaluation of energy efficient buildings from a user perspective includes research on the experience of indoor climate, heating, light, ventilation, local energy production and other technical installations, in relation to experienced housing quality in general. In this paper, “energy efficient buildings” is used as a collective term for different types of buildings made to reduce energy consumption to different degrees. The research presented includes studies on low-energy buildings, passive houses, LEED buildings and green buildings. The research is thematically categorized as “indoor climate”, “technical operation”, “user attitudes”, and “general satisfaction”.

1. INDOOR CLIMATE

1.1 Residential Buildings

Are the users satisfied with the indoor climate in energy efficient buildings? Isaksson & Karlsson (2006) has investigated the thermal environment and the space heating in 20 low-energy terraced houses in Lindås, south of Gothenburg, Sweden. They applied qualitative interviews with the occupants as well as measurements of physical parameters. The heating system in the terraced houses in Lindås is based on the emission of the household appliances, the occupants' body heat, and solar irradiation. Many agree that the heating system functions well. However, during wintertime when the heater is on, varying indoor temperature is experienced. The study shows that people experiment with warming up the house, as for instance by leaving doors open and lighting candles. When the houses are empty for some time, it takes half a day to warm it up. Therefore, some of the residents leave the heating on when they are away. Interestingly, when comparing the residents' opinions to the measured parameters, there were main differences between the measured indoor temperature and the occupants' experience of the thermal environment. The indoor temperature was often higher than experienced, indicating that the subjective experience differs from person to person (Isaksson & Karlsson 2006).

Another study on residential satisfaction with the indoor climate is a diploma work by Samuelsson & Lüdeckens (2009). They did a survey on three different passive houses in Sweden. Questions were asked about experienced temperature and temperature variations, draughts, and perceived indoor climate. They have also calculated the energy consumption and simulated the indoor climate for two of the projects. The results between the two models do not vary a lot, neither in terms of energy consumption, nor in terms of heating. The models

indicate that in theory, the heating unit is enough to heat up the houses during the winter. The results from the survey show, however, experienced problems with the indoor temperature during the winter. Especially in one of the three projects, where more than 50 per cent of the residents report that it is too hot in the summer and too cold in the winter. They criticised that they cannot adjust the temperature, and that weather conditions influence the indoor temperature. They also report temperature differences of 3-4 C between rooms during wintertime and that the ventilation system did not function sufficiently. They had to use additional heating during winter, which influenced the use of electricity. Similar discrepancies between the findings of the different methodologies (evaluation and simulation) were found by Isaksson & Karlsson (2006). Samuelsson & Lüddeckens (2009) state that the problem with the simulation model is that it cannot simulate reality in a sufficient way, and that it might not capture the problems experienced by the residents. Samuelsson & Lüddeckens (2009) cannot give a clear answer to why the residential satisfaction with the indoor climate differs between the cases. Their discussion shows how difficult it is to comprehensively predict indoor climate through simulations. Another challenge is the fact that people experience temperature and draughts differently.

Buber *et al.* (2007) investigated the meaning of the terms comfort, well-being, cosiness, and housing comfort in relation to experienced housing quality in passive houses. The personal opinions of residents were investigated in focus group interviews. Results show that the type of heating had a crucial influence on housing comfort, and thus on the well-being of its residents. None of the residents interviewed would have agreed on moving to a house that is just heated by the ventilation system. They wanted to have an additional heating, such as wall heating or wood pellet ovens. The visual and sensible effects were of importance for perceived comfort. In regard to fresh air supply, the ventilation system with frequent air exchange was seen as imperative for a high level of comfort.

In conclusion, studies of thermal comfort show that the way indoor thermal environment is evaluated depends on the relationship between people, climate and building and can vary over time (Nicol & Roaf 2005). This can explain the difference between experienced comfort and simulated indoor climate found by Samuelsson & Lüddeckens (2009). When users living in passive houses declare that they miss a fire place or wish for an additional heating it reflects that the feeling of a comfortable indoor climate is influenced by visual or sensible signs of heat. Differences between perceived and measured temperatures show that user satisfaction in domestic spheres includes subjective factors. While this is true for most evaluations, homes may be considered to be special ‘territories’ (Morley 2009) where demands for comfort are particularly high (Aune 2007).

1.2 Occupational Buildings

Leaman & Bordass (2007) have studied if occupational buildings designed for lower environmental impact are better than conventional buildings from the occupants’ point of view. They compared user experiences through surveys in 177 conventional buildings, with mixed modes or air conditioning, and green buildings, with natural or advanced natural ventilation. They found that green buildings scored better on: ventilation/air, health, design, image, lighting, overall comfort, and perceived productivity. While the best green buildings ranked higher than the best conventional buildings, a few of the lowest scores were also attained by green buildings. Many of the green buildings were experienced as too hot in summer, and seemed to have more ambient noise. The experience of indoor climate may also

be related to whether the occupants have single offices or open plan layout. In a single office an employee is more in control over the temperature, ventilation, lighting, and noise.

An article by Heerwagen & Zageus (2005) evaluates the Philip Merrill Environmental Center in Annapolis, Maryland, an educational institution. A survey on indoor environmental quality was distributed and a series of interviews and discussion groups were conducted. The findings show that occupants were highly satisfied with the building. Air quality, daylighting and artificial lighting, as well as the access to views, were rated positively by close to 90 per cent of the respondents. The evaluation also revealed critical aspects. Acoustic conditions, and also temperature conditions, noise distractions due to the open landscape, insufficient provision of meeting rooms, and glare from windows caused some concerns (Heerwagen & Zageus 2005).

Wagner *et al.* (2007) have also made a survey on workplace occupant satisfaction in 16 office buildings in Germany. This survey revealed that the occupants' control of the indoor climate, and moreover the perceived effect of their intervention, strongly influence their satisfaction with thermal indoor conditions. Another study by Barlow & Fiala (2007) also focuses on the occupants' ability to control the indoor climate, and how this increases their thermal comfort. They suggest that active adaptive opportunities should be made an important part of future refurbishment strategies for existing office buildings. In the study, opening windows was voted to be the most favourite adaptive opportunity followed by controlling solar glare, turning lights off locally and controlling solar gain. Occupants also expressed desires to intervene with heating and ventilation currently operated centrally.

The studies presented on user evaluations of indoor climate in energy efficient occupational buildings are *in general positive*, but when investigating more thoroughly, the users have complaints and frustrations that are important to notice. Different from residential buildings, control in occupational buildings is, at least in part, delegated to centralised control systems. Comfort experience varies greatly between individuals – what one person experiences as chilly may be too warm for another. This leads to many ways in which individuals manage comfort in their work environment, some of which may outright counteract the designers' intentions (Heerwagen & Diamond 1992, Hitchings 2009). Therefore, the users' perception about their ability to control the indoor climate is of great importance.

2. TECHNICAL OPERATION

2.1. Information and Knowledge

Leaman & Bordass' (2007) study of the difference between user satisfaction on green and conventional occupational buildings shows that users tend to have a higher tolerance for deficiencies in green buildings than in more conventional buildings. People seem to tolerate more discomfort in a green building *the more they know about how the building is supposed to operate*, and how they can use for example thermostats and window controls. Users are much less satisfied when they cannot understand how things work or how to control temperature and ventilation (Nicol & Roaf 2005, Leaman & Bordass 2007). Information on use and operation of technical facilities is therefore crucial.

The indoor climate in a residential building at Husby Amfi in Stjørdal was in general experienced as comfortable (Kleiven 2007). 70 per cent of the residents used the energy operating panel in these flats, and most residents experienced them as user friendly, intuitive, and simple. Most residents also put their flats into standby mode when they left, however, a

few residents found the energy operating panel difficult to understand. They wondered if it didn't work, or said that they had not been well enough trained in operating it. The flats had a web-based follow-up system for energy use, but this system was barely used, as it was experienced as too advanced.

In Isaksson (2009) and Isaksson & Karlsson's (2006) investigation of the houses in Lindås, the interviews showed that knowledge about the heating system was an important issue for the residents. Some residents told the authors that they did not have sufficient information about the heating system when moving in. Consequently, they tested the system during the first winter, something that resulted in varying indoor temperature and higher energy costs. The process of operating the energy system was a dynamic learning process. Isaksson (2009) emphasises the importance of learning-by-doing in operating energy efficient technology and concludes that implementing energy efficient buildings is not just a question of developing new technologies, but the great challenge is that "*tools must be developed that support people to choose the sustainable ways to use the new technology*" (Isaksson 2009:195).

To summarize, the studies show that the operation of energy efficient buildings may be difficult for the users, and that if the technology is experienced as too advanced, they are not used or not entirely understood. This may lead to uncomfortable indoor climate. The research also shows, once more, that perceived personal control and sufficient information on operation and use is crucial for an overall positive experience of the houses.

2.2 Motivation to Operate Energy Efficient Housing

Schnieders & Hermelink (2006) evaluate residential satisfaction with passive houses in two CEPHEUS projects (Cost Efficient Passive Houses as European Standards), Hannover-Kronsberg and Kassel. The development of the residents' opinions, attitudes, behaviour, and satisfaction over time were recorded. Several studies have shown a high level of satisfaction with living in the passive houses in Hannover-Kronsberg. The building in Kassel is the world's first multi-story passive house. The main difference between the projects in Hannover and Kassel is the type of occupancy. The houses in Hannover-Kronsberg are owner-occupied and therefore represent typical passive houses. This is in contrast with the multi-story passive house with 40 flats for low-income tenants. The project was built at low costs by a social housing company. A hypothesis was that the demand for heating energy might be much higher in the Kassel project than in other, owner-occupied cases because "*Tenants usually do not identify themselves as much with their dwelling and its characteristics as owners do. Therefore the motivation to deal with unfamiliar technologies and the willingness to change customs might be lower*" (Schnieders & Hermelink 2006:162).

The study investigated the tenants' ventilation behaviour. Keeping the windows shut is an important factor to keep the ventilation rate steady. The results showed that in general, the "forbidden" ventilation through windows stayed within a tolerable range that did not upset the energy balance as such. More interestingly, residents who showed a high level of window-ventilation expressed a low opinion of the controlled ventilation, probably because they interfered with the system which consequently did not work properly. The maximum ventilation switch is situated in the kitchen and the location leads to the misconception that it is dedicated only to kitchen odours, even though it affects the whole flat, including the toilet and bathroom. When an information letter was sent out, the use of maximum ventilation increased immediately. Prior to the first winter, many expressed worries that the ventilation system without additional radiators would not be enough to keep the flats warm. This scepticism was altered after the first winter. The average of satisfaction with the ventilation

system heating the flats was 4.7 on a scale from 1- 6. It was also assessed whether the residents were of the opinion that living in a passive house increased or decreased comfort. The results indicate a perceived increase of comfort. Most of the tenants adapted to the new building quickly and “*very easy control of the ventilation, very high thermal comfort and air quality make the tenants feel very comfortable. In addition, they are realizing that costs for heating are extremely low*” (Schnieders & Hermelink 2006:162).

This study indicates that type of occupancy is not necessarily relevant for the motivation to operate energy efficient buildings, or to identify with them, if good information on operation is provided and personal advantages are understood. The study also shows that user evaluations have to take into account what the occupants know and that their knowledge may be subject to change. Brown & Cole (2009) compared occupants in a conventional and a green building in British Columbia. They found that users in the green building were more interested in learning how the building and its controls work. However, while those who knew more about their building’s inner workings used the controls more extensively, they did not report higher degrees of perceived comfort. Thus, even though cognitive aspects like knowledge and learning are central for a well-functioning energy efficient building, and should be improved through easy to use controls and appropriate guidance and feedback, there are other factors at play. Furthermore, users have certain expectations towards energy efficient buildings.

3. USER ATTITUDES

3.1 Choosing an Energy Efficient House

Research shows that energy efficient houses are mainly bought or chosen for other reasons than the energy profile. Isaksson & Karlsson’s (2006) findings in the user evaluation of housing in Lindås show that the low-energy profile of the houses was positively evaluated, but the inhabitants’ main reason for moving there were the location and getting value for the money. Buber *et al.* (2007) state that passive houses are usually advertised as “houses without heating” and not as “comfortable houses”, even though housing comfort aspect is a crucial argument for potential (passive) house buyers, while the environmental effect might just be a side-effect for many.

Schnieders & Hermelink’s (2006) study of the Kassel project also focuses on the residents’ reasons for moving in. The first advertising campaign for flats was aimed at passive house characteristics and low energy demand. The response to this campaign was weak and only after advertising other characteristics such as attractive location, balcony and new buildings there was a great response.

In the study of the flats in Husby Amfi, the low-energy concept of the flats was important for only 1/3 of the buyers. Interestingly, most of the residents answered that living in a low-energy building had made them more aware of energy use and environment friendly behaviour (Kleiven 2007)

As a conclusion, energy efficient buildings are seldom sold due to their energy profile, but due to other aspects such as preferred location or having a balcony. Nonetheless, most residents seem to appreciate the environmental benefits over time, and become more aware of environmental issues. By the time the positive aspects of energy efficient buildings become

more generally acknowledged, the energy profile of buildings may become a more relevant marketing factor.

Regarding the findings that other aspects than the environmental profile are important for marketing energy efficient buildings, it is noteworthy that there are very few studies on aesthetic or architectural preference as perceived by the users. It can be assumed that architecture and aesthetics are important factors when choosing a house (Thomsen 2008). Architectural preferences in energy efficient buildings are not a main focus of any of the studies reviewed.

3.2 General Satisfaction

There are however, a few studies that evaluate more than indoor climate and operational aspects. They cover general satisfaction and the concept "comfort" in these studies is used in a wider sense than "thermal comfort". It may for example include comfort in relation to light, architecture and aesthetics.

This research is interested in if the improved thermal comfort and the architectural qualities affect the users' performance and well-being. Some of these studies indicate that energy efficient buildings have a positive impact on comfort, performance and well-being, other studies do not. Heerwagen and Zargeus' study on user evaluation of the Philip Merrill Environmental Center (Heerwagen & Zargeus 2005), focused on the impact of the different passive house features on the respondents' ability to work. Both temperature and acoustics were named as the conditions that can contribute positively, but that also can interfere with working abilities. Even though acoustics was a concern, the detailed assessment shows that most of the respondents seem to be able to concentrate and achieve privacy when needed. Lighting (74 per cent) and air quality (61 per cent) conditions in the centre were rated as enhancing the ability to work. For the Philip Merrill Environmental Center, also the building's overall aesthetics were named as a positive aspect. The educational institution had open plan offices that housed a staff of about 90. Social benefits such as improved communication and sense of belonging are linked to the buildings' design, as well as perceived psychosocial benefits. About 80 per cent experienced a high level of well being and sense of belonging at work, and 97 per cent felt proud when showing the office to visitors (Heerwagen & Zargeus 2005). Factors that influenced working ability negatively were distractions, interruptions, uncomfortable temperatures, and glare from windows. The authors also compare the results of the survey with results from evaluations of other LEED buildings that could be found in the database maintained by the Center for the Built Environment (CBE) in 2005 at the University of California, Berkeley and the results clearly show differences in user satisfaction with these LEED buildings. The Merrill Center is number 2 in the entire database (170 buildings) for overall satisfaction with the building. This is also a much higher score than any other of the LEED buildings achieve. The comparison of conventional buildings and LEED buildings also shows that LEED buildings in general are not equivalent with high user satisfaction.

Heerwagen & Zagreus (2005) indicates that energy efficient buildings can have a positive impact on well-being and daily performance while other studies do not confirm this. Paul & Taylor (2008) for instance, conclude that their study revealed insufficient evidence to support the hypothesis that green buildings are perceived as more comfortable than conventional buildings. They measured occupants' perception of comfort and satisfaction in three university buildings in Australia, one green building and two conventional university buildings. The survey found no evidence that the green building is perceived more

comfortable than the conventional buildings. The aspects of aesthetics, serenity, lighting, ventilation, acoustics, and humidity, were not perceived differently by the occupants of the two types of building, and the authors state that they were surprised by these findings (Paul & Taylor 2008).

In conclusion, these studies, which are based on more comprehensive accounts of comfort, show how the overall level of user satisfaction is influenced by a broad variety of factors. Floor plans, design, noise levels and many other parameters determine how occupants experience a building. The important finding of these studies, therefore, may be that there is not determinism in the relation between energy efficiency and user satisfaction: energy efficient buildings *can* be experienced very positively, but this depends on many other factors.

4. CONCLUSIONS AND FURTHER RESEARCH

Some buildings function very well and have a positive impact on well-being and performance, others do not. Some buildings have operational systems that are difficult to understand, or the users have not received good enough information on how to operate them. These in part contradictory results of the research presented above show that the connection between energy efficiency and user satisfaction in buildings is more complex than is usually assumed. Concluding, we propose three ways of improving the evaluation of energy efficient buildings:

4.1 The Meaning of Social Context in Evaluation of Energy Efficient Buildings

Heerwagen (2009) and Paul & Taylor (2008) state that in order to test the hypothesis that green buildings are perceived as more comfortable, and contribute to a healthier and better living and working environment, several case studies have to be conducted. The findings by Heerwagen (2005; 2009) are controversial to the findings by Paul & Taylor (2008). The articles of Heerwagen indicate that green buildings increase comfort, well-being and work performance, while Paul & Taylor (2008) could not find differences in perceived comfort between a green building and two conventional buildings. The differences in findings may be due to the features of the buildings, but as well to the attitudes and preferences of the users, e.g. whether they can identify with the concept of energy efficient building. When comparing energy efficient buildings with conventional buildings, it is important to consider the social context of the users, and process behind the building.

The research presented often lacks focus on the meaning of the social context, or it lacks focus on the attitudes and meaning the users associate with the building. Leaman & Bordass (2007) state that users tend to have a higher tolerance of deficiencies in “green buildings” than they do in more conventional buildings. This implies that image and process mean something for the evaluation of the building. According to Vischer (2008), it is important to conduct user evaluations of buildings on more than one level. Contextual variables cannot be ignored. Users in a new occupational building may be happy about receiving a completely new building, no matter if it is energy efficient or not. A new building signalizes that the employees are worth something, and it may contribute to a company’s positive image. It is then easier to evaluate a building as positive, and ignore frustrations with ventilation and comfort. In the same way, evaluations of occupational buildings may also be coloured by conflicts with leaders, colleagues, and a difficult organizational environment. Residential buildings are also evaluated on the background of the residents’ knowledge of the building

they live in. If the building has received attention in the media and among researchers, this will affect the evaluations.

The wish for an environmental friendly image or the wish to be ordinary may also colour the building evaluations. The intentions of the different stakeholders at Lindås Park was not to build housing that appealed only to environmental conscious people, but to ordinary people (Isaksson & Karlsson 2006). Indeed, there are only a few residents who see themselves as environmentally engaged persons, who found the environmental aspects important when choosing the house. They expected to use less energy than in a conventional house, and wanted to reduce their impact on the environment, which they perceived as an important contribution to their family and to nature (Isaksson & Karlsson 2006). Most of the other residents characterise themselves as being average people when it comes to environmental friendly living. This also corresponds with the image that the stakeholders wanted to promote when marketing the houses. However, Isaksson (2009) emphasises that both constructing and buying a passive house is something beyond the prevalent norm. It is most likely that people buying passive houses are aware of that. Going beyond the norm can also be viewed upon as "extreme" by outside observers. This might be appreciated by some of the residents, but not by others, who rather choose to characterise themselves as the "norm". Even though the majority of the residents names other reasons than the low energy profile as reasons for choosing a house at Lindås Park, they were aware of the concept in advance, and they have to handle it in their everyday life. That implies that the people who look upon themselves as "average" have to develop an attitude towards it as well. Maybe they even feel that they have to "justify" their choice to outsiders. This may be one reason why people seem more likely to tolerate deficiencies in low energy buildings than in conventional buildings. It is therefore crucial to map the context of the building evaluation, the users' attitudes, and their knowledge of the building.

- Future user evaluation should include focus on social context, process and image for a better understanding of why a building is evaluated the way it is. This also implies the significance of being aware of the gap between the outcome of simulations and experienced reality in indoor climate energy efficient buildings.
- Evaluations should focus on the users' reasons for choosing to live in energy efficient buildings, to be able to give input to how to market energy efficient buildings.

4.2 The Meaning of Architecture and Aesthetic in Energy Efficient Buildings

It has been mentioned previously that the architecture and aesthetics of energy efficient buildings may have a meaning for the users. There is a lack of research on this topic and very few of the studies presented have focused on the architectural and aesthetic aspects of the energy efficient buildings evaluated.

An energy efficient approach influences the design and layout of a building through for instance orientation or limited window area, material use, and construction. It is commonly acknowledged that a building's appearance mediates information about its purpose and use, and that architectural aspects can have a significant influence on user satisfaction (Thomsen 2008). Therefore it should be of interest whether the premises of energy efficient building results in specific architectural expressions, and how the aesthetics of energy efficient buildings are perceived and influence user satisfaction. Do the users find energy efficient architecture as aesthetically appealing, can they identify with it, and what role does the aspect of aesthetics play when choosing to live in an energy efficient house? Further research should

investigate these questions as they are main aspects of successful and comprehensive architectural concepts.

- Future evaluations should include more than indoor climate, temperature, air quality and operational aspects. Important aspects are perceived architectural quality and aesthetics, as well as light conditions.

4.3 The Meaning of Information and Training in Operation of Energy Efficient Buildings

Difficult energy operation systems are a common theme in the research presented, and is central to focus on in future building. It is of importance to make the operation of buildings understandable to the users to increase control over work or home environment, as well as to ensure the buildings optimum performance.

The lack of instructions on the adequate use of the building is a typical reason that people mention when having problems with the operation of their house or at their workplace (Kleiven 2007). In the study by Schnieders & Hermelink (2006) the handling of the ventilation system is not entirely understood. The maximum ventilation switch is situated in the kitchen and the location leads to the misconception that it is dedicated only to kitchen odours. Other problems they observed could be solved by better informing the residents about requirements, e.g. changing filters more often to avoid noise from the ventilation system. Schnieders & Hermelink (2006) also state that the results of informing people often are better if a qualified person explains and demonstrate the handling of the system as soon as a tenant moves in, rather than to provide written information. Also Isaksson (2009) points out that complicated technical descriptions are seldom read by users, especially if they are not interested in technical innovations. Only if the users can operate the building, the performance of the building will be close to calculations in the planning phase.

There is a lack of research on detailed evaluations of operation systems, and how information and training on use and operation should be given. How should energy operating panels be designed? Should there be differences according to resident groups and system operators? In what ways should information on use and operation be provided? How much information is needed, and should there be feedback on operation of energy efficient buildings over time?

Buildings and their users change over time (Brand 1995). Longitudinal studies focusing on operation and maintenance over years are significant for planning better and more usable energy efficient buildings.

- Future evaluations should be longitudinal, and focus on operation and maintenance over time.
- User evaluation must include a detailed focus on different types of user friendly operating systems. They should include a detailed focus on different ways of providing information and training for the users and system operators in energy efficient buildings.

References

- Aune, M., 2007, Energy comes home, *Energy Policy*, vol 35, p. 5457-5465
- Barlow, S., Fiala, D., 2007, Occupant comfort in UK offices - How adaptive comfort theories might influence future low energy office refurbishment strategies, *Energy and Buildings*, vol 39, p. 837-846
- Bordass, B. et al., 2004, Energy Performance of Non-Domestic Buildings: Closing the Credibility Gap, *Building Performance Congress*, Frankfurt, Germany
- Brand, S., 1995, *How buildings learn: what happens after they're built*, Penguin Books
- Brown, Z., Cole, R.J., 2009, Influence of occupants' knowledge on comfort expectations and behaviour, *Building Research & Information*, vol 37, p. 227-245
- Buber, R. et al., 2007, Wohnen in Passivhäusern. Der Einsatz des Fokusgruppeninterviews zur Identifikation von Wohlfühlkomponenten, in Buber, R., Holzmüller, H.H., (eds.) *Qualitative Marktforschung Konzepte - Methoden – Analysen*, Wiesbaden, Gabler Verlag
- Heerwagen, J., Zagreus, L., 2005, *The Human Factors of Sustainable Building Design: Post Occupancy Evaluation of the Philip Merrill Environmental Center*, UC Berkeley, Center for the Built Environment, retrieved March 2010 from <http://escholarship.org/uc/item/67j1418w>
- Heerwagen, J., Diamond, R.C., 1992, Adaptations and coping: Occupant response to discomfort in energy efficient buildings, in Economy A.C.f.a.E.E., (ed.) *ACEEE 1992 Summer School on Energy Efficiency in Buildings*, p. 83-90
- Heerwagen, J., 2001, *Do Green Buildings Enhance the Well Being of Workers?*, Retrieved November 2009 from:
<http://www.edcmag.com/CDA/Archives/fb077b7338697010VgnVCM100000f932a8c0>; 2001.
- Hinge, A. et al., 2008, Sustainability in commercial building: Bridging the gap from design to operations, *Green Building Insider* - 23 May
- Hitchings, R., 2009, Studying thermal comfort in context, *Building Research & Information* vol 37, p. 89-94
- Isaksson, C., Karlsson, F., 2006, Indoor climate in low-energy houses - an interdisciplinary investigation, *Building and Environment*, vol 41, p. 1678-1690
- Isaksson, C., 2009, *Uthålligt lärande om värmen? Domesticering av energiteknik i passivhus*, Dissertation, Linköping Linköpings Universitet
- Kleiven, T., 2007, *Brukerundersøkelse i Husby Amfi*, SINTEF Report SBF BY A07022, Trondheim, SINTEF Byggforsk
- Leaman, A., Bordass, B., 2007, Are users more tolerant of 'green' buildings?, *Building Research and Information*, vol 35, p. 662-673

Morley D., 2009, *Home territories : media, mobility, and identity*, New York, Routledge

New Building Institute, 2008, *Energy performance of LEED New Construction buildings*, retrieved April 2010 from: <http://www.gbc.org>ShowFile.aspx?DocumentID=3598>

Nicol, F., Roaf, S., 2005, Post-occupancy evaluation and field studies of thermal comfort, *Building Research and Information*, vol 33, p. 338-46

Paul, W.L., Taylor, P.A., 2008, A comparison of occupant comfort and satisfaction between a green building and a conventional building, *Building and Environment*, vol 43, p. 1858-70

Samuelsson, M., Lüddeckens, T., 2009, *Passivhus ur en brukares perspektiv*, Växjö, Sweden, Växjö universitet

Schnieders, J., Hermelink, A., 2006, CEPHEUS results: Measurements and occupants' satisfaction provide evidence for Passive Houses being an option for sustainable building, *Energy Policy*, vol 34, p. 151-171

Thomsen, J., 2008, *Student housing - student homes? Aspects of student housing satisfaction*, Dissertation, Trondheim, Norwegian University of Science and Technology

Vischer, J.C., 2008, Towards a user-centred theory of the built environment, *Building Research and Information*, vol 36, p. 231-240

Wagner, A. et al., 2007, Thermal comfort and workplace occupant satisfaction - Results of field studies in German low energy office buildings, *Energy and Buildings*, vol 39, p. 758-769

Endnote:

¹LEED, Leadership in Energy and Environmental Design, is an ecology-oriented building certification program run under the auspices of the U.S. Green Building Council (USGBC). LEED concentrates its efforts on improving performance across five key areas of environmental and human health: energy efficiency, indoor environmental quality, materials selection, sustainable site development, and water savings.

Renewable energy application in zero emission buildings – a case study

M. Haase¹ and V. Novakovic²

¹NTNU, Department of Architectural Design, History and Technology, Trondheim, Norway

²NTNU, Department of Process Engineering, Trondheim, Noray

ABSTRACT

The largest potential for decreasing green house gas emissions, and therewith mitigating the effects of global climate change, comes from improving energy efficiency. Once this is done an efficient way of renewable energy supply with low related CO₂ emissions is needed.

Utilizing solar power in buildings is a topic which received much attention in the past twenty years. In Norway, the potential for building integrated solar applications have long been underestimated. New building codes that will be published later this year (2010) will demand a fraction of between 50% and 60% which shall be covered by renewable energy sources.

This paper investigates the potential of different renewable energy application (solar thermal, PV, and wind) in a commercial building (office) for energy efficient buildings with very low heating demand. A cost effectiveness analysis was done and a sensitivity analysis on some of the input parameter was performed. In addition, CO₂ emissions from operation and production phase were compared and evaluated.

The results show that some solar applications are more cost effective than others. To integrate solar applications can help to find cost effective solutions that minimize total CO₂ emissions of the building.

Keywords: energy supply, CO₂ emissions, renewable energy

1. INTRODUCTION

The Linesøy project aims at renovating an existing building structure towards a minimized energy use in the operation of the building. The project is now under development with a passive house concept that minimizes energy use. The building owners asked to find possibilities for up to 100% renewable energy supply on the site. Here, it was assumed that the building provides the same amount of energy produced on-site from renewable sources (sun and wind) as it consumes over the whole year.

The project owners wants to develop a multipurpose building with different areas and use of the building, see Figure 1 and 2. Around half part of the ground floor is a residential unit (140m²) whiles the rest of the ground floor and the basement are divided into multifunctional spaces and a small café (220m²). The total area of the building is estimated to be approximately 360m².

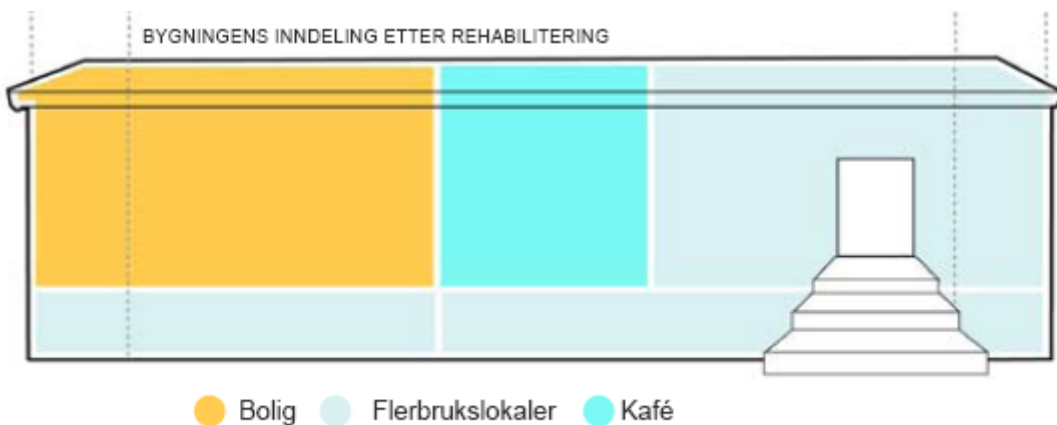


Figure 1: Functions of the building



Figure 2: Possible plan of the building with basement on the right and ground floor on the left

2. OBJECTIVES

The Linesøya project owner wanted to evaluate the potential of on-site renewable energy production and especially analyze cost implications.

The net zero energy concept was applied and CO₂ emission implications were determined.

3. METHODOLOGY

This report is divided into three steps. First, an energy budget was determined. Here, an estimate of areas used and installed power (according to NS3700) was made (NS3700, 2010). Assumptions about operation time for different parts of the building were determined which led to a calculation of energy demand (specific and total) with a division of energy need into heat and electricity.

Then, renewable energy supply for this project was determined. Here, estimations of solar radiation (monthly) and wind (annual) on the site was used to calculate a solar thermal system (for heat production), a PV system (for electricity production), and a wind turbine (electricity).

Finally, an economic analysis of the three systems was done by calculating investment and payback period of solar thermal system, PV system, and wind turbine. A comparison of results and analysis of saved CO₂ emissions gives a basis for possible decisions on an environmental investment strategy.

4. RESULTS

4.1 Energy budget

Then, an energy budget was estimated. As shown in Table 1 the residential area requires appr. 72 kWh/(m²a) total. Here, it was assumed constructing the building according to passive house standard (NS3700, 2010), with minimum heating need (only 1500h per year operation which leads to 15kWh/(m²a)) but with an additional heater for 420h of extra cold periods (as a safety measure). This is in total 25 kWh/(m²a) for heating purposes which is also discussed as a value in the passive house research community to be allowed in refurbishment projects.

The multifunctional part of the building (220m²) is assumed not to be operated in the winter. Thus, there is no energy budget for heating. The operation of the multifunctional part is limited to 900h per year reflecting the plan that it is used for events on weekends only. These assumptions lead to minimal energy budget of 22 kWh/(m²a).

Table 1: Energy budget for the Linesøya building

category	residential			office		
	power [W/m ²]	operation [h/a]	energy demand [kWh/(m ² a)]	power [W/m ²]	operation [h/a]	energy demand [kWh/(m ² a)]
space heating	23,8	420	10,0		not used in winter	
ventilation heating	10	1500	15,0		not used in winter	
domestic hot water	3,4	5824	19,8	1,6	900	1,44
fans and pumps	0,9	8736	7,9	0,9	900	0,81
lighting	1,3	5824	7,6	5,0	900	4,5
technical equipment	2,0	5824	11,6	6,0	900	5,4
cooling	-	-	-	-	-	-
cooling coil	-	-	-	33,3	300	10
sum			71,88			22,15

Total energy budget was calculated with the specific data and area data and divided into need for heat and electricity. Table 2 gives the sum for heating and electricity. Here, space and ventilation heating and warm water was assumed to be heat while electricity use was assumed for fans and pumps, lighting, technical equipment and cooling (assuming a heating system that is not based on electricity). With the assumptions described above the Linesøya project has an annual energy budget of 14937 kWh. This can be divided into 6589 kWh heat and 8348 kWh electricity. With these energy budget figures it is possible to estimate renewable energy supply systems.

Table 2: Annual energy budget

	heat kWh/a	electricity kWh/a	total kWh/a
space heating	1400		
ventilation heating	2100		
domestic hot water (DHW)	3089		
fans and pumps		1279	
lighting		2050	
technical equipment		2819	
cooling		2200	
cooling coil		0	
Sum	6589	8348	14937
kWh/(m ² a) (360m ²)	18.3	23.2	42

4.2 Renewable energy supply

PV system

In order to estimate the electricity that can be produced with a PV system the losses were estimated:

- Nominal power of the PV system: 10.0 kW (crystalline silicon)
- Estimated losses due to temperature: 7.7% (using local ambient temperature)
- Estimated loss due to angular reflectance effects: 3.0%
- Other losses (cables, inverter etc.): 14.0%

The combined PV system losses were thus estimated to 23.0%. Figure 3 gives the monthly produced energy of such a system.

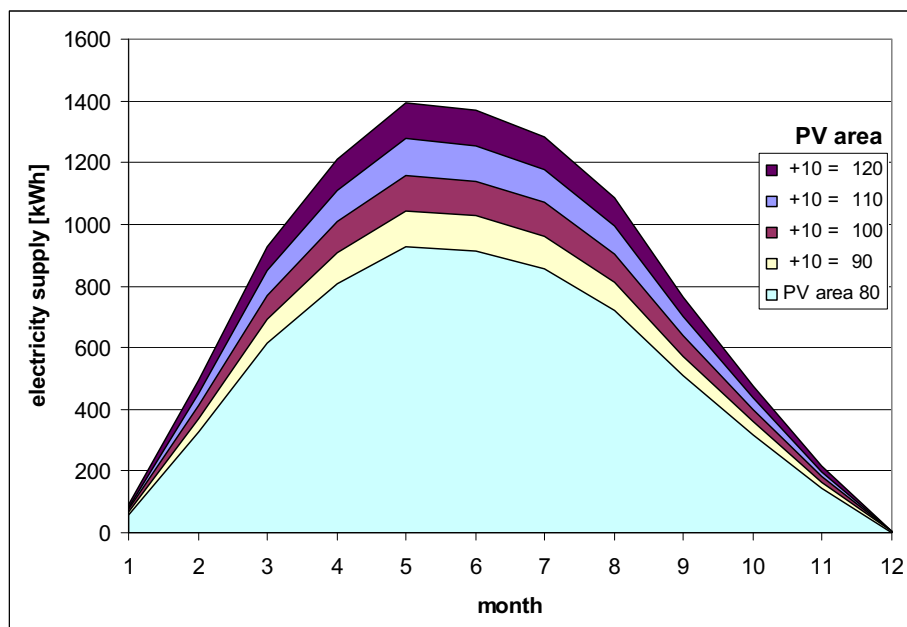


Figure 3: Estimated electricity production of PV system for Linesøya

Annual energy demand and production of electricity is shown in Figure 4. It can be seen that in order to match demand and supply the installed PV area needed is 108 m² (or 10.8 kWp installed power, assuming 10m² per kWp). But it can also be seen that a 10 % in demand changes the PV area needed by appr. 10m². If the estimated electricity demand changes due to changes in the use of the building, this will change the required area needed for PV modules (and related costs).

With estimated system costs of between 3.5 and 5 €/Wp (installed power) the PV system costs appear to be between 301260 and 430371 NOK (assuming 8NOK/€) which will give a simple payback period between 45 and 65 years (assuming constant saved energy costs of 0.8 NOK/kWh). Costs should be calculated taking integration effects into account (e.g. integrating PV in solar shading system and taking only extra costs into account). Assuming a necessary advanced shading system on the south facing façade with appr. 3500NOK/m² which will be integrated with a PV system (at 500€/Wp = 4000NOK/m²) will lead to 500NOK/m² extra costs for the PV system (with a simple payback period of 7.5 years). There are of course many assumptions in this calculation.

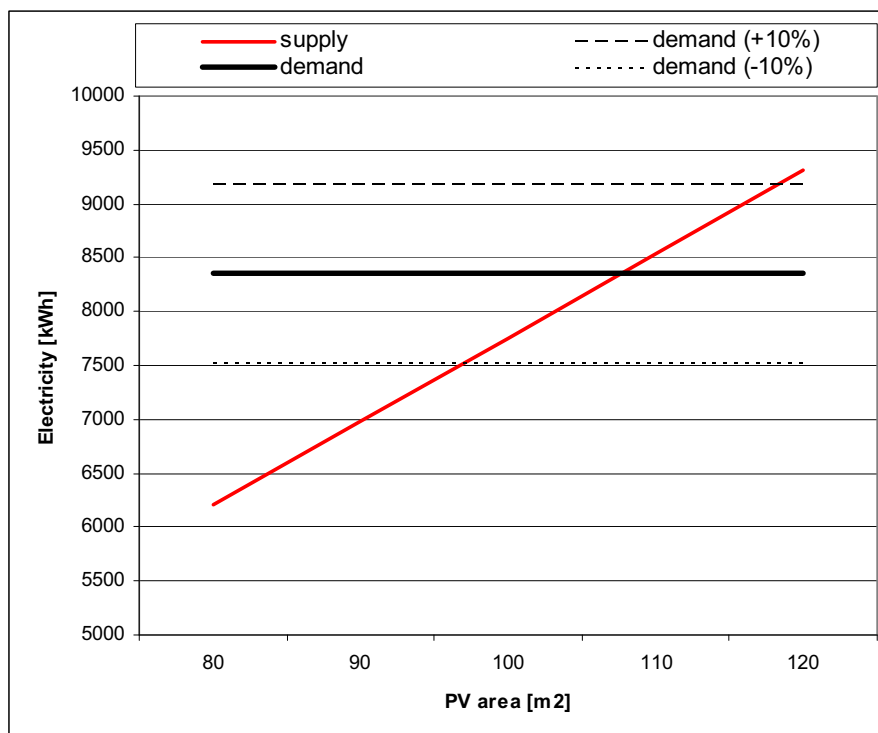


Figure 4: Annual energy demand and production of electricity

Solar thermal system

Figure 5 shows the relation of solar collector area to the solar fraction of a solar collector system for domestic hot water (DHW). This is based on a plate collector system with an inclination angle of 44 ° from the horizontal, oriented toward the south. Solar thermal system includes a storage tank of 200 liters. The annual DHW demand is 3000 kWh which is typical for a family of 3 persons (Andresen, 2008).

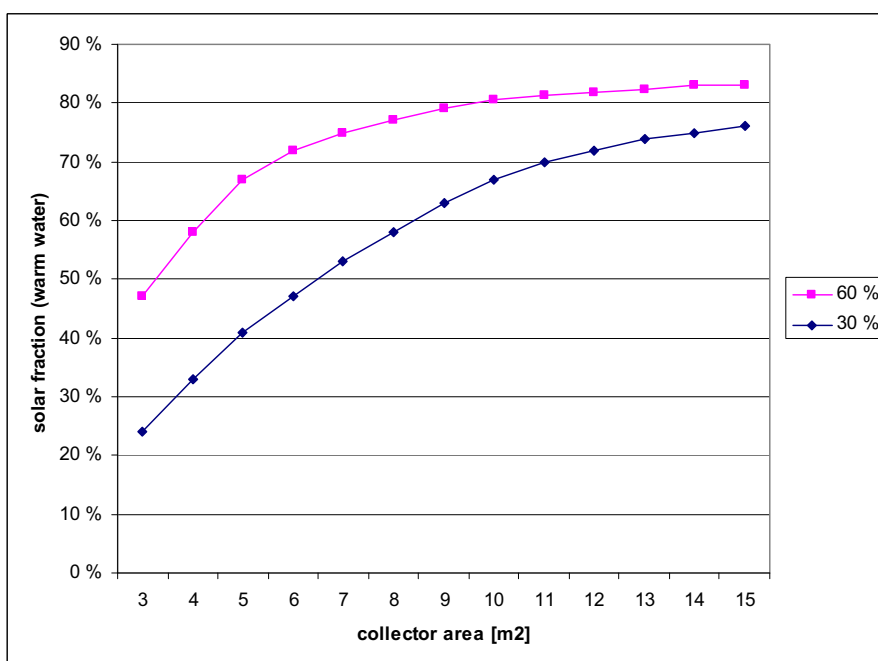


Figure 5: Solar fraction (domestic hot water) of two EPC systems (with 30% and 60% efficiency)

With a 7m^2 solar collector and system efficiency of 60% the heat supply was estimated and is shown in Figure 6. Here, different inclinations of the collectors were taken into consideration, reflecting different approaches of integrating them into the building. An inclination of 0° means horizontal collectors integrated into a flat roof while 30° and 44° indicate different roof angles or separate lifted installations. 90° inclination is relevant for integration in the vertical façade.

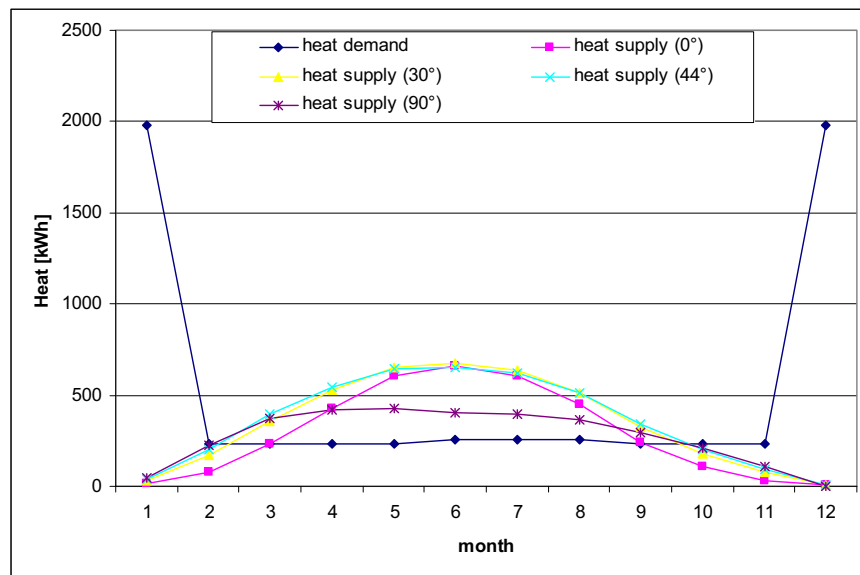


Figure 6: Heat demand and supply for different collector inclinations

It can be seen that there is a huge mismatch between delivered heat and heat demand (for heating and domestic hot water (DHW)). The heat demand during the winter cannot be covered with a solar collector while it produced excess heat during summer, spring and autumn (from March to September).

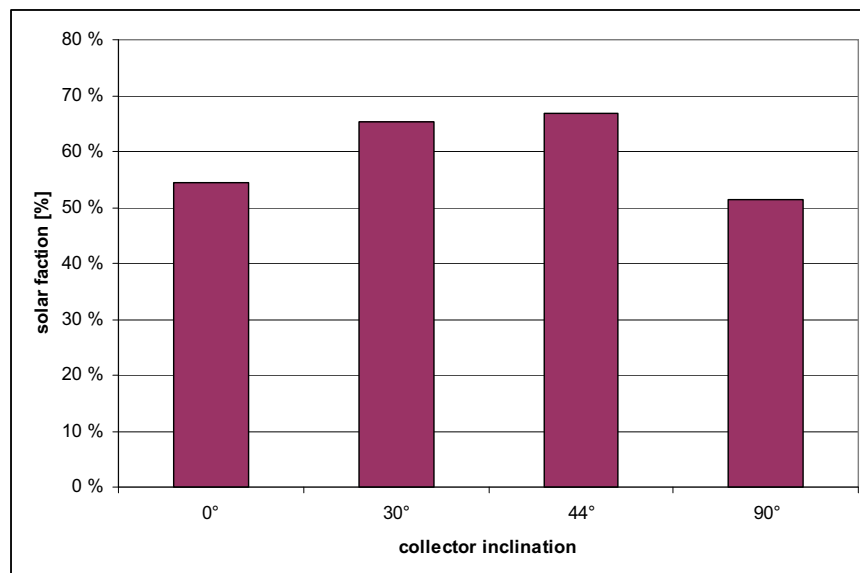


Figure 7: Solar fraction for different inclinations

Solar fraction for different inclinations was calculated and is shown in Figure 7. It can be seen that the inclination with 44° shows the highest solar fraction. This indicates that a solar

thermal system with this inclination manages to cover the maximum of heat. An increase in collector area would increase this annual solar fraction but is not recommended. The reason for that is that the solar thermal system is already sized large enough to cover the use of DHW. An increase in collector area would increase the production of heat when it is not needed. One possibility would be to examine a seasonal heat storage system that would enable to shift some of the supplied heat to the winter when it is needed. Such systems could consist of large buried and well insulated water tanks. Further investigation of such systems is recommended.

Mismatch between the different seasons was further analyzed and results are shown in Figure 8. All inclinations cover all heat demand (heating and DHW) during spring and summer. The solar fraction in winter is very low (due to the high heating demand) and ranges between 2.4 and 6.5 %. The inclination of 44° shows with 92 % the best solar fraction in the autumn season (and worst at 0° inclination with 55 %).

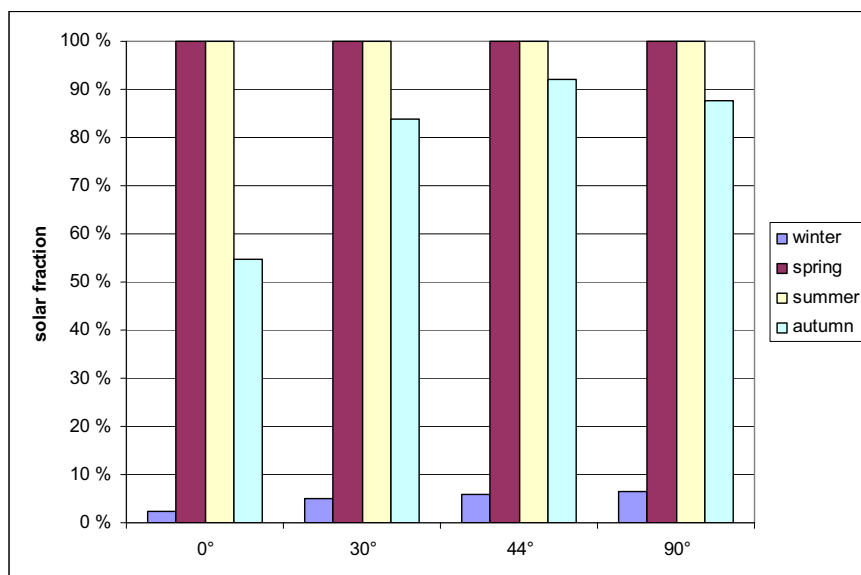


Figure 8: Mismatch between the different seasons

Additional costs for solar system relative to a conventional system based on only electricity will be appr. 30,000 NOK, because a hot water tank is certainly needed (cost 10,000 NOK). Solar heating plant is estimated to cover 60% of hot water needs, i.e. 2000 kWh / year. With an assumed average price of electricity at 80 cents / kWh, the following annual savings can be reached by replacing electric heating with solar heating:

Annual savings, $B = 2000 \text{ kWh} \cdot 0.80 \text{ NOK} / \text{kWh} = 1600 \text{ NOK}$. Simple payback period calculation results in a payback period of 19 years.

Wind turbine

For a 15m high wind turbine the electricity output of wind turbines was calculated using the formulas above. Calculations were done for two different capacity factors and different sizes of the rotors. The results are shown in Figure 9 where it can be seen that an increase in rotor size increases the electricity output (between 188 and 1176 kWh for 10% capacity factor) but the capacity factor is influencing the output to a large extent (between 1176 and 3530 kWh for the 5m radius wind turbine).

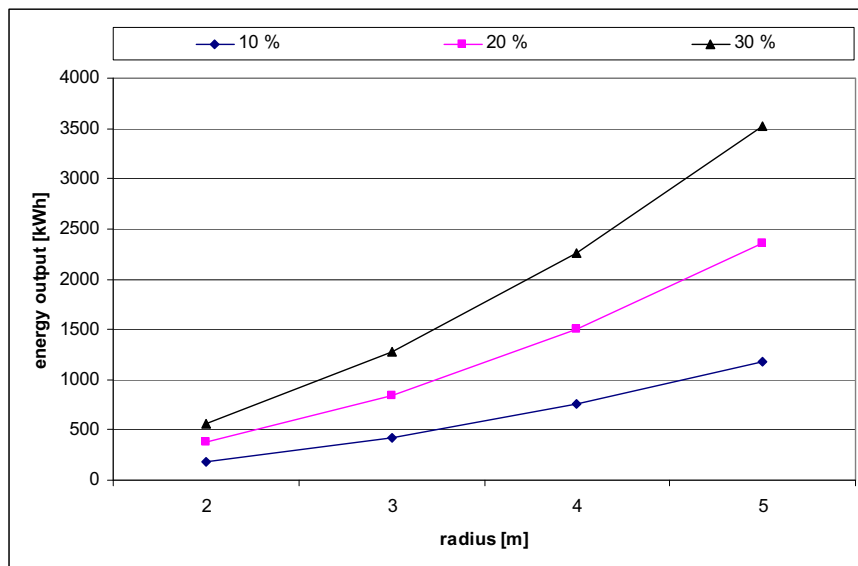


Figure 9: Energy output of different wind turbines and different capacity factors

According to BWEA (BWEA), the UK Government's Clear Skies grants programme "estimates that typical small system costs are €3000–6000 per kW capacity installed. The rooftop turbine market is still in the early stages of development, but manufacturers estimate that once mass production starts, an average 1–1.5 kW model will cost around €1250 per kW capacity installed. The cost of large, megawatt scale, wind turbines is today about €1000 per kW capacity."

The Swedish wind power society (Svensk Vindkraftförening, 2009) includes a survey of small wind turbines in Sweden. Investment costs are somewhat hard to compare due to variations of what is included in the price. Moreover, different models give rated power for different wind speeds, so a direct comparison of price per (rated) kW is unfair. Keeping these caveats in mind, a typical price seems to be in the order of 6000€/kW [16]. Assuming a 1.5 kW wind turbine for around 18000 NOK with 30% capacity factor will result in an annual energy output of 560 kWh. Simple payback period (assuming electricity costs of 0.8 NOK/kWh) results to 40 years.

4.2 Analysis and comparison

Table 3 summarizes the systems energy output, investments costs and simple payback period. It can be seen that none of the systems can deliver all energy needed. A mixture of systems should also take other energy supply systems into account (e.g. heat pumps). Especially solar thermal system is limited to a fraction of DHW supply and it became clear that heat supply for the heating season requires additional heat storage equipment. This should be investigated in the future.

Table 3: Renewable energy systems energy output, investments costs and simple payback period (at 0.8 NOK/kWh energy costs)

Renewable energy system	delivered energy [kWh]	investment costs [NOK]	Payback period [years]
Solar thermal system	2244	30000	16,7
PV system	8348	301260	45,1
Wind turbine	565	18000	39,8

The payback periods of three different energy supply systems range between 16 years (solar thermal system), 40 years (wind turbine), and 45 years (PV). An increase in energy costs would reduce the payback period of all systems.

Figure 10 shows results for simple payback period calculation for different energy costs. It can be seen that the payback periods is reduced most for PV and wind turbine systems. This is due to the higher energy savings of those two systems. But solar thermal system has higher savings than wind and PV. The lowest payback period still remains for the solar thermal system (11 years at energy costs of 1.2 NOK/kWh).

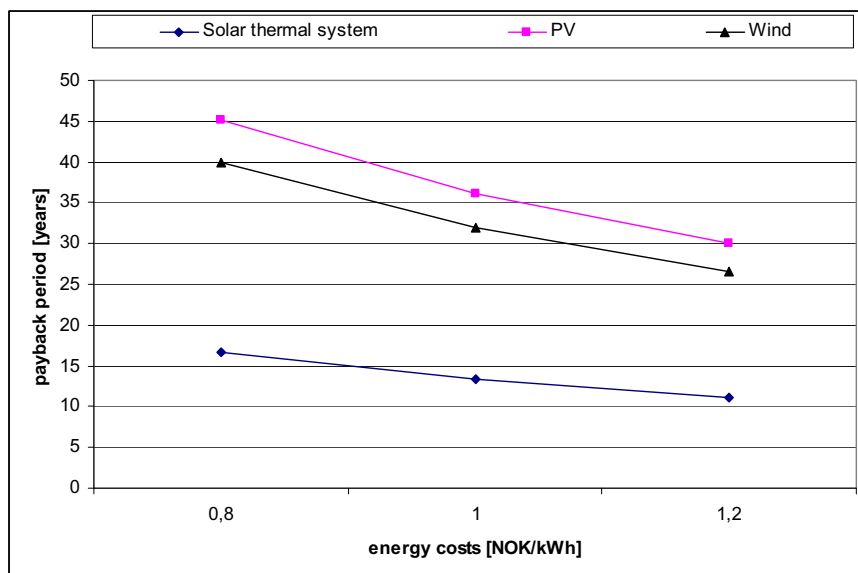


Figure 10: Payback period for different energy costs

Table 4: CO₂ factors for different energy sources (Hastings and Wall, 2007; NS-EN15603, 2008; Thyholt, 2006; Vold et al., 1999)

Energy system	CO ₂ -factor (g/kWh)
Solar thermal system ^a	51
PV system ^a	130
Wind turbine ^a	20
Biofuel ^b	14
District heating ^c	231
Gas (fossil) ^d	277
Oil ^d	330
Electricity from the grid ^d	617

^a taken from (Hastings and Wall, 2007)

^b taken from (Vold et al., 1999)

^c taken from (Thyholt, 2006)

^d taken from (NS-EN15603, 2008)

In order to calculate delivered energy and related CO₂ emissions according to the Norwegian building codes, calculation methods and CO₂ factors of different energy sources were collected in Table 4. There must be noted that there is no national agreement on the CO₂ factors and thus a great uncertainty in these figures, especially the CO₂ factors for electricity from the grid. Here, NS-EN15603 proposes to use provided figures until national figures are established. It can be seen that biofuel has the lowest related CO₂ emissions. Table 5 gives an overview of different energy supply system options with its related efficiencies that were

used to calculate delivered energy. Figures from Table 4 and 5 were then used to calculate the related CO₂ emissions. Results are shown in Figure 11

Table 5: supply systems efficiency according to (NS3031, 2007) and CO₂ factors according to Table 4

Supply system	1	2	3	4, 5	6,7	8,9,10	11,12	13,14
Supply of heating and hot water	el	oil boiler	gas boiler	DH	solar thermal	biofuel	biofuel/ PV	biofuel/ wind
efficiency factor	0.98	0.73	0.73	0.84	8.55	0.84	100	100
CO ₂ factor (g/kWh)	617	330	277	231	51	14	130	20
Supply of rest	el	el	el	el	el/ DH	el	PV	Wind
efficiency factor	0.98	0.98	0.98	0.98	0.98	0.98	100	100
CO ₂ factor (g/kWh)	617	617	617	617	617	617	130	20

el = electricity

PV = photovoltaic system

DH = district heating system

DHW = domestic hot water

Option 4: 50% supply of heating and DHW from DH, rest el.

Option 5: 100% supply of heating and DHW from DH

Option 6: 50% supply of DHW from solar thermal system, rest el.

Option 7: 100% supply of DHW from solar thermal system, rest DH

Option 8: biofuel boiler for heating and DHW

Option 9: biofuel CHP produces 100% heat (heating and DHW) with 30% el output

Option 10: biofuel CHP produces 100% electricity with heat production as by-product

Option 11: biofuel boiler for heating and DHW, PV system produces electricity

Option 12: PV system produces heat and electricity

Option 13: biofuel boiler for heating and hot water, wind turbine system produces electricity

Option 14: Wind turbine system produces heat and electricity

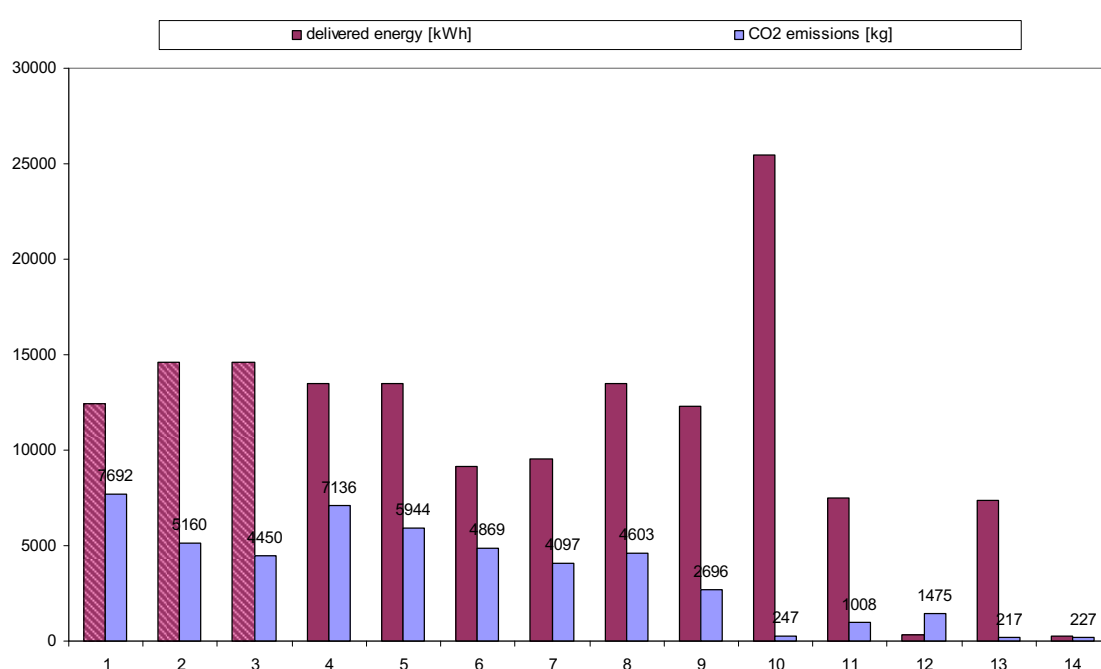


Figure 11: Delivered energy and CO₂ emissions of different supply options (Table 5)

Figure 11 shows the delivered energy from the grid and the CO₂ emissions per heated floor area for the different supply systems (options 1-11 from Table 8). It can be seen that options 2-5 and 8-10 result in higher overall delivered energy. The highest delivered energy is needed

for option 10 (biofuel CHP that produces 100% electricity). Options 1-3 do not fulfill the renewable energy share requirements in the Norwegian passive house standard which requires appr. 50% of DHW to be delivered by renewable energy sources (NS3700, 2010). Options 4-14 can be considered as appropriate solutions that fulfill the requirements in NS3700. Here, energy costs can help to optimize the supply system.

Another decision help are related CO₂ emissions. Here, all options result in reduced CO₂ emissions. Option 4 (district heating) results in slightly higher CO₂ emissions than option 3 (natural gas). It can further be seen that options 2 and 3 (gas and oil boiler respectively) results in CO₂ emissions reduction of 36% and 46%. The use of minimum district heating (50% of heating option 4) results in 3% CO₂ reduction while the use of 100% supply of heating and DHW from district heating reduces CO₂ emissions by 34% (option 5). Option 6 and 7 help to reduce delivered energy as well as CO₂ emissions but the later will not be feasible. Those options that use biofuel (options 8 to 11 and 13) result in a higher amount of delivered energy. This could affect results in an energy rating scheme (which relates energy performance to delivered energy) (Wigenstad et al., 2005). Note that option 10 deliverers more heat than needed in the building which could be used elsewhere.

A supply system with PV as energy supply (option 11 and 12) show slightly higher CO₂ emissions compared to option 10 due to relatively high emissions from PV. A supply system with wind turbines as energy supply (option 13 and 14) can help to minimize CO₂ emissions from operation of the building with option 13 showing a minimum of 217 kg CO₂ emissions per year. Again, there must be noted that there is a great uncertainty in these figures.

5. CONCLUSIONS

The total energy consumption in the Linesøya project was assumed to be minimized with different measures. First, the Norwegian passivhus standard (NS3700) was applied for the residential building part. Then, temporary use of the rest of the multipurpose building was assumed. This resulted in a total specific energy consumption of only 42 kWh/(m²a) with 44% heat and 56% electricity need.

This minimized energy budget was then a starting point for the analysis of different renewable energy supply systems. Costs should be calculated taking integration effects into account (e.g. integrating PV in solar shading system and taking only extra costs into account). Assuming a necessary advanced shading system on the south facing façade which will be integrated with a PV system (additional costs of appr. 50000NOK) will lead to a simple payback period of 2 years (at energy costs of 1.2NOK/kWh). There are of course many assumptions (not at least increased PV costs) in this calculation but it illustrates a large potential for integrated and cost effective solutions.

It will not be feasible to have an autarkic system rather a net energy and net emissions balance over the year. Here, a clear definition of the boundaries of the balance is needed in order to be able to optimize buildings energy performance with energy supply system and political goals of emission reduction. The size of the building is also an important factor for providing sufficient area for PV installation.

Another decision help is related CO₂ emissions, once national factors for electricity from the grid have been established. Here, different options result in reduced CO₂ emissions. A supply system of biofuel and wind (option 13) shows a minimum of 217 kg CO₂ emissions per year. It can be seen from the results that none energy supply system can completely avoid CO₂

emissions. Here, a CHP system that produces its own electricity from biofuel (option 10) deliverers more heat than needed in the building. If this heat could be used elsewhere, e.g. a neighboring building so could this lead to a negative CO₂ emission balance. It remains to be seen whether or not this option will be allowed under new NZEB definitions that are under development.

The relatively low energy use of large parts of the building due to the projected minimal use of the building during the winter period makes it difficult to draw too general conclusions. This is a special case that allows the use of renewable energy sources to meet the energy needs on an annual balance. Investment costs far below the live span of the building indicate sustainable solutions but the life span of the systems is normally considered much shorter. In addition, the payback periods of all supply systems analyzed indicate that they are not considered to be cost effective investments. Here, further research should investigate incentive systems and develop economic models that take societal costs and benefits on a macroeconomic level into account.

ACKNOWLEDGEMENTS

This work has been supported by the Research Council of Norway and several partners through the SINTEF/NTNU research project “*The research Centre on Zero Emission Buildings*” (ZEB).

REFERENCES

- Andresen I, 2008, Planlegging av solvarmeanlegg for lavenergiboliger og passivhus, Prosjketrapport nr. 22 S Byggforsk (SINTEF Byggforsk, Oslo)
- BWEA, "Small Wind Turbine FAQ", <http://www.bwea.com/small/faq.html>
- Hastings R, Wall M, 2007 *Sustainable solar housing - strategies and solutions* (Earthscan)
- NS3031, 2007, Calculation of energy performance of buildings – Method and data, (Standard Norge)
- NS3700, 2010, Criteria for low energy and passive houses - Residential buildings, (Standard Norge)
- NS-EN15603, 2008, Energy performance of Buildings - Overall energy use and definition of energy ratings, (Standard Norge)
- Svensk Vindkraftförening, 2009, Marknadsöversikt små vindkraftverk i Sverige 2009,
- Thyholt M, 2006 *Varmeforsyning til lavenergiboliger i områder med fjernvarmekonsesjon*, Department of Architectural Design, History and Technology, NTNU, Trondheim
- Vold M, Modahl S, Rønning A, 1999, Miljømessig sammenligning av foredlet biobrensel og fyringsolje i et livsløpperspektiv, O.R. 07.99 S Østfoldforskning (Stiftelsen Østfoldforskning, Statoil Norge)
- Wigenstad T, Dokka T H, Pettersen T, Myhre I, 2005, Energimerking av næringsbygg, STF50F05117 (SINTEF Building and Infrastructure, Trondheim)

Nanotechnology and Possibilities for the Thermal Building Insulation Materials of Tomorrow

Bjørn Petter Jelle^{ab*}, Arild Gustavsen^c, Steinar Grynning^a, Erlend Wegger^b, Erland Sveipe^b and Ruben Baetens^d

^aDepartment of Materials and Structures,
SINTEF Building and Infrastructure, Trondheim, Norway.

^bDepartment of Civil and Transport Engineering,
Norwegian University of Science and Technology (NTNU), Trondheim, Norway.

^cDepartment of Architectural Design, History and Technology,
Norwegian University of Science and Technology (NTNU), Trondheim, Norway.

^dDepartment of Civil Engineering,
Catholic University of Leuven (KUL), Heverlee, Belgium.

*Corresponding author: E-mail: bjorn.petter.jelle@sintef.no, Phone: 47 73 59 33 77

The work presented within this article is based on B. P. Jelle, A. Gustavsen and R. Baetens, "The Path to the High Performance Thermal Building Insulation Materials and Solutions of Tomorrow", Accepted for publication in *Journal of Building Physics*, 2010.

ABSTRACT

Nanotechnology and possibilities for the thermal building insulation materials of tomorrow are explored within this work. That is, we are looking beyond both the traditional and the state-of-the-art thermal building insulation materials and solutions, e.g. beyond vacuum insulation panels (VIP).

Thus advanced insulation material (AIM) concepts like vacuum insulation materials (VIM), gas insulation materials (GIM), nano insulation materials (NIM) and dynamic insulation materials (DIM) are introduced and defined.

The VIMs and GIMs have closed pore structures, whereas the NIMs may have either open or closed pore structures. The objective of the DIMs are to dynamically control the thermal insulation material properties, e.g. solid state core conductivity, emissivity and pore gas content.

In addition, fundamental theoretical studies aimed at developing an understanding of the basics of thermal conductance in solid state matter at an elementary and atomic level will also be carried out. The ultimate goal of these studies will be to develop tailor-make novel high performance thermal insulating materials and dynamic insulating materials, the latter one making it possible to control and regulate the thermal conductivity in the materials themselves, i.e. from highly insulating to highly conducting.

Keywords: Nano insulation material, NIM, Vacuum insulation, Building, Tomorrow.

1. BACKGROUND

Buildings constitute a substantial part of the world's total energy consumption, thus savings within the building sector will be essential, both for existing and new buildings. The thermal building insulation materials and solutions constitute one of the key fields. Recent studies (McKinsey 2009) point out that energy efficiency measures are the most cost-effective ones, whereas measures like e.g. solar photovoltaics and wind energy are far less cost-effective than insulation retrofit for buildings.

2. THE TRADITIONAL THERMAL INSULATION OF TODAY

The traditional thermal building insulation materials of today includes:

- **Mineral Wool**
- **Expanded Polystyrene (EPS)**
- **Extruded Polystyrene (XPS)**
- **Cork**
- **Polyurethane (PUR)**

3. THE STATE-OF-THE-ART THERMAL INSULATION OF TODAY

The state-of-the-art thermal building insulation materials and solutions of today includes:

- **Vacuum Insulation Panels (VIP)**
"An evacuated foil-encapsulated open porous material as a high performance thermal insulating material"
 - Core (silica, open porous, vacuum)
 - Foil (envelope)
- **Gas-Filled Panels (GFP)**
- **Aerogels**
- **Phase Change Materials (PCM)**
 - Solid State ↔ Liquid
 - Heat Storage and Release
- **Beyond State-of-the-Art High Performance Thermal Insulation Materials?**

Phase change materials (PCM) are normally not regarded as thermal building insulation materials. Nevertheless, the PCMs are mentioned for the sake of completeness as they may be part of a high performance thermal building envelope, contributing to the total thermal building envelope performance by heat storage and release during solid state to liquid phase transformations. However, the PCMs are not treated further in this context.

4. THERMAL CONDUCTIVITY

The typical thermal conductivity values for the traditional and state-of-the-art thermal building insulation materials are:

- **Concrete**
 - 200 - 2000 mW/(mK)
- **Mineral Wool, Expanded Polystyrene (EPS), Extruded Polystyrene (XPS) and Cork**
 - 32 - 40 mW/(mK)
- **Polyurethane (PUR)**
 - 20 - 30 mW/(mK)
- **Vacuum Insulation Panels (VIP)**
 - 4 mW/(mK) fresh
 - 8 mW/(mK) 25 years ageing (moisture and air penetration)
 - 20 mW/(mK) perforated
- **Gas-Filled Panels (GFP)**
 - 40 mW/(mK)
- **Aerogels**
 - 12 – 20 mW/(mK)

Note that concrete is normally not regarded as a thermal insulation material, but rather as a construction material. Nevertheless, due to its widespread use and for comparison reasons, the thermal conductivity range of concrete is also included here.

Polyurethane (PUR) is also applied as a thermal insulation material, but even if PUR is safe in its intended use it rises serious health concerns and hazards in case of a fire. During a fire PUR will when burning release hydrogen cyanide (HCN) and isocyanates, which is very poisonous. The HCN toxicity stems from the cyanide anion (CN^-) which prevents cellular respiration. Generally, hydrogen cyanide may be found in the smoke from nitrogen (N) containing plastics.

In order to reach sufficient low thermal transmittances (U-values) for buildings in cold and/or changing climates where the outdoor temperature may drop well below 0°C, other thermal insulation materials or solutions than the traditional ones are needed to avoid too thick buildings envelopes, e.g. walls with thicknesses between 40 cm to 50 cm as to satisfy passive house or zero energy building requirements.

5. VACUUM INSULATION PANELS

Vacuum insulation panels are superior compared to traditional thermal insulation materials with respect to achieving the lowest possible thermal conductivity. However, the VIPs do also have several drawbacks:

- Thermal bridges at panel edges
- Currently expensive, but calculations show that VIPs may be cost-effective even today
- Ageing effects – Air and moisture penetration
- Vulnerable towards penetration, e.g nails
- Can not be cut or adapted at building site
- Condensation issues through thermal building envelope (i.e. as VIPs are moisture tight)

Although the commercially available VIPs are rather expensive, calculations show that VIPs may already offer competitive thermal insulation solutions where the area is restricted (Grynnning et al. 2009, Tenpierik 2009).

For further information and details about VIPs it is referred to Baetens et al. (2010) and Tenpierik (2010).

6. GAS-FILLED PANELS

Gas-filled panels which applies a gas less thermal conductive than air, e.g. argon (Ar), krypton (Kr) and xenon (Xe), exhibit the same major disadvantages as the VIPs. Besides, although much lower theoretical values have been calculated, the lowest reported thermal conductivities are around 40 mW/(mK) in the pristine condition, thus at the high end compared to traditional thermal insulation. Thus, the future of GFPs in buildings may be questioned, as the VIPs seem to be a better choice both for today and tomorrow.

7. AEROGELS

Aerogels represent another state-of-the-art thermal insulation solution, and maybe the most promising with the highest potential of them all at the moment. The aerogel costs are still quite high, though. Using carbon black to suppress the radiative transfer, thermal conductivities as low as 4 mW/(mK) may be reached at a pressure of 50 mbar. However, commercially available state-of-the-art aerogels have been reported to have thermal conductivities between 13 to 14 mW/(mK) at ambient pressure (Aspen Aerogels 2008ab). Furthermore, it is noted that aerogels can be produced as either opaque, translucent or transparent materials, thus enabling a wide range of possible building applications. The coming years will show how far and extensive the aerogels will be applied in the building sector

8. THE REQUIREMENTS OF THE THERMAL INSULATION OF TOMORROW

As low thermal conductivity as possible is both desired and required for the thermal insulation materials and solutions of tomorrow. In addition, the thermal conductivity should not increase too much over a 100 year or more lifetime span. Furthermore, these materials and solutions should also be able to maintain their low thermal conductivity even if they are perforated by external objects like nails, except the increase due to the local heat bridges. Technologies based on vacuum may have problems with maintaining a low thermal conductivity over a long time span stretching over several decades, due to loss of vacuum with air and moisture uptake during the years.

A crucial requirement for the future thermal insulation materials is that they can be cut and adapted at the building site without loosing any of their thermal insulation performance. The VIP solution with an envelope barrier around an open pore structure supposed to maintain a vacuum does not satisfy this specific requirement, as cutting a VIP will result in a total loss of vacuum and an increase of thermal conductivity up to typically 20 mW/(mK).

Several other properties also have to be addressed, and Table 1 summarizes the various properties with their proposed requirements.

Table 1. The high performance thermal insulation materials and solutions of tomorrow and their proposed requirements (Jelle et al. 2010).

Property	Requirements
Thermal conductivity - pristine	< 4 mW/(mK)
Thermal conductivity - after 100 years	< 5 mW/(mK)
Thermal conductivity - after modest perforation	< 4 mW/(mK)
Perforation vulnerability	not to be influenced significantly
Possible to cut for adaption at building site	yes
Mechanical strength (e.g. compression and tensile)	may vary
Fire protection	may vary, depends on other protection
Fume emission during fire	any toxic gases to be identified
Climate ageing durability	resistant
Biological growth (e.g. fungi)	resistant
Freezing/thawing cycles	resistant
Water	resistant
Dynamic thermal insulation	desirable as an ultimate goal
Costs vs. other thermal insulation materials	competitive
Environmental impact (including energy and material use in production, emission of polluting agents and recycling issues)	low negative impact

9. ADVANCED INSULATION MATERIALS (AIM)

In the following, *advanced insulation materials* (AIM) and concepts are introduced:

- Vacuum Insulation Materials (VIM)
- Gas Insulation Materials (GIM)
- Nano Insulation Materials (NIM)
- Dynamic Insulation Materials (DIM)

For further elaborations and details it is referred to Jelle et al. (2010).

10. VACUUM INSULATION MATERIALS (VIM)

A *vacuum insulation material* (VIM) is basically a homogeneous material with a closed small pore structure filled with vacuum with an overall thermal conductivity of less than 4 mW/(mK) in pristine condition (Fig.1).

The VIM can be cut and adapted at the building site with no loss of low thermal conductivity. Perforating the VIM with a nail or similar would only result in a local heat bridge, i.e. no loss of low thermal conductivity.

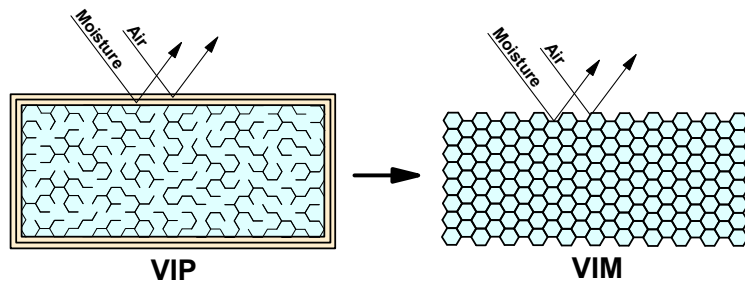


Figure 1. The development from VIPs to VIMs (Jelle et al. 2010).

11. GAS INSULATION MATERIALS (GIM)

A *gas insulation material* (GIM) is basically a homogeneous material with a closed small pore structure filled with a low-conductance gas, e.g. argon (Ar), krypton (Kr) or xenon (Xe), with an overall thermal conductivity of less than $4 \text{ mW}/(\text{mK})$ in the pristine condition.

That is, a GIM is basically the same as a VIM, except that the vacuum inside the closed pore structure is substituted with a low-conductance gas.

12. NANO INSULATION MATERIALS (NIM)

The development from VIPs to *nano insulation materials* (NIM) is depicted in Fig.2. In the NIM the pore size within the material is decreased below a certain level, i.e. 40 nm or below for air, in order to achieve an overall thermal conductivity of less than $4 \text{ mW}/(\text{mK})$ in the pristine condition.

That is, a NIM is basically a homogeneous material with a closed or open small nano pore structure with an overall thermal conductivity of less than $4 \text{ mW}/(\text{mK})$ in the pristine condition.

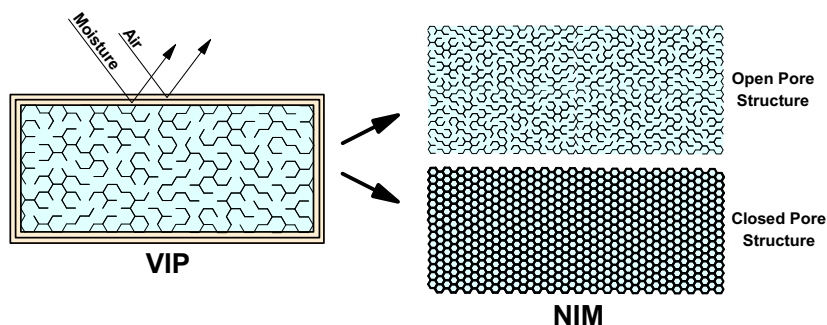


Figure 2. The development from VIPs to NIMs (Jelle et al. 2010).

Note that the grid structure in NIMs do not, unlike VIMs and GIMs, need to prevent air and moisture penetration into their pore structure during their service life for at least 100 years.

But how do the NIMs achieve their low thermal conductivity without applying a vacuum in the pores?

13. THE KNUDSEN EFFECT – NANO PORES IN NIMS

Decreasing the pore size within a material below a certain level, i.e. a pore diameter of the order of 40 nm or below for air, the gas thermal conductivity, and thereby also the overall thermal conductivity, becomes very low (< 4 mW/(mK) with an adequate low-conductivity grid structure) even with air-filled pores.

This is due to the so-called Knudsen effect where the mean free path of the gas molecules is larger than the pore diameter. That is, a gas molecule located inside a pore will ballistically hit the pore wall and not another gas molecule. The gas thermal conductivity λ_{gas} taking into account the Knudsen effect may be written in a simplified way as (Handbook of Chemistry and Physics 2003-2004, Schwab et al. 2005, Baetens et al. 2010, Jelle et al. 2010):

$$\lambda_{\text{gas}} = \frac{\lambda_{\text{gas},0}}{1 + 2\beta\text{Kn}} = \frac{\lambda_{\text{gas},0}}{1 + \frac{\sqrt{2}\beta k_B T}{\pi d^2 p \delta}} \quad (1)$$

where

$$\text{Kn} = \frac{\sigma_{\text{mean}}}{\delta} = \frac{k_B T}{\sqrt{2}\pi d^2 p \delta} \quad (2)$$

where

λ_{gas} = gas thermal conductivity in the pores (W/(mK))

$\lambda_{\text{gas},0}$ = gas thermal conductivity in the pores at STP (standard temperature and pressure) (W/(mK))

β = coefficient characterizing the molecule - wall collision energy transfer efficiency (between 1.5 - 2.0)

k_B = Boltzmann's constant $\approx 1.38 \cdot 10^{-23}$ J/K

T = temperature (K)

d = gas molecule collision diameter (m)

p = gas pressure in pores (Pa)

δ = characteristic pore diameter (m)

σ_{mean} = mean free path of gas molecules (m)

The Knudsen effect is visualized in a 2D and a 3D graphical plot in Figs 3-4, respectively, also depicting the low thermal conductivity threshold value of 4 mW/(mK). Note that these plots are logarithmic with respect to the pore diameter and the pore pressure.

The hard sphere collision diameters have been applied for d in the calculations, i.e. 3.66, 3.58, 4.08 and 4.78 Å for air, Ar, Kr and Xe, respectively (given at 298.15 K, Handbook of Chemistry and Physics 2003-2004). That is, the covalent diameters of the gas molecules have not been employed in these calculations. Furthermore, $\beta = 1.75$ and $T = 300$ K have been chosen in the calculations. In addition, $\lambda_{\text{gas},0}$ values of 26.2, 17.9, 9.5 and 5.5 mW/(mK) have been applied for air, Ar, Kr and Xe (at 300 K), respectively. In Fig.3 a pore gas pressure of 100 000 Pa (≈ 1 atm = 101 325 Pa) has been chosen.

For these chosen values in Figs.3-4, a rapid decrease between pore diameters 1 µm - 10 nm and pore pressures 10 Pa - 0.1 Pa is demonstrated in the gas thermal conductivities for all the four gases. For further calculation details and more graphical plots it is referred to Jelle et al. (2010).

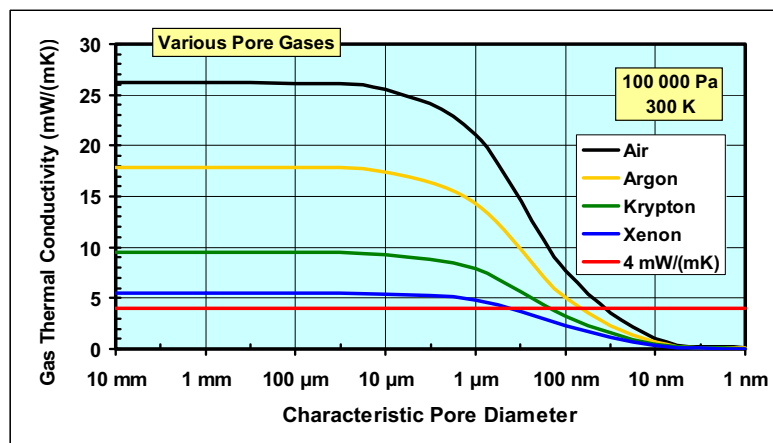


Figure 3. The effect of pore diameter on the gas thermal conductivity for air, argon, krypton and xenon. From Eqs.1-2 (Jelle et al. 2010).

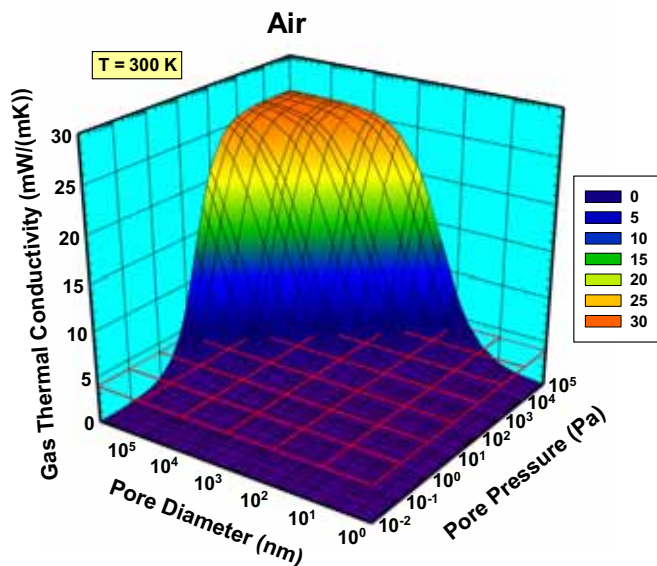


Figure 4. The effect of pore diameter and gas pressure in pores on the gas thermal conductivity visualized in a 3D plot for air. From Eqs.1-2 (Jelle et al. 2010).

14. THERMAL RADIATION IN NIMS

Applying the Stefan-Boltzmann relationship it may be shown that the radiation thermal conductivity decreases linearly with decreasing pore diameter, where the emissivity of the inner pore walls determine the slope of the decrease. That is, the smaller the pores, and the lower the emissivity, the lower the radiation thermal conductivity will be.

However, various works (e.g. Joulain et al. 2005, Mulet et al. 2002, Zhang 2007) describe a large increase in the thermal radiation as the pore diameter decreases below the wavelength

of the thermal (infrared) radiation (e.g. 10 µm), where tunneling of evanescent waves may play an important role.

The work by Mulet et al. (2002) and Joulain et al. (2005) indicate that the large thermal radiation is only centered around a specific wavelength (or a few). That is, this might suggest that the total thermal radiation integrated over all wavelengths is not that large. How much this actually contributes to the total (overall) thermal conductivity is not known by the authors at the moment, although we believe it is at least rather moderate. Nevertheless, these topics are currently being addressed in on-going research activities. Jelle et al. (2010) elaborates more on these thermal radiation issues.

15. TOTAL THERMAL CONDUCTIVITY IN NIMS

The solid state lattice conductivity in the NIMs has to be kept as low as possible in order to obtain the lowest possible overall thermal conductivity. If a low-conductivity solid state lattice and a low gas thermal conductivity are achieved, and which still dominate the thermal transport, i.e. larger than the thermal radiation part, then NIMs may become the high performance thermal insulation material of tomorrow and the future.

16. DYNAMIC INSULATION MATERIALS (DIM)

A *dynamic insulation material* (DIM) is a material where the thermal conductivity can be controlled within a desirable range.

■ **Thermal conductivity control may be achieved by:**

- Inner pore gas content or concentration including the mean free path of the gas molecules and the gas-surface interaction
- The emissivity of the inner surfaces of the pores
- The solid state thermal conductivity of the lattice

■ **What is really solid state thermal conductivity? Two models:**

- Phonon thermal conductivity - atom lattice vibrations
- Free electron thermal conductivity

■ **What kind of physical model could describe and explain thermal conductivity?**

■ **Could it be possible to dynamically change the thermal conductivity from very low to very high, i.e. making a DIM?**

Could other fields of science and technology inspire and give ideas about how to be able to make DIMs, e.g. from the fields?:

- Electrochromic Materials
- Quantum Mechanics
- Electrical Superconductivity
- Others?

The thermal insulation regulating abilities of DIMs give these materials a great potential. However, first it has to be demonstrated that such robust and practical DIMs can be manufactured. Again, it is referred to Jelle et al. (2010) for further details and elaborations.

17. MATERIALS AND SOLUTIONS NOT YET THOUGHT OF ?

The thermal solution of tomorrow might be found in materials and solutions not yet thought of, which requires that we may have to *think thoughts not yet thought of*.

18. POTENTIAL OF THE STATE-OF-THE-ART AND BEYOND

A short summary of the potential of the state-of-the-art and beyond with respect to becoming the high performance thermal insulation materials and solutions of tomorrow is given in Table 2.

Table 2. The potential of state-of-the-art solutions and beyond for becoming the high performance thermal insulation materials and solutions of tomorrow.

Thermal Insulation Materials and Solutions	Low Pristine Thermal Conductivity	Low Long-Term Thermal Conductivity	Perforation Robustness	Possible Building Site Adaption Cutting	Load-Bearing Capabilities	A Thermal Insulation Material and Solution of Tomorrow ?
Traditional						
Mineral Wool and Polystyrene	no	no	yes	yes	no	no
Todays State-of-the-Art						
Vacuum Insulation Panels (VIP)	yes	maybe	no	no	no	today and near future
Gas-Filled Panels (GFP)	maybe	maybe	no	no	no	probably not
Aerogels	maybe	maybe	yes	yes	no	maybe
Phase Change Materials (PCM)	-	-	-	-	no	heat storage and release
Beyond State-of-the-Art – Advanced Insulation Materials (AIM)						
Vacuum Insulation Materials (VIM)	yes	maybe	yes	yes	no/maybe	yes
Gas Insulation Materials (GIM)	yes	maybe	yes	yes	no/maybe	maybe
Nano Insulation Materials (NIM)	yes	yes	yes, excellent	yes, excellent	no/maybe	yes, excellent
Dynamic Insulation Materials (DIM)	maybe	maybe	not known	not known	no/maybe	yes, excellent
Others?	-	-	-	-	-	maybe

19. CONCLUSIONS

New concepts of advanced insulation materials (AIM) have been introduced, i.e. vacuum insulation materials (VIM), gas insulation materials (GIM), nano insulation materials (NIM) and dynamic insulation materials (DIM).

Nano insulation materials (NIM) seem to represent the best high performance low conductivity thermal solution for the foreseeable future. Possible applications of NIMs cover all building types including timber frame and concrete buildings.

Dynamic insulation materials (DIM) have great potential due to their controllable thermal insulating abilities.

ACKNOWLEDGEMENTS

This work has been supported by the Research Council of Norway and several partners through the SINTEF and NTNU research projects *Robust Envelope Construction Details for Buildings of the 21st Century (ROBUST)* and the Concrete Innovation Centre (COIN).

REFERENCES

- Aspen Aerogels, Spaceloft® 3251, 6251, 9251, "Flexible insulation for industrial, commercial and residential applications", Retrieved October 7, 2008, from www.aerogel.com, 2008(a).
- Aspen Aerogels, Spaceloft™ 6250, "Extreme protection for extreme environments", Retrieved October 7, 2008, from www.aerogel.com, 2008(b).
- R. Baetens, B. P. Jelle, J. V. Thue, M. J. Tenpierik, S. Grynning, S. Uvsløkk and A. Gustavsen, "Vacuum Insulation Panels for Building Applications: A Review and Beyond", *Energy and Buildings*, **42**, 147-172, 2010.
- S. Grynning, R. Baetens, B. P. Jelle, A. Gustavsen, S. Uvsløkk and V. Meløysund, "Vakuumisolasjonspaneler for bruk i bygninger – Egenskaper, krav og muligheter" ("Vacuum insulation panels for application in buildings – Properties, requirements and possibilities"), (in Norwegian), *SINTEF Byggforsk Prosjektrapport*, nr. 31, 2009.
- Handbook of Chemistry and Physics, 84th edition, pp. 6-47 and 6-195, *CRC Press*, 2003-2004.
- B. P. Jelle, A. Gustavsen and R. Baetens, "The Path to the High Performance Thermal Building Insulation Materials and Solutions of Tomorrow", Accepted for publication in *Journal of Building Physics*, 2010.
- K. Joulain, J.-P. Mulet, F. Marquier, R. Carminati and J.-J. Greffet, "Surface electromagnetic waves thermally excited: Radiative heat transfer, coherence properties and Casimir forces revisited in the near field", *Surface Science Reports*, **57**, 59-112, 2005.
- McKinsey, "Pathways to a low-carbon economy. Version 2 of the global greenhouse gas abatement cost curve", McKinsey & Company, 2009.
- J.-P. Mulet, K. Joulain, R. Carminati and J.-J. Greffet, "Enhanced radiative heat transfer at nanometric distances", *Microscale Thermophysical Engineering*, **6**, 209-222, 2002.
- H. Schwab, U. Heinemann, A. Beck, H.-P. Ebert and J. Fricke, "Dependence of thermal conductivity on water content in vacuum insulation panels with fumed silica kernels", *Journal of Thermal Envelope & Building Science*, **28**, 319-326, 2005.
- M. J. Tenpierik, "Vacuum insulation panels applied in building constructions (VIP ABC)", *Ph.D. Thesis*, Delft University of Technology (Delft, The Netherlands), 2009.
- Z. M. Zhang, "Nano/microscale heat transfer", McGraw-Hill, 2007.

Dynamic Solar Radiation Control in Buildings by Applying Electrochromic Materials

Bjørn Petter Jelle^{ab}* and Arild Gustavsen^c

^aDepartment of Materials and Structures,
SINTEF Building and Infrastructure, Trondheim, Norway.

^bDepartment of Civil and Transport Engineering,
Norwegian University of Science and Technology (NTNU), Trondheim, Norway.

^cDepartment of Architectural Design, History and Technology,
Norwegian University of Science and Technology (NTNU), Trondheim, Norway.

*Corresponding author: E-mail: bjorn.petter.jelle@sintef.no, Phone: 47 73 59 33 77

ABSTRACT

Smart windows like electrochromic windows (ECWs) are windows which are able to regulate the solar radiation throughput by application of an external voltage. The ECWs may decrease heating, cooling and electricity loads in buildings by admitting the optimum level of solar energy and daylight into the buildings at any given time, e.g. cold winter climate versus warm summer climate demands.

In order to achieve as dynamic and flexible solar radiation control as possible, the ECWs may be characterized by a number of solar radiation glazing factors, i.e. ultraviolet solar transmittance, visible solar transmittance, solar transmittance, solar material protection factor, solar skin protection factor, external visible solar reflectance, internal visible solar reflectance, solar reflectance, solar absorbance, emissivity, solar factor and colour rendering factor. Comparison of these solar quantities for various electrochromic material and window combinations and configurations enables one to select the most appropriate electrochromic materials and ECWs for specific buildings. Measurements and calculations were carried out on two different electrochromic window devices, where one ECW was substantially darker than the other in the coloured state.

Keywords: Solar Radiation, Glazing Factor, Electrochromic Window, Building, Transmittance, Reflectance, Absorbance, Emissivity, Solar Material Protection Factor, Solar Skin Protection Factor, Window Pane, Glass.

1. INTRODUCTION

The electrochromic windows (ECWs) aim at controlling the solar radiation throughput at the earth's surface, which is roughly located between 300 nm and 3000 nm. The ECW solar control is achieved by application of an external voltage. The visible (VIS) light lies between 380 nm and 780 nm. Ultraviolet (UV) and near infrared (NIR) radiation are located below and above the VIS region, respectively. Above 3000 nm, and not part of the direct solar radiation, lies the thermal radiation called infrared (IR) radiation, which all materials radiate

above 0 K, peaking around 10 000 nm (10 μm) at room temperature. However, the ECWs are not aimed at controlling the IR radiation. Normally, as low as possible heat loss through windows is desired, i.e. low U-value, which is accomplished by the application of various static low emissivity coatings on the window glass panes. Some commercial ECWs are already on the market (Baetens et al. 2009).

Glass with material additives and different surface coatings may be tailor-made and chosen in order to fulfil the various requirements for the actual building type and function, e.g. office building, hospital, family dwelling etc. The glass and window properties are selected with respect to several, often contradictory, considerations. Generally, a window is supposed to let in as much daylight as possible, give comfortable luminance conditions, give satisfactory view out of (and often into) buildings, transmit a minimum of heat from the interior to the exterior in order to reduce the heating demand, transmit solar radiation from the exterior to the interior in order to reduce the heating demand (i.e. in winter), shut off solar radiation by reflection which otherwise might cause too much heating with subsequent cooling load, not induce air current problems or give a poor thermal comfort and not induce unacceptable interior or exterior water condensation.

In addition to the pure energy and daylighting aspects, it is also important to emphasize the degradation of building materials by solar radiation, especially organic matter where the chemical bonds may be broken up by the more energetic parts of the solar spectrum, i.e. ultraviolet (UV) light. A substantial part of the UV light is blocked by the glass itself, but nevertheless a significant amount of UV light passes through the glass and into the buildings. Generally, the most important solar radiation glazing factors are:

- Ultraviolet Solar Transmittance, T_{uv}
- Visible Solar Transmittance, T_{vis}
- Solar Transmittance, T_{sol}
- Solar Material Protection Factor, SMPF
- Solar Skin Protection Factor, SSPF
- External Visible Solar Reflectance, $R_{\text{vis,ext}}$
- Internal Visible Solar Reflectance, $R_{\text{vis,int}}$
- Solar Reflectance, R_{sol}
- Solar Absorbance, A_{sol}
- Emissivity, ϵ
- Solar Factor, SF (from T_{sol} , R_{sol} and ϵ)
- Colour Rendering Factor, CRF

All these factors will be a number between 0 and 1, where in common usage the factors may often be chosen in percentage, i.e. between 0 and 100 %.

Hence, the solar radiation regulation in ECWs enables a dynamic control of the solar radiation glazing factors given above, where this work presents and summarizes in a very abridged way these solar glazing factors together with measurements and calculations carried out on two ECWs. For calculations with ECWs incorporated in two-layer and three-layer window panes, including spectroscopical measurements on float glass and low emittance glass, it is referred elsewhere (Jelle and Gustavsen 2010).

2. EXPERIMENTAL

To illustrate various transmittance levels in the solar spectrum, two electrochromic window (ECW) devices, one ECW substantially darker than the other in the coloured state, were selected as examples. Based on the ECW transmittance measurements the solar radiation glazing factors were calculated. The actual fabrication and miscellaneous testing of the ECWs are described elsewhere (Jelle et al. 1998a, 1998b, 1999, 2007).

A Cary 5 UV-VIS-NIR spectrophotometer, with an absolute reflectance accessory (Strong-type, VW principle), was used to measure the transmittance and reflectance of various glass samples in the ultraviolet (UV), visible (VIS) and near infrared (NIR) region, from 290 nm to 3300 nm. However, at the moment of the fabrication and characterizing of the ECW devices, no laboratory resources for determining the absolute reflectance of the ECWs were available. Nevertheless, as the two ECWs consist of solar absorbing electrochromic materials, and not reflecting modulating electrochromics, the measured (low) reflectance values for float glass are applied in the calculation of the various reflectance based solar radiation glazing factors.

The standard ISO/FDIS 9050:2003(E) refers to ISO 10292:1994 E for emissivity determinations, which according to ISO 10292:1994(E) are to be carried out with an infrared spectrometer, measuring the near normal reflectance ($\leq 10^\circ$) at a temperature of 283 K. More details of the emissivity determinations and measurements are found in EN 12898:2001 E. In order to minimize polarization effects, the angle of incidence with respect to the normal of the sample must be 10° or less (ASTM E 1585-93). For other ambient temperatures than 283 K ($\approx 10^\circ\text{C}$), the emissivity is not strongly dependent on the mean temperature (ISO 10292:1994(E)).

The emissivity may also be determined by applying a heat flow meter apparatus according to the standard EN 1946-3:1999 E. For theoretical considerations, referral is made to EN 1946-2:1999 E and EN 1946-3:1999 E.

Furthermore, the emissivity may also be determined by measuring the directional hemispherical reflectance (DHR, direct mode) or the hemispherical directional reflectance (HDR, reciprocal mode). In the DHR method the sample is illuminated from a single direction and all the reflected radiation into the hemisphere surrounding the sample is measured. In the HDR method the sample is uniformly illuminated from all directions by use of a hemisphere and the radiation reflected into a single direction is measured. For both the DHR and HDR methods the single direction may be varied for miscellaneous instruments, i.e. illuminating or detecting at varying angles, respectively.

In this work, a float glass and a low emittance glass were measured by the hemispherical directional reflectance method by applying a SOC-100 HDR Hemispherical Directional Reflectometer from Surface Optics Corporation connected to a Thermo Nicolet 8700 FTIR Spectrometer. The reflected radiation from the sample was detected at the following incident angles: 10, 20, 30, 40, 45, 50, 55, 60, 65, 70, 75 and 80° . 32 scans were performed with 2 repeats at a resolution of 16 cm^{-1} in the wavelength range $2 - 25\text{ }\mu\text{m}$. The IR source temperature was 704°C . The results were $\epsilon_{\text{float}} = 0.836$ and $\epsilon_{\text{lowe}} = 0.071$, for the float and low emittance glass, respectively. The ϵ_{float} value was applied in the calculation of the solar factor (SF) for both the float glass and the low emittance glass as the ϵ value in the SF calculations is with respect to the inside facing surface of the innermost glass pane, i.e. normally a float glass. Hence, the ϵ_{lowe} value is not applied in this context. At the moment of the fabrication and characterizing of the ECW devices, no laboratory resources for determining the emissivity of the ECWs were available, so the nominal value $\epsilon_{\text{float}} = 0.837$ for float glass is applied in the calculation of SF for the ECWs.

3. SOLAR RADIATION GLAZING FACTOR DEFINITIONS

The ***Ultraviolet Solar Transmittance*** (T_{uv}) is given by the following expression:

$$T_{uv} = \frac{\sum_{\lambda=300nm}^{380nm} T(\lambda)S_\lambda \Delta\lambda}{\sum_{\lambda=300nm}^{380nm} S_\lambda \Delta\lambda} \quad (1)$$

The ***Visible Solar Transmittance*** (T_{vis}), often denoted Light Transmittance, is given by:

$$T_{vis} = \frac{\sum_{\lambda=380nm}^{780nm} T(\lambda)D_\lambda V(\lambda) \Delta\lambda}{\sum_{\lambda=380nm}^{780nm} D_\lambda V(\lambda) \Delta\lambda} \quad (2)$$

The ***Solar Transmittance*** (T_{sol}) is given by:

$$T_{sol} = \frac{\sum_{\lambda=300nm}^{2500nm} T(\lambda)S_\lambda \Delta\lambda}{\sum_{\lambda=300nm}^{2500nm} S_\lambda \Delta\lambda} \quad (3)$$

The ***Solar Material Protection Factor*** (SMPF) is given by:

$$SMPF = 1 - \tau_{df} = 1 - \frac{\sum_{\lambda=300nm}^{600nm} T(\lambda)C_\lambda S_\lambda \Delta\lambda}{\sum_{\lambda=300nm}^{600nm} C_\lambda S_\lambda \Delta\lambda} \quad (4)$$

The ***Solar Skin Protection Factor*** (SSPF) is given by:

$$SSPF = 1 - F_{sd} = 1 - \frac{\sum_{\lambda=300nm}^{400nm} T(\lambda)E_\lambda S_\lambda \Delta\lambda}{\sum_{\lambda=300nm}^{400nm} E_\lambda S_\lambda \Delta\lambda} \quad (5)$$

The ***External Visible Solar Reflectance*** ($R_{vis,ext}$), often denoted External Light Reflectance, is given by:

$$R_{vis,ext} = \frac{\sum_{\lambda=380nm}^{780nm} R_{ext}(\lambda)D_\lambda V(\lambda) \Delta\lambda}{\sum_{\lambda=380nm}^{780nm} D_\lambda V(\lambda) \Delta\lambda} \quad (6)$$

The **Internal Visible Solar Reflectance** ($R_{vis,int}$), often denoted Internal Light Reflectance, is given by:

$$R_{vis,int} = \frac{\sum_{\lambda=380nm}^{780nm} R_{int}(\lambda) D_\lambda V(\lambda) \Delta\lambda}{\sum_{\lambda=380nm}^{780nm} D_\lambda V(\lambda) \Delta\lambda} \quad (7)$$

The **Solar Reflectance** (R_{sol}), implicitly external solar reflectance, is given by:

$$R_{sol} = \frac{\sum_{\lambda=300nm}^{2500nm} R_{ext}(\lambda) S_\lambda \Delta\lambda}{\sum_{\lambda=300nm}^{2500nm} S_\lambda \Delta\lambda} \quad (8)$$

The **Solar Absorbance** (A_{sol}) is calculated from T_{sol} and R_{sol} in Eq.3 and Eq.8 using the fact that $T + A + R = 1$, giving the following expression:

$$A_{sol} = 1 - T_{sol} - R_{sol} = 1 - \frac{\sum_{\lambda=300nm}^{2500nm} T(\lambda) S_\lambda \Delta\lambda}{\sum_{\lambda=300nm}^{2500nm} S_\lambda \Delta\lambda} - \frac{\sum_{\lambda=300nm}^{2500nm} R_{ext}(\lambda) S_\lambda \Delta\lambda}{\sum_{\lambda=300nm}^{2500nm} S_\lambda \Delta\lambda} \quad (9)$$

The **Emissivity** (ϵ), implicitly corrected emissivity, may be determined from specular IR reflectance measurements by:

$$\epsilon = c_{corr} \epsilon_n = \frac{\epsilon}{\epsilon_n} \epsilon_n = c_{corr} (1 - R_n) = c_{corr} \left[1 - \frac{1}{30} \sum_{i=1}^{30} R_n(\lambda_i) \right] \quad (10)$$

or by heat flow meter measurements by:

$$\epsilon = \frac{2(q_{tot} - \frac{\kappa}{d} \Delta T)}{4\sigma T_m^3 \Delta T + q_{tot} - \frac{\kappa}{d} \Delta T} \quad (11)$$

or as the total hemispherical emissivity by applying a hemispherical reflectometer and integrating over the hemisphere by

$$\epsilon = 2 \int_0^{\pi/2} \epsilon_t(\theta) \sin \theta \cos \theta d\theta \quad (12)$$

The **Solar Factor** (SF) is the Total Solar Energy Transmittance and is given by:

$$SF = T_{sol} + q_i \quad (13)$$

The **Colour Rendering Factor** (CRF) is given by:

$$CRF = \frac{R_a}{100} = \frac{1}{800} \sum_{i=1}^8 R_i \quad (14)$$

where

λ = wavelength (nm)

$\Delta\lambda$ = wavelength interval (nm)

$T(\lambda)$ = spectral transmittance of the glass

$R_{ext}(\lambda)$ = external spectral reflectance of the glass

$R_{int}(\lambda)$ = internal spectral reflectance of the glass

R_n = average spectral reflectance calculated by summation of spectral reflectance values at 30 distinct wavelengths and divided by 30 as shown in Eq.10 above

λ_i = wavelength and λ_i values for the 30 wavelengths are given in ISO 10292:1994(E) and EN 12898:2001 E

S_λ = relative spectral distribution of ultraviolet solar radiation or solar radiation (ISO/CDIS 9050:2003(E), ISO 9845-1:1992(E))

D_λ = relative spectral distribution of illuminant D65 (ISO/CDIS 9050:2003(E), ISO 10526:1999(E))

$V(\lambda)$ = spectral luminous efficiency for photopic vision defining the standard observer for photometry (ISO/CDIS 9050:2003(E), ISO/CIE 10527:1991(E))

$S_\lambda \Delta\lambda$ values at different wavelengths for ultraviolet solar radiation or solar radiation are given in ISO/CDIS 9050:2003(E)

$D_\lambda V(\lambda) \Delta\lambda$ values at different wavelengths are given in ISO/CDIS 9050:2003(E)

τ_{df} = CIE damage factor (ISO/CDIS 9050:2003(E), CIE No 89/3:1990)

$C_\lambda = e^{-0.012\lambda}$ (λ given in nm)

$C_\lambda S_\lambda \Delta\lambda$ values at different wavelengths are given in ISO/CDIS 9050:2003(E)

F_{sd} = skin damage factor (ISO/CDIS 9050:2003(E), McKinlay and Diffey 1987)

E_λ = CIE erythemal effectiveness spectrum

$E_\lambda S_\lambda \Delta\lambda$ values at different wavelengths are given in ISO/CDIS 9050:2003(E)

q_{tot} = total heat flow density between two parallel, flat infinite isothermal surfaces (W/m^2) (EN 1946-2:1999 E, EN 1946-3:1999 E)

κ = thermal conductivity of the medium separating the two surfaces ($W/(mK)$)

$\kappa = \kappa_{air} = 0.0242396(1 + 0.003052\theta - 1.282 \cdot 10^{-6}\theta^2)$ ($W/(mK)$)

(values accurate to 0.6 % between $\theta = 10^\circ C$ and $\theta = 70^\circ C$)

(θ given in $^\circ C$) (EN 1946-2:1999 E, EN 1946-3:1999 E)

$\theta = (T_m - 273.15 K)^\circ C/K$ ($^\circ C$)

T_m = mean temperature of the two surfaces (K)

ΔT = temperature difference between the two surfaces (K)

d = distance between the two surfaces (m)

$\sigma = \pi^2 k^4 / (60 h^3 c^2)$ = Stefan-Boltzmann's constant $\approx 5.67 \cdot 10^{-8} W/(m^2 K^4)$

$$\varepsilon_t(\theta, \phi, \lambda) = 1 - \frac{\int_0^\infty R(\lambda) P(\lambda, T) d\lambda}{\int_0^\infty P(\lambda, T) d\lambda} \quad (\text{Surface Optics Corporation 2009})$$

$$P(\lambda, T) = \frac{8\pi hc}{\lambda^5 (e^{hc/(\lambda kT)} - 1)} = \text{Planck's function} \quad (\text{Surface Optics Corporation 2009})$$

R = hemispherical reflectance

T = temperature (K)

θ and ϕ are integrating angles over the hemisphere

h = Planck's constant $\approx 6.63 \cdot 10^{-34}$ Js

k = Boltzmann's constant $\approx 1.38 \cdot 10^{-23}$ J/K

c = velocity of light $\approx 3.00 \cdot 10^8$ m/s

T_{sol} = solar transmittance (Eq.3)

$A_{sol} = q_i + q_e$ (A_{sol} from Eq.9)

q_i = secondary heat transfer factor towards the inside

q_e = secondary heat transfer factor towards the outside

$$q_i = A_{sol} \frac{h_i}{h_e + h_i} \text{ for a single pane window}$$

$$h_e = 23 \text{ W/(m}^2\text{K)}$$

$$h_i = \left(3.6 + \frac{4.4\epsilon}{0.837} \right) \text{ W/(m}^2\text{K)}$$

ϵ = emissivity of the innermost glass inside surface (ϵ of other surfaces is taken care of by the reflectance values)

(complete details for calculation of SF, also including two-layer and three-layer window panes, are given in ISO/FDIS 9050:2003(E), with additions in ISO 10292:1994(E) and EN-ISO 6946:1996, note that ϵ and R_{sol} enter into q_i in Eq.13, R_{sol} from A_{sol})

$$R_a = \frac{1}{8} \sum_{i=1}^8 R_i = \text{general colour rendering index (EN 410:1998 E)}$$

$R_i = 100 - 4.6\Delta E_i = \text{specific colour rendering index}$

$$\Delta E_i = \sqrt{(U_{t,i}^* - U_{r,i}^*)^2 + (V_{t,i}^* - V_{r,i}^*)^2 + (W_{t,i}^* - W_{r,i}^*)^2} = \text{total distortion of colour } i$$

(complete details for calculation of CRF given in EN 410:1998 E)

For further and complete calculation details, it is referred to the literature in the reference list.

The emissivity (ϵ) is a measure of a material's radiative properties, i.e. the emission of infrared radiation. The higher emissivity, the higher emission. Highly reflective materials of infrared radiation have low emissivity values, e.g. polished surfaces of gold, silver or copper. The ϵ value will be a number between 0 and 1. Oxidation of metallic surfaces will increase the emissivity substantially, e.g. polished aluminium with $\epsilon = 0.05$ (reflectance 0.95) and

oxidized aluminium with $\epsilon = 0.30$ (reflectance 0.70). Determination of the emissivity is required in order to further determine the solar factor (SF) and the thermal transmittance (U-value).

The Colour Rendering Factor (CRF) expresses synthetically a quantitative evaluation of the colour differences between eight test colours lighted directly by the reference illuminant D65 and by the same illuminant transmitted through the glazing. The CRF value will thus be a number between 0 and 1, calculated in the visible part of the solar spectrum, i.e. 380-780 nm. A high number indicates a good colour rendering. Ideally, the maximum value of 1 will be obtained by glazing whose spectral transmittance is completely constant in the whole visible spectral range, i.e. no variation of transmittance with wavelength. A CRF value > 0.9 characterizes a very good colour rendering and CRF > 0.8 represents a good colour rendering (ISO/FDIS 9050:2003(E), EN 410:1998 E).

4. ELECTROCHROMIC WINDOW MEASUREMENTS

Electrochromic windows (ECWs) are able to control the colour of the window, thereby also the solar radiation throughput, by varying the applied electrical potential. Schematic drawings of two ECWs are shown in Fig.1, constructed in a sandwich form from the electrochromic materials polyaniline (PANI), prussian blue (PB) and tungsten oxide (WO_3), transparent conducting glass plates with an indium-tin oxide coating (indium oxide doped with tin, $In_2O_3(Sn)$, ITO, typical surface resistivity of $90 \Omega/\square$) and the solid state polymer electrolyte poly(2-acrylamido-2-methyl-propane-sulphonic acid) (PAMPS) as an ionic conductor. Both the PANI, PB and WO_3 coating thicknesses have been less than 1 μm , while the PAMPS layer thickness has been about 0.1 mm. Applying a positive potential to the PANI/PB electrode, both PANI, PB and WO_3 turn to a blue colour, while the window is bleached (made almost transparent) by reversing the polarity of the electrodes. Only a small charge density of about 3 mC/cm^2 , corresponding to a low energy consumption of about 5 mWh/m^2 , is required for either the colouring or the bleaching process (Jelle et al. 1998a).

A high transmission regulation and solar modulation (solar regulation 53 %, calculated based on the solar spectral irradiance given in CRC Handbook of Chemistry and Physics 1989-1990) (Jelle et al. 1998a) have been achieved with this type of ECW (ECW1, left Fig.1), which is depicted in Fig.2 covering the whole solar spectrum. The inclusion of PB in PANI enhances the colouration (wavelength dependent absorption), while the adhesion of PB is improved by PANI, i.e. in this respect there exists a symbiotic relationship between PANI and PB (Jelle et al. 1998a). Transmittance curves for a second ECW (ECW2, right Fig.1) of the same construction, though with PANI-PB multilayers and a very dark colour in the coloured state, are shown in Fig.2 (solar regulation 49 %) (Jelle et al. 1998b). These solar regulations might be compared to the ΔT_{sol} values of 0.57 and 0.51 for ECW1 and ECW2, respectively, thus obtaining somewhat larger values when using the same calculation method but with a bit different solar reference spectrum.

In addition to their evident potential benefits and savings in solar energy control, the ECWs may also be employed in order to achieve the desired protection of materials and human skin inside buildings during direct sunlight. That is, the dynamic characteristics of ECWs may allow diffuse daylight through the window panes in the required amount in order to obtain a satisfactory room illumination, whereas at direct sunlight exposure, the SMPF and SSPF values for the window panes may be increased to a sufficient high protection level.

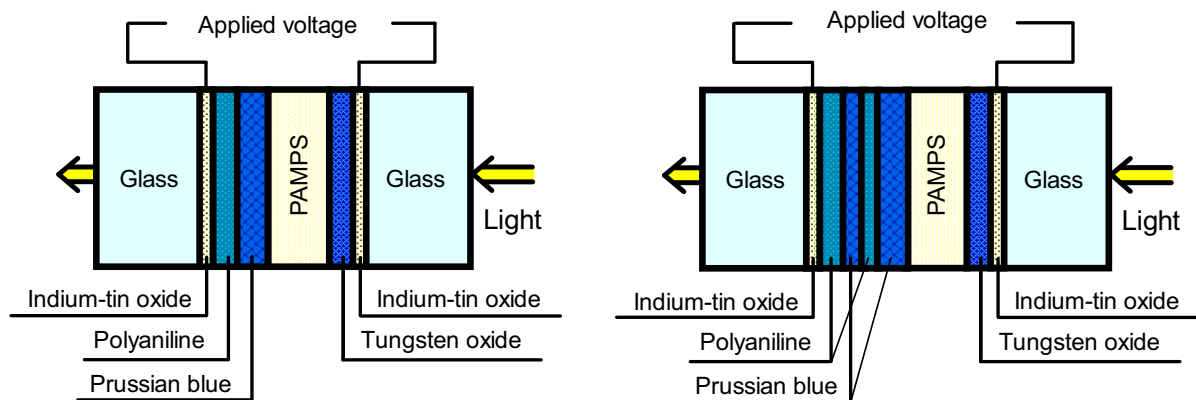


Fig.1. Schematic drawing of the two electrochromic window configurations ECW1 (left) and ECW2 (right, PANI-PB multilayer) based on the electrochromic materials polyaniline (PANI), prussian blue (PB) and tungsten oxide (WO_3). From Jelle and Hagen (1999).

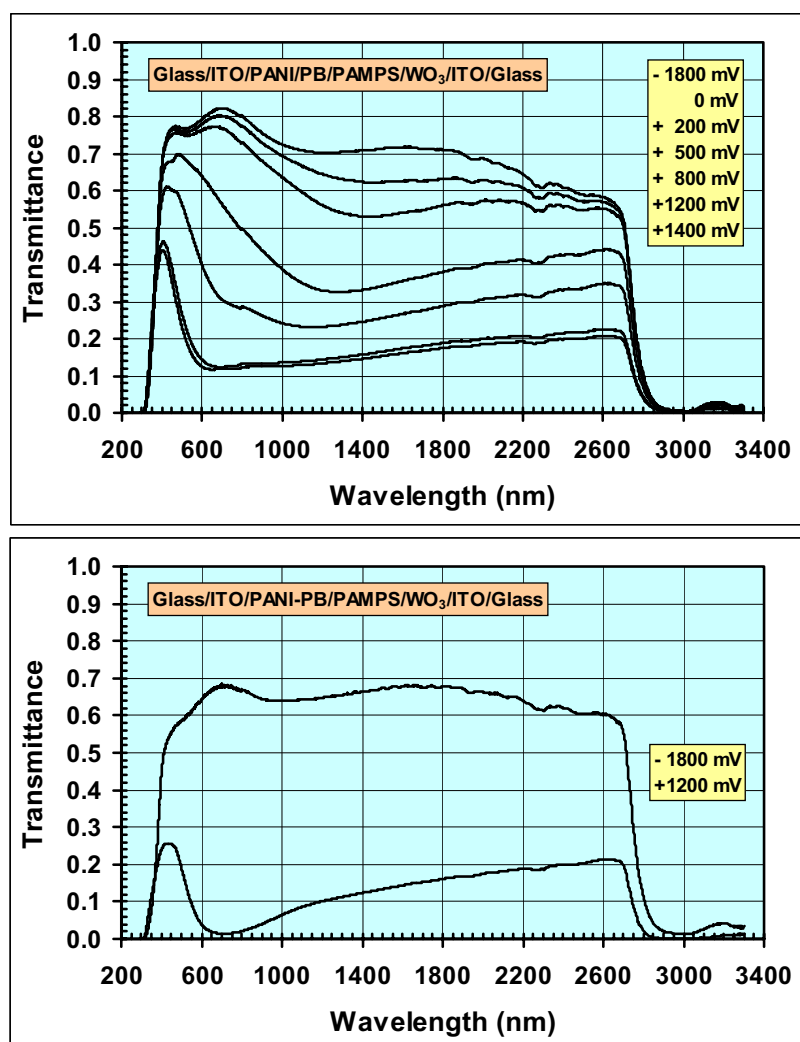


Fig.2. Transmittance vs. wavelength in the whole solar spectrum measured for two different ECWs at various applied potentials. Highest colouration level is at +1400 mV (ECW1, top) and +1200 mV (ECW2, bottom). Redrawn from Jelle et al. (2007).

5. SOLAR RADIATION GLAZING FACTOR CALCULATIONS

Solar radiation glazing factors for different colouration levels, i.e. at different applied potentials, in two electrochromic windows (ECW) are given in Table 1. From Table 1 it is observed that various solar radiation glazing factors may obtain both high and low values depending upon the applied electrical potential (intermediate values not shown here), e.g. changing the T_{vis} value from 0.78 to 0.17 for the ECW1 device and from 0.62 to 0.10 for the darker ECW2 device. It is also noted that these ECWs contain solar radiation absorbing electrochromic materials, i.e. not reflecting materials, as the changes with applied potential occur in the transmittance (e.g. T_{sol}) and absorbance (e.g. A_{sol}) values, and not in the reflectance (e.g. R_{sol}) values. As expected, the highest colouration level gives the largest SMPF values, i.e. the best protection of materials is achieved with the darkest ECW, e.g. compare a SMPF value of 0.71 for ECW1 and 0.82 for ECW2 in the coloured state.

Incorporating the ECWs into two-layer and three-layer window pane configurations reduces the total solar energy throughput in the windows, e.g. as seen in the T_{sol} and SF values, as several layers of glass and coatings will increase the total reflectance and absorbance. Note that some of the reflectance values $R_{vis,ext}$, $R_{vis,int}$ and R_{sol} may have errors due to parallel displacement of solar radiation through glass causing parts of the radiation to not enter the spectrophotometer detector during the measurements. For daylight and solar energy control the T_{vis} , T_{sol} and SF values are among the most crucial factors to be determined for ECWs working in the absorption mode.

Furthermore, solar radiation glazing factor modulations are calculated for the two different electrochromic windows ECW1 and ECW2 and given in Table 1. The modulation level is calculated by subtracting the solar radiation glazing factors for the same ECW at the high and low potentials given in Table 1, e.g. $\Delta T_{sol} = 0.74 - 0.17 = 0.57$ for ECW1.

Table 1. Calculated solar radiation glazing factors, and modulations, for two different electrochromic windows ECW1 (left) and ECW2 (right) at different colouration levels, i.e. at different applied potentials. Highest colouration level is at +1400 mV (ECW1) and +1200 mV (ECW 2, PANI-PB multilayer). Corresponding transmittance spectra are given in Fig.2. Reflectance values of the ECWs have not been measured, but as the (absorbing) electrochromic coatings are located between two glass plates, the (low) reflectance values will be close to the values for float glass, and these are hence employed in the current calculations. As there at the time of ECW fabrication were no resources for emissivity determinations, the nominal value of 0.837 for float glass was assumed (ϵ). The calculation of the SF is performed with respect to ϵ of the inside facing surface of the innermost glass pane, i.e. normally a float glass.

Solar Radiation Glazing Factor	ECW at -1800 mV	ECW at +1400 mV	Change in Solar Radiation Glazing Factor	ECW from -1800 mV to +1400 mV
T_{uv}	0.23	0.23	ΔT_{uv}	0.00
T_{vis}	0.78	0.17	ΔT_{vis}	0.61
T_{sol}	0.74	0.17	ΔT_{sol}	0.57
SMPF	0.43	0.71	$\Delta SMPF$	-0.28
SSPF	0.93	0.93	$\Delta SSPF$	0.00
$R_{vis,ext}$	0.09	0.09	$\Delta R_{vis,ext}$	0.00
$R_{vis,int}$	0.09	0.09	$\Delta R_{vis,int}$	0.00
R_{sol}	0.08	0.08	ΔR_{sol}	0.00
A_{sol}	0.18	0.75	ΔA_{sol}	-0.57
ϵ	0.837	0.837	$\Delta \epsilon$	-
SF	0.79	0.37	ΔSF	0.42

Solar Radiation Glazing Factor	ECW at -1800 mV	ECW at +1200 mV	Change in Solar Radiation Glazing Factor	ECW from -1800 mV to +1200 mV
T_{uv}	0.10	0.12	ΔT_{uv}	-0.02
T_{vis}	0.62	0.10	ΔT_{vis}	0.52
T_{sol}	0.61	0.10	ΔT_{sol}	0.51
SMPF	0.61	0.82	$\Delta SMPF$	-0.21
SSPF	0.97	0.97	$\Delta SSPF$	0.00
$R_{vis,ext}$	0.09	0.09	$\Delta R_{vis,ext}$	0.00
$R_{vis,int}$	0.09	0.09	$\Delta R_{vis,int}$	0.00
R_{sol}	0.08	0.08	ΔR_{sol}	0.00
A_{sol}	0.31	0.82	ΔA_{sol}	-0.51
ϵ	0.837	0.837	$\Delta \epsilon$	-
SF	0.69	0.31	ΔSF	0.38

Note that incorporating the ECWs into two-layer and three-layer window pane configurations (not depicted here) reduces the total solar energy throughput modulation in the windows, as several layers of glass and coatings will increase the total reflectance and absorbance, i.e. less solar radiation left for the ECWs to modulate (regulate). That is, the solar radiation regulation by an ECW will decrease with the number of glass panes and low emittance coatings added to the total window configuration. It is observed that the Δ SSPF modulation is more or less insignificant for the ECW glass configurations given in Table 1, as the change in ECW colouration state at low wavelengths is almost negligible due to the highly increasing absorption in the glass system from 400 nm and below (see Fig.2).

Thus, the ECWs may contribute to elegant, flexible glazing systems with dynamical control of the solar radiation, both with regard to daylight, energy aspects and protection of materials inside buildings. The ECWs may readily be characterized by spectroscopic measurements and subsequent calculations of the solar radiation glazing factors.

6. CONCLUSIONS

Solar radiation glazing factors, i.e. ultraviolet solar transmittance, visible solar transmittance, solar transmittance, solar material protection factor, solar skin protection factor, external visible solar reflectance, internal visible solar reflectance, solar reflectance, solar absorbance, emissivity, solar factor and colour rendering factor, characterize window panes and other glass structures in buildings. These factors for different glass fabrications may readily be compared in order to choose the most appropriate glass material for the building in question. Spectroscopical measurements and corresponding calculations of the solar radiation glazing factors were performed on two electrochromic window devices, and selected two-layer and three-layer window pane combinations incorporating electrochromic materials. It is concluded that the solar radiation glazing factors offer a suitable and powerful characterizing tool for comparing electrochromic windows at their various colouration states.

ACKNOWLEDGEMENTS

This work has been supported by the Research Council of Norway through the SINTEF research project "*Environmentally Favourable Energy Use in Buildings*" and the Research Council of Norway, AF Gruppen, Glava, Hunton Fiber as, Icopal, Isola, Jackon, maxit, Moelven ByggModul, Rambøll, Skanska, Statsbygg and Takprodusentenes forskningsgruppe through the SINTEF/NTNU research project "*Robust Envelope Construction Details for Buildings of the 21st Century*" (ROBUST).

REFERENCES

- ASTM E 1585-93, "Standard test method for measuring and calculating emittance of architectural flat glass products using spectrometric measurements", 1993.
- R. Baetens, B. P. Jelle and A. Gustavsen, "Properties, requirements and possibilities of smart windows for dynamic daylight and solar energy control in buildings: A state-of-the-art review", *Solar Energy Materials & Solar Cells*, **94**, 87-105, 2010.
- CIE No 89/3:1990, "On the deterioration of exhibited museum objects by optical radiation", 1990.
- CRC Handbook of Chemistry and Physics 1989-1990, R.C. Weast, D.R. Lide, M.J. Astle, W.H. Beyer (Eds.), 70th Ed., CRC Press, Boca Raton, Florida, p. F-167, 1989-1990.
- EN 410:1998 E, "Glass in building - Determination of luminous and solar characteristics of glazing", 1998.

EN 1946-2:1999 E, "Thermal performance of building products and components - Specific criteria for the assessment of laboratories measuring heat transfer properties - Part 2: Measurements by guarded hot plate method", 1999.

EN 1946-3:1999 E, "Thermal performance of building products and components - Specific criteria for the assessment of laboratories measuring heat transfer properties - Part 3: Measurements by heat flow meter method", 1999.

EN 12898:2001 E, "Glass in building - Determination of the emissivity", 2001.

EN ISO 6946:1996, "Building components and building elements. Thermal resistance and thermal transmittance. Calculation method", 1996.

ISO/DIS 9050:2001, "Glass in building - Determination of light transmittance, solar direct transmittance, total solar energy transmittance, ultraviolet transmittance and related glazing factors", 2001.

ISO/FDIS 9050:2003(E), "Glass in building - Determination of light transmittance, solar direct transmittance, total solar energy transmittance, ultraviolet transmittance and related glazing factors", 2003.

ISO 9845-1:1992(E), "Solar Energy - Reference solar spectral irradiance at the ground at different receiving conditions - Part 1: Direct normal and hemispherical solar irradiance for air mass 1.5", 1992.

ISO 10292:1994(E), "Glass in building - Calculation of steady-state U values (thermal transmittance) of multiple glazing", 1994.

ISO 10526:1999(E), "CIE standard illuminants for colorimetry", 1999.

ISO/CIE 10527:1991(E), "CIE standard illuminants for colorimetry", 1991.

B. P. Jelle, G. Hagen and Ø. Birketveit, "Transmission properties for individual electrochromic layers in solid state devices based on polyaniline, prussian blue and tungsten oxide", *Journal of Applied Electrochemistry*, **28**, pp. 483-489, 1998(a).

B. P. Jelle and G. Hagen, "Electrochemical multilayer deposition of polyaniline and prussian blue and their application in solid state electrochromic windows", *Journal of Applied Electrochemistry*, **28**, pp. 1061-1065, 1998(b).

B. P. Jelle and G. Hagen, "Performance of an electrochromic window based on polyaniline, prussian blue and tungsten oxide", *Solar Energy Materials & Solar Cells*, **58**, 277-286 (1999).

B. P. Jelle, A. Gustavsen, T.-N. Nilsen and T. Jacobsen, "Solar material protection factor (SMPF) and solar skin protection factor (SSPF) for window panes and other glass structures in buildings", *Solar Energy Materials & Solar Cells*, **91**, 342-354 (2007).

B. P. Jelle and A. Gustavsen, "Solar radiation glazing factors for electrochromic windows for building applications", *Proceedings of the Building Enclosure Science & Technology (BEST 2 - 2010)*, Portland, Oregon, U.S.A., 12-14 April, 2010.

K. I. Kimura, "Scientific basis of air conditioning", pp. 99-105, Applied Science Publishers, London, 1977.

A. F. McKinlay and B.L. Diffey, "A reference action spectrum for ultraviolet induced erythema in human skin", *CIE Journal*, **6**, pp. 17-22, 1987.

M. Rubin, K. von Rottkay and R. Powles, "Window optics", *Solar Energy*, **62**, 149-161, 1998.

Surface Optics Corporation, "SOC-100 User's Manual", San Diego, U.S.A., June 2009.

Rock Core Samples Cannot Replace Thermal Response Tests - A Statistical Comparison Based On Thermal Conductivity Data From The Oslo Region (Norway)

H.T. Liebel¹, K. Huber², B.S. Frengstad³, R. Kalskin Ramstad⁴ and B. Brattli¹

¹ Department of Geology and Mineral Resources Engineering, Norwegian University of Science and Technology (NTNU), NO-7491 Trondheim; E-mail: heiko.liebel@ntnu.no

² Department of Geology, University of Bayreuth, Universitätsstr. 30, D-95440 Bayreuth, Germany

³ Geological Survey of Norway (NGU), NO-7491 Trondheim

⁴ Asplan Viak AS, Postbox 6723, NO-7490 Trondheim

ABSTRACT

Borehole heat exchanger (closed-loop) systems coupled to a ground-source heat pump are applied for space heating and cooling using the ground as energy source or storage medium. For accurate dimensioning of a ground-source heat installation, knowledge of the thermal conductivity of the subsurface is vital.

Thermal response tests (TRT) are widely used to measure the *in situ* thermal conductivity in a well. Alternatively, the thermal conductivity in a borehole is approximated from rock core samples based on lab measurements. Rock core data and thermal conductivity maps are financially more attractive for planning purposes than expensive TRTs. The value of both approaches was statistically tested using data from the geologically diverse Oslo region (Norway).

Effective thermal conductivity data measured *via* TRTs show a clear trend towards higher thermal conductivity values in comparison to lab measured thermal conductivity values from rock cores (in 82 % of cases). The deviation from the rock core samples, however, varies strongly as several geological layers may be represented in one single well. Furthermore, the thermal conductivity of the rock core samples varies strongly within individual geological units.

The comparison of both techniques of thermal conductivity measurement shows that the *in situ* thermal conductivity at a location cannot be predicted from rock core data of a geological unit.

The results of this study indicate that the dimensioning of a large ground-source heat project cannot be based on rock core measurements or thermal conductivity maps only, without analysing the *in situ* thermo-, hydro- and geological conditions in fractured rocks.

Keywords: Thermal response test, thermal conductivity, ground-source heat, hard rock, thermal conductivity map.

1. INTRODUCTION

The so-called “Stern review”, published in 2006, was the first report focussing on the effect of global warming on the world economy. Among other things, it shows the relative greenhouse gas emissions per sector. The space-heating and cooling of buildings account for 8 % of the total greenhouse gas emissions, or possibly even 20 % if upstream emissions associated with electricity and heat are included (Stern, 2006).

Low-temperature geothermal energy applications, also called shallow geothermal energy or ground-source heat applications, are considered one of the key technologies to reduce greenhouse gas emissions in the buildings sector (Sims *et al.*, 2007).

The most common type of ground-source heat applications for space-heating and cooling in Europe is the closed-loop borehole heat exchanger system. Shallow boreholes (< 200 m) are drilled for this purpose in different kinds of rocks or unconsolidated sediments. Collector pipes, U-shaped or coaxial, are installed in the boreholes and connected to a ground-source heat pump, which helps heat to flow from a low-temperature environment to a high-temperature one. Ground-source heat pumps can effectively be switched into reverse, from heating to cooling mode, so that heat from the inside of a building is pumped away to the borehole. This is more efficient than air-to-air heat pumps in warm weather (Banks, 2008). This type of closed-loop system with a ground-source heat pump is widely used in Scandinavia for heating and cooling of single households with a single or few non-grouted boreholes. Larger buildings require more boreholes to meet the demands for heating and cooling. For the estimation of the required borehole length to deliver a certain amount of energy to a building, some ground parameters should be known, including the thermal conductivity. If the thermal conductivity for a certain rock type is assumed and not certain, some extra meters of borehole are usually drilled to avoid underdimensioning the system.

Another possibility is to perform a thermal response test (TRT) in a test well to measure the *in situ* thermal conductivity (Austin, 1998; Gehlin, 1998) and then drill the required boreholes depending on the measured value. Thermal response tests are often performed for larger ground-source heat projects. One disadvantage, however, is that it is a costly procedure. Alternatively, thermal conductivity data from rock cores may be used in planning and dimensioning of large ground-source heat installations, if these data are available.

For the Oslo region, the most densely populated area of Norway, such a database, including a thermal conductivity map, exists at the Geological Survey of Norway (NGU). This study investigates statistically the applicability of such a thermal conductivity map for the dimensioning of large ground-source heat pump projects by comparing its entries with data from TRTs performed in the same geological units.

2. MATERIAL AND METHODS

2.1 Thermal conductivity data from rock cores

Surface rock cores from 1398 sample locations within the area of the bedrock map of the Oslo region (based on Lutro and Nordgulen, 2004) were drilled and analyzed for their thermal conductivity in the laboratory of the Geological Survey of Norway. Ramstad *et al.* (2008a) presented these data as a map showing the thermal conductivity of the different geological units of the Oslo region (Fig.1). For every geological unit a median thermal conductivity value was calculated and then given a colour according to a colour classification code. Each of the 24 geological units is represented with 10 to 219 locations.

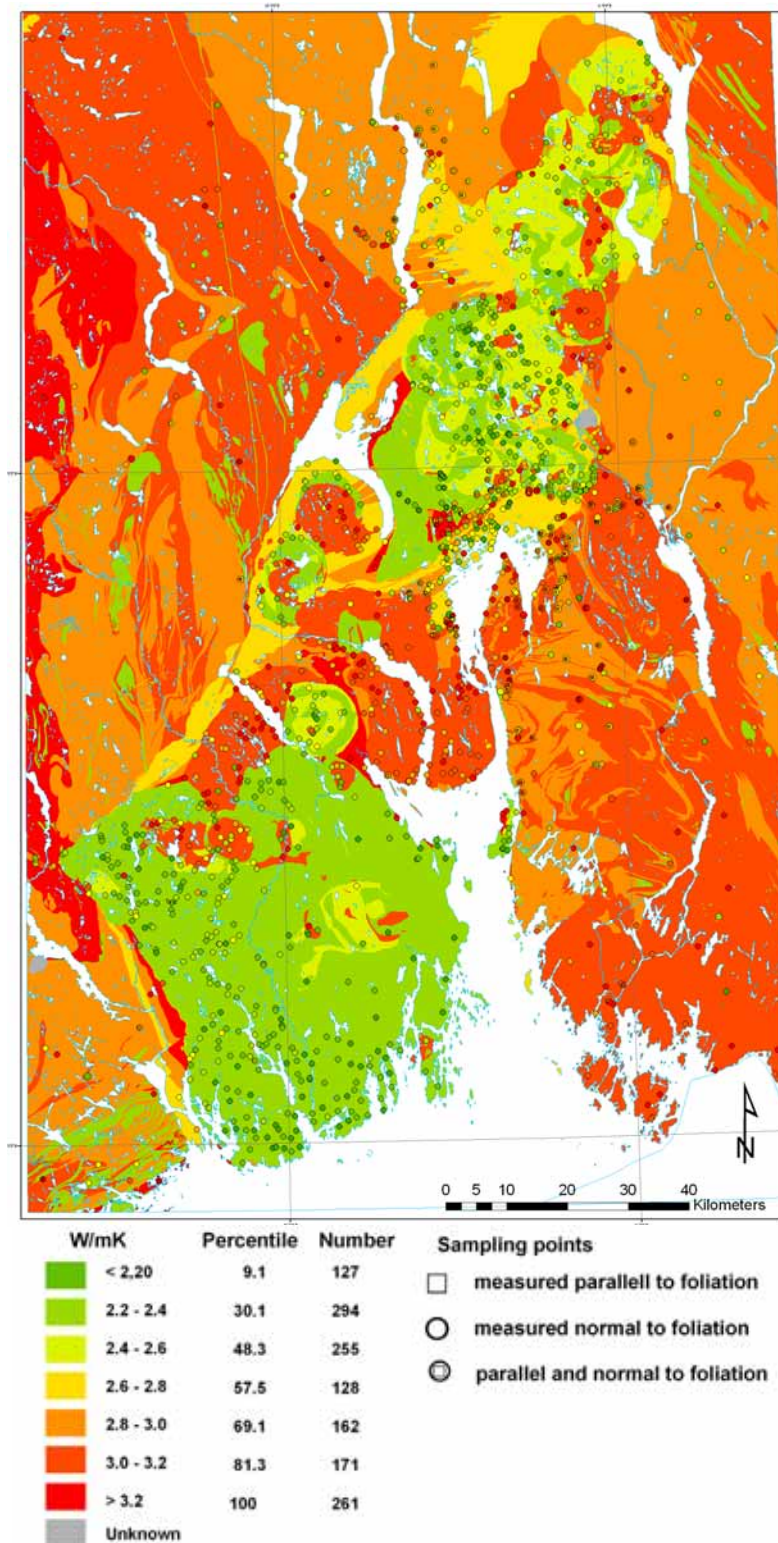


Figure 1: Median values of thermal conductivity of geological units are presented on map sheet “Oslofeltet” where sampling points indicate measured values (Ramstad *et al.* 2008a).

The laboratory procedure to estimate the thermal conductivity of a rock core follows Middleton’s approach (1993) where a constant heat source (144 or 300 °C) is applied few millimeters above the vertically positioned rock core sample at room temperature. The temperature increase at the base of the rock core is measured. From the measurement of the

thermal diffusivity (α) of the sample, the thermal conductivity (λ) is calculated according to equation 1.

$$\lambda = \rho C_p \alpha \quad (1)$$

where

- λ : Thermal conductivity [$\text{W m}^{-1}\text{K}^{-1}$]
- ρ : Density [kg m^{-3}]
- C_p : Specific heat capacity [$\text{J kg}^{-1}\text{K}^{-1}$]
- α : Thermal diffusivity [$\text{m}^2 \text{s}^{-1}$]

A detailed description of the method development and quality control routines of the thermal conductivity measurement at the laboratory at the Geological Survey of Norway is found in Ramstad *et al.* (2008b).

One drawback of the method is that fractures and fissures in the rocks are filled with water at the location but they are dry in the lab. Air has a lower thermal conductivity than water so that *in situ* measurements in water-saturated conditions should lead to slightly higher thermal conductivity values (Ericsson, 1985). Further, a strong anisotropic thermal behaviour of some rocks has been shown by Clauser and Huenges (1995) among others, where the thermal conductivity is high parallel to the foliation and low perpendicular to the foliation. The direction of foliation, however, may vary strongly in folded rocks within the same geological unit, which will give varying thermal conductivity values.

One final limitation of the dataset is that only surface bedrock cores are taken into account while several rock types may occur vertically along a borehole used for a ground-source heat pump installation.

2.2 Thermal conductivity data from thermal response tests

Thermal response tests are often applied in Scandinavia to test the *in situ* or effective thermal conductivity in a borehole. For this purpose the TRT equipment is connected to the collector pipes of the energy well. Heating elements in a portable TRT trailer heat the water that is circulating through the closed-loop system. The connection between the trailer and the borehole has to be well insulated, to avoid heat loss in cold weather or heat gain through sun irradiation. The circulation pump creates a turbulent flow in the pipes to get best heat transport from the collector towards the ground. The undisturbed ground temperature (measured before the TRT) and the temperature increase in the water during a test run are used to calculate the effective thermal conductivity of the ground (λ_{eff}) and the borehole resistance (R_b) which is from contact between the borehole heat exchanger and the well. The calculation of λ_{eff} and R_b follows the suggestions of Gehlin (2002), which are based on the infinite line source theory (Ingersoll, 1948). A TRT typically lasts 72 hours (Gehlin, 1998). In this time range the analytical solution of the infinite line source shows a very low error level compared to the alternative exact solutions of the finite line source and the infinite cylindrical source theory (Philippe *et al.*, 2009).

Possible sources of error during a TRT are: 1) heat loss and gain, 2) variable electric power supply, 3) accuracy of the determination of the undisturbed ground temperature, 4) free convection of water in non-grouted boreholes (standard for energy wells in Scandinavia; Gustafsson *et al.*, 2010), 5) gradient-driven horizontal groundwater flow and 6) density-driven vertical groundwater flow (e.g. thermosiphon effect, Gehlin *et al.*, 2003, Gustafsson, 2006).

Data from 67 standard TRTs from the Oslo region performed with the test equipment of the Geological Survey of Norway and the consulting company Geoenergi AS are statistically evaluated in this study. Statistical analyses were performed with SPSS 17.0

(SPSS, Chicago, IL, USA), box and whisker plots were calculated and drawn with SigmaPlot 11.0 (Systat Software, Chicago, IL, USA).

3. RESULTS

Median thermal conductivities of different rock types from the Oslo region measured in rock cores and in TRTs show a similar range and vary from 2.3 to $3.5\text{ W m}^{-1}\text{ K}^{-1}$ and 2.6 to $3.7\text{ W m}^{-1}\text{ K}^{-1}$, respectively (see Table 1). The lowest thermal conductivity is found in monzonites and monzodiorites (quartz-poor rock). The highest values from rock cores are measured in late Silurian sandstones (quartz-rich rock) while the highest effective thermal conductivity (measured in TRTs) was found in granitic to tonalitic gneisses. The borehole resistance varies from 0.06 to $0.07\text{ K W}^{-1}\text{ m}^{-1}$, with the exception of one measurement in an alum shale ($0.09\text{ K W}^{-1}\text{ m}^{-1}$). Convection occurs in non-grouted, water-filled boreholes during heat injection, which reduces the calculated borehole resistance so that a slightly higher value is expected for a ground-source heat pump system in operation during heating mode (Gustafsson *et al.*, 2010).

Table 1: Mean values for the borehole resistance, R_b , and median values of the thermal conductivity (λ) measured in TRTs ("eff") and from rock core samples ("Geomap") for 14 different rock units (Geomap number) based on the geological map 1:250 000 of Oslo (Lutro and Nordgulen, 2004). Number of analyses shown by (n).

Rock type	$R_b [\text{K W}^{-1}\text{ m}^{-1}] \pm \text{SD (n)}$	$\lambda_{\text{eff}} [\text{W m}^{-1}\text{ K}^{-1}] (\text{n})$	$\lambda_{\text{Geomap}} [\text{W m}^{-1}\text{ K}^{-1}] (\text{n})$	Geomap number
Monzonite, monzodiorite (larvikite and kjelsåsite)	0.07 (2)	2.6 (2)	2.3 (219)	14
Biotite syenite (e.g. Grefsen syenite)	0.06 ± 0.01 (7)	2.8 (8)	2.4 (58)	7
Syenite porphyry (ring-dykes)	0.06 (1)	2.9 (1)	2.5 (18)	9
Dioritic to tonalitic gneiss (in places metagabbro; 1550 Ma)	0.07 ± 0.00 (3)	3.1 (3)	3.1 (11)	42
Shale, marl and limestone, Mid to Late Ordovician age	0.07 ± 0.01 (17)	3.2 (20)	2.7 (79)	26
Mica gneiss, often with garnet, kyanite or sillimanite (1590-1490 Ma)	0.06 ± 0.01 (8)	3.2 (8)	3.0 (91)	44
Granite, granodiorite	0.06 ± 0.01 (4)	3.3 (4)	3.0 (157)	5
Granite (ca. 925 Ma, Flå- and Iddefjordgranites)	0.07 (2)	3.4 (2)	3.2 (32)	30
Sandstone, Late Silurian age	0.07 ± 0.01 (3)	3.5 (3)	3.5 (24)	24
Latite (rhomb porphyry)	0.06 (2)	3.5 (2)	2.3 (54)	19
Limestone, shale and sandstone, Early Silurian age	0.06 ± 0.01 (8)	3.5 (8)	2.9 (48)	25
Alum shale, sandstone, conglomerate and limestone, Cambrian to Ordovician age	0.09 (1)	3.5 (1)	2.6 (13)	27
Granitic to tonalitic gneiss (1500-1550 Ma)	0.07 ± 0.01 (4)	3.7 (4)	3.0 (95)	41
Mica schist, metasandstone, amphibolite, granitic to tonalitic gneiss	0.07 (1)	3.7 (1)	2.9 (77)	50

The thermal conductivity values from the two different measurement techniques show a significant positive correlation (Pearson product-moment correlation coefficient, normally

distributed data) for the 14 different investigated rock types ($r = 0.534$, $P = 0.049$, $n = 14$). A linear regression gives a poor fit to the dataset, however (see Fig. 2).

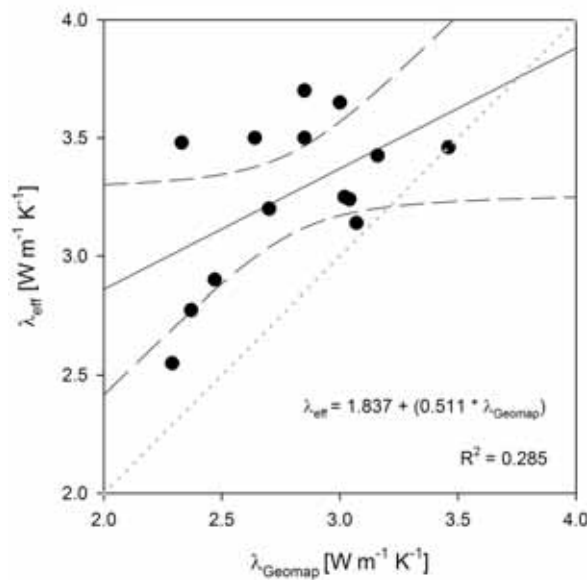


Figure 2: Median values of the thermal conductivity from TRTs ("eff") versus values from rock core samples ("Geomap") for 14 different geological units. The linear regression (solid line) is shown with 95 % confidence intervals (dashed line).

In all cases the effective thermal conductivity is higher (or equal) than the thermal conductivity measured in rock cores. If thermal conductivities from single TRT results ($n = 68$) are compared to the median thermal conductivity from rock cores, 82 % plot above the 1:1 line and show accordingly higher thermal conductivities compared to rock cores.

All locations of this study were classified according to the surface bedrock in sedimentary, metamorphic and igneous rocks. The single thermal conductivity measured with TRTs was then compared to the median value from rock cores as a ratio for the according rock type. All median thermal conductivity ratios are higher than 1 (Fig. 3).

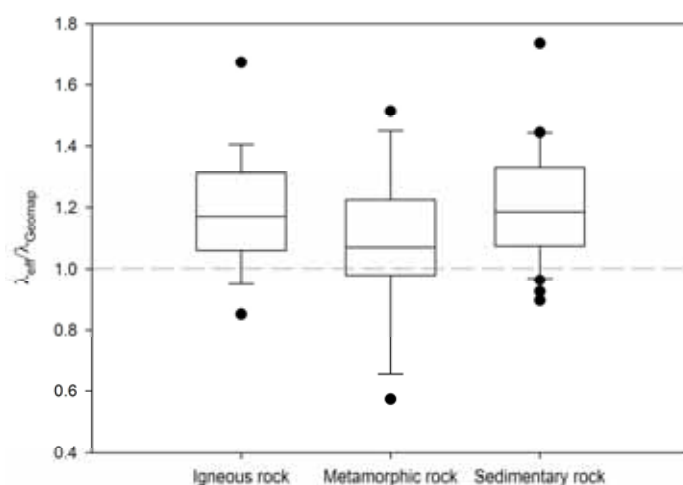


Figure 3: Box and whisker plot for the ratio between the effective thermal conductivity and the median thermal conductivity (rock core samples) for igneous ($n = 19$), metamorphic ($n = 17$) and sedimentary rocks ($n = 32$).

A Kruskal-Wallis nonparametric test (data are not normally distributed) shows that no significant difference ($\chi^2 = 1.404$, $df = 2$, $n = 68$, $P = 0.496$) can be proven in the thermal conductivity ratios between sedimentary, metamorphic and igneous rocks. A remarkable higher variation in its thermal conductivity ratio, however, is found in metamorphic rocks. Also the median thermal conductivity ratio of the metamorphic rocks is lower than the ones of igneous and sedimentary rocks.

The dataset for effective thermal conductivity values in the Oslo region of 68 samples opposes 1843 rock core samples. Statistical comparisons and cautious interpretations are still possible. Box and whisker plots are used as descriptive statistics to compare visually the results from the rock core samples with the thermal conductivity data from TRTs. Sufficient data is available for four different geological units: Syenite (igneous rock), Silurian and Ordovician sediments and mica gneiss (metamorphic rock; Fig. 4).

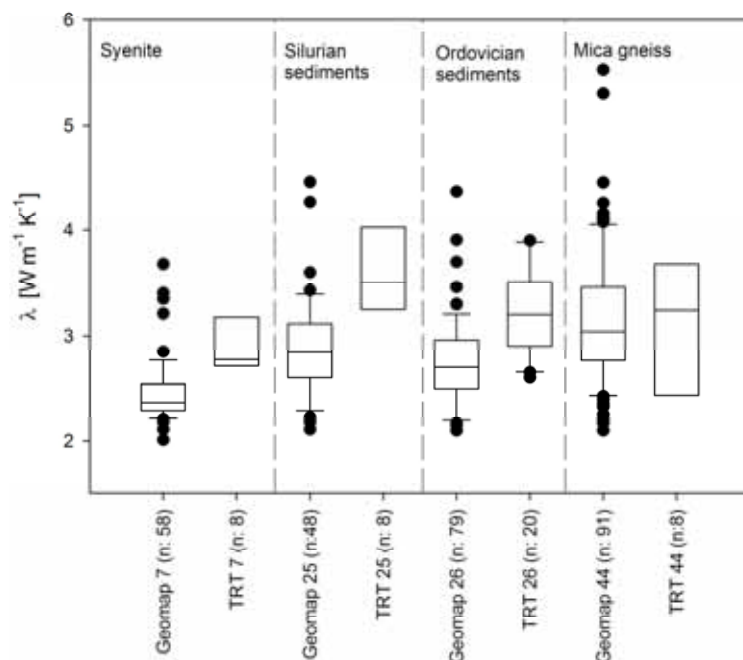


Figure 4: Statistical variations of the thermal conductivity (25 % percentile, median, 75 % percentile, whiskers indicate 10 % and 90 % percentiles if more than 9 samples are available, outliers are dotted) for four geological units of the Oslo region according to the geomap of Lutro and Nordgulen (2004) for data from rock core samples and from TRT data.

Nonparametric Mann-Whitney U tests (no equality of variance in the datasets) show that the thermal conductivities of the rock core samples are significantly different from the values measured in TRTs in syenites (Mann-Whitney $U = 83.0$, $P = 0.003$), Silurian (Mann-Whitney $U = 37.0$, $P < 0.001$) and Ordovician sediments (Mann-Whitney $U = 300.0$, $P < 0.001$). Instead, no significant difference could be found in the data for the mica gneiss (Mann-Whitney $U = 322.0$, $P = 0.590$). Large variations within the thermal conductivity measurements appear in all rock types regardless of the measurement type.

The inverted approach to search statistically for groups (e.g. cluster of entries belonging to a geological unit) within the two overall thermal conductivity datasets was done with the help of a hierarchical cluster analysis (Squared Euclidean distance, Ward's Linkage). For this purpose the effective thermal conductivity and the median rock core value of the same geological unit were chosen as input data. No pattern could be found, however.

4. DISCUSSION

Generally, the effective thermal conductivity is higher than the rock core data would suggest. Effective heat transport through groundwater advection has been shown to be the most important cause through field experiments (Witte 2002, 2007) and numerical modelling (e.g. Fujii *et al.*, 2005; Fan *et al.*, 2007). No hydraulic yield or other hydrogeological data is available for the wells of this study.

Morland (1997) however, studied well yields of wells in different geological units throughout Norway.

In syenites, he found a normalised median yield of 22.4 l hr^{-1} per drilled meter, which is one of the highest yields of the different rock types of this study. The median of the effective thermal conductivity measured in syenites is 15 % higher than the thermal conductivity from rock core samples, which may be explained by groundwater flow through fracture networks.

In Ordovician and Silurian sediments, the median of the effective thermal conductivity measured is respectively 16 and 19 % higher than the thermal conductivity from the rock core samples. Groundwater flow through fractures and karst systems in the limestones can be expected. A median normalised yield of 11.4 l hr^{-1} per drilled meter in Cambro-Silurian meta-sediments, however, is a surprisingly low value. One problem of the results of Morland (1997) is, that his group of Cambro-Silurian meta-sediments includes both stronger metamorphosed sedimentary rocks from the Caledonian mountain chain (low yields) and weakly metamorphosed sedimentary rocks of the Oslo region where higher yields are expected.

In micaceous gneisses the median effective thermal conductivity is only 6 % higher than the thermal conductivity from rock cores and the variation within the different samples of the same geological unit is the largest of all rock types of this study. Morland found a median well yield of 16.7 l hr^{-1} for Precambrian gneisses from all over Norway. Advective groundwater flow is expected in many wells drilled in gneisses as well. The thermal anisotropy of micas may explain the large variation in thermal properties. Clauser and Huenges (1995) investigated the thermal conductivity of biotites. They measured $3.1 \text{ W m}^{-1} \text{ K}^{-1}$ parallel to the sheets and $0.5 \text{ W m}^{-1} \text{ K}^{-1}$ perpendicular to the sheets. The orientation of the foliation in the mica gneisses is not known and it may vary along the boreholes due to folding.

An inverse approach is to classify the thermal conductivity data to find homogeneous groups belonging to one or several rock types with the help of a hierarchical cluster analysis. This approach failed, as it shows that the variability within the geological units is large and that no systematic cluster following the rock type classification can be found.

5. CONCLUSION AND FURTHER WORK

Despite the variations within individual geological units, rock core thermal conductivity values give a good qualitative indication of the effective thermal conductivity expected at a planned ground-source heat pump site. If the linear regression would yield a better fit, the regression equation could be used to predict the effective thermal conductivity of a geological unit. The data of this study, however, shows that the variations are large, due to thermal anisotropic rock properties and variable groundwater influence. The dimensioning of a high-capacity ground-source heat pump installation based on rock core data or the thermal conductivity map of the Oslo region only is not recommended, despite the extensive dataset available.

Further work could test whether a better correlation can be found if only the rock core thermal conductivity from the outcrop closest to the TRT site is used. If this succeeds, a geographic information system (GIS) could be built up that gives information about the thermal conductivity of the closest rock core sample and its distance to the planned ground-source heat site. Additionally, thermal and hydrogeological information can be made available linking relevant databases available at the Geological Survey of Norway.

ACKNOWLEDGEMENTS

The authors are thankful for having gotten access to the GEOS database of the Geological Survey of Norway. TRT data made available by Geoenergi AS, Futurum Energi AS, the Geological Survey of Norway and the Norwegian Geotechnical Institute (NGI) are gratefully acknowledged. We like to thank Båsum Boring AS for their valuable cooperation offering eight energy wells for thermal response testing and Allan Krill (Norwegian University of Science and Technology, NTNU) for giving valuable comments to the manuscript. The study was financed by the Geological Survey of Norway and the Norwegian University of Science and Technology, Trondheim.

REFERENCES

- Austin, W.A., 1998, *Development of an in situ system for measuring ground thermal properties*. M.Sc. Thesis. Oklahoma State University, Stillwater. OK, USA, 177 p.
- Banks, D., 2008, *An introduction to thermogeology – Ground source heating and cooling*, Blackwell Publishing Ltd., Oxford, UK, 339 p.
- Clauser, C., Huenges, E., 1995, Thermal conductivity of rocks and minerals, In: Ahrens T.J., *Rock physics and phase relations – A handbook of physical constants*, Am. Geophys. Union, Washington, USA: p. 105-126.
- Ericsson, L.O., 1985, *Värmeutbyte mellan berggrund och borrhål vid bergvärme-system*, Dep. of Geol., Chalmers Univ. of Techn. and Univ. of Göteborg, Publ. A 52, Göteborg, Sweden.
- Fan, R., Jiang, Y.Q., Yao, Y., Shiming, D., Ma, Z.L., 2007, A study on the performance of a geothermal heat exchanger under coupled heat conduction and groundwater advection, *Energy* vol. 32: p. 2199-2209.
- Fujii, H., Itoi, R., Fujii, J., Uchida, Y., 2005, Optimizing the design of large-scale ground-coupled heat pump systems using groundwater and heat transport modeling. *Geothermics* vol. 34: p. 347-364.
- Gehlin, S., 1998, *Thermal response test. In situ measurements of thermal properties in hard rock*, Licentiate thesis, Luleå Univ. of Techn., 1998:37.
- Gehlin, S., 2002, *Thermal response test. Method development and evaluation*, Doctoral thesis, Luleå Univ. of Techn., 2002:39.

Gehlin, S.E.A., Hellström, G., Nordell, B., 2003, The influence of the thermosiphon effect on the thermal response test, *Renew. Energy*, vol. 28: p. 2239-2254.

Gustafsson, A.M., 2006. *Thermal Response Test – Numerical simulations and analyses*. Licentiate thesis. Luleå University of Technology, 2006:14, 141 p.

Gustafsson, A.M., Westerlund, L., Hellström, G., 2010, CFD-modelling of natural convection in a groundwater-filled borehole heat exchanger, *Appl. Thermal Eng.*, vol. 30: p. 683-691.

Ingersoll, L.R., 1948, *Heat conduction – With engineering and geological application*, McGraw-Hill Book Comp., New York, USA. 278 p.

Lutro, O., Nordgulen, Ø., 2004, *Oslofeltet, berggrunnskart M 1:250 000*, Geol. Surv. of Nor..

Middleton, M.F., 1993, A transient method of measuring the thermal properties of rocks. *Geophysics*, vol. 58: p. 357-365.

Morland, G., 1997, *Petrology, lithology, bedrock structures, glaciation and sea level. Important factors for groundwater yield and composition of Norwegian bedrock boreholes?* Geol. Surv. of Nor., Rep. 97.122, 274 p.

Philippe, M., Bernier, M., Marchio, D., 2009, Validity ranges of three analytical solutions to heat transfer in the vicinity of single boreholes, *Geothermics* vol. 38: p. 407-413.

Ramstad, R.K., Tiarks, H., Midttømme, K., 2008a, Ground source energy – Thermal conductivity map in the Oslo region, Poster shown at the stand of the Geol. Surv. of Nor., 33rd Int. Geol. Congr. Oslo, August 6-14th.

Ramstad, R.K., de Beer, H., Midttømme, K., Koziel, J., Wissing, B., 2008b, *Thermal diffusivity measurement at NGU – Status and method development 2005-2008*, Geol. Surv. of Nor., rep. 2008.050, 41 p.

Sims, R.E.H., Schock, R.N., Adegbululgbe, A., Fenhan, J., Konstantinaviciute, I., Moomaw, W., Nimir, H.B., Schlamadinger, B., Torres-Martínez, J., Turner, C., Uchiyama, Y., Vuori, S.J.V., Wamukonya, N., Zhang, X., 2007, Energy supply, In: Metz, B., Davidson, O.R., Bosch, P.R., Dave, R., Meyer, L.A., *Climate Change 2007: Mitigation. Contribution of Working Group III to the Fourth Assessment Report of the Intergovernmental Panel on Climate Change*, Cambridge University Press, Cambridge, UK and New York, USA, p. 252-322.

Stern, N., 2006, *The Stern review on the economics of climate change*, Cambridge University Press, UK, 692 p.

Witte, H., 2002, Ground thermal conductivity testing: Effects of groundwater on the estimate, Abstract, 3. Kolloquium d. Arbeitskr. Geothermik d. DGG, Aachen, Germany, October 3rd-4th.

Witte, H., 2007, Advances in Geothermal Response Testing, In: Paksoy, H.Ö., *Thermal Energy Storage for Sustainable Energy Consumption*, Springer Netherlands, p. 177-192.

Thermosyphon Heated Thermal Store, the Influences of Valve Opening on flow, an Experimental Analysis

J. N. Macbeth¹, H. Smith¹, Dr. J. Currie², Dr. N. Finlayson¹

¹*Greenspace Research, Lewis Castle College UHI, Stornoway, Isle of Lewis, HS1 0XR, UK*

²*Edinburgh Napier University, Schools of Engineering and the Built Environment, 10 Colinton Rd, Edinburgh, EH10 5DT, UK*

ABSTRACT

This paper outlines initial findings from the design of a Thermal Energy Storage (TES) system whose principal objective is to promote stratification when charged by an intermittent electrical supply. This concept will offer an efficient solution to the heating and provision of domestic hot water within buildings when coupled with a renewable energy source such as wind power.

The principal of operation is to add the energy to the tank through a side arm that creates a thermosyphon and returns the water to the top of the tank at a desired temperature. A system of extraction points will then be employed to prioritise the replenishment of individual tank nodes from top to bottom, thus increasing the useful energy content of the system.

In this paper initial investigations on the control mechanism required to achieve the desired mass flow rate have been carried out experimentally on a 750 litre tank. The tank was charged under steady input power with different valve opening angles, the results from which show the formation of temperature gradients through the tank's vertical plane.

It is found that the importance of the valve opening lies mainly in permitting large changes in the power inputs to the store. It also allows for small and large temperature rises to be achieved across the side arm, thus enabling nodes to be "topped-up". The requirements to compensate for the changes in driving force are found to be less critical than first anticipated.

Keywords: Intermittent electrical supply, stratification, thermosyphon, charge-cycle.

1. INTRODUCTION

Thermal energy storage (TES) systems have been used in many situations as a buffer between the energy supply system and a building's demand for domestic hot water and space heating, thus allowing smaller power sources to be used to provide the end user with high intermittent bursts of power. In the last few decades, many studies have been carried out on the benefits and the means to achieve stratification within a TES. Stratification is the phenomenon where hot water accumulates in a layer on top of cooler, denser water. As well as benefitting the efficiency of some energy supply equipment by providing cooler return

temperatures, this process can be used to increase the usable energy in the system. Most forms of renewable energy, such as solar and wind, are well known for their intermittent patterns which directly impact on the power available from the energy converter.

The use of solar energy for domestic hot water (DHW) and space heating provision is a well understood process where, as mentioned above, stratification plays an important role in increasing the efficiency of the solar collector as well as compensating for the diurnal patterns in energy availability, Hollands (1989).

In most studies, however, the electrical energy is usually considered to be a “back up”, with few restrictions on its quantitative and/or temporal availability. In this research the electrical supply is treated as a principal energy supply but has an intermittent regime in terms of its available power. Thus a system that has the ability to maximize the storage potential of this energy when it is available is desired.

The main principle of operation being tested consists of adding the energy through a side arm as demonstrated in figure 1. This method, referred to as a thermosyphon, was believed to be the easiest way to bring the energy into the tank with minimal infrastructure and disturbance. Furbo (2005) found in side-by-side testing that this mechanism could lead to a large increase in solar collector performance as well as reduced auxiliary energy requirements over conventional systems. In his control mechanism, the upper layers of the tank were supplied with the correct amount of energy at the correct times, bringing the desired volume of water needed by the load to the set point temperature. The system investigated by the authors, in addition to the side arm, would have a number of extraction points that prioritise the areas of the tank needing energy.

The aim of this paper is to evaluate, through theoretical and experimental analyses, the control required in charging a tank using a side arm in the instances where variable temperatures as well as power inputs are encountered.

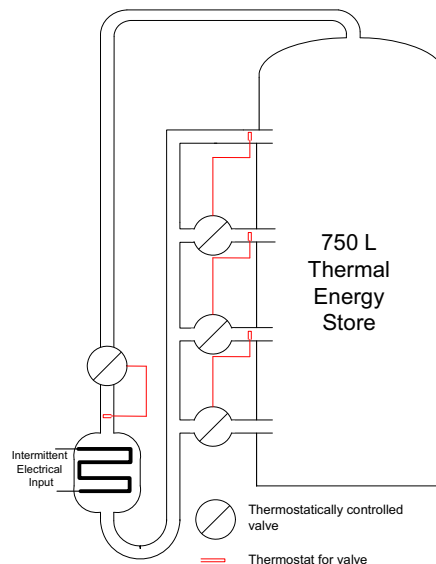


Figure 1: Layout of the TES including control valves (not to scale)

2. THEORETICAL INVESTIGATION

The operation of the system is governed by two fundamental equations. The first determines the desired mass flow rate ($m\dot{\&}$), Eq. (1), for a given set of operating conditions and at any one point in time.

$$m\dot{\&} = \frac{\dot{Q}}{cp.\Delta T} \quad (1)$$

Where \dot{Q} is the electrical power input to the heat box and $\Delta T = T_{set} - T_{out}$. T_{set} is the desired set point temperature for the water re-entering the tank after having been heated by the heat box and T_{out} is the temperature of the water flowing out of the tank towards the heat box. cp is the specific heat capacity of the water.

The second equation looks at the driving force in the system. This force is dependent on temperature and must therefore be summed, for all layers on the vertical axis within the tank that have different temperature, as found by Eq. (2);

$$P = \sum \Delta\rho.h.g \quad (2)$$

Where $\Delta\rho$ is the density difference between the horizontal layers on the vertical axis of the side arm and its equivalent layer on the tank. h is the height of the layer and g is gravity. The derived units are Pa .

To maintain the desired set point temperature, the friction loss around the loop encountered by the water travelling at flow $m\dot{\&}$ must equal that of the driving force created by the density difference between the tank and side arm.

As the system must be able to cope with a wide range of input powers, leading to large variations in $m\dot{\&}$, it is not possible to depend solely on the friction found in the pipes and bends. A valve or throttling device must therefore be employed to provide the correct friction at any one point in time, thus maintaining the set point temperature at the outlet of the heat box.

The valve selection was made according to manufacturer's datasheets. Valves are characterized by the friction factor, kv , which corresponds to the volume of water that passes through the valve when a pressure drop of 1 bar occurs across it. A percentage of the "kv-factor" is then given for various valve opening angles. Due to the very low flow rates and pressure drops encountered in this system, the data was extrapolated to obtain the desired openings under different states of charge. Initial experimentation revealed that this data, once extrapolated and added to the friction losses in the pipes, heat box and tank, was too inaccurate to provide satisfactory levels of control as too many errors in the assumption made accumulated through the calculations. An experimental approach was therefore adopted to evaluate the performance.

3. EXPERIMENTAL INVESTIGATION

Experimental Rig

The experimental rig is made up of a *750 litre* tank made of stainless steel with a wall thickness of *2mm*. The domes are of a heavier gauge (*6mm*). This was necessary in order to provide the required strength at the bottom for support. The dimensions of this vessel are given in Figure 2. The pipe-work connecting the tank to the heat box has an internal diameter of *37mm* and is made of polypropylene in order to withstand the heat. All connections on this pipe work are listed in Table 1, along with the valve and heating element details. The heat box was constructed of *2mm* stainless steel and of dimensions shown in figure 2.

Power input was changed by lowering the input voltage to the heating element using a transformer; due to the voltage fluctuations on the grid, the power was found to be variable. From the measurement the fluctuations were +3% and -3% of the mean measured power for the experimental run. The accuracy of the voltage and current transducers was found to be quite poor only once the experiments were over. Calibration exercises were undertaken and corrections to the recorded data were made accordingly.

The tank was divided into forty controlled volumes. The volumes are made up of ten horizontal layers, each divided into equal quarters. The thermocouples were held in place at the correct height by using four glass fibre tubes as shown in Figure 2. When assembled, the tips of the thermocouple were within a maximum of 5mm from their desired location on the vertical axis. The thermocouples and data logging equipment were calibrated prior to assembly and found to be within 1 degree of a calibrated thermometer.

The tank was insulated using glass wool with a minimum thickness of *100mm*. The pipes and heat box were not insulated.

2.1 Experimental procedures

The tank was allowed to settle for 40 minutes after being mixed using a pump to achieve a uniform temperature throughout. In some experiments, however, some residual heat from the heat box, that had not been mixed, created a top layer a couple of degrees higher than the rest of the tank. The data was gathered at a rate of 1 sample every 5 seconds for temperature, RMS voltage and current.

2.2 Results

Experimental runs were carried out with five valve openings and two distinctive power inputs; all of which were held constant for the duration of the experiment. Plots of temperature over time were created using the measurements. Figures 3, 4 and 5 show the results from valve openings of 15%, 20% and 50%. The input power to these runs was approximately 4.7 kW; further detail of the power input is listed in the caption. The following graphs, Fig, 6, 7 and 8 show the results from three individual three-hour runs. These performed with a combination of two valve openings and two input powers.

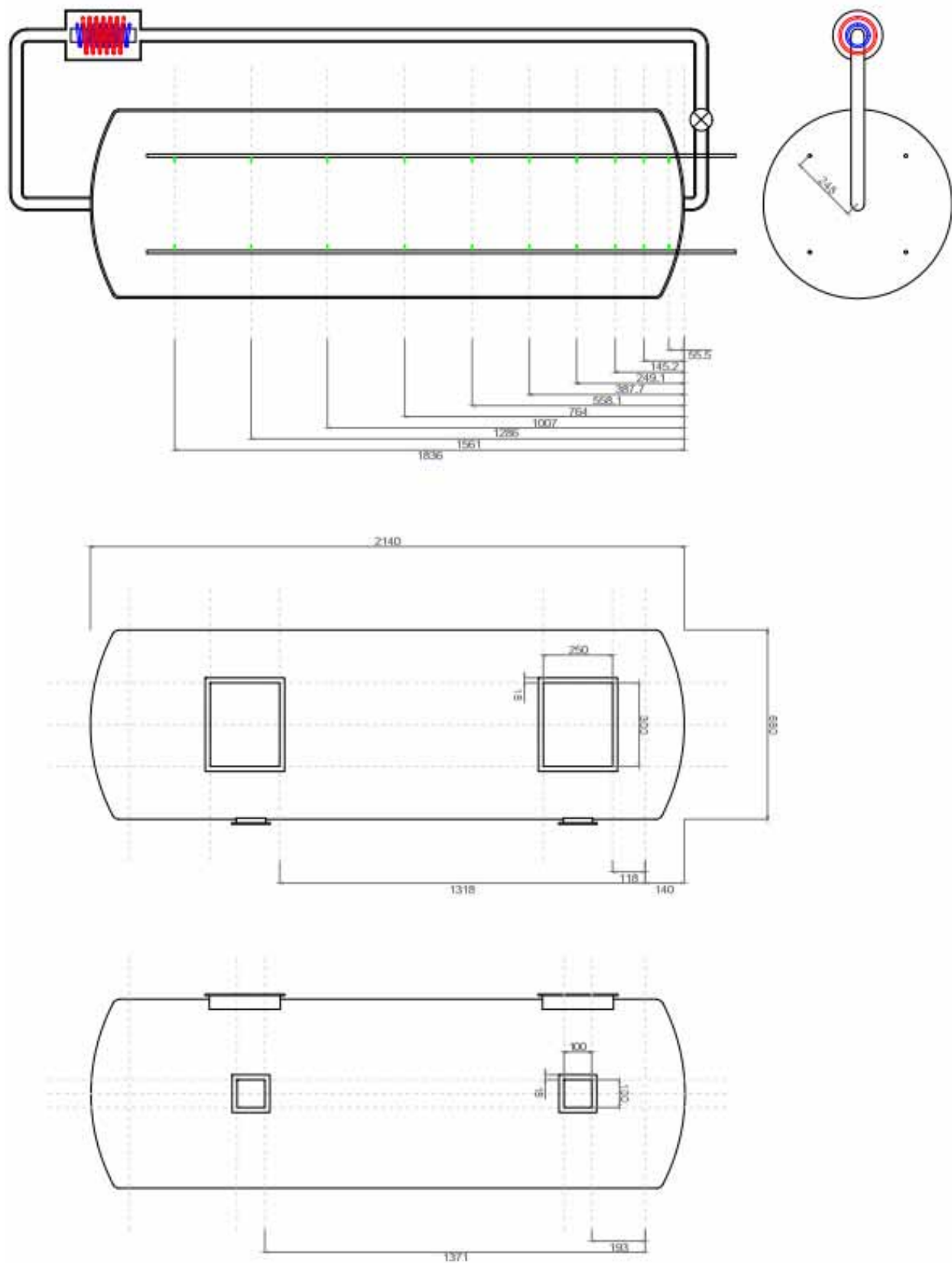


Figure 2: Experimental rig, general layout and dimensions.

Ball Valve	DN 40, PN 20
Ball Valve Actuator	Nenutec NABM 1.1-10
Pipes	37mm ID, 47mm OD, POLYPROPENE
Fittings	1 ½" BSP threaded <ul style="list-style-type: none">• 2 × Straight couplings• 2 × 90° bends (top),• 2 × tees with blanks (bottom bends).
Insulation	Glass Wool, 100 mm thickness
Heating element	2 × 2440mm, 8mm OD, coiled to specified diameter. 13500 W/m ² at 3.5 kW input

Table 1: Experimental specification.

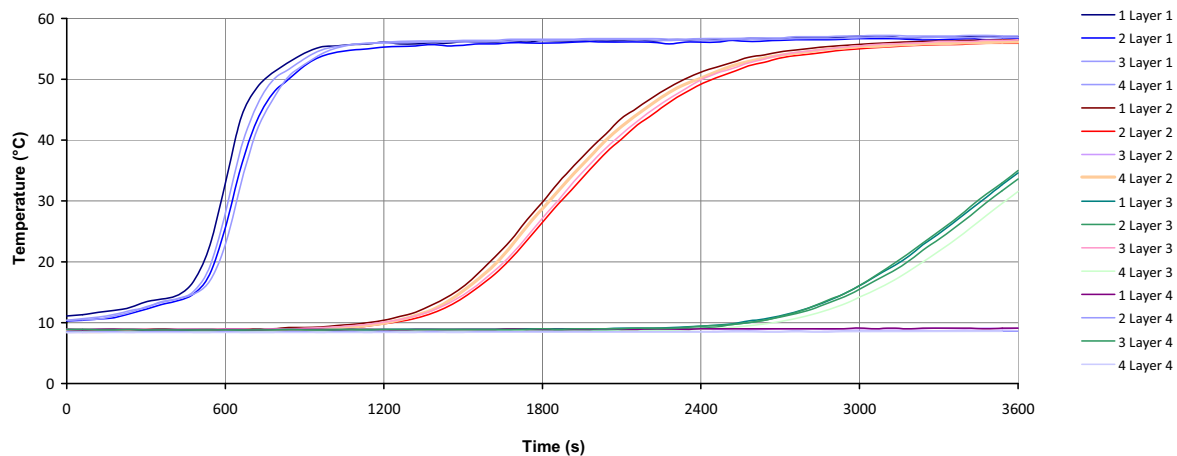


Figure 3: 4.9 kW mean electrical input, 15% valve opening.

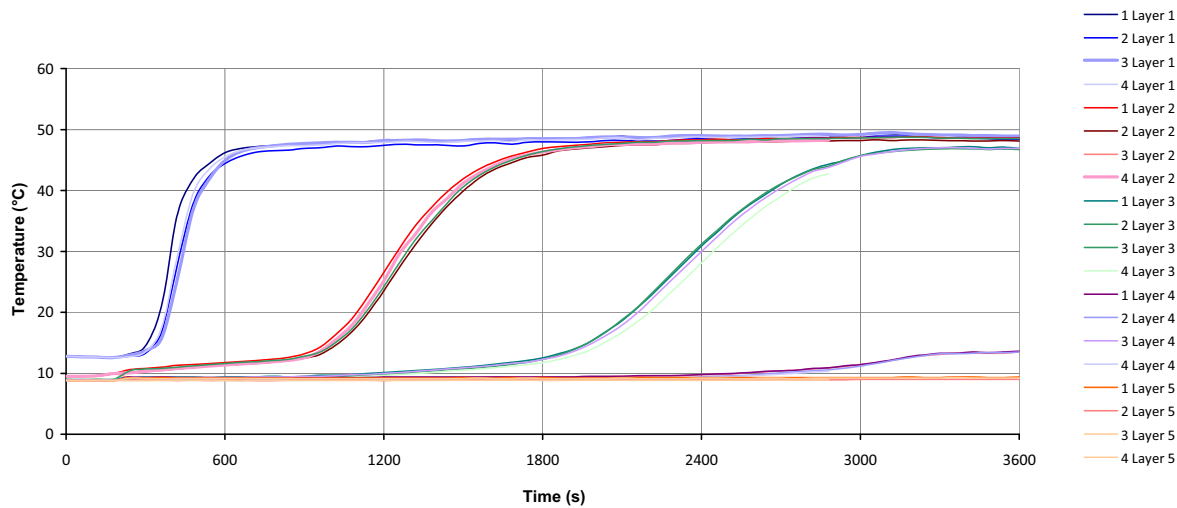


Figure 4: 4.75 kW mean electrical input, 20% valve opening.

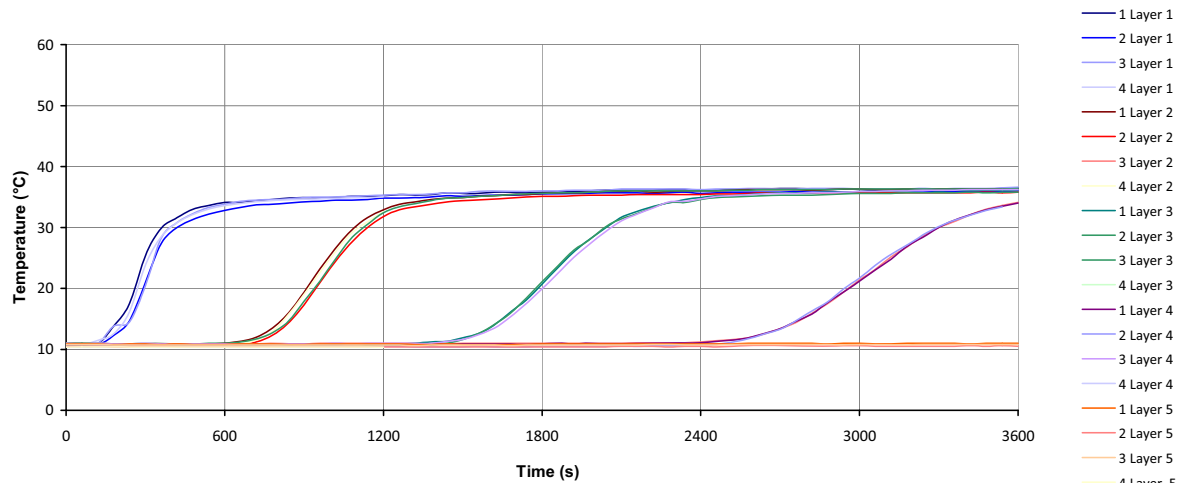


Figure 5: 4.88 kW mean electrical input, 50% valve opening.

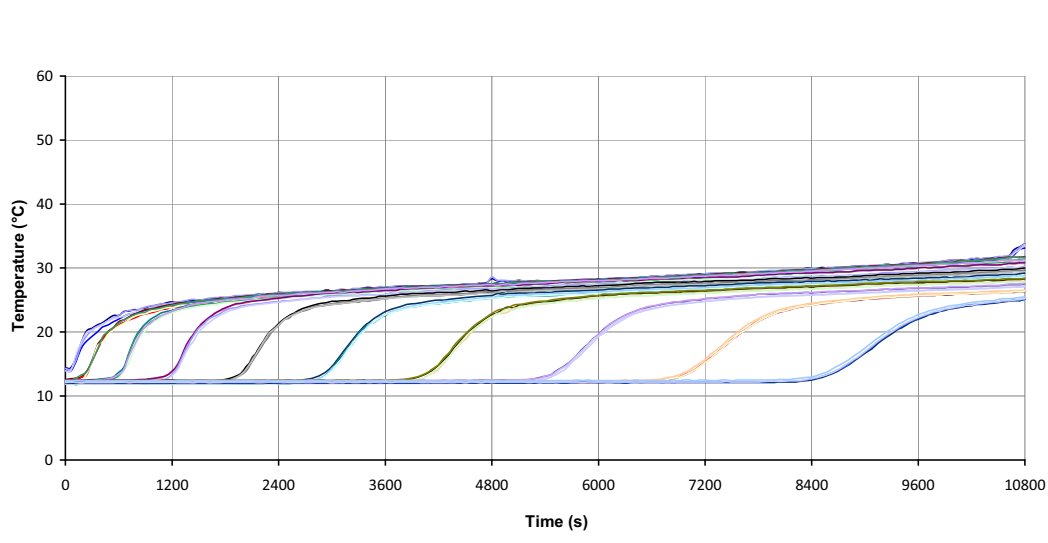


Figure 6: 4.8 kW mean electrical input, 100% valve opening.

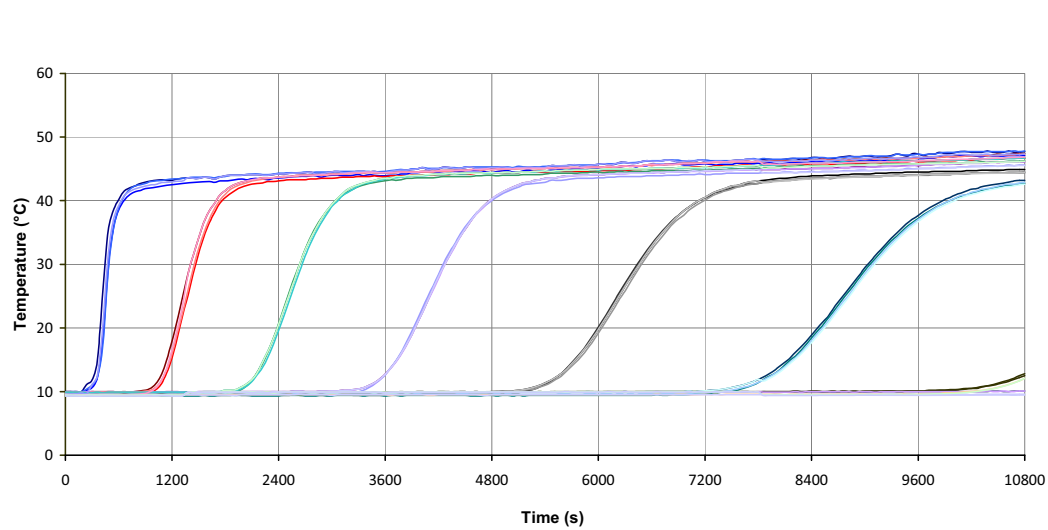


Figure 7: 4.88 kW mean electrical input, 25% valve opening.

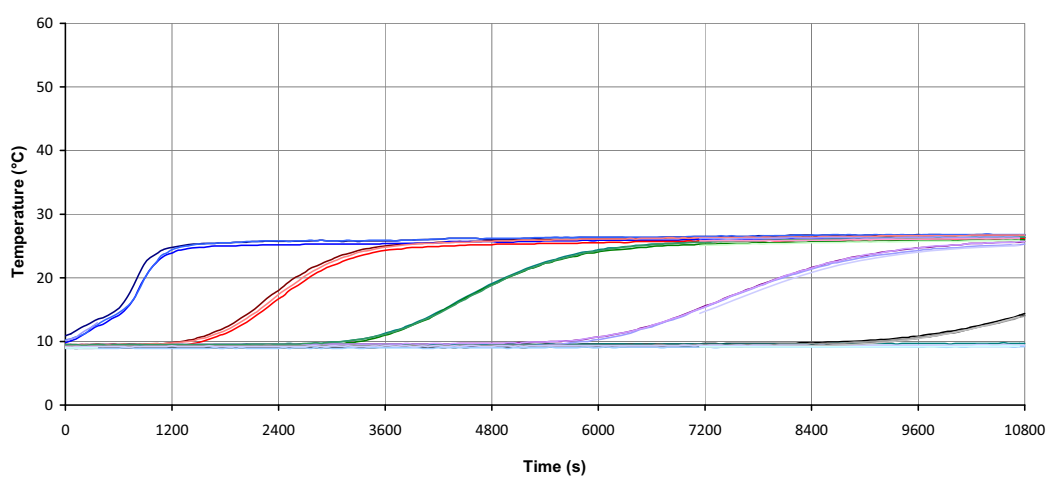


Figure 8: 1.31 kW mean electrical input, 25% valve opening.

4. ANALYSIS and DISCUSSION

The results show that the valve opening has a large influence on the temperature rise across the side arm. A plot of temperature over time, Fig 9, was carried out using the data from Node 1.1 of each of the experiments with high input power. It can be seen that the time taken for the node to get up to a steady temperature is increased for smaller valve openings. The 25% opening, is the exception in this plot, due to a slightly lower ΔT than in the rest of the plots. The temperature at time *1200 seconds* was plotted for the various valve openings in Fig. 10 to reveals the valve operating characteristics

The increased temperature of the water entering the tank, due to the driving force decreasing as the charge progresses, is visible but may not be as large as one could expect. One reason for this is that the experimental length is too short to reflect this clearly, especially in the situations were the valve has a small opening angles, Fig 3, 4 and 7, due to very low n and therefore a small section of the tank being heated.

The driving force, eq. (2), was computed for each recording, allowing a plot of pressure vs. ΔT to be made, please refer to Fig 11, 12 and 13. This plot was constructed using the following method. The temperature recordings were used to represent the whole of the controlled volume they are in, therefore no thermo-clines within any particular node were shown. The temperature of the side arm was taken as the temperature of the top node. The graphs produced break down the charge cycle in to a series of events. In all situations the pressure increases with the temperature difference until a steady state is reached, after which, the decreasing driving force leads to a higher temperature entering the top of the tank. In Fig 11, due to the fully open valve the tank fully replenished itself in the *10800 seconds*. Between the period of *8200 to 9780 seconds*, ΔT and P drop before starting a new stabilization cycle at time *9780 seconds*. This drop in ΔT and P is unlikely to be as pronounced in real life as it appears on the graph. This due to the time lag associated with using the upper and lower node temperatures to compute the driving force and the temperature of the side arm.

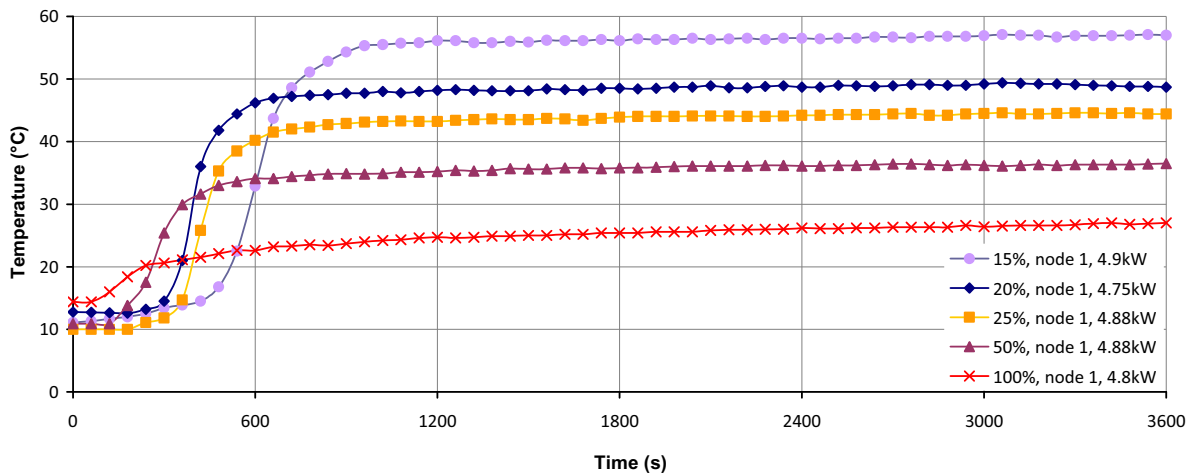


Figure 9: Temperature profile for nodes 1 layer 1

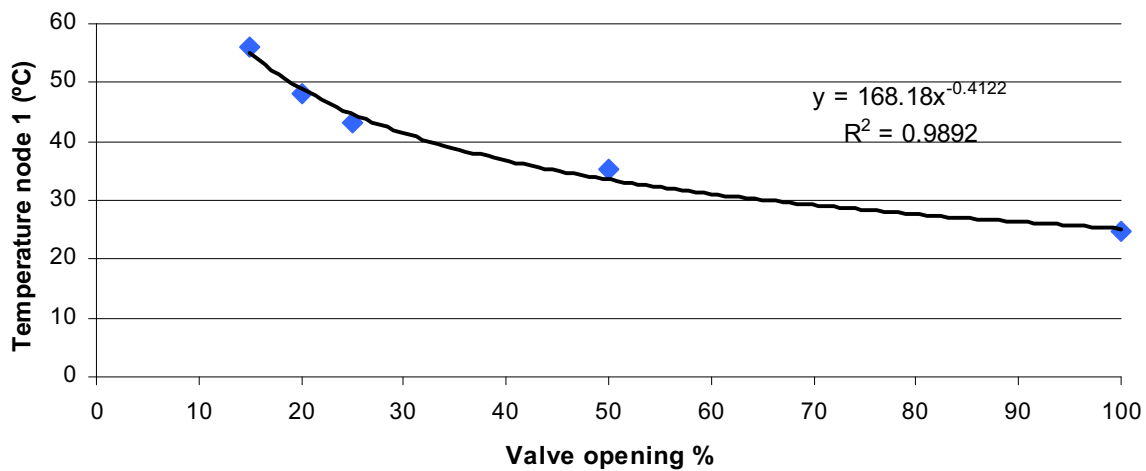


Figure 10: Temperature rise through valve at time 1200 seconds

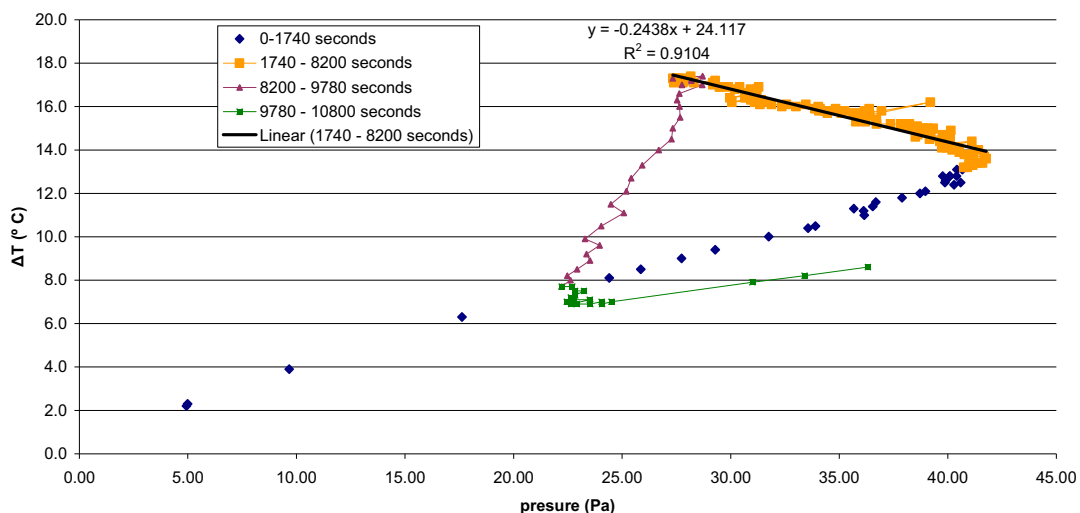


Figure 11: Pressure vs. temperature rise. 4.8 kW, 100% valve opening.

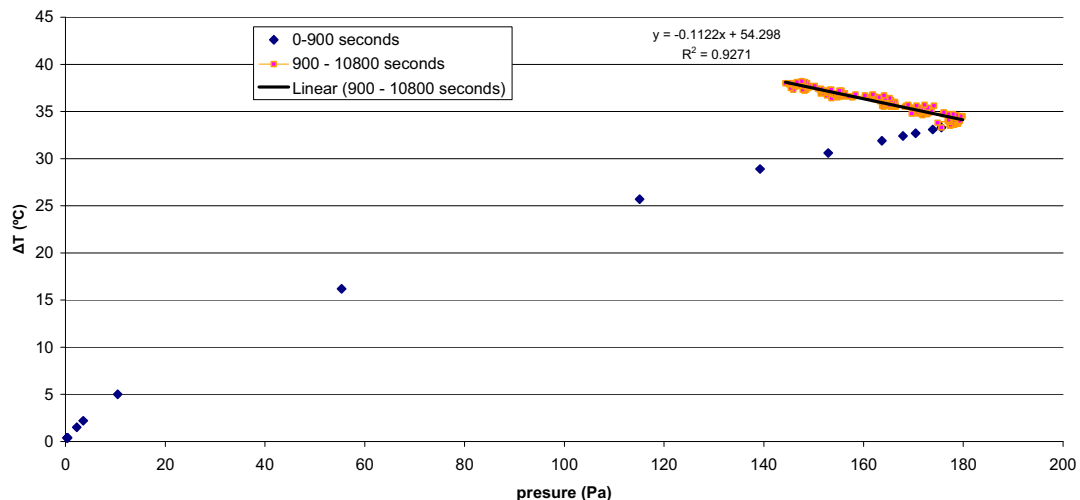


Figure 12: Pressure vs. temperature rise. 4.88 kW, 25% valve opening.

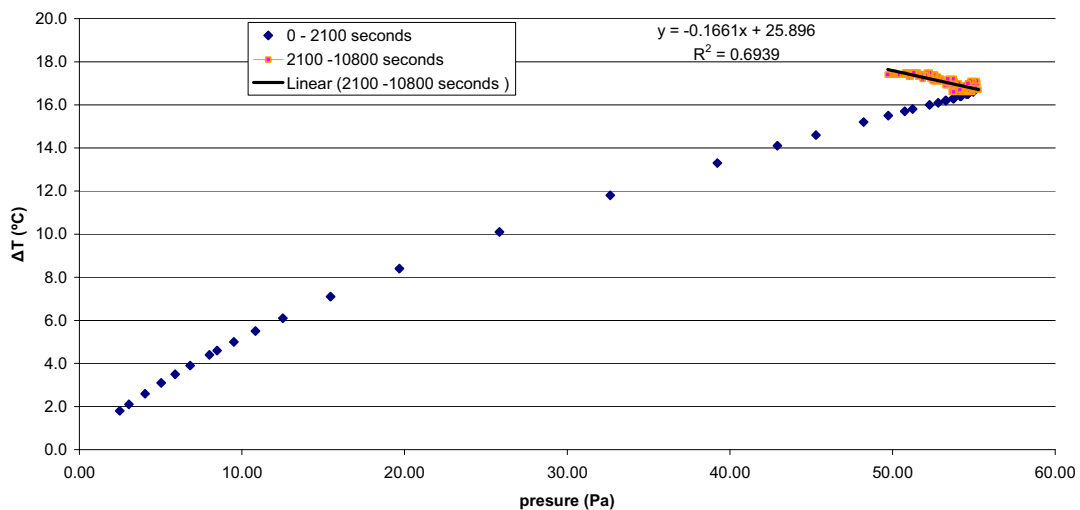


Figure 13: Plot of pressure vs. temperature rise. 1.31 kW, 25% valve opening.

5. CONCLUSIONS

Due to the time lag between the water exiting the side arm and reaching the top thermocouples, it is difficult to compute accurately the exact temperature in the side arm. It is recommended that a few measurements be made along the length of the riser to facilitate computation as well as providing real data for its operation.

The domes weigh 18 kg each and have an estimated specific heat capacity of 90 kJ/kg.k each. This, combined with the thermal mass of the tank walls, can be seen to have an impact on the thermo-cline created within the tank. The first layers to enter the tank are cooled rapidly as they descend. Quantifying this in a plug flow model would help with the estimation of the effectiveness of the system to promote stratification.

Changes in viscosity will influence the flow rate too, as the water heats up the friction encountered at a given mass flow rate will decrease. Experiments with higher initial temperature should be carried out to quantify this.

The results show clearly that the valve adds enough control to permit “topping up” of individual nodes were ΔT of 10 or 20 C are required as well as allowing very small Δt to be controlled when the driving force is at its highest.

Work in the immediate future will try and extract a function that depicts the desired valve opening for a set of operating conditions. The level of stratification achieved will also be quantified.

ACKNOWLEDGEMENTS

This research was carried out with support from the UHI Strategic Development Body, the European Regional Development Fund, Highlands and Islands Enterprise and Comhairle nan Eilean Siar.

REFERENCES

Furbo, S., Andersen, E., Knudsen, S., Vejen, N.K., Shah, L.J., 2005, Smart solar tanks for small solar domestic hot water systems, Solar Energy., vol. 78, p. 269-279.

Hollands K.G.T., Lightstone M.F., 1989, A review of low flow, stratified-tanks solar water heating systems, Solar Energy., vol. 78, p97-105

North European Understanding of Zero Energy/Emission Buildings

Anna Joanna Marszal^a, Julien S. Bourrelle^b, Jyri Nieminen^c,

Björn Berggren^d, Arild Gustavsen^b, Per Heiselberg^a, Maria Wall^d

^aAalborg University, ^bNorwegian University of Science and Technology

^cVTT Technical Research Centre of Finland, ^dLund University

ABSTRACT

The worldwide CO₂ emission mitigation efforts, the growing energy resource shortage and the fact that buildings are responsible for a large share of the world's primary energy use drives research towards new building concepts, in particular Zero Energy/Emission Buildings (ZEBs). Unfortunately, the lack of a common understanding for this new type of building results in most countries to have their own, unique approaches. This paper presents the northern (Danish, Finnish, Norwegian and Swedish) understanding of ZEBs and gathers together information related to ZEBs in these countries. Generally, we may observe a correlation between the zero energy/emission building approach adopted by a country and this particular country's utility grid characteristics. Moreover, it is to be noted that the ZEB concept is not well defined at the national level in northern Europe and that all of the participating countries are still to adopt a national definition for these types of buildings. This results often in more than one understanding of ZEBs in each country.

This study provides a concise source of information on the north European understanding of zero energy/emission buildings. It puts forward a number of similarities among the four studied approaches while highlighting that each country adopts a slightly different ZEB concept depending on its particular realities. This work may be viewed as a useful input to the coordination of sustainable building research in northern Europe and as a good source of information on different possible approaches towards ZEBs.

Keywords: zero energy building, zero emission building, Nordic countries, requirements, multi-disciplinary.

1. INTRODUCTION

Energy use in the building sector accounts for about 40% of world's final energy use and 33% of direct and indirect greenhouse gas emissions, IEA (2008). This fact together with the issue of climate change and the growing energy resource shortage drive research towards continuous improvement of energy efficiency measures. However, the incremental increase in energy efficiency is not sufficient anymore and new solutions for decreasing building's energy use need to be defined in order to cope with the incessant growth of the world's energy consumption. The concept of ZEBs is a promising solution currently gaining in popularity.

The ZEB concept is not a new idea. Literature exists from 1970's, 80's and 90's which describes zero energy/emission buildings; Esbensen and Korsgaard (1977), Gilijamse (1995). Yet, just a few years ago this concept attracted the attention of a wide international audience and a worldwide discussion began. A number of international and national research programmes started to focus on investigating and implementing the ZEB in the real life i.e.

the IEA SHC Task 40 / ECBCS Annex 52 ‘Towards Net Zero Energy Solar Buildings (NZEBs)’, The Strategic Research Centre on Zero Emission Buildings in Denmark, The Research Centre on Zero Emission Buildings (ZEB) in Norway and Zero Carbon Hub in the United Kingdom. In the April 2010 recast of the Energy Performance of Building Directive (EPBD), the European Parliament and Commission declared that by 31 December 2020 all new buildings must be nearly zero energy buildings, however all public owned new buildings must be nearly zero buildings from 31 December 2018. Within the EPBD recast the nearly energy building is understood:

“(...) a building that has very high energy performance (...) and the nearly zero or very low amount of energy required should to a very significant extent be covered by energy from renewable sources, including renewable energy produced on-site and nearby”.

The European Parliament and the Commission advice the Member States to prepare national plans for increasing the number of nearly zero energy buildings. The national plans should at least include:

- *“A detailed application in practice of the definition of nearly zero energy buildings, reflecting their national, regional or local conditions (...)”*
- *“intermediate targets for improving the energy performance of new buildings for 2015(..)”*
- *“information on the policies and financial or other measures undertaken nearly zero energy buildings, including details of national requirements and measures concerning the use of energy from renewable sources in new buildings and existing buildings”*

Despite the numerous international/national actions towards ZEBs and the excitement of the term ‘zero’, major challenges need to be met in the development of such building concept, in particular in relation to the lack of common understanding. In a number of publications, Torcellini and Crawley (2006), Laustsen (2008), Crawley et al. (2009), Marszal and Heiselberg (2009), authors present the wide variety of ZEB definitions and highlight the significant influence the understanding of the zero energy and/or emission building concept has on design and performance of ZEBs.

This paper presents the Nordic (Danish, Finnish, Norwegian and Swedish) understanding of zero energy/emission buildings. It puts forward a number of similarities among the different approaches, while highlighting that each country-specific zero energy/emission building concept deriving from local realities. None of the participating countries have yet adopted an official definition/understanding of ZEB concept. This paper thus focuses on the general trend in each of the countries’ different possible approaches.

2. DENMARK

The first zero energy building was build in Denmark already in late 1970’s, Esbensen and Korsgaard (1977), however it was just a single demonstration project with no significant influence on the Danish building sector at this time. Moreover, in this project the ‘zero’ reflects solely the thermal energy consumption (space heating and domestic hot water). The real discussion and the intensive investigation of the zero energy and/or emission building concept started around 2007. The Danish approach is more focus on the zero energy buildings. Firstly, since Denmark has a long tradition in calculating and evaluating the building performance based on the building’s energy balance. Secondly, due to the fact that

the zero energy buildings are seen as a possibility for increasing the share of renewable energy sources in the national energy infrastructure. Denmark has not yet adopted the national definition for ZEBs concept, however in 2009 the Strategic Research Centre on Zero Emission Buildings was established with the main objective of development the zero energy building concept in the Danish context. The centre is a joint collaboration of two main Danish universities: Aalborg University and Danish Technical University and the key Danish companies in the building and energy sector. The lack of common understanding for the zero energy buildings concept results in unofficial approaches, often assign to a single project. In Denmark two main ZEB demonstration projects with well defined approach towards this building concept exist: *Bolig+* and *Active House 'House for life'*.

2.1 Bolig+ concept

The Bolig+ concept was initiated in connection with the EnergyCamp05 where a number of representatives from different parts of the building sector spent 36 hours to solve the task: *How can we develop energy-efficient housing for the growing world population*. The workshop resulted in the development of a unique and dogmatic approach towards residential zero energy buildings. The five (5) dogmas embrace not only the energy issue but also the indoor climate, flexibility of use and architectural quality. In order to meet the requirements of the Bolig+ concept all 5 dogmas have to be satisfied.

The first dogma is *energy neutral on an annual basis*. It means that the total energy use, including heating, cooling, domestic hot water, ventilation, lighting, household electricity, operational energy etc. is optimized to the local context and the energy purchased from the utility grid is offset by produced renewable energy fed back to the utility grid. This dogma sets additional requirement for the building-grid interaction, in particular that the energy delivered back to the national grid must be at least the same quality and usability as the energy taken from the grid. In other words, you cannot buy heat in the winter time and feed it back in the summer period, since the heat usability is different in summer and winter. Moreover, strict building constraints require the fulfilment of the Danish Building Regulations low energy class 1 without including the electricity production. Since the energy balance also includes the electricity for the households, the Bolig+ consortium stated that this should not exceed 1725 kWh/year per apartment.

The second dogma calls for an *intelligent and user friendly house*. A ZEB should be equipped with intelligent energy control systems that both reduce energy use and improve the indoor climate by using the building services in a smart and optimized manner. The control and the monitoring data systems should be easily accessible for the occupants in order to make them constantly aware of their energy use.

The Bolig+ concept requires that the ZEB is *flexible in daily use and over time*. This third dogma focuses on three different types of flexibility. First and foremost, it refers to the flexibility in the building envelope in a way that the thermal envelope will react and adjust to the building's annual and daily rhythm (variable over the year and/or day energy demands and indoor climate conditions) as well as to the changeable weather conditions. Secondly, it means flexibility in easily adapting the dwellings to the individual and varying needs of diverse user profiles. The different room-requirements of family of 2 adults and 2 children or of an elderly couple should be easily met. Finally, it is important that the building construction ensures flexibility in replacing individual building components without destroying other parts of the building.

The long tradition in Denmark of focusing during the building design on reducing the energy use as well as on providing a healthy indoor environment maintains also in the Bolig+

concept. Therefore, the fourth dogma emphasizes the *good and healthy indoor climate in the house*. The focus is put on the daylight and artificial light, atmospheric indoor climate, indoor temperature, air quality, acoustics and finally on choice of the sustainable and healthy building materials.

The last dogma sets the requirement for *high architectural quality and adaptation to the local context*. It states that the ZEB should be a design in agreement with the surrounding architectural style but at the same time express the period of construction. Moreover, it should satisfy the human expectations to harmony and balance while having an innovative and challenging design. Finally, the ZEB must be constructed from environmentally friendly and low polluting materials that suit the local environment.

2.2 Active house – ‘House for life’

The Active house concept is initiated by the industrial investor - VKR Holding with the objective of constructing eight demonstration houses in different European countries. The Active house concept strives to design buildings that are energy efficient and with all energy produced by renewable energy sources and/or supplied from the nearby collective energy system (i.e. local district heating grid) and electricity grid. Moreover, it should have healthy indoor climate, positive influence on the environment throughout the total life cycle and finally high architectural qualities in agreement with the local context. Furthermore, the Active house concept applies to all types of residential and non-residential new-build and renovated buildings. The initiators of this approach emphasize that in order to design and construct the Active house all the above mentioned parameters should be balanced. The best explanation of the idea behind the concept is Fig.1, where all three elements: energy, indoor climate and environment create a common framework of the Active house vision.

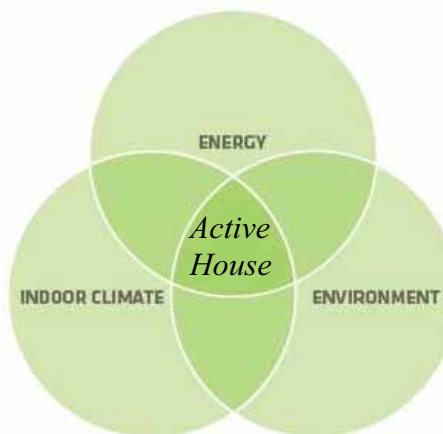


Figure 1. Active house concept. [Active house, 2010]

The first Active house in Denmark the ‘Home for life’ was built in 2009. Taking the main framework from the Active house concept the working group has moved a step further by designing a plus energy house with the main focus on the comfort of its occupants. The annual renewable energy production surplus should offset within 30-50 years both the energy embodied in the building materials and the energy used for constructing the house. With this approach the ‘Home for life’ can be seen as a life cycle zero energy building.

2.3 Conclusion

Denmark lacks a national, standardised approach for zero energy buildings. However, two concepts: Bolig+ and Active house can be seen as an initial framework for a future Danish zero energy building definition. Both concepts aim to reach zero energy goal thus put great focus on energy efficiency, healthy indoor climate and architectural qualities. Furthermore, the Danish understanding of a zero energy building concept would probably include one more important aspect; in particular the requirements for the building-grid interaction, since the ZEB buildings are seen in Denmark as a solution for increasing the share of renewable energy in the total national primary energy supply. To conclude Denmark aims to adopt a net zero energy building definition.

3. FINLAND

The Finnish climate and energy policies have two major focus areas. The strategy is to increase the share of renewable and emission free energy in the national primary energy consumption. The national aim is to increase the amount of renewable energy from the present level of 20% up to 38% of the total primary energy by the year 2020. The Finnish climate and energy policies include supply subsidies (e.g. wind power) and a program to substantially increase biomass as the alternative energy source. However, the present government has initiatives to combine the biomass scheme into construction of new nuclear power plants. Furthermore, the Finnish building code will be renewed step vice towards 2020. The main objective is that with a number of intermediate steps, near zero energy house requirements will be set for new buildings in 2020.

There is no commonly agreed definition for a zero energy house in Finland. However, all the zero energy projects utilize the definition of a net zero energy building. Net zero energy building is commonly understood as a building that uses energy from energy grids but at the same time produces energy to be fed into the energy grid. The amount of energy provided by on-site renewable energy sources is equal to the amount of energy used by the building. A net zero energy building should be based on a very low-energy building concept in order to minimise the energy demand. The low energy demand defines the design of the building integrated renewable energy production systems. There are two important ZEB pilot projects in Finland that follow the above mentioned definition: the IEA5 Solar House in Pietarsaari constructed in 1994 and two twin net zero apartment buildings under construction in Kuopio (latitude 62,9°) and in Järvenpää (latitude 60,5°). Moreover, with the second project Finland attempts to verify the possibilities for constructing zero energy buildings at high latitudes.

3.1 IEA5 Solar House, Pietarsaari

The project IEA Task 13 "Advanced solar low-energy houses", a part of the Solar heating and cooling programme (SHC) of the International Energy Agency (IEA), aimed at promoting use of solar energy in buildings. The IEA5 Solar house, see Fig. 2, was built at the Pietarsaari housing fair in 1994, Hestnes et al., (1997). The house is a single family house that fulfils the present Finnish passive house and very low-energy houses definitions. The performance of the house has been monitored until the end of 1996 and checked every year since 1996. The results prove that the yearly purchased energy consumption was only 7900 kWh, corresponding to 48 kWh/gross m². The average space heating energy consumption was 13 kWh/m². The owner of the house is upgrading the building so that it will be a net zero energy building.

The heating system is based on a ground source heat pump with a capacity of 8 kW that is supported by a roof integrated 10 m² solar thermal collector system. Heat from the 3 m³

storage tank is distributed to the rooms with a low-temperature floor heating system. The 48 m² photovoltaic system consists of 45 solar panels (amorphous silicon modules) with 2 kWp output power.



Figure 2. IEA5 Solar House

The upgrading of the building includes refurbishing of the ground source heat pump, ventilation system and the PV system. Table 1 shows the energy balance of the original composition of the house together with the assessed new balance with upgraded systems. The performance of the heat pump has now been tested for a period of some months and shows important increase in the COP (3.5 – 4.0) compared to the original over the year COP of 2.4. The assessment shows that the upgrading improves the performance so that the net zero energy level can be reached. The monitoring system has also been renewed and the performance of the building will be available on-line.

Table 1. Energy balance as built and after renewal (1994 normal/**2010 bold**).

Consumption	Demand kWh/m ²	Produced kWh/m ²	Ground heat kWh/m ²	Purchased energy kWh/m ²
Heating - heat pump - boosting for water heating - solar heating	65/ 60		27/ 30	20/ 12 6/ 6
Electricity (household, systems) - grid electricity - solar electricity	33/ 25			33/ 25 -11/- 43
Total	98/ 85	23/ 55	27/ 36	48/ 0

3.2 Net zero energy buildings in Kuopio and Järvenpää

The buildings serve for the national roadmap towards nearly zero energy buildings referred in the Energy Performance of Buildings Directive under preparation at the EU. The Kuopio building is a student apartment house and the Järvenpää building is a home for elderly people, see Fig. 3. The gross floor area of each building is 2124 m². The Kuopio building is located in the dense centre of the City of Kuopio. This location limits the implementation of renewable energy producing technologies to solar thermal panels and solar

cells. The Järvenpää building is located in a rather open area at the outskirts of the centre which provide a favourable context to support photovoltaic system by building integrated windmills. At this moment no decision is made on how much of the total electricity demand should be covered by solar electricity production or other renewable technologies and, thus, further studies are needed. Both buildings use district heat and are connected to the local grid. The Kuopio and Järvenpää projects will be finished in 2010 and 2011, respectively.



Figure 3. Net zero energy buildings in Kuopio (left) and Järvenpää (right).

Table 2 shows the energy demand of the Kuopio and Järvenpää buildings. It is important to notice that, even if within the Finnish climate conditions the predominant part of the total energy demand in buildings is associated to space heating in those two projects the space heating is not the dominating energy consumption. The major part of the energy use is associated users. Therefore, it is a key issue for achieving the net zero energy level that the occupants are supported and guided in how they should correctly use the building.

Table 2. Energy demands

Energy demand	Space heating	Water heating	Electricity for the systems	Household electricity
	MWh	MWh	MWh	MWh
Järvenpää	18.8	37.8	9.8	28.1
Kuopio	24.5	28.2	11.7	33.1

3.3 Conclusion

The net zero energy building concept is a rather challenging target in the Finnish climate. The approach of nearly zero energy buildings referred in the EPBD under preparation at the EU seems to be more rational for cold climates. The definition implies that the renewable energy can be produced by building integrated energy production or nearby the building. The aim to increase the use of renewable sources by the energy production buildings is generally considered to be the right path towards reduction of fossil fuels and related emissions. In the most cities in Finland combined heat and power production is the dominating source of energy; increasing the share of renewable energy sources in the power and heat generation facilitates will help reaching the ZEB target. This may require the development of a definition for a near zero energy building.

4. NORWAY

Norway is peculiar in ways that influence the local approach to ZEBs. A very large proportion of its electrical production derives from hydropower. The climate is cold and rainy in many locations and, as for Sweden and Finland, large parts of the country are affected by important variations of solar radiation throughout the year. To cope with these realities and promote the development of emission-free buildings, Norway started financing in 2009 The Research Centre on Zero Emission Buildings (hereafter referred to as ZEB-Centre).

Within the ZEB-Centre, work is divided into five (5) focus areas: material technologies, low-energy envelope technologies, energy supply system and services, energy efficient use and operation, concepts and strategies for ZEBs, ZEB-Centre (2009). These focus areas are set up as work packages which are led by experts from various fields, thus highlighting the centre's commitment to a multi-disciplinary approach to the development of ZEBs.¹

4.1 Sustainability and the United Nation Environmental Programme

The commitment of Norway towards sustainability and the findings of the Intergovernmental Panel on Climate Change (IPCC), Levine *et al.* (2007), are depicted in its approach to ZEBs. While the energy savings and related economical benefits to the development of ZEBs are very well understood, Norway makes reducing the emission of greenhouse gases (GHG) its priority and thus looks at ZEBs as Zero *Emission* Buildings. Furthermore, the approach is meant to encompass a complete life cycle analysis of buildings were mitigation of GHG emissions should take place in the production, operation and demolition phase of buildings.

4.2 A European Approach

Hydropower provides most of Norwegian buildings with a highly renewable mix of energy. In certain countries, reaching a ZEB-status requires only to balance the non-renewable part of the energy consumed by a building during its operational phase, Marszal *et al.* (2010). As such, reaching a ZEB-status in Norway would require balancing only relatively small amounts of energy. In order for a building to reach a ZEB-status over its complete life cycle, aspects related to embodied emissions in materials and the emissions linked to the demolition and end of life should be considered. Norway tends to adopt a broad perspective in which it is understood that the renewable hydroelectricity not consumed by buildings inland may be used to electrify transportation and off-shore installations or may be exported, thus indirectly reducing GHG emissions. Consequently, Norway is to evaluate its buildings' emission footprint based on the European electricity mix, resulting in a more stringent zero-emission target. Doing so, Norway highlights the importance of looking at the European grid as one entity, ease the comparison of European ZEBs and aim at reducing emissions globally, thus tackling climate change from a global perspective.

4.3 A Norwegian approach

The Norwegian approach puts a strong emphasis on the high level of energy efficiency required for a building to reach the ZEB-status. Based on the IPCC findings, improving energy efficiency is the most effective option to mitigate GHG emissions in the building sector. Energy efficiency is part of a larger set of requirements which ZEBs should fulfil prior to offsetting their energy consumption from on-site renewable energy production. This

¹ The Research Centre on Zero Emission Buildings (www.zeb.no)

set of requirements deals, among other things, with minimum levels of comfort and indoor atmosphere aspects. Defining requirements for ZEBs will influences the co-benefits associated with these buildings. Out of the six co-benefits identified by the IPCC, Levine *et al.* (2007), three are of special importance within the Norwegian realities: (1) Improved health, quality of life and comfort, (2) improved productivity and (3) employment creation. These co-benefits are important drivers for the adoption of ZEBs by the users, the industry and by the society as a whole and thus a central focus area of the Norwegian approach.

The Norwegian approach also highlights the importance the users play in the energy consumption of building. To that extend, a dedicated work package studies how energy-efficient use and operation of ZEBs may be achieve, notably by understanding user behaviours. It focuses on approaches and processes which are inter-disciplinary and seek to include end-users.

Globally, the ZEB-Centre advocates for an Integrated Design Process (IDP) where the building performance is optimized through an iterative process that involves the most important members of the design team and inputs from the user community. Such design process may help prevent irreversible choices typically made in the early design phase of buildings and which may limit their energy performance.

Due to the slow regeneration of the building stock and in order to efficiently mitigate GHG emissions from the built environment, the ZEB-Centre also deals with finding retrofitting options for existing buildings, ZEB-Centre (2009). Retrofitting of existing building is linked with the development of ZEB as it uses similar technologies to increase energy efficiency in existing buildings, thus indirectly reducing GHG emissions.

Finally, considering the inevitable changes within the energy supply system, different scenarios are looked upon which depict several possible futures in terms of two main uncertainties: technology development and public attitude towards ZEBs. These scenarios are meant to help develop consistent strategies and indirectly influence the definition of ZEBs. A formal definition for ZEBs in Norway is still to be adopted. At the time of writing, a draft proposal including a set of criteria was under review at The Research Centre on Zero Emission Buildings Sartori *et al.* (2010).

4.4 Conclusions

The Norwegian understanding advocates for a global European ZEB-approach in line with the IPCC findings on the mitigation of climate change in the building sector. ZEBs are understood as zero emission buildings and looked upon from a life cycle perspective. The approach to the design of ZEBs is multi-disciplinary, looks into requirements for energy efficiency and understands the importance of co-benefits in the development of ZEBs.

5. SWEDEN

The Swedish environment policy is based on goals defined within sixteen environmental quality objectives adopted by the Swedish Parliament in 1999 and 2005. The goals, that are ecologically sustainable, describe a desired quality and condition of the Swedish environment. In November 2005 the Swedish parliament adopted 72 interim targets to concretize the work towards reaching the goals. One of the interim targets, within the main objective called “A Good Built Environment”, applies among others to energy use in buildings Naturvårdsverket (2009):

"Total energy consumption per unit area heated in residential and commercial buildings will decrease, with target reductions of 20% by 2020 and 50% by 2050, compared with consumption in 1995. By 2020 dependence on fossil fuels for the energy used in the built environment sector will be broken, at the same time as there will be a continuous increase in the share of renewable energy."

In order to reach the above mentioned goals Sweden promotes energy efficiency through several projects, mostly supported by the Swedish energy agency - Energimyndigheten. Moreover, the National Board of Housing, Building and Planning - Boverket has gradually sharpened the Swedish building regulations regarding the energy requirements. New building regulations with more strict energy requirements are planned to come in force in 2011, Regeringskansliet (2009). Furthermore, in order to evaluate energy use based on various energy carriers a system based on weighting factors has been proposed in the Swedish Energy Efficiency Inquiry, Regeringskansliet (2008). The system includes local Swedish weighting factors. These weighting factors have not yet been implemented within the Swedish Building regulations.

5.1 Swedish zero energy house

The Swedish government or Boverket has not yet adopted the national understanding of the ZEB concept. However, an organization – FEBY has presented a concept to certify and verify a zero-energy house. It is included in the voluntary criteria for the passive houses in Sweden, FEBY (2009).

The Swedish requirements for a passive house aim to minimize the peak load for space heating in buildings so that the required thermal comfort can be obtained in a rational manner. This is based on the functional definition of the Passive House, namely that the heat should be possible to supply with a distribution of heat through hygiene air flow (Feist, 2005). For the construction of zero energy houses, an additional note states that, on an annual basis the energy use should be less than or equal to the total produced energy and the same weighted energy form factors should be used for both used and generated energy. Unfortunately, there are no known existing buildings within Sweden that fulfill the requirements of above mentioned zero energy house concept. However, there is a single-family house in the south of Sweden, Villa Åkarp, where the constructor/builder states that the house they constructed is plus energy house.

In addition to the voluntary criteria presented above there have also been suggestions for three other definitions of a zero energy house concept, Blomsterberg (2009), in particular: *zero primary energy use, zero energy costs, zero energy emissions*. All of the four above concepts are based on an annual balance.

5.2 Conclusions

There is no official standard for a ZEB-concept in Sweden. The voluntary standard and the published suggestions for ZEB-concepts are all based the annual energy consumption and generation balance. This may in the future cause problems concerning grid interaction due to the fact that zero energy buildings in a Nordic climate possibly will produce most of the energy in the summertime while using more during winter. To address this problem there is a need for a better defined standard, were the use of different energy carriers and the possible imbalance between production and use of energy in time is taken into consideration. The

question of the balancing period: year, month, day or hour will be a fundamental issue that will affect the future design of all upcoming ZEB-projects.

Any concept for ZEB should be based on trying to minimize peak loads and ensuring a very low energy demand of the building. A discussion for a national strategy to achieve zero energy buildings until 2020 has only begun in Sweden.

6. CONCLUSIONS

This paper provided an overview of the Nordic (Danish, Finnish, Norwegian and Swedish) understanding of zero energy/emission buildings. Discussion on ZEBs is at a different stage in each country. Denmark and Norway have already established research centers, which focus on ZEBs concept, whereas in Sweden and Finland the ZEB development is in an early stage. However, all four countries have common aims: to adopt a definition which will reduce the energy use in building, and which will include ZEBs in the national strategies for integration of renewable sources. Investigating the best interaction between zero energy/emission buildings and the national energy infrastructure differentiate the Nordic approach from other national understandings.

The Finish, Danish and Swedish understanding of ZEBs are more focused on zero energy buildings, since it is more in line with their utility grid characteristics. Norway due to large share of hydropower in the national grid strives for adopting zero emission buildings concept that is closer to the country's particular realities and the findings of the IPCC.

Although each country's understanding of ZEB concept is unique and very much related to each specific national context, they all have common features. Firstly, all countries emphasize the importance of energy efficiency measures before the integration of on-site energy production technologies. By adopting such requirement the countries want to eliminate low-quality ZEBs with high energy use and oversized on-site energy producing systems. Secondly, most of the ZEB approaches agree upon the significant influence of the occupants on the energy use in buildings. Therefore, it is a key issue to develop a ZEB definition that aims for user-friendly buildings. Finally, all different understandings highlight that ZEB concepts should focus on energy issues as well as on a good and healthy indoor climate, thus meeting the energy requirements should be balanced with an acceptable indoor environment.

The concept of zero energy/emission building is a challenging target especially for the Nordic countries in which cold climates and large variations in solar radiation need to be dealt with. However, this paper indicates that Denmark, Finland, Norway and Sweden do make efforts to bring the concept into the reality.

ACKNOWLEDGEMENT

The authors would like to thank Kim B. Wittchen for the exhaustive information about the Bolig+ concept, and Anne Grete Hestnes, Inger Andresen, Igor Sartori and Thomas Berker for their valuable inputs on the Norwegian understanding.

REFERENCES

- Active house project: www.activehouse.info/
Blomsterberg Å., 2009, *Lågenergihus - En studie av olika koncept*, Lund University, Sweden, 88p.
Bolig+ project: www.boligplus.org/

- Marszal A. J., Bourrelle, J.S., Musall E., Gustavsen A., Heiselberg P., Voss K., 2010, Net Zero Energy Buildings: Calculation Methods and Input Variables - An International View, *EuroSun 2010*, (un-published)
- Boverket, 2009, *Boverkets byggregler, avsnitt 9 BFS 2008:20*, Karlskrona 2008 p: 13-23.
- Crawley, D., Pless, S., Torcellini, P., 2009, Getting to net zero, *ASHRAE Journal* vol. 51, no. 9: p.18-25
- Esbensen, T.V., Korsgaard, V., 1977, Dimensioning of the solar heating system in the zero energy house in Denmark, *Solar Energy* vol. 19, no. 2: p. 195-199
- Danish Building Regulations, 2008, Copenhagen, Denmark, 224p.
- Danish Energy Agency, 2010, *Energy policy report 2009*, Copenhagen, 19 p.
- FEBY, 2009, *Kravspecifikation för Passivhus*, Sweden, p. 1-20
- Feist W., 2005, First Steps: What can be a Passive House in Your Region with Your Climate?, The Passive House Institute, Darmstadt, Germany
- Gilijamse, W., 1995, Zero-energy houses in the Netherlands, *Proc. of Building Simulation '95*, p. 276–283
- Hestnes, A.G., Hastings, R., Saxhof, B. (editors), 1997, *Solar Energy Houses. Strategies. Technologies. Examples*. IEA, James & James, London, 170 p.
- House for life project: www.velfac.dk/Global/Home_for_life
- International Energy Agency (IEA), 2008, *Energy Technologies Perspectives: Scenarios and Strategies to 2050*, OECD/IEA, Paris, 650 p.
- IEA SHC Task 40 / ECBCS Annex 52 www.iea-shc.org/task40/index.html
- Laustsen, J., 2008, *Energy Efficiency Requirements in Building Codes, Energy Efficiency Policies for New Buildings*, OECD/IEA, Paris, 85p.
- Levine, M., D. Ürge-Vorsatz, K. Blok, L. Geng, D. Harvey, S. Lang, G. Levermore, A. Marszal, A.J., Heiselberg. P., 2009, A literature review of Zero Energy Buildings (ZEB) definitions, DCE Technical Report No. 78, Aalborg University
- Mongameli Mehlwana, S. Mirasgedis, A. Novikova, J. Rilling, H. Yoshino, 2007: *Residential and commercial buildings. In Climate Change 2007: Mitigation. Contribution of Working Group III to the Fourth Assessment Report of the Intergovernmental Panel on Climate Change* [B. Metz, O.R. Davidson, P.R. Bosch, R. Dave, L.A. Meyer (eds)], Cambridge University Press, Cambridge, United Kingdom and New York, USA
- Naturvårdsverket, 2009, *Sweden's environmental objectives* www.miljomal.se/Environmental-Objectives-Portal
- The Research Centre on Zero Emission Buildings www.zeb.no
- Regeringskansliet, 2008, *SOU 2008:25 Ett energieffektivare Sverige*, Stockholm p. 369-396
- Regeringskansliet, 2009, *Regeringens proposition 2008/09:162 – En sammanhållen klimat och energipolitik*, Stockholm ,144 p.
- Regeringskansliet, 2010, 1994:1215 The Ordinance on Technical Requirements for Construction Works, etc.
- The Strategic Research Centre on Zero Emission Buildings www.zeb.aau.dk/
- Sartori, I., Bakken, B. H., Graabak, I., 2010, *Zero Emission Buildings Scenario and Definition Methodology*, Internal Memo – The Research Centre on Zero Emission buildings
- Torcellini, P.A., Crawley, D.B., 2006, Understanding zero-energy buildings. *ASHRAE Journal* vol. 48, no. 9: p. 62-69
- ZEB-Centre, 2009, *The Research Centre on Zero Emission Buildings - Project Description*, Internal document
- Zero Carbon Hub <http://www.zerocarbonhub.org/>

Proposal of a Norwegian ZEB definition: Storylines and Criteria

I. Sartori^{a*}, I. Graabak^b and T. H. Dokka^a

^a SINTEF Building and Infrastructure P.O. Box 124, N-0314 Blindern, Oslo, Norway

^b SINTEF Energy Research, Sem Saelands vei 11, Trondheim , Norway

* corresponding author, tel: +47 22965541, email: igor.sartori@sintef.no

ABSTRACT

A clear and agreed definition of Zero Emission Building (ZEB) is yet to be achieved, both internationally and in Norway. However, it is understood that both the definition and the surrounding energy supply system will affect significantly the way buildings are designed to achieve the ZEB goal. Since the energy system in Europe is expected to change significantly in the coming decades, especially for electricity, it is indispensable to tie the definition of ZEB to possible scenarios on such development of the energy system. A scenario is defined as a combination of options chosen within a framework of different uncertain futures. Two uncertainties are identified as most important for the development and deployment of ZEB: Technology development and Public attitude. These two uncertainties are used to span out a set of four relevant futures, also termed storylines, as a common background for scenario analysis. A formal definition of ZEB is characterized by a set of criteria that are: the system boundary, feeing-in possibilities, balance object, balancing period, credits, crediting method, energy performance and mismatch factors. For each criterion different options are available, and the choice of which options are more appropriate to define ZEBs may depend on the storyline features.

Keywords: ZEB definition, scenarios, storylines.

1 INTRODUCTION

The primary objective for the Zero Emission Building (ZEB) centre is to develop solutions for existing and new buildings, both residential, commercial and public owned, in order to bring about a breakthrough for buildings with zero greenhouse-gas (GHG) emissions associated with their construction, operation, and demolition.

However, a clear and agreed definition of Zero Emission Building (ZEB) is yet to be achieved, both internationally and in Norway. Relevant works on the subject as Torcellini *et al.* (2006), Marszal and Heiselberg (2009) and ECEEE (2009) can be a useful introduction to the issue. ZEBs are of great interest both in the US (US DOE, 2010) and in Europe. In the ongoing process to recast the EU directive on energy performance of buildings there is a certain focus on ZEBs, even though with some reserves because the directive refers to nearly zero energy buildings (EU, 2010):

In Article 2:

(1a) “nearly zero energy building” means a building that has a very high energy performance [...]. The nearly zero or very low amount of energy required should to a very significant extent be covered by energy from renewable sources, including renewable energy produced on-site or nearby;

In Article 9:

- a) by 31 December 2020, all new buildings are nearly zero energy buildings [...]
- b) after 31 December 2018, public authorities that occupy and own a new building shall ensure that the building is a nearly zero energy building [...]

[...] Member States shall [...] stimulate the transformation of buildings that are refurbished into nearly zero energy buildings [...]

A parallel work is ongoing in a project of the International Energy Agency (IEA) under the joint Solar Heating and Cooling programme (SHC) Task 40 and the Energy Conservation in Buildings and Community Services programme (ECBCS) Annex 52: “Towards Net Zero Energy Solar Buildings”(Task 40/Annex 52, 2008). In this project the various definitions found in literature are revised, state of the art examples of zero or close to zero energy buildings are collected into a database, and a thorough analysis of a possible set of definitions is in progress.

Conceptually, a *Zero Energy Building* is a building with greatly reduced energy demand, such that the energy demand can be balanced by an equivalent generation of electricity (or other energy carriers) from renewable sources. In a *Zero Emissions Building* such balance is achieved not directly on the energy demand and generation but on the associated carbon equivalent emissions. The energy imported from the grids into the building is accountable for certain emissions. The export of renewable energy from the building to the grids is accountable for avoiding similar emissions by other (non-renewable) energy producers connected to the same energy grids.

Therefore, the definition of ZEB is intrinsically connected to the energy infrastructure, which the buildings are part of. It is understood that both the definition and the surrounding energy supply system will affect significantly the way buildings are designed to achieve the goal. Since energy production in Europe is expected to change significantly in the coming decades, especially for electricity, it is indispensable to tie the definition of ZEB to possible scenarios on such development of the energy system. This evolution has to be captured in the definition to avoid a situation where a building is designed and constructed to be a ZEB today, but it is no longer such after some years because electricity from the grid has got a higher share of RES in the generation mix.

2 STORYLINES

2.1 *Developing Consistent Scenarios*

The following are steps commonly used in scenario planning:

- Define a focal point, an issue on which it is important to develop insight. For the ZEB centre the key focal point/question is: How can we best promote the development and deployment of zero emission buildings towards 2030 and further towards 2050?
- Identify the primary driving forces (for this focal point); these usually fall into the following categories: Social, Economic, Policy and Technological issues.

- Identify predetermined uncertainties as driving forces that are outside of the control of the decision maker(s) involved in the process.
- Group uncertain driving forces into possible futures according to some commonality. Preferably simplify remaining list into a few dimensions of uncertainties. These dimensions should be proxies for other related drivers moving in similar direction. If we have 2 dimensions of uncertainties, four fundamentally different futures should be developed.
- Identify options that can be chosen/employed as a strategy by the decision maker(s)
- Specify the scenarios as combination of options chosen within the different futures.

The methodology is illustrated in Figure 1, and is the same adopted in the EU project for large integration of renewable energy sources into future energy infrastructure (SUSPLAN, 2009). Each future consists of a set of *uncertainties* which are external and internal factors/developments that cannot be directly controlled by the decision makers. Each strategy contains a combination of technical and non-technical *options* which can be chosen/implemented by decision makers. Some uncertainties and some options will be global, others will be specific in a given nation or region. Each *scenario* is then a combination of a possible *future* and a *strategy* (Action Plan) for how to act within that future. The maximum theoretical number of scenarios is the number of possible futures multiplied by the number of alternative strategies.

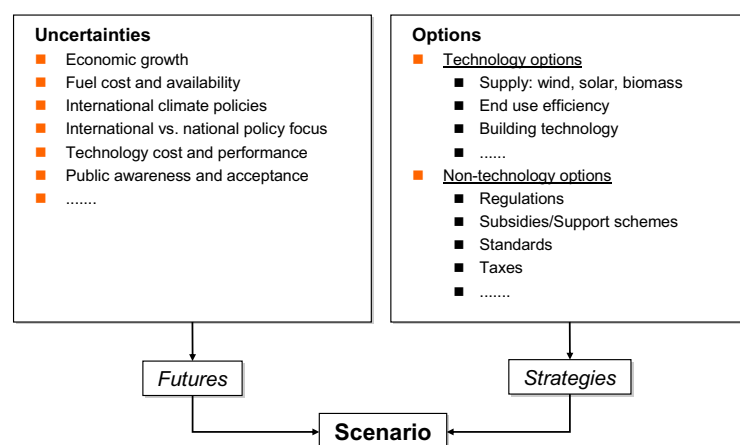


Figure 1. Methodology for establishing scenarios.

ideally all possible combinations of relevant uncertainties and options should be tested. However, the combination of many uncertain future developments and strategies leads to a multitude of combinations, and the amount of scenarios has to be limited to be able to derive credible practical implementation plans for decision makers and stakeholders.

The most challenging task in this context is to limit the number of uncertain, non-controllable future developments. This is done by the identification of the two primary driving forces (typically a "hardware/technology" driver and a "soft" driver) according to degree of uncertainty and relevance for the task. These two uncertainties are used to span out a set of 4 most relevant futures, also termed *storylines*, as a common background for scenario analysis.

2.2 Description of the Storylines

The storylines are used to create four fundamentally different pictures of "the rest of the world" in which to design, build and operate zero emission buildings. The storylines are based on the basic assumptions that there is a strong political will in Norway (and Europe) to promote the deployment of zero emission buildings, and that the greenhouse gasses emissions (GHG) in the

future European energy system will be contained compared to the current situation. The kernel of analysis is how to get maximum deployment of zero emission buildings towards 2030 and further to 2050.

Relevant uncertainties are evaluated to identify the two most important ones with respect to the main objectives. We emphasize that uncertainties here mean future developments that may be influenced but cannot be directly controlled by the relevant decision makers. The following uncertainties have been considered and discussed in detail: Technology development, Transmission grids and international energy trade, Fuel cost and availability, International climate policies, International versus national focus, Economic growth, Public attitude and Venture capital availability.

A comprehensive analysis and discussion of relevant uncertainties is performed in Sartori *et al.* (2010), which cannot be reproduced here for matters of space. The two uncertainties identified as most important for ZEB storylines are: *Technology development* and *Public attitude*. These two uncertainties are used to create the 4 storylines shown in Figure 2, forming a space with four quadrants. Note that the "colour codes" are preliminary and may be changed to more intuitive names.

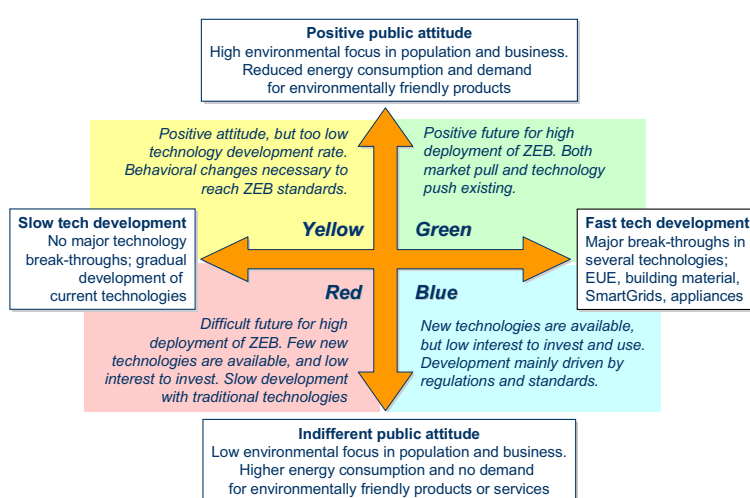


Figure 2. Overview of the four different storylines in ZEB.

Once the storylines are described in detail it is possible to perform a quantitative analysis and the average emission factors between today and 2050 can be calculated for each storyline. In this way the definition of ZEB will be based on emission factors that are meaningful throughout the life time of a building; at least as long as it is reasonable to foresee the electric system evolution.

It is important to remind that the authors do not currently consider any of the storylines more likely to happen than the others.

3 CRITERIA FOR ZEB DEFINITION

3.1 *The ZEB Balance Inequality*

The concept of balance is central in the definition of zero energy/emissions buildings. A ZEB is connected to one or more energy infrastructures, such as electricity grid, district heating and cooling system, gas pipe network, biomass and biofuels distribution networks. These infrastructures are here addressed with the general term energy grids. Figure 3 shows a sketch of the connection between buildings and energy grids, reporting the most important terminology.

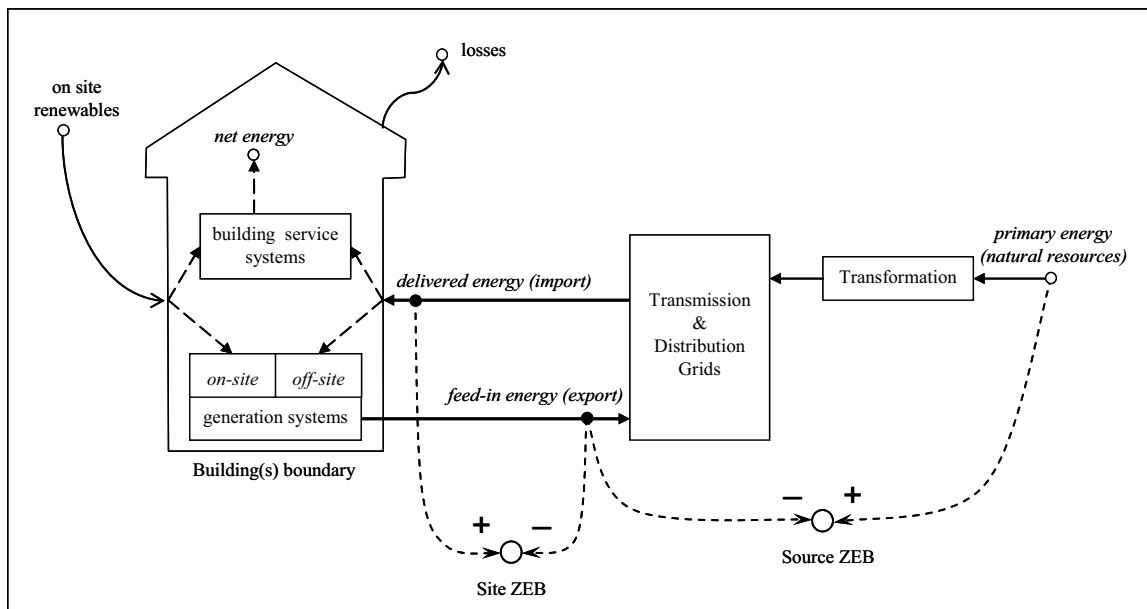


Figure 3. Connections between buildings and grids.

The term *net energy* indicates the total demand for energy services in a building, i.e. heating, cooling, hot water, lighting and so on. Net energy demand can partly be satisfied by direct exploitation of renewable energy sources available on site, e.g. solar energy. The term *delivered energy* indicates the total amount of energy supplied by the grids to the building in order to satisfy the remainder of the net energy demand. The losses arrow in the figure represents both envelope thermal losses and systems' inefficiencies. Passive houses and, to some extent low energy buildings make thorough use of both passive and active measures to achieve high energy efficiency, and so they require significantly less delivered energy than conventional buildings found in the stock.

ZEBs can also *feed-in energy* into the grids, and that happens primarily by means of generating electricity. In general, also other energy carriers can be considered; i.e. a district heating system able to supply and receive hot water at predefined conditions. Distinction shall be made between *on-site* and *off-site* generation. Systems such as PV and mini wind turbines generate electricity exploiting renewable energy sources available at the building site, and so they are called on-site options¹. On the other hand, generation of electricity from cogeneration (CHP) or fuel cells rely on fuels that are not available on site and need to be imported; e.g. biofuels from a distribution network. Thereof these options are called off-site.

For a ZEB the balance between energy *export* (feed-in energy) and *import* (delivered energy) over a period of time must be zero, or even positive, i.e. when embodied energy/emission in materials also have to be balanced off. The following balance inequality defines a ZEB:

$$\text{ZEB: } |\text{export}| - |\text{import}| \geq 0 \quad (1)$$

¹ In 0 a further distinction is made between *footprint* and *on-site* options, here both summarized with the term on-site.

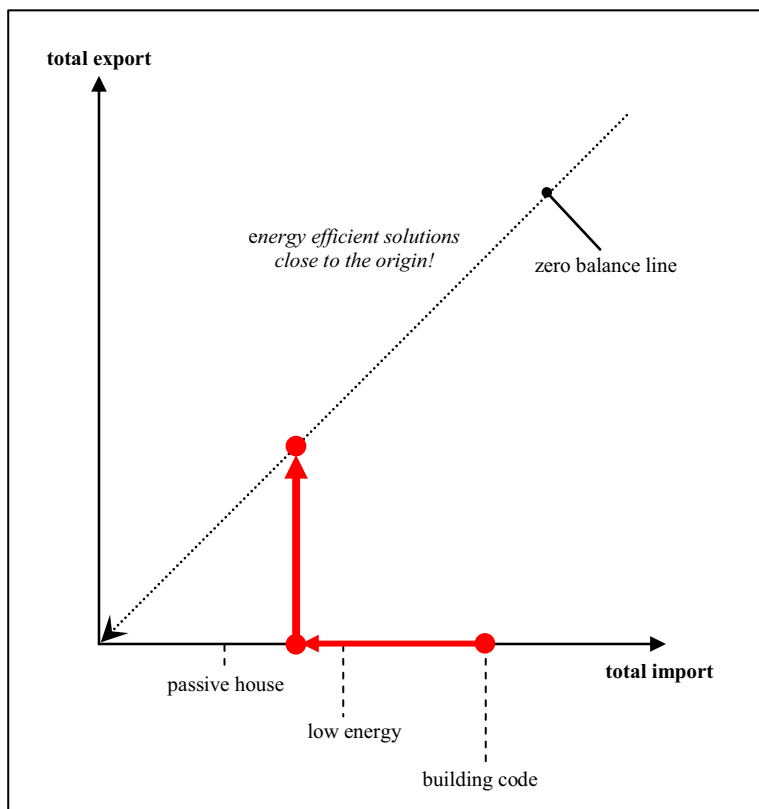


Figure 4. Graphical representation of the pathway to ZEB. First step: Reduce energy demand, or related carbon emissions. Second step: Generate renewable energy to get enough credits to achieve the balance.

system. To be able to grasp such differences it is necessary to use some conversion factors, or credits, that value the quantity of interest, as total primary energy or CO₂ equivalent emissions, etc. In this case the definition is called *Source-ZEB* (Torcellini *et al.*, 2006).

The terms of the above ZEB balance inequality are then expressed as follows:

$$\text{import} = \sum_i \text{delivered_energy}(i) \times \text{credits}(i) \quad (2)$$

$$\text{export} = \sum_i \text{feed-in_energy}(i) \times \text{credits}(i) \quad (3)$$

where i = energy carriers

Due to the complexity of the energy infrastructure, it is normally feasible to estimate such credits only as average values for a period of time and for a specific energy infrastructure. The credits will then vary over time and from location to location. Electricity may be considered with average European values, as the European electricity grid and market will eventually become fully integrated; while other energy carriers, i.e. district heating or biomass, should be credited according to the national or regional context, according to the actual availability of resources in the area.

Figure 4 gives a graphical representation of a general pathway to the design of ZEB. First step: reduce energy demand, or related carbon emissions. Second step: generate renewable energy to get enough credits to achieve the balance.

The balance is normally calculated by means of some sort of "credits" rather than directly on physical units of energy. A definition based on direct measurement of physical units of energy is called *Site-ZEB* (Torcellini *et al.*, 2006). This definition has the advantage of being easy to understand and measure, but it has the disadvantage of not valuing the differences between energy carriers. Indeed, in terms of natural resources use, emissions, environmental costs etc. one kWh of electricity has a different value than a kWh of thermal energy contained in refined gas or hot water in a district heating

The next step consists in identifying a series of criteria that characterise a ZEB definition. Evaluation of such criteria and selection of related options becomes a methodology for elaborating sound ZEB definitions in a formal, systematic and comprehensive way.

3.2 Description of the Criteria

A series of criteria need to be evaluated in order to achieve a sound ZEB definition. Some of these might be covered by national building energy codes already. The criteria are interconnected and choices on one could influence or eventually force the choices on another one. Furthermore, the choice of the most appropriate options may be influenced by the storyline under consideration.

1. System boundary: Is the boundary on a single building or on a cluster of buildings? Photovoltaic installation, e.g. on the roof, belongs to the building or to the grid?

The Norwegian ZEB centre is primarily oriented to research on buildings. However, building settlements may be considered as well. Where to put the boundary would affect, for example, the evaluation of a local district heating system. Suppose there is a small scale district heating system in place that serves a neighbourhood. If the entire neighbourhood is to be defined as ZEB, then the carbon emissions to offset are calculated considering the fuel mix and the efficiency of the actual plant in use, because it is inside the system boundary. Alternatively, if each single building is to be defined as ZEB, the carbon emissions to offset could be calculated differently. The energy imported into the system (one building) is in the form of hot water. Then it would make sense, for the sake of generality and/or for lack of specific data, to refer to regional or national aggregated data on fuel mix and efficiency of district heating systems.

It follows that a ZEB definition for a settlement would be easier to achieve when the local energy grid performs better than the national average. Consider for example the small district heating of above as running exclusively on biomass and/or biofuels. Internalising such a plant into the system boundary does reduce the amount carbon emissions to offset, when compared to the average district heating system that uses a mix of waste, renewable source, fossil fuels and electricity.

2. Feed-in possibilities: How can the building feed-in energy into the grids? Is electricity the only option or are there other carriers available, e.g. hot water in district heating system?

The simplest situation is when only electricity is available as a form of energy export from the building to the grid. Alternatively, it is possible to export energy in the form of other energy carriers, in case the grids are predisposed for it. This the case of hot and chilled water in a district heating and cooling system that works two-ways, or hydrogen produced on site from electrolysis with surplus electricity from a photovoltaic roof, in a hypothetical hydrogen infrastructure.

3. Balance object: What goes into the balance of a ZEB definition? Divided in two parts:

3.1 Balance object I, Life time: What is the scope of the definition? Is it solely the energy used for operation of the building? Or the energy calculated from a complete LCA analysis? Or a

middle way, e.g. energy for operation and embodied energy in materials and technical installations?

The definition could focus solely on the balance of emissions during the normal operation of the building. Alternatively the definition could consider the complete Life Cycle Analysis (LCA) of the building, which includes the emissions embodied in materials and technical installations and emissions caused in construction, renovation and demolition phases, eventually considering also material recycling and waste management options. Another option is to balance emissions caused by operation of the building and emissions embodied in materials and technical installation, while neglecting the construction and demolition phases, knowing a priori that they are far less significant.

When the balance is not solely on the operation of the building the implication is that the building must achieve an excess of emission credits, i.e. it must produce more energy than it consumes, in order to payback also for the embodied emissions.

3.2 Balance object II, Operation: What comfort standards have been followed to calculate the building loads, i.e. for heating, cooling and ventilation? Are user loads, i.e. domestic hot water, lighting, plug loads, included in the balance? Are electric vehicles included in the balance?

In Norway the physical parameters of comfort and standardized user loads to be used as the basis for design and evaluation of energy performance are defined in the norm NS-3031 (2007).

Charging of electric vehicles in the garage is not considered in the Norwegian normative. However, this is a form of user load and even though it does not contribute to the building's internal gains, it may represent a form of storage of excess electricity produced on-site. Load from charging of electric vehicles could be considered. Other loads may also be worth considering, such as server rooms and water treatment.

4. Balancing period: What is the basis for calculating the balance? Yearly, seasonal or monthly balance? or a balance upon many years, e.g. a reference period of 30-50 years?

The first intuitive choice is to calculate the balance of emissions over a year. Alternatively, a monthly or seasonal period could be chosen. These options would capture variable availability of renewable energy and discourage great disparity between winter demand and summer generation. In both cases the embodied emissions, if considered, should be normalized on a yearly basis. Furthermore, changes in the climate are likely to happen in the forthcoming decades and average temperatures and precipitations are already different today than how they are in reference weather data files (given as averages over the last 30 years). If this aspect is to be considered, then yearly and sub-yearly evaluations should be performed with a set of different reference climatic years, known and forecasted.

Alternatively, the balance can be performed over a period of many years, i.e. 30 or 50 years. This option reckons the fact that after such a period a building is likely to undergo major renovation work and alter significantly its properties. In this case the calculations could be performed with stochastic weather input.

5. *Credits:* What is the metric to calculate the balance? Is it energy measured at site or source level? Or is the balance calculated on carbon emissions or other environmental indicators associated with energy? Is there any crediting of activities related to external investments such as wind farm shares etc. or green electricity?

The target of the Norwegian ZEB centre is to do research on zero emission buildings. However, carbon emissions are not always the most obvious choice and it is worth analysing also other possible credits.

The most intuitive way to give credits for the energy demand and generation of a building would be based on energy units itself. Such credits would then look different depending on where the energy is measured in the energy chain, i.e. delivered or primary energy as shown in Figure 3. Such cases are regarded in literature as site ZEB and source ZEB (Torcellini *et al.*, 2006), respectively. A summary of pros and cons of each choice is given in Table 1. In case of source ZEB the credits could be given on total primary energy or on the non-renewable part of primary energy.

Table 1. Comparison of site and source ZEB definitions.

Type of definition	Pluses	Minuses	Notes
Site ZEB	Emphasis on energy efficiency. Easy to measure. Robust, repeatable and consistent.	Blind on primary energy (hence emissions). May favour all electric buildings.	
Source ZEB	Easier to achieve than Site ZEB. Values primary energy. Better model for national energy policy.	May favour generation options vs. energy efficiency.	Site-to-Source conversion factors needed (<i>credits</i>).

The choice of crediting carbon equivalent emissions implies the adoption of a source ZEB definition, because it is at source level that a direct correspondence between energy and emissions can be calculated. It shall be noticed that not all renewable energy sources are equally abundant or available on the planet, i.e. biomass vs. solar. Renewable energy resources with low GHG emissions are not necessarily equally environmental friendly and beneficial from a local perspective. An option for the ZEB definition could then be to account for some sort of environmental credits that are defined with a broader scope than just GHG emissions, i.e. environmental cost analysis.

Other options could be to give credits on the basis of energy or emission costs, or on exergy. The former option is likely to be very unstable and imprecise due to energy price volatility and economic externalities. The latter may be difficult to understand for anybody not acquainted with such a physical property as exergy. It is even debatable whether exergy would actually be a good proxy of environmental performance of buildings.

6. Crediting method: How are the credits accounted for? Statically with average values? Or dynamically on a hourly basis? Or a semi-dynamic accounting with average values but with daily bands for base/peak load? Furthermore, is electricity from gas fueled cogeneration and fuel cells to be considered in the balance?

A static crediting method is based on average values of the electricity generation mix. Such evaluation should be regularly updated, i.e. every 5 or 10 years. As mentioned it is meaningful to use the generation mix at European level, because of the expected integration of the EU electric grid. In reality though, the generation mix does vary both with the time of the year and the hours of the day, according to load levels (base or peak generation technology), availability of intermittent RES at local and regional level, storage capacity and trans-national power transmission. To account for such variations a dynamic crediting method should be used, based on hour-by-hour evaluation of the credits, e.g. from the hourly clearing of the electricity market. This option is more meaningful because it would reflect nearly real time, on the spot, what is the actual impact of the electricity consumption by the building. However, it is more difficult to implement. It is already standard procedure for the electricity market to operate on hourly prices, but it is debatable to what extent electricity prices can be a good proxy of the associated environmental impact. An intermediate solution could be a semi-dynamic crediting method where average values are considered together with an hour-of-the-day classification into different levels, i.e. corresponding to average load levels.

It shall be noticed that some of the energy carriers, i.e. electricity, should be evaluated at European level, while others like gas, biomass, biofuels and district heating/cooling should be evaluated considering the regional and local infrastructure.

A controversial issue is how to consider the off-site generation, see Figure 3, based on natural gas rather than biomass or biofuels. The electricity so generated cannot be said to come from renewable sources. However, the overall efficiency of electricity and heat generation is high (often > 80%) because the waste heat can be directly used for meaningful purposes in the building, without heat transmission losses. So, this use of gas is more efficient than in a gas power plant where the waste heat is dispersed in a cooling tower. As long as the electricity grid has a poor environmental performance, i.e. it is largely based on fossil fuels, it may be justifiable to credit also gas fueled off-site generation.

7. Energy performance: Is it necessary to specify explicit minimum requirements? If yes what standards would define, for example, low energy and passive house buildings?

A major advantage of the ZEB approach is claimed to be the absence of energy performance indicators, hence avoiding the need to set internationally agreed limits. So, the first option is to give no requirements. With reference to Figure 4 this means letting the balance between import and export credits to be found anywhere in the graph area. This means that energy consumed and produced is valued equally, and cost optimisation will determine where the balance is to be found case by case.

Alternatively it is possible to set minimum requirements, which in Figure 4 it means to work as close as possible to the origin. This corresponds to value energy conservation more than energy

production, according to the principle that the best form of clean and renewable energy is the energy which is not used.

In Norway a standardised definition of *low energy* and *passive house* buildings for residential buildings is found in the norm NS-3700 (2009) and for non-residential buildings in SINTEF Byggforsk project report SB pr. 42 (2009). One option is to require that a ZEB must be at least a low energy building in terms of its energy efficiency. Alternatively, it could be stated that a ZEB must be a low energy building when it uses thermal carriers for heating while it must be a passive house if it is an all-electric building. This would give a rough yet helpful *a priori* consideration that electricity is an energy carrier more valuable than thermal carriers and should be devoted to other purposes than heating, especially outside of the building sector.

8. *Mismatch factors*: is it necessary to define requirements on the mismatch between energy generation and the building load? And the needs of a grid? And the substitution of fuels?

The mismatch factors give a better appreciation of the qualities of ZEBs than the simple overall balance of credits. Mismatch requirements assure higher design standard and lower stress on the grids. Mainly three different forms of mismatch are under analysis in the activities of IEA Task40/Annex52 (Voss *et al.*, 2010):

- the temporal mismatch of the energy generation with the building load: building performance mismatch
- the temporal mismatch of the energy transferred to a grid with the needs of a grid: grid interaction mismatch
- the mismatch between the type of energy imported and exported: fuel switching mismatch

The first two forms of mismatch are correlated. The temporal mismatch may occur at daily level, e.g. excess PV generation at daytime and consumption of electricity during night, and it can occur at seasonal level, e.g. the highest load in winter while generation mainly in summer. Strategies for reducing building performance and grid interaction mismatches are under evaluation. However, solutions that tend to improve the matching between load and generation in the building will automatically contribute also to reduce the mismatch with the grid, because more energy is used on site and less is fed back into the grid.

It has also been suggested to incorporate the two factors in one single indicator: the storage mismatch. A ZEB uses the grids as a storage system, feeding in energy when there is an excess generation and taking it back when needed. This differentiates a ZEB from an autarchic building that must have its own storage systems. The storage mismatch then corresponds to the amount of storage capacity theoretically needed to “convert” a grid connected ZEB into an autarchic building. This indicator would, indeed, measure how much the building uses the grid as its storage system. Better design solution would reduce the storage mismatch; as for example using cogeneration in cold climates rather than an oversized PV system gives a better seasonal load matching, and adoption of batteries for short term storage and smart metering allow feeding in electricity when convenient for the grid. The storage mismatch indicator can be applied to the electric grid as well as to a two-way district heating and cooling system.

Finally, the balance of primary energy or emission budget might result from energy source switching, such as taking natural gas from a grid during the heating season and feeding solar electricity back into another grid during summer. This may be a good strategy for the building as it avoids seasonal storage. On the other hand it might not match with the needs of the grids. Ways to quantify this aspect are also under evaluation.

REFERENCES

- ECEEE (2009), Net zero energy buildings: definitions, issues and experience, *European Council for an Energy Efficient Economy (EU)*.
- EU (2010), Directive of the European Parliament and of the Council on the energy performance of buildings (recast), dated 07/04/2010 Brussels, 2008/0223 (COD).
- Marszal, A. and Heiselberg, P. (2009), A literature review on ZEB definitions, *Aalborg University (DK)*.
- NS-3031 (2007) Beregning av bygningers energiytelse- Metode og data, *Standard Norge*.
- NS-3700 (2010), Kriterier for lavenergi- og passivhus- Boligbygninger, *Standard Norge*.
- Sartori, I., Bakken, B. H. and Graabak, I. (2010) Zero Emission Buildings – Scenario and Definition Methodology, *ZEB centre internal memo*, dated 17.01.2010.
- SB pr. 42 (2009), Kriterier for passivhus- og lavenergibygger – Yrkesbygg, *SINTEF Byggforsk prosjektrapport 42*, forfattere: Tor Helge Dokka, Michael Klinski, Matthias Haase og Mads Mysen.
- SUSPLAN (2009), Development of regional and Pan-European guidelines for more efficient integration of renewable energy into future infrastructure “SUSPLAN”, Deliverable D1.1: Setup of SUSPLAN Scenarios, *Seventh Framework Programme project nr. 218960 (EU)*, www.susplan.eu, accessed 14/12/2009.
- Task 40/Anenx 52 (2008), Towards Net Zero Energy Solar Buildings, *IEA SHC Task 40 and ECBCS Annex 52*, <http://www.iea-shc.org/task40/index.html>, accessed 10/12/2009.
- Torcellini, P., Pless, S., Deru, M. and Crawley, D. (2006), Zero Energy Buildings: A Critical Look at the Definition, *National Renewable Energy Laboratory and Department of Energy*, (US).
- US DOE (2010), Building Technologies Program, Department Of Energy, US <http://www1.eere.energy.gov/buildings/goals.html>, accessed 14/01/2010.
- Voss, K., Sartori, I., Musall, E., Napolitano, A., Geier, S., Hall, M., Karlsson, B., Heiselberg, P., Widen, J., Candanedo, J. A. and Torcellini, P. (2010) Load Matching and Grid Interaction of Net Zero Energy Buildings, to be presented at *EuroSun 2010*, Gratz, AT.

ZEB Definition: Assessing the Implications for Design

Igor Sartori^{a*}, Inger Andresen^a and Tor Helge Dokka^a

^a SINTEF Building and Infrastructure, P.O. Box 124, N-0314 Blindern, Oslo, Norway

* corresponding author, tel: +47 22965541, email: igor.sartori@sintef.no

ABSTRACT

Conceptually a Zero Emission Building (ZEB) is a building with greatly reduced energy demand and able to generate electricity (or other carriers) from renewable sources in order to achieve a carbon neutral balance. However, a rigorous and agreed definition of ZEB is yet to come. A parallel paper in this conference explains how a formal and comprehensive ZEB definition can be based on the evaluation of certain criteria. These criteria are extensively discussed in ongoing projects, both in Norway and internationally. The objective of this paper is to focus on two of these criteria: energy performance and credits used to measure the ZEB balance. For each criterion different options are considered and the implications they have on the building design are assessed. The case study is on a typical Norwegian single family house. It is shown that for certain choices on the two criteria options, a paradoxical situation could arise. When using off-site generation based on biomass/biofuels, achieving the ZEB balance may be easier for high energy consuming buildings than for efficient ones. This is the exact opposite of what ZEBs are meant to promote: design of energy efficient buildings with on-site generation options. Recommendations on how to avoid such a paradox are suggested.

Keywords: ZEB definition, design, low energy, passive house.

1 INTRODUCTION

A series of criteria to characterise a formal and comprehensive ZEB definition has been presented in Sartori *et al.* (2010). The objective of this paper is to focus on two of these criteria: *credits* used to measure the balance and the building's *energy performance*. For each criterion, different energy supply and demand options are considered and the implications they have on the building design are assessed. A summary of the important terminology necessary to understand the content of this paper is taken from Sartori *et al.* (2010) and reported below.

The term *net energy* indicates the total demand for energy services in a building, i.e. heating, cooling, hot water, lighting and so on. Net energy demand can partly be satisfied by direct exploitation of renewable energy sources available on site, e.g. solar energy. The term *delivered energy* indicates the total amount of energy supplied by the grids to the building in order to satisfy the remainder of the net energy demand.

ZEBs can also *feed-in energy* into the grids, and that happens primarily by means of generating electricity. In general, also other energy carriers can be considered; i.e. a district heating system able to supply and receive hot water at predefined conditions. Distinction shall be made between *on-site* and *off-site* generation. Systems such as PV and mini wind turbines generate electricity exploiting renewable energy sources available at the building site, and so they are called *on-site* options¹. On the other hand, generation of electricity from cogeneration (CHP) or fuel cells rely on fuels that are not available on site and need to be imported; e.g. biofuels from a distribution network. Thereof these options are called *off-site*.

It is still a matter of debate how to consider the off-site generation based on natural gas rather than renewable fuels. The electricity so generated cannot be said to come from renewable sources. However, the overall efficiency of electricity and heat generation is high (often > 80%) and as long as the electricity grid has a poor environmental performance, i.e. it is largely based on fossil fuels, it may be justifiable to credit also gas fueled off-site generation. For the sake of completeness, in this work the off-site generation based on natural gas is considered as an available option.

For a ZEB the balance between energy *export* (feed-in energy) and *import* (delivered energy) over a period of time must be zero, or even positive. The following balance inequality defines a ZEB:

$$\text{ZEB: } |\text{export}| - |\text{import}| \geq 0 \quad (1)$$

The balance is normally calculated by means of some sort of *credits* rather than directly on physical units of energy. The terms of the above ZEB balance inequality are then expressed as follows:

$$\text{import} = \sum_i \text{delivered_energy}(i) \times \text{credits}(i) \quad (2)$$

$$\text{export} = \sum_i \text{feed-in_energy}(i) \times \text{credits}(i) \quad (3)$$

where i = energy carriers

The *credits* are therefore the metric used to calculate the balance. Two types of credits are considered in this paper: primary energy credits and carbon emission credits.

The *energy performance* is given in three cases for a typical Norwegian single family house. The three cases represent a typical house found in the building stock, a house built according to the new building code and a passive house.

Concerning other criteria described in Sartori *et al.* (2010), the following options hold true for the work presented in this paper. The boundary is on a single building and the sole feed-in possibility considered is electricity. The balancing object is solely the energy used during the operational life time of the building, hence no embodied energy is

¹ In 0 a further distinction is made between *footprint* and *on-site* options, here both are summarized with the term *on-site*.

considered, and it includes the building load and the user loads. The balancing period is one year and the crediting method is static, hence based on average values, and no mismatch factor is considered.

2 METHODOLOGY

A theoretical case is presented based on a typical Norwegian housing unit in the Oslo climate. The house has a heated floor area of 160 m², divided in two storeys, for a total air volume of 440 m³. Windows cover an area equal to 20% of the floor area.

Energy performance is considered in three levels: a house representative of the stock, a house built according to the new building code TEK-2010 following the prescriptive requirements of §14.3, and a house built according to the Norwegian passive house standard defined in NS 3700 (2010). More in detail, the passive house has a heating demand < 20 kWh/m²a and is equipped with a solar thermal system that covers 50% of the domestic hot water demand. The “House TEK-2010” and the “Passive House” have a balanced ventilation system supplying a constant airflow of 1,2 m³/h·m² day and night. The “Stock house” has natural ventilation assumed at a constant air change of 0,5 ach. Internal loads are taken from NS 3031 (2007) for the Stock house and the House TEK-2010, while for the Passive House they are taken from NS 3700. Other relevant parameters are reported in Table 1.

The Norwegian labelling system for the energy performance of buildings is based on delivered energy. The energy classes are labelled with letters from A to G, where A is the most energy efficient class and G the least efficient. Assuming as an explanatory case that the three versions of the single family house are all heated with direct use of electricity, they would be labelled as follows. The Stock house would receive a label of energy class E (on the border to class D); the House TEK-2010 would receive a class C and the Passive House a class A.

Table 1. Main parameters for the three cases.

Parameter	Stock house	House TEK-2010	Passive House
U-value outer walls [W/m ² K]	0.40	0.18	0.11
U-value roof [W/m ² K]	0.28	0.13	0.10
U-value ground floor [W/m ² K]	0.33	0.15	0.13
U-value windows [W/m ² K]	2.9	1.2	0.8
Thermal bridge normalized [W/m ² K]	0.10	0.03	0.01
Infiltration (at 50 Pa) [ach]	3.0	2.5	0.6
Heat recovery ventilation, yearly [%]	0	70	90
Specific Fan Power (SFP) [kW/m ³ /s]	0	2.5	1.5

Two different credits are considered for measuring the balance between imported and exported energy: primary energy factors, as found in IEA 28-books (2007) and EN 15603 (2008), and CO₂ equivalent emission factors, as found in SB pr. 42 (2009). A summary of the credit values is shown in Table 2. The credits are converted into electricity equivalent figures in order to allow a direct comparison between electricity and the thermal carriers. When thermal carriers are used for heating purposes, the equivalent amount of electricity

is used to calculate the imported credits, see Eq. (2). When excess electricity is generated (no matter if on-site or off-site generation) and exported to the grid the exported credits are calculated, see Eq. (3). To achieve the ZEB balance the imported credits have to be equal or higher than the sum of all imported credits, as given by Eq. (1).

Table 2. Credits for the different energy carriers considered.

Energy carrier	Primary energy credits		Emission credits	
	kWh _{prim} / kWh _{del}	electricity equiv.	gCO _{2eq} / kWh	electricity equiv.
Electricity	3.31	1.00	395	1.00
District heating	1.12	0.34	231	0.58
Gas	1.36	0.41	211	0.53
Biomass/Biofuel	1.10	0.33	14	0.04

A number of different heating systems is considered as shown in Table 3, including cogeneration and fuel cell systems that can generate electricity while supplying heat to the building. Data on the efficiency of heating systems are taken from Pettersen *et al.* (2005).

Table 3. Heating system characteristics.

Heating system	Heat load covered	Heating efficiency (Back-up system)	Electricity generation efficiency
	%	η	ε
Direct electricity	100	0.98	-
Heat pump	75	2.20 (0.98)	-
District heating	100	0.88	-
Gas	100	0.81	-
Biomass	100	0.77	-
CHP gas	100	0.50	0.30
CHP biofuel	100	0.50	0.30
Fuel cell gas	100	0.40	0.40
Fuel cell biofuel	100	0.40	0.40

Calculations of the building energy demand are performed according to the Norwegian calculation procedure NS 3031 (2007), using the software SIMIEN. For each heating system it is calculated the amount of on-site electricity generation needed – i.e. how big the PV system should be – to achieve the ZEB balance.

3 RESULTS AND DISCUSSION

Results for the three different levels of energy performance are reported in Table 4, Table 5 and Table 6 for the Passive House, the House TEK-2010 and the Stock house, respectively; a graphical visualisation is given in Figure 1, Figure 2 and Figure 3. Results show how the differences between the various cases can be significant, and how certain choices on the two criteria may favour one design solution or another.

The tables show the amount of net energy required by the building together with the delivered energy and corresponding energy class label obtained with the different heating systems. Depending on the energy carrier used for heating the total amount of credits

necessary to achieve the zero balance varies. The amount of credits also varies according to the credit metric adopted, whether primary energy or carbon emission, according to the values given in Table 2.

When a building is all electric, i.e. the heating system is based on direct use of electricity or heat pump, the credits balance is achieved generating as much on-site electricity as it is consumed by the building. When thermal carriers are used for heating, the required electricity generation is always less than in an all electric building, see Table 2. This implies, for example, that a smaller PV system is sufficient to achieve the ZEB balance.

When the heating system is run by a cogeneration machine (micro CHP) or a fuel cell, a certain amount of electricity is generated; this is the off-site generation. The remainder of the credits (total minus off-site) has to be generated on-site in order to achieve the ZEB balance.

It follows that when a building with high heating demand is equipped with CHP or Fuel cell, the off-site electricity generation is also high. This is because the cogeneration in buildings is driven by the heating demand and electricity is seen as the by-product; the opposite of what happens in power plants with cogeneration. The off-site generation of electricity may eventually be enough to provide all the necessary credits, or even give a surplus.

This leads to the absurd consequence that using off-site generation options, i.e. CHP and fuel cells, it is easier to achieve the ZEB balance with a high energy consuming building than with an efficient one, see tables below.

Table 4. Results the Passive House.

Heating system based on	Passive House			Electricity generation credits [kWh/m ² a]				
	Delivered energy [kWh/m ² a]	Class	Primary energy credits			Carbon emission credits		
(Net demand)	(69)		Total	Off-site	On-site	Total	Off-site	On-site
Direct electricity	71	A	71	0	71	71	0	71
Heat pump	58	A	58	0	58	58	0	58
District heating	75	A	49	0	49	58	0	58
Gas	78	A	53	0	53	58	0	58
Biomass	81	B	50	0	50	37	0	37
CHP gas	105	B	64	21	43	73	21	52
CHP biofuel	105	B	58	21	37	38	21	17
Fuel cell gas	123	C	71	35	36	82	35	47
Fuel cell biofuel	123	C	64	35	29	38	35	3

Table 5. Results for the House TEK-2010.

Heating system based on	House TEK-2010		Electricity generation credits [kWh/m ² a]					
	Delivered energy [kWh/m ² a]	Class	Total	Off-site	On-site	Total	Off-site	On-site
(Net demand)	(137)							
Direct electricity	139	C	139	0	139	139	0	139
Heat pump	101	B	101	0	101	101	0	101
District heating	150	C	82	0	82	107	0	107
Gas	158	D	93	0	93	107	0	107
Biomass	164	D	86	0	86	52	0	52
CHP gas	227	D	121	54	68	143	54	90
CHP biofuel	227	D	107	54	53	54	54	0
Fuel cell gas	272	E	140	90	50	167	90	78
Fuel cell biofuel	272	E	122	90	32	56	90	0

Table 6. Results for the Stock house.

Heating system based on	Stock house		Electricity generation credits [kWh/m ² a]					
	Delivered energy [kWh/m ² a]	Class	Total	Off-site	On-site	Total	Off-site	On-site
(Net demand)	(247)							
Direct electricity	251	E	251	0	251	251	0	251
Heat pump	163	D	163	0	163	163	0	163
District heating	275	E	120	0	120	177	0	177
Gas	295	E	145	0	145	176	0	176
Biomass	308	F	129	0	129	50	0	50
CHP gas	453	F	210	124	86	261	124	137
CHP biofuel	453	F	177	124	54	55	124	0
Fuel cell gas	556	G	252	206	46	316	206	110
Fuel cell biofuel	556	G	212	206	5	59	206	0

The results can be plotted as in the following figures in order to give an immediate visual understanding. For each of the three energy performance levels two graphs are shown; one for the primary energy credits and one for the carbon emission credits. Delivered energy, blue bars, and on-site electricity generation needed to achieve ZEB balance, yellow bars, are shown (*y*-axis) for the different heating systems considered (primary *x*-axis). The energy class label, A-G, is also shown (secondary *x*-axis). The green bar on the left hand side of the graphs shows the net energy demand.

The horizontal black line shows the amount of electricity that can be generated on-site by a PV system mounted on the roof. The average production is assumed being 120 kWh/a per square meter of PV area, and the available roof area is assumed equal to the building's footprint area, i.e. the area of one storey. The PV generation capacity is normalized per square meter of heated floor area in order to be directly comparable with the other variables. It follows that the generation capacity is 60 kWh/m²a.

It shall be reminded that all cases shown in the figures satisfy the ZEB balance inequality given in Eq. (1).

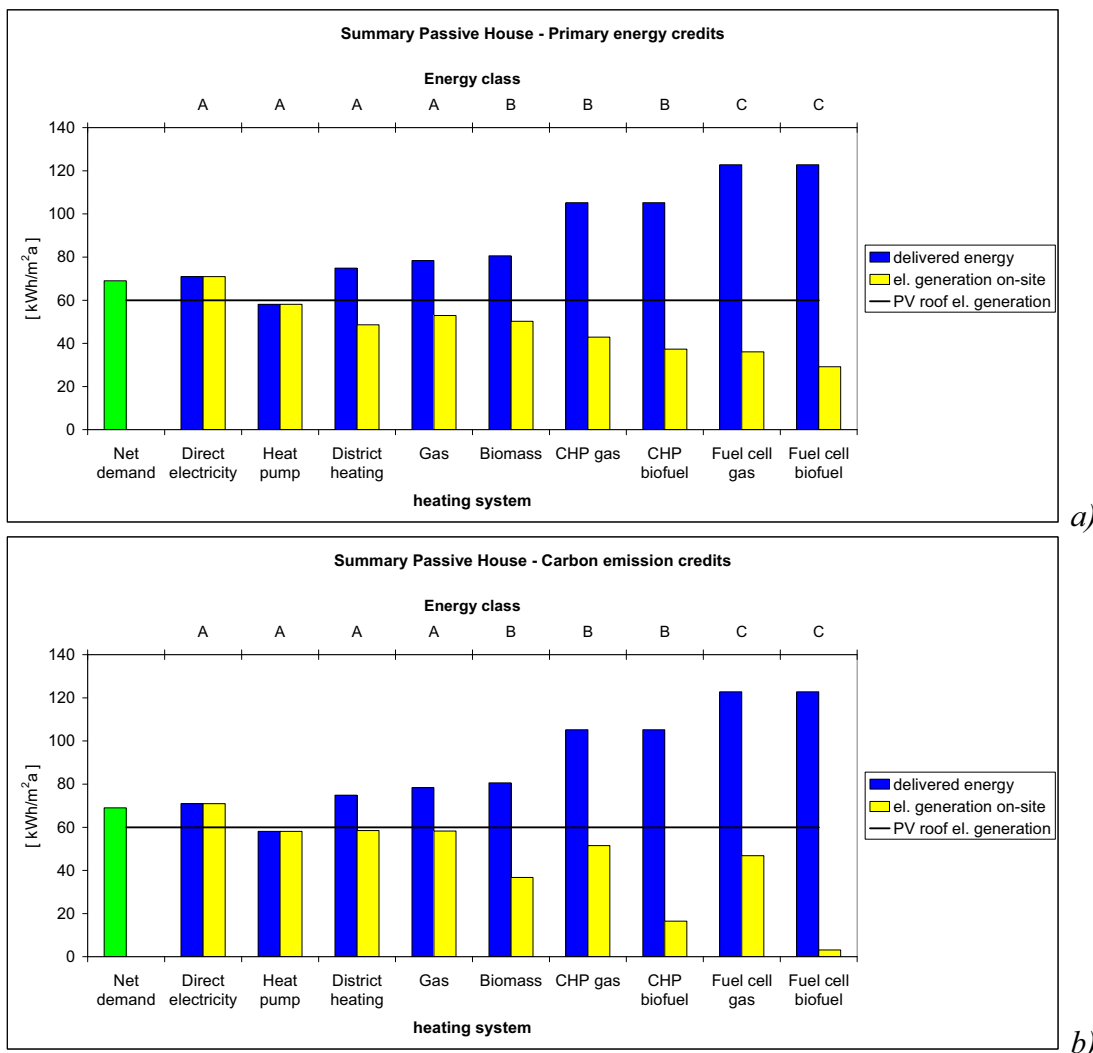


Figure 1. Summary graph for the Passive House when using a) Primary energy credits and b) Carbon emission credits.

Figure 1 shows the case of the Passive House. The net energy demand is 69 kWh/m² and the end of scale value for the y-axis is 140 kWh/m². When the house is heated with direct use of electricity the PV roof generation capacity is not enough to achieve the ZEB balance, while it is enough when adopting a heat pump. For all other heating systems, proceeding from left to right the delivered energy increases due to the diminishing efficiencies, as given in Table 3. The corresponding energy class varies from A up to C in the worst cases. According to conversion factors given in Table 2, adopting primary energy credits, Figure 1a), the necessary on-site generation decreases from left to right; while adopting carbon emission credits, Figure 1b), gives especially low generation requirements for the systems running on biomass and biofuels. In either case the PV roof is always sufficient to satisfy the ZEB balance.

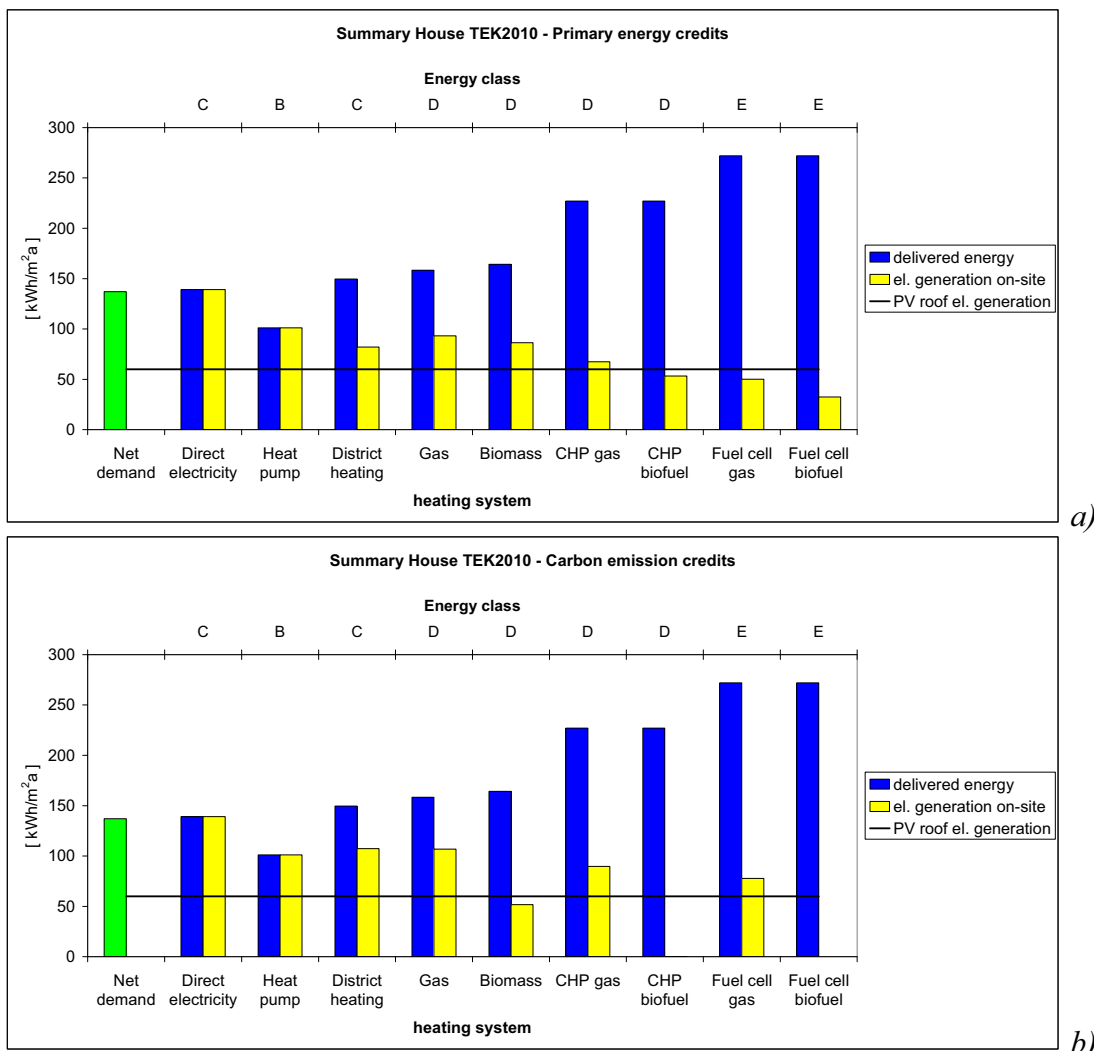


Figure 2. Summary graph for the House TEK-2010 when using a) Primary energy credits and b) Carbon emission credits.

Figure 2 shows the case of the House TEK-2010. The net energy demand is 137 kWh/m² and the end of scale value for the y-axis is 300 kWh/m². As before, for all heating systems except heat pump, proceeding from left to right the delivered energy increases. The corresponding energy class varies in this case from C up to E in the worst cases. Adopting primary energy credits, Figure 2a), the PV roof is sufficient only for the three right-most cases. Adopting carbon emission credits, Figure 2b), the PV roof is sufficient only when using biomass or biofuels based systems. In all other cases the generation from the PV roof is not enough and additional on-site generation capacity is needed. This could be provided, for example, by extra PV capacity or mini wind turbines mounted on the building site. However, it is worth focusing the attention on the fact that with carbon emission credits and using CHP or fuel cell run on biofuel the credits obtained with off-site generation are already equal or higher than the total necessary credits. Therefore, in these cases a PV roof becomes superfluous for achieving the ZEB balance.

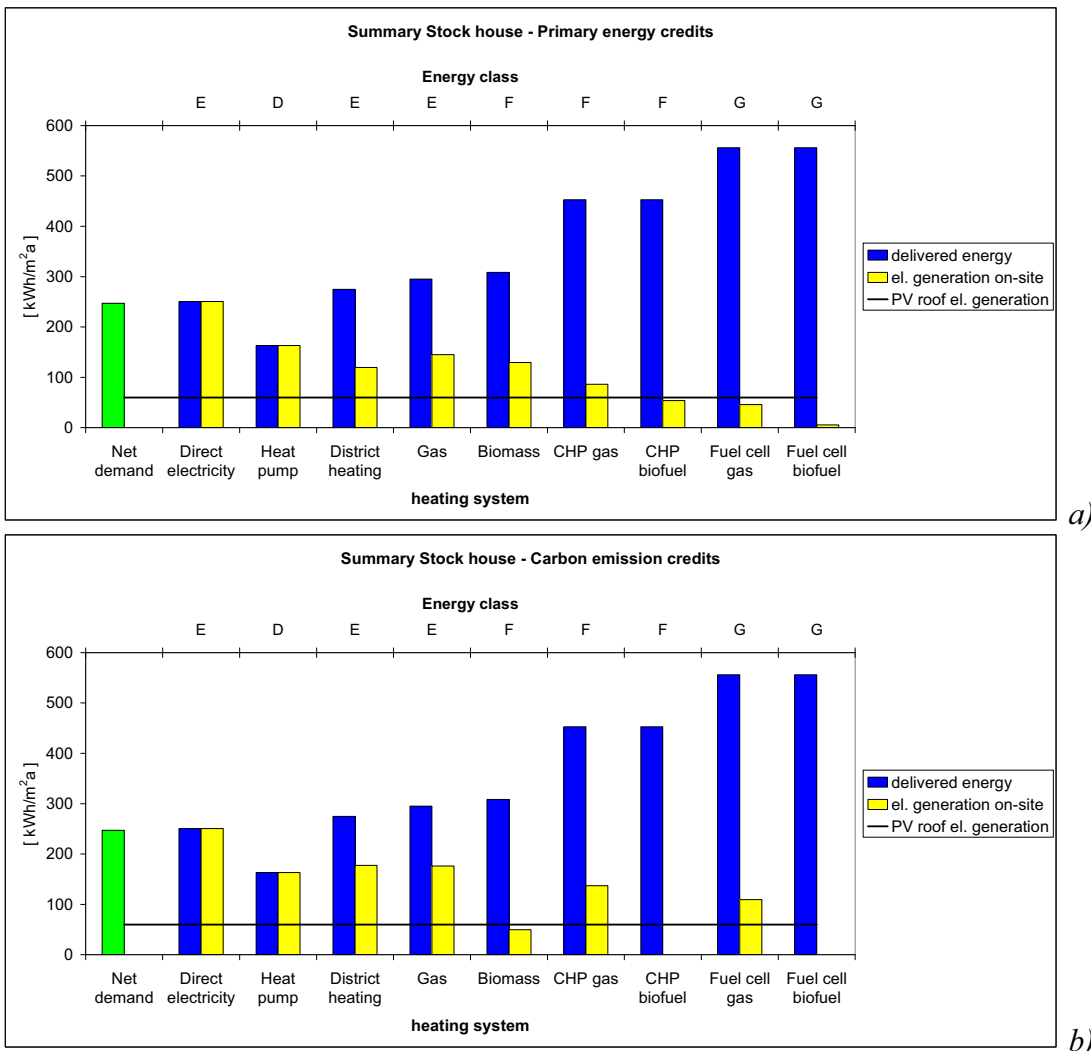


Figure 3. Summary graph for the Stock house when using a) Primary energy credits and b) Carbon emission credits.

Figure 3 shows the case of the Stock house. The net energy demand is 247 kWh/m² and the end of scale value for the y-axis is 600 kWh/m². As before, for all heating systems except heat pump, proceeding from left to right the delivered energy increases. The corresponding energy class varies in this case from E up to G in the worst cases. As for the House TEK-2010, adopting primary energy credits, Figure 3a), the PV roof is sufficient only for the three right-most cases; and adopting carbon emission credits, Figure 3b), the PV roof is sufficient only when using biomass or biofuels based systems. Once again, it is worth focusing the attention on the fact that with carbon emission credits and using CHP or fuel cell run on biofuel the credits obtained with off-site generation are already equal or higher than the total necessary credits. Therefore, in these cases a PV roof becomes superfluous for achieving the ZEB balance.

The above considerations bring to the conclusion that when using off-site generation based on biomass/biofuels, achieving the ZEB balance is easier for high energy

consuming buildings than for efficient ones. This is the exact opposite of what ZEBs are meant to promote: design of energy efficient buildings with on-site generation options.

In order to avoid this paradoxical situation the following recommendations should be considered. The first recommendation is on the ZEB definition criterion *energy performance*, see Sartori *et al.* (2010): establish clear minimum requirements, so that only energy efficient buildings are eligible as ZEB. In Norway this can be achieved adopting the definition of low energy and passive house buildings given in NS 3700 (2010). This is also in line with the recast of the EU directive on energy performance of buildings, EU (2010) that calls for the establishment of “cost optimal energy efficiency” requirements at national level. However, such requirements are yet to be defined as well as the common methodology for their evaluation; this should be defined at EU level within 2011.

The second recommendation is on the ZEB definition criterion *credits*, see Sartori *et al.* (2010): adopt credits that do not overemphasize the benefit of biomass and biofuels. Such a choice would reflect the fact that biomass is a limited resource and its availability varies significantly with the geographical area. On the contrary, solar energy is virtually unlimited and is available everywhere, even though with the due differences between low and high latitudes. To this respect primary energy credits seem to be more suitable than carbon emission credits. Alternatively, other credits could be defined. In Norway an example of alternative credits is given by the weighting factors described in Pettersen *et al.* (2005), which are based on the environmental cost analysis of various energy carriers. Given that electricity has a weighting factor of 1, the weighting factor they suggest for biomass is 0,35. This value is very different from the electricity equivalent factor of 0,04 give in Table 2 for carbon emission credits. Not surprisingly, it is similar to the value of 0,33 given here in the same table for primary energy credits.

Finally, another recommendation is to assign a sort of priority to the generation options to be adopted for achieving the ZEB balance. This is what is done in Torcellini *et al.* (2006), where the generation options are categorised in four levels, and on-site generation options are given priority over the off-site generation options.

REFERENCES

- EN 15603 (2008) Energy performance of buildings – Overall energy use and definition of energy ratings.
- EU (2010), Directive of the European Parliament and of the Council on the energy performance of buildings (recast), dated 07/04/2010 Brussels, 2008/0223 (COD).
- <http://www.energimerking.no/no/Energimerking-Bygg/Om-energimerkesystemet-og-regelverket/Energimerkeskalaen/>, accessed 30.04.2010.
- IEA 28-books (2007) Sustainable Solar Housing 2, Ed: Robert Hastings and Maria Wall.
ISBN: 978-1-84407-326-9.
- NS-3031 (2007) Beregning av bygningers energiytelse- Metode og data, *Standard Norge*.

- NS-3700 (2010), Kriterier for lavenergi- og passivhus- Boligbygninger, *Standard Norge*.
- NVE (2010), Norwegian labeling system on the energy performance of buildings, *Norges Vassdrags- og Energidirektoprate*, see
- Pettersen, T. D., Myhre, L., Wigenstad, T. and Dokka, T. H. (2005) Energimerking av boliger, *Byggforsk Report for NVE*, O 20461.
- Sartori, I., Graabak, I. and Dokka, T. H. (2010) Proposal of a Norwegian ZEB definition: Storylines and Criteria, *In the Proceedings of Renewable Energy Beyond 2020*, Trondheim, NO.
- SB pr. 42 (2009), Kriterier for passivhus- og lavenergibygg – Yrkesbygg, *SINTEF Byggforsk prosjektrapport 42*, forfattere: Tor Helge Dokka, Michael Klinski, Matthias Haase og Mads Mysen.
- TEK-2010 Forskrift om tekniske krav til byggverk (Byggteknisk forskrift), *Kommunal- og Regionaldepartementet*, Oslo, NO.
- Torcellini, P., Pless, S., Deru, M. and Crawley, D. (2006), Zero Energy Buildings: A Critical Look at the Definition, *National Renewable Energy Laboratory and Department of Energy*, (US).

Application of Vacuum Insulation Panels in Retrofitting of Timber Frame Walls – An Experimental Investigation

Erland Sveipe ^a, Bjørn Petter Jelle ^{ab*}, Erlend Wegger ^a, Sivert Uvsløkk ^b, Jan Vincent Thue ^a, Steinar Grynning ^b, Ole Aunrønning ^a, Egil Rognvik ^b, Arild Gustavsen ^c

^a Department of Civil and Transport Engineering, Norwegian University of Science and Technology (NTNU), NO-7491 Trondheim, Norway.

^b Department of Materials and Structures, SINTEF Building and Infrastructure, NO-7465 Trondheim, Norway.

^c Department of Architectural Design, History and Technology, Norwegian University of Science and Technology (NTNU), NO-7491 Trondheim, Norway.

* Corresponding author: bjorn.petter.jelle@sintef.no (e-mail), 47-73-593377 (phone), 47-73-593380 (fax)

ABSTRACT

A large amount of the buildings in Norway is from the 1970s. Many of these buildings have timber frame walls and are now ready to be retrofitted. Application of vacuum insulation panels (VIPs) can make it easier to improve the thermal insulation in building walls with a minimal additional thickness. Retrofitting of buildings using VIPs may therefore be done without large changes to the building, e.g. extension of the roof protruding and fitting of windows. Additionally, U-values low enough to fulfil passive house standards or zero energy building requirements may be achieved. Thus, contribute to a reduction of the energy use and CO₂ emissions within the building sector. This work investigates two different ways of retrofitting timber frame walls, one with VIPs on the cold side and one with VIPs on the warm side. A wall module containing four different fields is built and tested between two climate rooms with indoor and outdoor climate, respectively. The module consists of one reference field representing a timber frame wall built according to regulations in the 1970s in Norway, and three fields representing different ways of improving the thermal insulation of the reference field with VIPs. As VIP is a vapour tight barrier, the fields are tested with respect to condensation risk. A new sensor for measuring surface condensation called the wetness sensor is introduced. The results of the experiment show that this method of retrofitting may be acceptable in certain structures within limited climate zones, humidity classes, and building envelopes.

Keywords: Thermal insulation, Retrofitting, Timber frame wall, Vacuum insulation panel, VIP

1 INTRODUCTION

A large amount of the buildings in Norway is built after the second world war, especially many in the 1970s (Statistics Norway 2009). The building tradition in Norway and Scandinavia implies that a large amount of these buildings have timber frame walls and are now ready to be retrofitted. The building regulations required in the 1970s a U-value of 0.35 W/(m²K) (about 10 cm mineral wool) in walls (Building regulations of 1969). Today the requirement is a U-value of 0.18 W/(m²K) (TEK 1997) and passive houses have even more strict requirements. That is, the allowed energy loss through a wall structure is close to halved in the past 40 years. Even if the new requirements do not have retroactive effect, the potential of saving energy is rather large in these old buildings.

Vacuum insulation panel (VIP) is a high thermal insulating *material solution* with thermal conductivity in the order of 0.004 W/(mK). The VIP is built up of a fumed silica core enclosed by a high barrier envelope to maintain the vacuum. More information on the VIP's build-up may be found in e.g. Baetens et al. (2010). The ageing of VIP is mainly caused by increased moisture content and a reduction of vacuum over time, a thorough description of the ageing effects is found in e.g. Wegger et al. (2010) and Baetens et al. (2010). A major challenge using VIP is the risk of puncturing. A punctured panel has about 5 times higher thermal conductivity than an intact one, i.e. increases to about 0.02 W/(mK) (Binz et al. 2005). A puncture may be crucial with regard to condensation in the structure. In addition, the use of VIPs requires a precise design of the structure and high accuracy in the craftsmanship because the VIP cannot be adjusted or cut at the construction site.

Use of VIPs can make it easier to improve the thermal insulation in walls with a minimal additional thickness. Retrofitting of buildings using VIPs may therefore be done without large changes to the building, e.g. extension of the protruding roof and fitting of windows. At the same time, U-values low enough to fulfil the passive house standard may be achieved. In addition, many of the buildings from the 1970s have a need for changing the facades in any case.

Traditional advices for retrofitting timber frame walls, are adding insulation on the outside of the existing wall. This prevents moisture problems because the temperature in the old wall structure rises. In addition, the thermal bridges in the old wall structure become insulated. However, this way of improving thermal insulation can not uncritically be implemented using vapour tight VIPs. Introducing a vapour tight layer on the cold exterior side of a wall increases the risk of condensation inside the wall. However, VIPs have very good insulating properties and the temperature at the warm interior side of the VIPs might therefore be high enough to avoid condensation. SINTEF Building Research Design Guides (SINTEF 523.002) allow installing the vapour barrier 50 mm inside a 200 mm thick wall of regular mineral wool, e.g. $\frac{3}{4}$ of the total amount of insulation must be located on the cold side of the vapour barrier. The case of VIP applied on the cold side may be compared with such a case. Due to the differences in thermal conductivity a thin layer of VIP on the outside of a mineral wool wall may still represent $\frac{3}{4}$ or more of the total thermal resistance of the wall.

This work investigates two different ways of retrofitting timber frame walls, one with VIPs on the cold side and one with VIPs on the warm side. A wall module containing four different fields is built and tested between two climate rooms with indoor and outdoor climate, respectively. The moisture and temperature conditions in the wall were logged and analysed.

Furthermore, a new way of fastening the VIPs (not described in this paper), and a new way of measuring moisture close to a material surface is introduced. Calculations and simulations of thermal and moisture conditions in the different fields are also carried out and the experimental and theoretical results are compared and analysed.

2 EXPERIMENTAL

A full size realistic laboratory test may provide different results than a numerical analysis because of the complex mechanisms that a numerical model may not handle. Figure 1 illustrates the test module and the four fields in 3D, seen from the bottom.

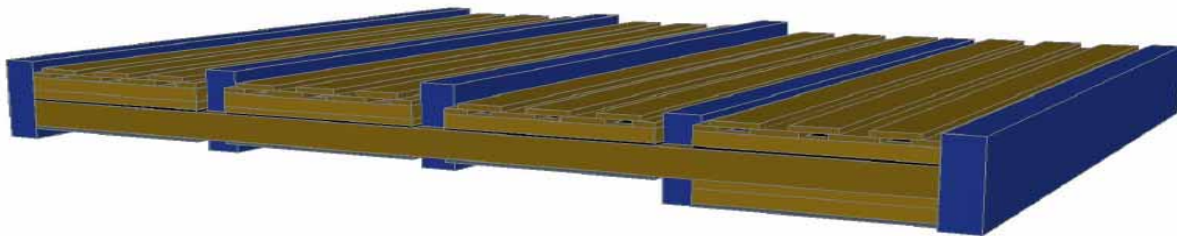


Figure 1. The test module in 3D view, seen from the bottom.

2.1 Description of Test Fields

The test module contains four fields seen in Figure 1 - 3. Field 3 (F3) is built without VIP and represents the original structure before retrofitting, i.e. a reference field of a timber frame wall from the 1970s. The three other fields (F1, F2 and F4) represent three different ways of improving thermal insulation of the reference field (Figure 2):

- F1: Outside 30 mm VIP
- F2: Outside 20 mm VIP
- F3: Reference field
- F4: Inside 30 mm VIP.

The four fields are separated by plastic film and extruded polystyrene (XPS), i.e. separated with respect to moisture and heat transport. Field 1 and field 4 have a initial U-value about 0.12 W/(m²K) with VIPs in their pristine condition.

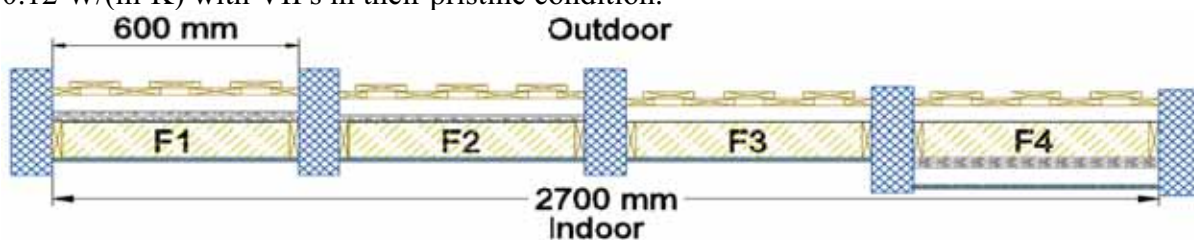


Figure 2. Horizontal cross-section of the test module. Note that the fields have no vapour barrier.

The build-up of Field 2 from outdoor to indoor (Figure 2 and Figure 3):

- Vertical weather boarding
- Furring strip (attached with a developed fastener, not shown here)
- VIP, joint not taped (attached with the same developed fastener)
- Wind barrier (bitumen-impregnated paper)
- Mineral wool
- Plasterboard

Normally, the wall should have a vapour barrier as well but this was omitted due to a short timeframe for the experiment. Not installing a vapour barrier represents a conservative modification and might be considered as a worst-case scenario.



Figure 3. Vertical cross-section of the test module. Note that the field has no vapour barrier, only the vapour tight VIPs at the cold exterior side (F2, see Figure 2).

The vacuum insulation panels used in the experiments in this work are of the type Vacupor NT - B2 from the producer Porextherm. Vacupor NT – B2 is a micro porous insulation material and consists of inorganic oxides. The main constituent is fumed silica. The other components are opacifiers for minimizing infrared radiation, and silicates. The panel is heat sealed with a high barrier film to maintain the vacuum (Porextherm 2009).

2.2 Temperature and Moisture Measurements

36 sensors of three different types were used in experiment:

- Thermocouple
- Air humidity sensor including thermocouple (two logging channels)
- New developed moisture sensor (Figure 4)

The thermocouple is familiar and consists of a cable with two separate conductors (copper and constantan). The cables are twined and soldered together at the tip where the measurement takes place based on varying electrical potential. The air humidity sensors were of the type “VAISALA Humidity and temperature transmitter TYPE HMP233”, which here are abbreviated as *RH air sensors*. These sensors were calibrated at 75.36 % relative humidity (RH), at 23 °C over a water solution of NaCl. The calibration was later re-examined by measuring the RH over a water solution of KNO₃ (94.0 % RH at 23 °C). The three different sensors are depicted in Figure 5.

In the process of planning the experiment, the idea of a new moisture sensor came up. The background for this new sensor is that the point of measurement using regular air-humidity sensors may be eccentric from the surface of the material-layer where the measurement is wanted. Condensation might therefore occur on a cold material surface while the air-humidity sensor shows a RH below 100 %. The idea was therefore to measure the electrical resistance on a thin material taped on the respective surface, this way the measurement could come as close to the material surface as possible. Different materials for use in the moisture sensor were considered and tested. Finally, the choice was as simple as regular copy paper (Lyreco BUDGET, 80 g/m²). The sensor is built up of double-sided tape, plastic-insulated single-wire 1.5 mm² cables, and copy paper. The moisture sensor is henceforth called the *wetness sensor*, and is shown in Figure 4.

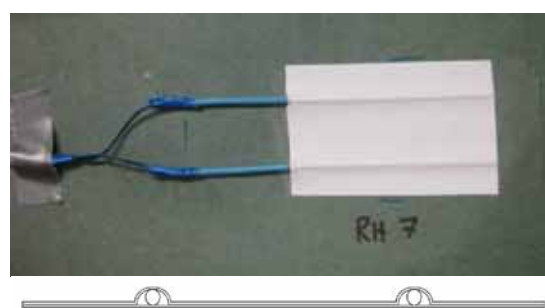


Figure 4. New developed moisture sensor consisting of double-sided tape, single-wired cable and copy paper.

The electrical resistance of the wetness sensor was measured with a wood moisture content meter, i.e. the electrical resistance was expressed by the moisture content in spruce at 20 °C. The sensor was calibrated in advance by measuring moisture content values for different RH and temperatures in a climate chamber. The result of this calibration made it possible to convert the logged moisture content to RH by a linear function on the form $y=ax+b$, where "a" and "b" were calculated. The moisture content measured for the case of condensation on the sensor was also noted. However, this method provides for several unknown errors, i.e. the sorption curve for paper is not in linear equivalence with the sorption curve for spruce. The fact that the sorption curves and the electrical resistance at different moisture contents change with temperature is neither accounted for. In addition, the size of errors of the manufacturing and the errors of materials used is not known. Therefore, the wetness sensor is to be considered as an indicator of RH and condensation, and must be further verified.

The most critical location for condensation was considered to be on the warm side of the VIPs in Field 1 and 2 (Figure 6), and at the warm side of the wind barrier at the reference field (F3). The thermal resistance of the wind barrier is marginal and the type of wind barrier used has a small water vapour resistance so condensation was expected to occur at the wind barrier as well as on the VIP surface. Hence, for practical reasons and the desire of having the sensors at the same locations for all four fields, most of the sensors in the experiment were located at the warm side of the wind barrier. However, there were also sensors at other locations in the wall. A wetness sensor were glued directly over the VIPs joint in F1 and F2 as shown in Figure 6, i.e. F1 and F2 had wetness sensors on both sides of the wind barrier located in the middle of the field. There were thermocouples in all four ventilated air cavities, located as seen in Figure 6. In addition, air temperature and RH were measured in both climate rooms.

Figure 7 show the location of the sensors on the wind barrier. The sensors at the top and the bottom are located 100 mm from the sills where convection in the mineral wool is considered to have the largest influence. The sensors at the middle are located directly within the joints of the VIPs, i.e. 1200 mm above the bottom sill.

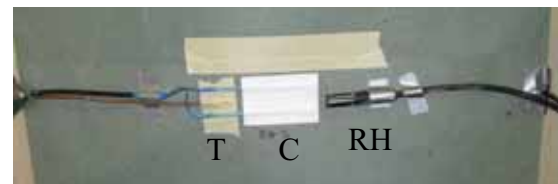


Figure 7. From the left: Thermocouple (T), new wetness sensor (C), and RH air sensor (RH) was installed on the wind barrier before the mineral wool was installed. The location of the sensors is seen in Figure 7.

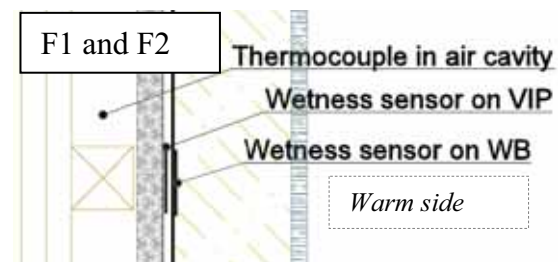


Figure 7. F1 and F2 had a wetness sensor both on the wind barrier and on the VIPs joint at the middle of the fields. The thermocouple in air cavity is also depicted.

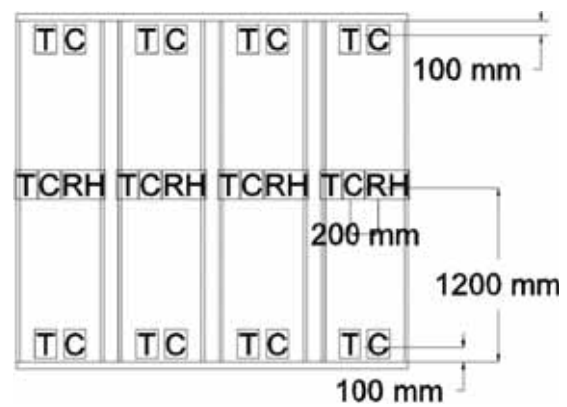


Figure 7. A section plane just within the warm side of the wind barrier. The timber frame and the wind barriers in the module seen from the warm side.

T – thermocouple,

RH – RH air (included thermocouple),

C – wetness sensor.

2.3 Data Logging

The 36 sensors gave a total amount of 42 logging channels because of six combined Humidity and temperature (RH air) sensors. Three different logging systems were used in the experiment. Because of the large number of sensors the thermocouples and the air humidity sensors were logged by two systems; *Solartron 35951C I.M.P.* connected to *Orchestrator 1.4.7* software, and *FLUKE Hydra data logger 2625A* with appurtenant software, respectively. The new moisture sensors required a separate logging system. This was a logger made by SINTEF and contained a *Greisinger GMH 830 Material moisture meter*. The logger was connected to a computer via *LabVIEW8.6* and the result logged to a data file.

2.4 Procedure

The test module was built between two climate rooms in the laboratory. The temperature at the cold side was intended to be - 20 °C, but the climate room did not manage to maintain this temperature. The outdoor temperature was therefore adjusted to - 18 °C. The relative humidity in the outdoor climate was not controlled, but was in the order of RH ~ 60 %.

The relative humidity in the indoor climate was adjusted in steps of 10 % while the temperature was held constant at 20 °C:

1. RH 30 % (Internal moisture excess ~ 4 g/m³)
2. RH 40 % (Internal moisture excess ~ 6 g/m³)
3. RH 50 % (Internal moisture excess ~ 8 g/m³)
4. RH 60 % (Internal moisture excess ~ 10 g/m³)

These moisture levels are henceforth called *climate steps*. The term *internal moisture excess* (ISO 13788) represents the difference in moisture content (g/m³) from the indoor to the outdoor air, where the indoor moisture production and degree of ventilation is taken into account. The term is useful in practical condensation calculations and divides different type of buildings into *humidity classes* as seen in Table 1.

Table 1. Internal humidity classes, derived from buildings in Western Europe (ISO 13788).

Humidity class	Internal moisture excess	Type of building
1	< 2 g/m ³	Warehouse
2	< 4 g/m ³	Office, shop
3	< 6 g/m ³	Home with few residents
4	< 8 g/m ³	Home with many residents, sports centre, kitchen, canteen
5	> 8 g/m ³	Special buildings, e.g. laundry, indoor swimming pool, brewery

3 RESULTS AND DISCUSSION

3.1 Wetness Sensor

The wetness sensor has proven to be quite trustworthy during this laboratory test. Even though the sensor was made as an indicator for condensation, the sensor has also proven to be reliable for RH around 80 – 90 %. The wetness sensor and the RH air sensor were in good agreement when they were at approximately the same location, as in the middle of field 1 and 2 (see Figure 8 to 11, especially Figure 9). However, the wetness sensor is primarily an indicator and the reliability must be tested further, e.g. for repeated cycles between low and high moisture levels. Note that the value of the wetness sensor goes beyond 100 in the plots of the results. This is because of the mentioned errors concerning use of the wood moisture sensor mentioned earlier. The values below 100 are equivalent with percent air RH. The values above 100, however, indicate condensation at the sensor. Calibration results have shown that values above 105 are to be considered as condensation, this includes a small safety margin. Thus the ordinate axes of Figure 8 to Figure 11 have not been denoted as % RH.

3.2 Measurements

The climate room on the cold side had problems keeping the temperature at -18 °C any longer than about 5 days (as seen in Figure 12). Still, the results from the laboratory test are according to what was expected from calculations.

None of the fields experienced condensation during step 1 or 2 (described in the procedure), with a RH of and ~40 %, respectively. Hence, day 1 to day 15 of the experiment are only plotted for field 2, see Figure 8. The alternation of RH in the climate room might be seen in the figure. The variation is up to 25 percentage points from the lowest to the highest value. This problem was however reduced past test day 15, when a different humidifier was installed.

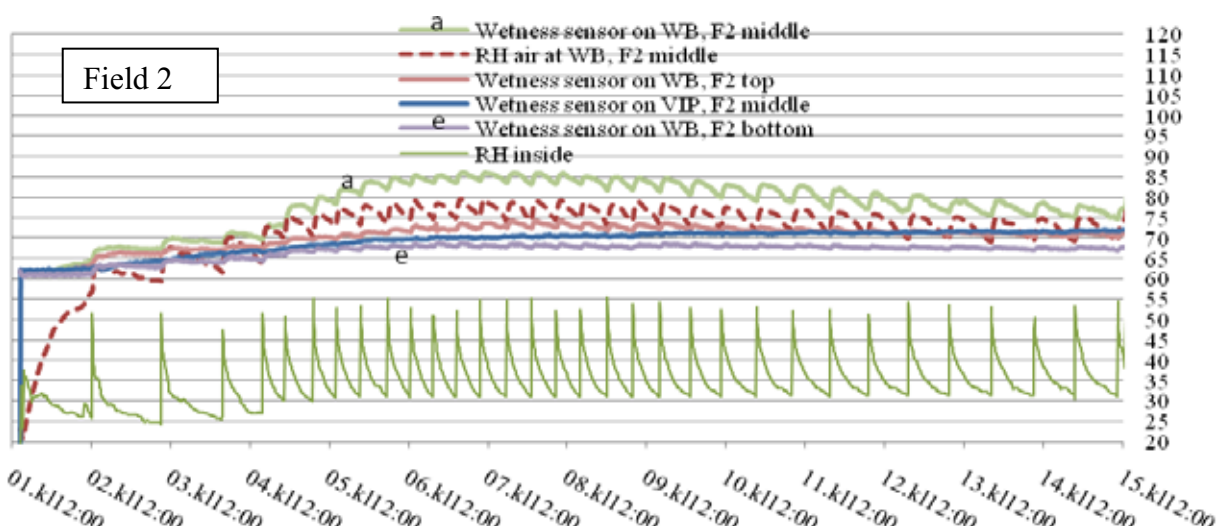


Figure 8. Moisture sensors in field 2 during climate step 1 and 2. The RH equivalent values of the four wetness sensors, as well as the RH air sensor are shown. The location of sensors is depicted in Figure 6 and Figure 7. The climate room RH was ~30 % from day 1 to 4.2, and ~40 % from day 4.2 to 15 (the lower plot).

In climate step 3 and 4 condensation was measured in field 1 and 2 as shown in Figure 9 and Figure 10. The RH inside the climate room is shown in the lower plot of the figures, and has a variation of about 10 percentage points from the lowest to the highest value.

Figure 9 shows field 1 that has 30 mm VIP on the outside, during the two climate steps with RH \sim 50 % and \sim 60 %. The field had condensation at RH \sim 50 %, which was not expected for this climate step compared to numerical simulations, at least not after that short period of exposure. This might be caused by the alternations in RH inside the climate room. The moisturising at the RH peak is possibly larger than the exsiccatting at the RH bottom. Small air leakages in the structure might also contribute to the measured condensation.

The wetness sensor shows condensation (value of 105) when the RH air sensor shows about 95 % RH. A possible explanation is that the RH air sensor is located about 5 mm from the wind barrier. Moreover, the wetness sensor is more influenced by condensed water on the vapour barrier than the RH air sensor. The wetness sensor located on the VIP joint has lower values than the wetness sensor on the wind barrier. Assuming that both sensors have the same temperature, condensation may be caused by the small vapour resistance of the wind barrier. The wetness sensor on the VIP (behind the wind barrier) then becomes moisturised by the wet wind barrier, which causes the sudden increase at the wetness sensor on the VIP. Another factor is the convection over the VIP joints (about 2 mm opening) that might dry the sensor somewhat. A third aspect may be time delay due to the small vapour resistance of the wind barrier, but this should not result in a sudden increase.

The wetness sensors at the top and the bottom have different development at the end of climate step 3. A possible explanation is that the wetness sensor at the top experiences a lower RH caused by an increase in the outdoor temperature. The increase at the wetness sensor at the bottom may be condensed water that runs down the vapour barrier and moisturises the sensor.

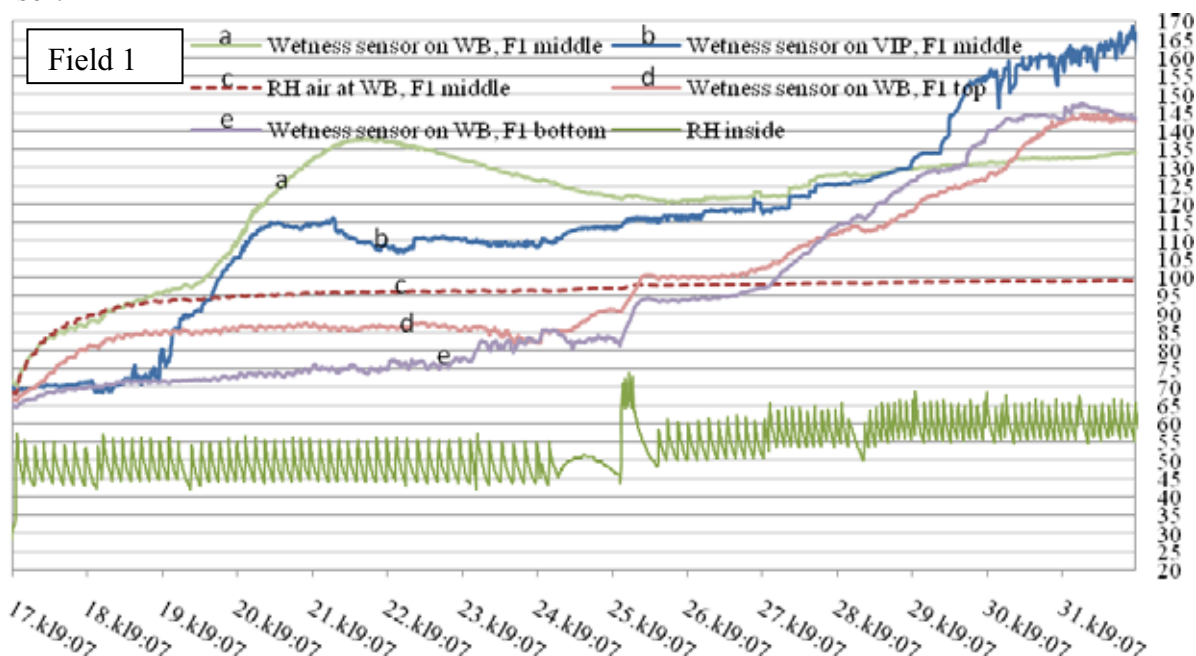


Figure 9. Moisture sensors in field 1 during climate step 3 and 4. The RH equivalent values of the four wetness sensors, as well as the RH air sensor are shown. The location of sensors is depicted in Figure 6 and Figure 7. The climate room RH was \sim 50 % from day 17 to 24, and \sim 60 % from day 25.5 to 32 (the lower plot).

Figure 10 shows field 2 that have 20 mm VIP on the outside, during the two climate steps with RH \sim 50 % and \sim 60 %. In accordance with numerical simulations, the field had condensation at both climate steps 3 and 4. However, an interesting difference between field 1 and 2 is the wetness sensors on the VIPs. In field 1 this sensor (on the VIPs) measures condensation at both climate steps. In field 2 however, the sensor measures condensation only for climate step 4 even if this field is less insulated (only 20 mm VIP). The temperatures measured at the warm side of the wind barrier (not plotted here) show that the wetness sensor at field 1 has a higher temperature than the wetness sensor in field 2. This is according to what one should expect, so the reason why the wetness sensor at the VIP joint in field 2 does not show condensation is unclear. It might be caused by difference in workmanship of the wall. The stiff wind barrier was hard to fit properly and this might cause air cavities between the VIP and the wind barrier that is different from field 1 to field 2. Another unexplainable occurrence is the sudden drop at the wetness sensor at the VIP joint in Figure 10. What might have caused this is not investigated.

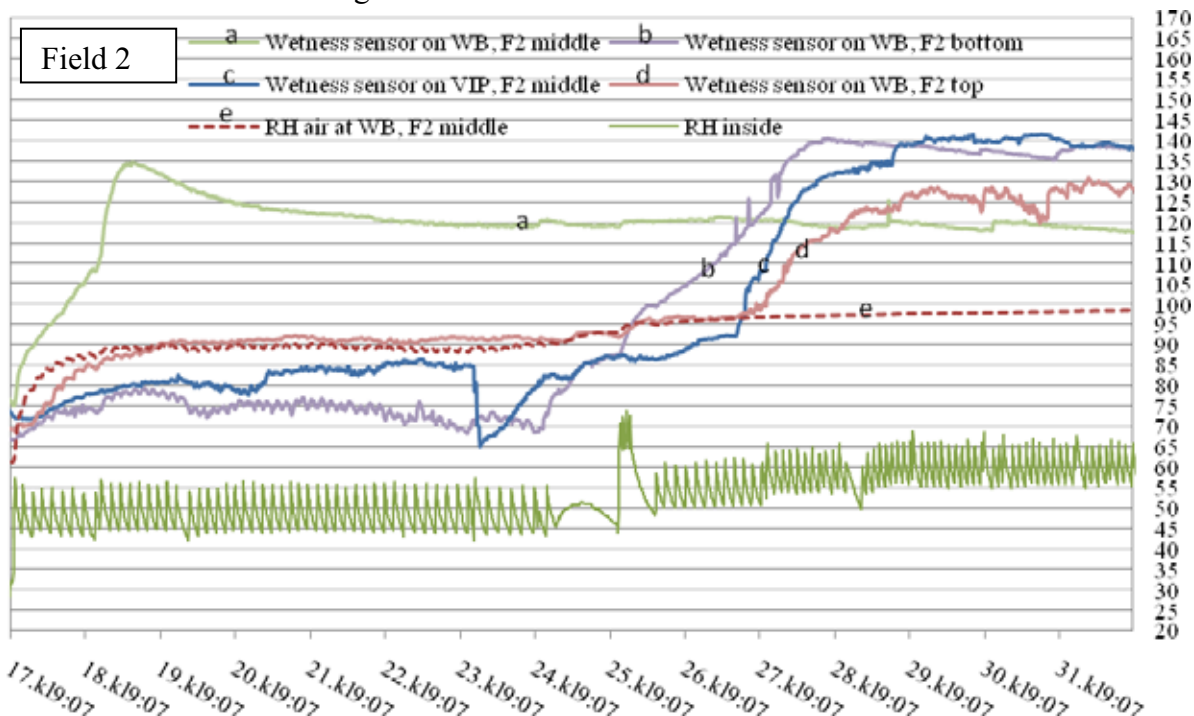


Figure 10. Moisture sensors in field 2 during climate step 3 and 4. The RH equivalent values of the four wetness sensors, as well as the RH air sensor are shown. The location of sensors is depicted in Figure 6 and Figure 7. The climate room RH was \sim 50 % from day 17 to 24, and \sim 60 % from day 25.5 to 32 (the lower plot).

Both Figure 9 and Figure 10 show a peak at the wetness sensors during condensation. The cause of this peak might be the different sorption curves for spruce and paper, i.e. that the measured electrical resistance is in a sensitive area of the curve that describes the electrical resistance as a function of moisture content for spruce (the moisture meter is calibrated with respect to spruce). A small decrease in RH might then give a large effect on the output value of the moisture meter.

Figure 11 shows the reference field (F3) during the two climate steps 3 and 4. None of the sensors shows condensation. The wetness sensors are not tested for temperatures below 0 °C and are therefore less trustworthy in field 3. It is reasonable that the electrical resistance increases at low temperatures. Therefore, the values from the wetness sensors are in this field lower than the RH air sensor.

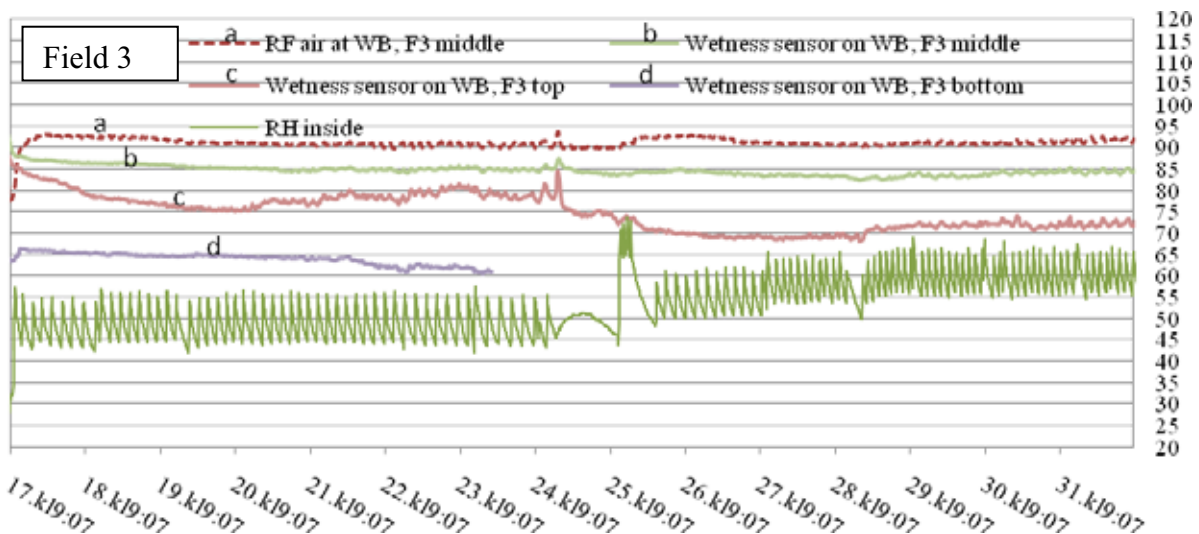


Figure 11. Moisture sensors in field 3 during climate step 3 and 4. The RH equivalent values of the three wetness sensors, as well as the RH air sensor are shown. The wetness sensor at the bottom was to dry and stopped giving reliable outputs. The location of sensors is depicted in Figure 6 and Figure 7. The climate room RH was ~ 50 % from day 17 to 24, and ~ 60 % from day 25.5 to 32 (the lower plot).

Condensation might be present in this field without being measured. The time frame of the test is not necessarily long enough to give condensation, because this field will experience a certain exsiccation to the outside climate room. The outside temperature is in addition increasing from the start of the climate step to the end as seen in the lower plot of Figure 12 (the cooling unit was manually de-iced for each climate step). This contributed to hold the RH air sensor on the wind barrier stable, as seen in Figure 11.

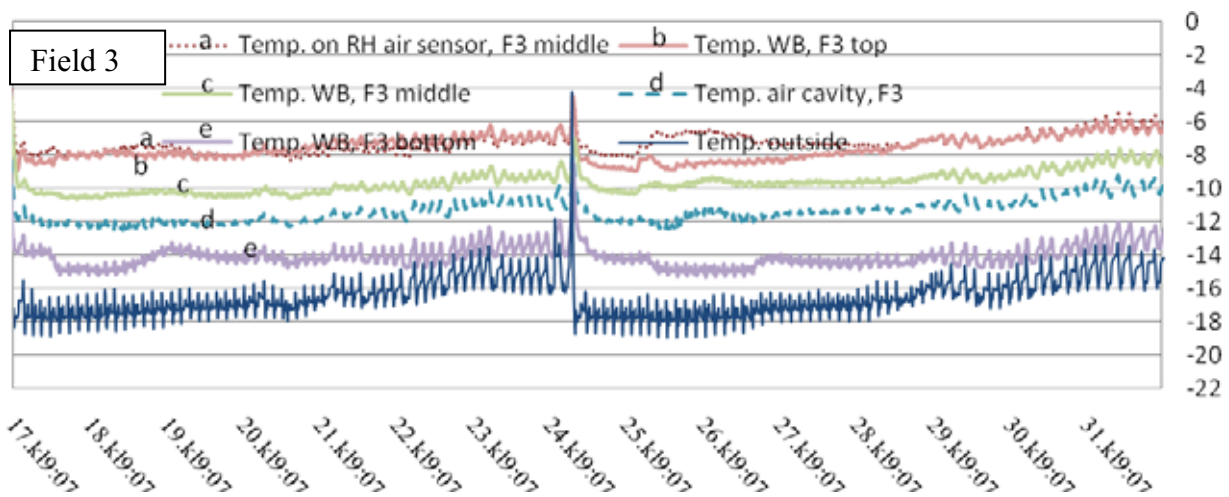


Figure 12. Temperatures in field 3 measured at the warm side of the wind barrier (WB) over the same time span and at the same locations as the wetness sensors shown in Figure 11. In addition, the temperature on the RH air sensor, temperature in air cavity inside the weatherboards, and outside temperature (in the climate room) are given.

Field 4 preformed well during the entire test, i.e. no condensation occurred. RH at the middle of the wind barrier was around 50 %, thus far from the risk of condensation. The results from this field are therefore not shown in graphical plots.

The results of the experiment show that 20 mm and 30 mm VIPs may be used at the outside of a 100 mm mineral wool wall to improve thermal insulation. Provided that the building has an internal moisture excess less than 6 g/m³ and do not experience exterior climate conditions more severe than - 18 °C/RH 60 %, and interior climate conditions more severe than 20 °C (RH ~ 40 % with 6 g/m³ internal moisture excess). Consequently, this method of retrofitting requires limitations to climate zone, humidity class, and the building envelope of a structure. Note that these results might not be valid for aged or punctured VIP with higher thermal conductivity.

4 CONCLUSIONS

Experimental work has been carried out on a test module consisting of four fields. One reference field representing a timber frame wall built according to regulations from the 1970s in Norway and three fields represent different ways of improving the thermal insulation of the reference field. During this work, a new sensor for measuring surface condensation called the wetness sensor was introduced.

The results of the experiment show that this method of retrofitting may be acceptable with respect to condensation risk in certain structures within limited climate zones, humidity classes, and building envelopes.

5 ACKNOWLEDGEMENTS

This work has been supported by the Research Council of Norway and several partners through the SINTEF/NTNU research project "*Robust Envelope Construction Details for Buildings of the 21st Century*" (ROBUST) and "*The Research Centre on Zero Emission Buildings*" (ZEB). Franco Blöchliger from Metallplan and the manufacturer Porextherm is acknowledged for supplying the vacuum insulation panel test samples.

REFERENCES

- R. Baetens, B. P. Jelle, J. V. Thue, M. J. Tenpierik, S. Grynning, S. Uvsløkk and A. Gustavsen, "Vacuum Insulation Panels for Building Applications: A Review and Beyond", *Energy and Buildings*, **42**, 147-172, 2010.
- A. Binz, A. Moosmann, G. Steinke, U. Schonhardt, F. Fregnan, H. Simmler, S. Brunner, K. Ghazi, R. Bundi, U. Heinemann, H. Schwab, J. M. Cauberg, M. J. Tenpierik, G. Johannesson, T. Thorsell, M. Erb, B. Nussbaumer, "Vacuum Insulation in the Building Sector. Systems and Applications (Subtask B)", Final report for the IEA/ECBCS Annex 39 HiPTI-project, 2005.
- Building regulations, "kap. 54 –Varmeisolering og tetthet", (Norwegian building regulations of 1969, chapter 54 –Thermal insulation and air tightness), 1969.
- ISO 13788, Hygrothermal performance of building components and building elements - Internal surface temperature to avoid critical surface humidity and interstitial condensation - Calculation methods, NS-EN ISO 13788:2001, 2001.
- Porextherm, "Vacupor NT – B2, data sheet", http://www.porextherm.com/web/pdfdownload.htm?ID=255&doctype=PDF_EN&lang=en&externeswindow=2&ts=1270722658 (Received 08.04.2010), 2009.
- SINTEF 523.002, SINTEF Building Research Design Guides no. 523.002, "Yttervegger over terreng. Egenskaper og konstruksjonsprinsipper. Krav og anbefalinger (Properties and construction principles of building envelopes above ground, requirements and recommendations.)", SINTEF Building and Infrastructure, Norway, 2008.
- Statistics Norway, "Boliger, etter bygningstype og byggår (K)", (Buildings, ranged by type of building and year of construction), Table 06266, 2009.
- TEK, §8-2, Energibruk (energikrav revidert i 2007), (Building regulations of 1997 (energy demands corrected in 2007), §8-2, Energy), 1997.
- E. Wegger, B. P. Jelle, E. Sveipe, S. Grynning, A. Gustavsen, R. Baetens, J. V. Thue, "Ageing Effects on Thermal Properties and Service Life of Vacuum Insulation Panels", Submitted for publication in *Journal of Building Physics*, 2009.

Utilisation of Geothermal Heat Pumps within Permeable Pavements for Sustainable Energy and Water Practices.

Kiran Tota-Maharaj^{a*} (k.tota-maharaj@ed.ac.uk),
Miklas Scholz^a (m.scholz@ed.ac.uk.)
Stephen J. Coupe^b (Stephen.Coupe@Formpave.co.uk)

^a*Institute for Infrastructure and Environment, School of Engineering, University of Edinburgh, William Rankine Building, The King's Buildings, Edinburgh, UK. EH9 3JL*

^b*Hanson Formpave Tufthorn Avenue Coleford Gloucestershire GL16 8PR*

ABSTRACT

Global warming and climate change is a reality faces the world today and as a result increases the use of sustainable practices for both energy and water minimising CO₂ emissions. Geothermal heat pumps (GHPs) are an attractive proposition for renewable energy worldwide as it uses energy naturally stored in the earth. The Earth is a very resourceful form of energy, using the natural solar energy collection and heat storage capabilities as an infinite heat source/heat sink at the base of permeable pavements can provide an excellent temperature gradient for which the GHP's harnesses. Two experimental rigs were setup up at The University of Edinburgh for a combined permeable pavement and GHP system. At the base of a pavement structure (approximately 1 meter) below the ground's surface, temperatures are constant of 10°C in the U.K all year round. The GHP performance efficiency was analysed by the coefficient of performance (COP) in a heating cycle and the energy efficiency ratio (EER) in a cooling cycle. The Mean COP and EER for both systems averaged between 2-4.5 and 3-5 respectively. The combined GHP and pavement structure operated at an optimum efficiency for both heating and cooling cycles and has shown to be unaffected by higher summer or lower winter temperatures. This hybrid system is an attractive renewable energy technology and has additional environmental benefits with regards to urban runoff reuse and recycling for the production domestic hot water.

Keywords: earth energy systems, permeable pavements, pervious pavements, sustainable urban drainage (SUDS), thermo-geologic efficiency.

1. Introduction

The concept of deriving beneficial uses from treated urban runoff coupled with increasing pressures on energy resources has prompted the emergence of a hybrid stormwater reclamation, treatment and reuse system in addition to renewable energy applications of ground-source heating and cooling. Advances in the effectiveness and reliability of permeable pavements as a stormwater treatment technology has improved not only the capacity by the quality of reclaimed urban runoff that can be utilized as a supplemental water source in addition to meeting water quality protection and pollution abatement practices (Tota-Maharaj and Scholz 2009).

The rapid growth of urbanisation has led to increased areas of impermeable surfaces, which, in times of heavy rainfall, results in increased pressure on existing drainage systems (Scholz 2006). When drainage system exceeds its design capacity, the surplus runoff must then be diverted to local watercourses without treatment (Butler and Davies, 2004). Pollutants such as heavy metals, hydrocarbons and other suspended solids are then washed into possible drinking water sources (Tota-Maharaj and Scholz, 2009). Energy consumption and the source of our energy has also become a major issue in recent years. With the threat of impending commercial carbon tax many companies have been searching for ways to reduce their energy consumption. One tried and tested method is Geothermal Heat Pumps (GHP) also known as earth energy systems harness the earth's heat to produce energy in a highly efficient manner. GSHP can be used for heating or cooling and have a coefficient of performance (COP) of approximately 3, this means output energy is 3 times greater than input. Geothermal heat pumps provide an energy efficient method of retrieving heat from the ground (Tota-Maharaj *et al.*, 2009). It utilises this renewable energy by transferring the heat in the ground to the areas it is required using water in pipes buried in the ground. The system can also be reversed to provide cooling during the warmer summer months.

At the University of Edinburgh an experiment, sponsored by Hanson Formpave Ltd., was undertaken to investigate combining both Geothermal Heat Pumps (GHP's) and Permeable Pavement Systems (PPS) for simultaneously stormwater treatment and reused whilst using the heat transfer at the base for residential, commercial or even industrial heating and cooling applications. The GHP can be used to provide heating to the sub-base of the pavement in winter and cooling to it in summer. Combined GHP and PPS does not alter the treatment efficacy of pervious pavements (Grabowiecki, 2010). Scholz and Grabowiecki (2009) found that the regulated yearly temperatures do not encourage pathogenic microbial growth for the combined systems and does not reduce how well the pavement treats runoff.

1.1 Urban Runoff Recycling and Flood Risk Management with Permeable Pavements

The destruction of flooding which occurred in the summer of 2007 in the UK resulted in over £3.2 billion in infrastructural damages. This stresses on the urgency for the applications and rapid installations of sustainable urban drainage systems (SUDS) techniques such as permeable (pervious) pavements. SUDS like pervious pavements combat surface water flooding and reduces the requirement for treatment (Butler and Davies, 2004). Permeable pavements are capable of infiltrating almost 50% of the total rainfall that falls on their surface during that period of rain. This is likely to increase as the duration of rainfall increases (Butler and Davies, 2004). PPS also provide a large area of infiltration with a hard surface suitable for areas such as car-parks, driveways, pedestrianised shopping streets and other moderately trafficked areas (Scholz and Grabowiecki, 2007).

A typical pavement consists of a permeable concrete paving layer, bedding layer, upper base and sub-base. A geotextile layer is placed between the bedding layer and the base to prevent the fine sand in the bedding layer from moving down into the aggregate below which would create air pockets in the bedding layer and, thus, resulting in an unstable surface. The geotextile also encourages microbial activity in this area, which treats the runoff (Tota-Maharaj and Scholz, 2009). The bedding layer is generally made up of fine sand suitable for trapping and removing contaminants from the runoff. The aggregate in the base and sub-base should be specified so that the pavement is capable of draining the storm-water rapidly, while also providing sufficient storage of the runoff so as to avoid localised flooding. It is also important that the pavement is capable of carrying the light traffic loads to which it will be

exposed (Tota-Maharaj and Scholz, 2009). An impermeable membrane can be introduced to the base and sides of the pavement would act as a reservoir to retain the infiltrated runoff for further treatment or reuse.

1.2 Geothermal Renewable Energy Solutions with Ground-Source Heat Exchange

Geothermal Heat pumps (GHPs) are an attractive proposition for renewable energy. They use energy naturally stored in the earth and are an energy-efficient alternative to fossil fuel boilers. A very efficient source of energy for water source heat pump systems is the Earth itself; using the Earth's natural solar collection and heat storage capabilities as an infinite heat source/heat sink (Banks, 2008). Below 3m, the ground's temperature is a constant 10°C all year round and these relatively constant, dependable temperatures can be harnessed using ground source heat pumps. The constant ground temperatures allow the heat pump to operate at optimum efficiency in both heating and cooling, unaffected by high summer or low winter temperatures. Heat is extracted or rejected into the ground using water, which is pumped through a network of plastic pipes. They make use of renewable energy stored in the ground, making it one of the most energy efficient methods of producing heat energy (Omer, 2006). GHP's can transfer the heat stored in the Earth into a building during the winter, and transfer heat out of the building during the summer (Omer, 2006). Rather than creating heat through combustion, they simply transfer heat from one place to another. The system relies on the fact that, at a certain depth, the Earth has a relatively constant temperature which is warmer than the air temperature in winter (heat source) and cooler than the air in summer (heat sink). GHP's circulate a mixture of water and anti-freeze around a ground loop which can be buried in residential gardens. As the liquid travels around the loop it absorbs heat from the surrounding ground, which is then used to heat the building during winter (Banks, 2008). In summer, the system is reversed to transfer heat out of the building, where it uses the cooler ground as a heat sink (Omer, 2006).

They use between 40% and 80% less fossil fuel energy than conventional heating systems and give the user control of supply and much more control of the price as seen in Figures 1(a) and 1(b) respectively. GHPs are receiving increasing interest because of its potential to reduce primary energy consumption, reduce emissions of greenhouse gases and thus reduce the effects of climate change (Figure 1(a), and Figure 1 (b)). GHP's are environmentally friendly tools that provide clean, efficient, energy saving heating and cooling all year round. They use less energy than conventional heating and cooling systems, which helps to conserve our natural resources. GHP's, while being quiet in operation and pollution free it is completely covered underground or within the building and does not mar the surrounding landscape.

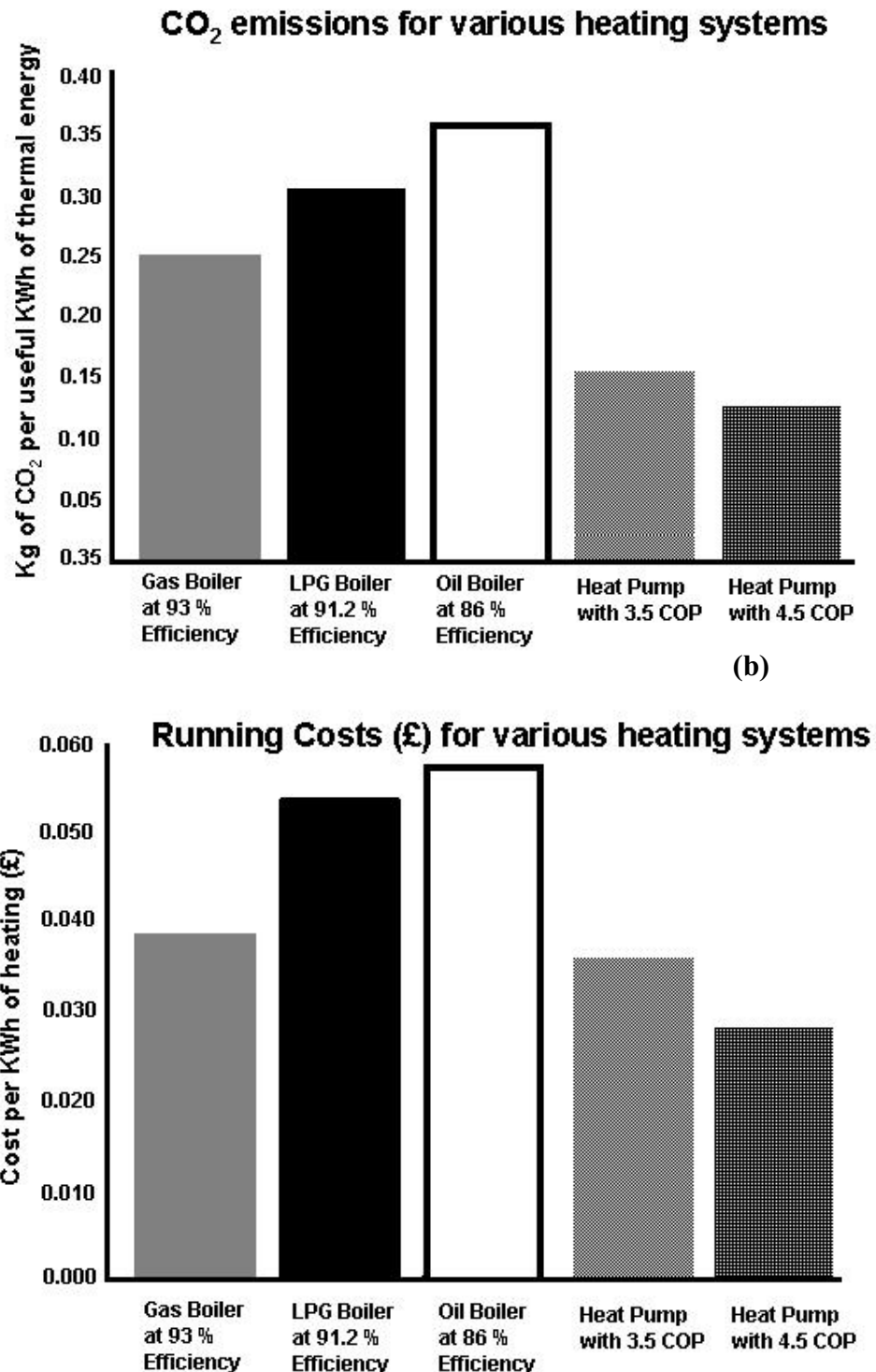


Figure 1: Comparison of Geothermal Heat Pumps to conventional heating systems for (a) CO₂ emissions, and (b) Financial cost for systems

1.2.1 The Efficiency of Geothermal Heat Pumps

Geothermal heat pumps sources of environmental energy are the ground or mediums thermally coupled to the ground, in our case the sub-base of a permeable pavement system. As the heat extracts heat energy flux form the water beneath the pavement, its temperature will drop. There is a theoretical limit of the efficiency of a geothermal heat pump. Ideally, a

geothermal heat pumps works on the reverse principals of an ideal heat engine. Assuming that energy losses due to acoustic noises is negligible and that all extracted heat is efficiently transferred to a point of use, the efficiency η of the GHP can be defined as the ratio of heat delivered (H) at elevated temperature (θ_1) to the work performed done (W). Therefore by using an idealised Carnot cycle, (Banks, 2008):

$$\eta_{MAX} = H / W = \theta_1 / (\theta_1 - \theta_2) \quad (1)$$

Where θ_2 is the lower temperature which is usually significantly below the environmental source temperature in order to ensure a kinetically rapid transfer of heat. The efficiency of the GHP is usually referred to as its Coefficient of Performance (COP) in a heating cycle, where (Banks, 2008):

$$COP_{Heating} = H / W = \theta_1 / (\theta_1 - \theta_2) \quad (2)$$

The GHP can be switched into reverse so that it can extract heat from the inside of a building and reject it to the ground or to ground-coupled medium such as the water beneath a permeable pavement system. The water in the saturated zone acquires heat from the GHP and its temperature increases a few degrees °C rather than decreases as in the heating mode. The COP in a cooling cycle is also referred to as the Energy Efficiency Ratio (EER) and is computed by (Banks, 2008):

$$EER[COP_{Cooling}] = C / W = \theta_2 / (\theta_1 - \theta_2) \quad (3)$$

2. Objectives

The main objectives of the research are to evaluate the effects of pollutant removal efficiency and evaluate the thermogeologic performance of geothermal heat pumps integrated within permeable pavements in terms of the Coefficient of Performance (COP) in a heating cycle and the Energy Efficiency Ration (EER) in a cooling cycle.

3. Experimental Methodology

The experiment was setup at the King's Building Campus, University of Edinburgh, Scotland. The integration of both systems included a tanked experimental rig constructed of permeable pavement blocks, a geotextile layer, an upper sub-base consisting of pea gravel and stone, a lower sub-base zone, containing crush rocks and gravel and finally the saturated zone where the filtered water was stored in addition to providing the heat flux system for the geothermal heating cooling coils. The lower sub-base was 500mm in lengths and the aggregate size used was determined by the manufacturer (Hanson Formpave, 2009). The aggregate used in the lower sub-base was a crushed rock/gravel of sizes ranging from 10-63mm in diameter. The Upper sub-base was 100mm in length and was composed of aggregate (stone) with sizes ranging from 5-20mm in diameter. GHP simulation was achieved by installing reinforced 5-mm polypropylene tubes placed in the lower sub-base. Seven to nine loops were folded within (total length of 10m). Both ends of each tube were located in a plastic water vessel. One end was connected to the pump and the other was used as an orifice for discharges. This arrangement provided closed circulation of water (Scholz and Grabowiecki, 2008) and achieved higher temperatures ($>20^{\circ}\text{C}$) in a heating cycle and cooler temperatures ($<8^{\circ}\text{C}$) in a

cooling mode. The heating-cooling coils were completely submerged by the filtered stormwater for maximum possible heat transfer. Just above the upper sub-base, an inbitex geotextile membrane was installed (2mm thick). Inbitex geotextile is a porous layer composed of polypropylene and polyethylene fibers. The fibers provide an ideal surface on which a bio-film can develop (Coupe *et al.*, 2008). A composite impermeable membrane can be added to the geotextile layer to form a geocomposite layer. The geotextile layer is pivotal to the performance of the system as it boost microbial activity (Coupe *et al.*, 2009). Above the geotextile layer is a base layer consisting of clean stone 5mm in diameter and 50mm in depth and directly above this the permeable pavements supplied from Hanson Formpave were fixed (80 mm in depth). The gaps between the blocks were filled with 3mm clean pea-gravel and aggregate.

4. Data Analysis

Four major water quality parameters were assessed including (i) Biochemical Oxygen Demand (BOD), (ii) Chemical Oxygen Demand (COD), (iii) turbidity and (iv) Suspended solids to test the permeable pavement systems environmental and water quality performance. Biological Oxygen Demand (BOD) is a measure of the oxygen used by microorganisms in decomposing organic matter. If there is large quantities of organic waste in stormwater, there will be several bacteria present degrading this. Chemical oxygen demand (COD) is a measure of the capacity of water to consume oxygen during the degradation or decomposition of organic matter and the oxidation process of inorganic chemicals such as ammonia and nitrite. COD measurements assay the oxygen-demanding strength of wastewater and are empirically related to BOD. Turbidity is a unit of measurement quantifying the degree to which light travelling through a water column is scattered by the suspended organic (including algae) and inorganic particles. The scattering of light increases with a greater suspended load. Turbidity is measured in Nephelometric Turbidity Units (NTU). Suspended solids refers to minute solid particles which remain in suspensions as a colloid in water. Suspended solids removal is essential as pollutants and pathogenic organisms are carried on the surface of particles in water. The measurements and analysis for these water parameters followed the American standards for the examination of water and wastewater quality (APHA 1998). The thermodynamic efficiencies were evaluated by the temperature variations throughout from the higher reservoir to the saturated zone at the base of the pavement system (Tota-Maharaj *et al.*, 2009).

5. Results and Discussion

Figure 2 (a) and (b) illustrates the Coefficient of Performance (COP) for the heating mode, and the Energy Efficiency Ratio (EER) for the cooling mode for rig 1, combined permeable pavements and geothermal heating cooling and rig 2 (without geotextile membrane). The rigs were analysed for a two (2) year period from March 2008-March 2010. During the heating cycle temperatures ranged between 20-27 °C whilst the cooling cycle temperatures dropped from 4-8 °C. The both rigs were compared for its thermodynamic performance in addition to its water quality treatment abilities. Figure 3 illustrates that the presence of the geotextile membrane results in an increased efficiency for the removal of BOD, COD, turbidity and suspended solids. The BOD, COD, suspended solids and turbidity removal rates ranged from

83% to 99% for both rigs respectively. However, rig 2 (without geotextiles) still performed well for organic removal. The biodegradation process with permeable pavement systems have shown to be more effective than rigs without (Tota-Maharaj and Scholz, 2009).

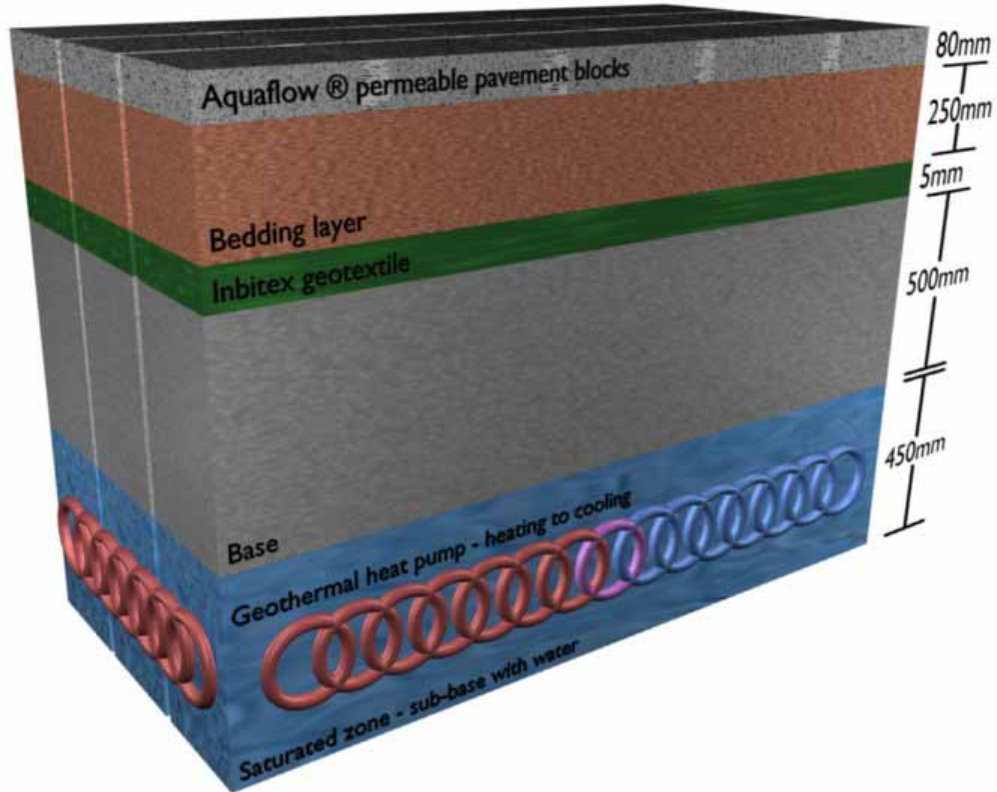


Figure 2: Experimental system for Geothermal Heat Pumps integrated with Permeable Pavements

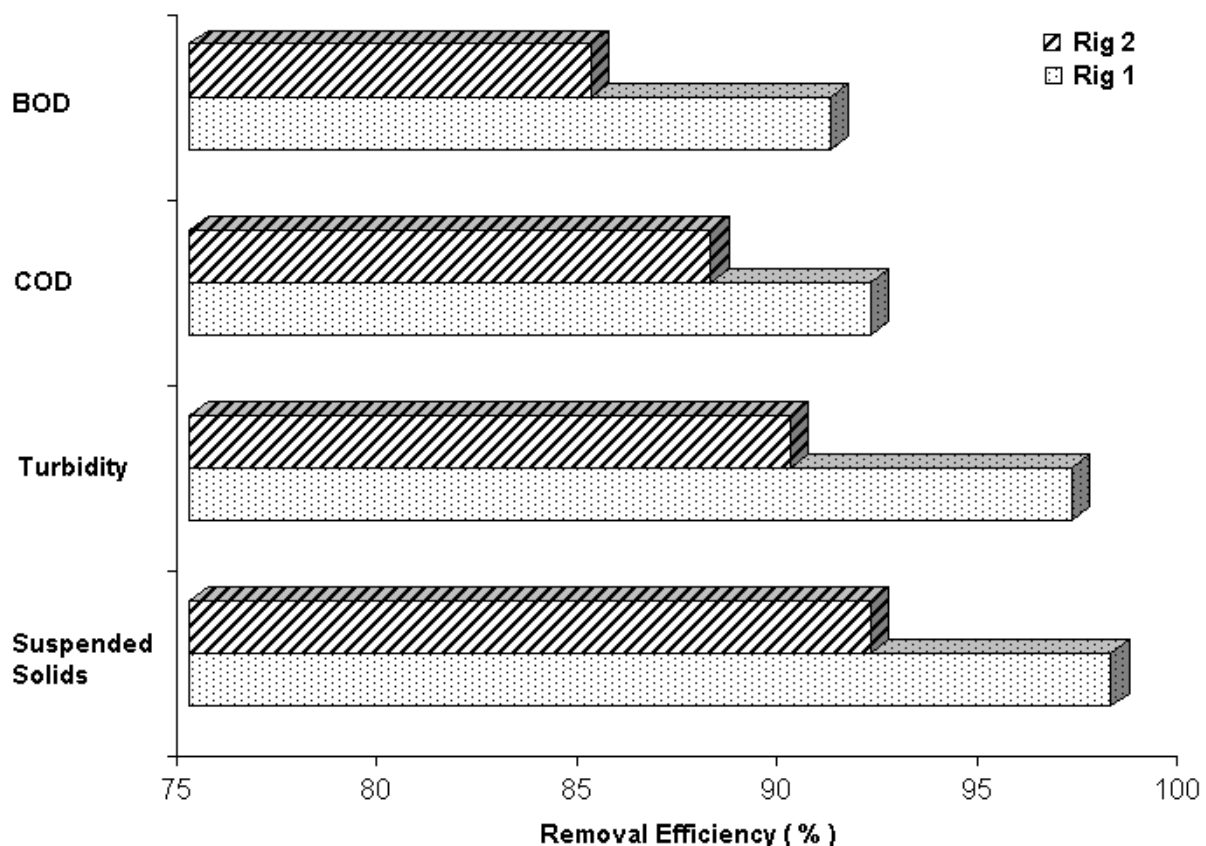


Figure 3: Mean removal efficiency for BOD, COD, Turbidity and suspended solids for Rig 1 and Rig 2(without geotextile membrane) from March 2008-March 2010.

In addition, it can be noted that for both the computed thermo-geologic efficiencies, the presence of the geotextile rig does not affect the Coefficient of Performance (COP) or the Energy Efficiency Ratio (EER). The EER varied between 3.1-4.8 for rig 1 and 2.-4.9 for rig 2 respectively. Similar performance occurred for the heating cycle with COP values ranging from 2.4-4.6 for rig 1 and 3.2-4.9 for rig 2 respectively. This illustrates as shown in Figure 1, for every 1 unit of work in a heating or cooling cycle the GHP gives back a range between 2.5-4.8 units of work. The integration of GHPs does not alter the removal efficiencies for stormwater treatment. Figure 3 shows the mean removal efficiency

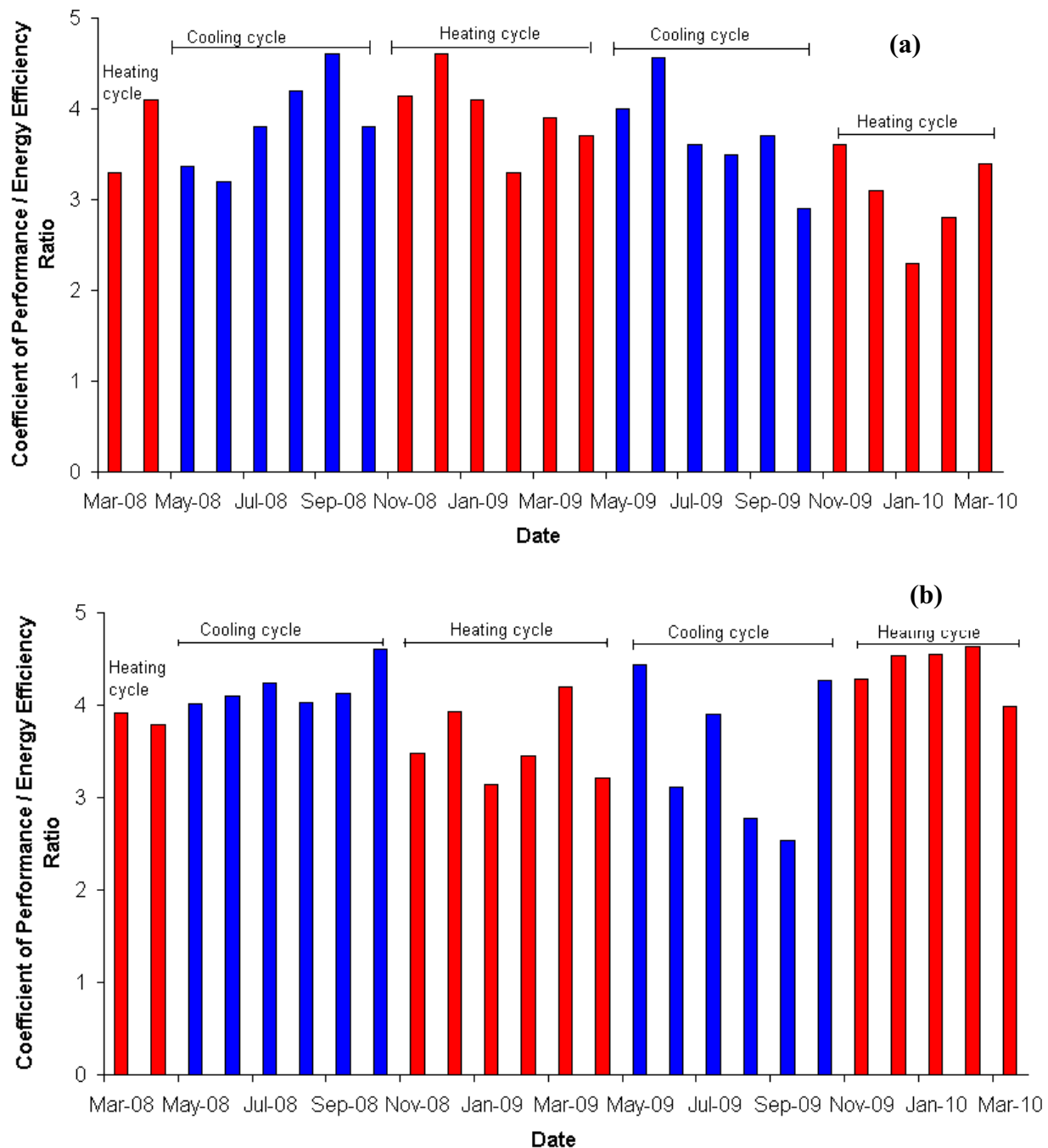


Figure 4: Coefficient of Performance (COP) for the heating mode, Energy Efficiency Ratio (EER) for the cooling mode for rig 1 (a) with geotextile and Rig 2 (b) without geotextile membrane, March 2008–March 2010.

6. Conclusion

Permeable pavements are excellent urban runoff treatment systems for the removal of contaminants when applied for grey-water recycling and reuse purposes. Permeable

pavements contribute to a positive effect on urban runoff water quality by providing mechanism that encourages filtration, sedimentation, adsorption, biodegradation and storage. The base of a permeable pavement is well suited for solar gain and energy transfers when integrated with geothermal heat pumps. The combined ground-source heat pump and permeable pavement system can be applied as an alternative heating-cooling technology when compared to conventional ones. In addition, as a substitute for traditional paving materials such as impermeable asphalt or concrete where appropriate such as pathways, pedestrian zones, driveways and golf courses permeable pavements can be used. The presence of the geotextile layer does not affect the geothermal heat flux across the system when switched from either a cooling cycle or a heating mode but improves the removal efficiency of pollutants present in storm water. The GHP when combined with permeable pavements can efficiently provide heating, and space cooling applications to nearby residential buildings.

Acknowledgments

The authors would like to thank Hanson Formpave Ltd for providing funding and support. The authors are grateful to Dr. Piotr Grabowiecki from the Environment Agency UK for his insightful comments and support throughout the research.

REFERENCES

- APHA., 1998, *Standard methods for the examination of water and wastewater* 20th Edition Washington D.C., America Public Health Association, American Water Works Association, Water Pollution Control Federation.
- Banks, D., 2008, *An Introduction to Thermogeology Ground Source Heating and Cooling*, Blackwell Publishing Ltd, Oxford, UK, p 339.
- Butler, D and Davies J.W., 2004, *Urban Drainage* 2nd Edition, Spon Press, London, U.K, p 543.
- Coupe, J.S., O Nnadi, E. and Oyekemi, O., 2008, Water recycling using permeable paving as the source: biological water safety and the fate of introduced microbial contaminants, *11th International Conference on Urban Drainage*, Edinburgh, Scotland, UK, p. 1-10.
- Coupe, S. J., Tota-Maharaj, K., Scholz, M., & Grabowiecki, P. (2009). Water stored within permeable paving and the effect of ground source heat pump applications on water quality. *9th International Conference on Concrete Block Paving*. Buenos Aires, p. 1-10.
- Grabowiecki, P., 2010, *Combined Permeable Pavement and Ground Source Heat Pump Systems*, PhD Thesis, University of Edinburgh, Scotland U.K, p 333.
- Hanson Formpave., 2009, *Stormwater source control system, aquafloow permeable paving leaflet*, available online at: <http://www.heidelbergcement.com/uk/en/hanson/products/blcok> paving and suds [Accessed October 2009]
- Omer, A.M., 2008, Ground source heat pumps applications, *Renewable and Sustainable Energy Reviews*, vol. 12, no. 2: p 344–371.

Scholz, M., 2006, *Wetland Systems to Control Urban Runoff*, Elsevier, Amsterdam, Netherlands, 360 p.

Scholz, M., and Grabowiecki, P., 2007, Review of Permeable Pavement Systems. *Building and Environment* vol.42, no. 11:p 3830-3836.

Scholz, M., and Grabowiecki, P., 2009, Combined permeable pavement and ground source heat pump systems to treat urban runoff. *Journal of Chemical Technology and Biotechnology*, vol. 84, no 3: p 405-413.

Tota-Maharaj, K., and Scholz, M., 2009, Permeable (pervious) pavements and geothermal heat pumps: addressing sustainable urban stormwater management and renewable energy. *International Journal of Green Economics*, vol. 3 no 3/4 :p 447-461.

Tota-Maharaj, K., Grabowiecki, P., and Scholz, M. (2009). Energy and temperature performance analysis of geothermal (ground source) heat pumps integrated with permeable pavement systems for urban runoff reuse. *International Journal of Sustainable Engineering*, vol. 2 no 3 : p 201-213.

Accelerated Ageing of Vacuum Insulation Panels (VIPs)

Erlend Wegger^a, Bjørn Petter Jelle^{ab}, Erland Sveipe^a,
Steinar Grynning^b, Arild Gustavsen^c, Jan Vincent Thue^a

^a Department of Civil and Transport Engineering,
Norwegian University of Science and Technology (NTNU), Trondheim, Norway

^b Department of Materials and Structures,
SINTEF Building and Infrastructure, Trondheim, Norway

^c Department of Architectural Design, History and Technology,
Norwegian University of Science and Technology (NTNU), Trondheim, Norway

ABSTRACT

Vacuum insulation panels (VIP) is a high performance thermal insulation material solution with thermal conductivity values reaching as low as 4.0 mW/(mK). With time the thermal performance of the VIPs will degrade as moisture and gas permeate through the barrier envelope of the panels. To better evaluate these ageing effects, accelerated ageing experiments are needed. VIPs consist of a porous core of pyrogenic silica (SiO_2) and a gas and vapour tight envelope. The external factors that are found to contribute most to ageing of VIPs are temperature, moisture and pressure.

Several experiments have been initiated to evaluate the acceleration effects by the application of severe temperature, moisture and pressure conditions, including:

1. Thermal ageing at 80°C for 180 days according to CUAP 12.01/30
2. Exposure to cyclic climate in a vertical climate simulator according to NT Build 495. One VIP sample is fully exposed in the simulator and one is placed in a wooden frame structure.
3. Exposure to high vapour pressure by storage at 70°C and 90-100 % RH for 90 days.

The increases in thermal conductivity during ageing were relatively small compared to the initial thermal conductivity of the VIPs, which is in agreement with the theoretical predictions. The temperature and moisture experiment seemed to achieve a rather large acceleration effect.

In addition, the thermally aged VIP and the exposed VIP in the climate simulator show physical alterations. E.g. swelling, curving and delamination of the outer fire protection layer are observed.

Keywords: Vacuum Insulation Panel, VIP, accelerated ageing, thermal insulation

1. INTRODUCTION

For several decades, thermal insulation has been the preferred way to improve buildings energy efficiency, and the thermal insulation requirements have increased steadily. In Norway the requirement of a wall construction in 2010 is an U-value of $0.18 \text{ W}/(\text{m}^2\text{K})$, which is equivalent to 250 mm mineral wool insulation. Future requirements in order to obtain zero emission standards may require wall thicknesses up to 500 mm filled with mineral wool. Obviously, such wall thicknesses and amounts of insulation are a challenge both for architects and engineers in building aesthetically, economically and in accordance with sound building physical principles.

Vacuum insulation panels (VIP) might offer a solution to this problem. VIPs consist of a solid, porous core which is sealed with an air- and watertight laminate maintaining a vacuum in the core. VIPs have thermal conductivities that are 5-10 times lower than for traditional thermal insulation. It will thus be possible to reduce the thickness of the building walls, and at the same time retain or even increase the thermal resistance.

As an innovative material, special concern is given to the performance of VIPs over time. The thermal performance will decrease over time, as air gases and water vapour penetrate through the barrier envelope. To evaluate the performance and ageing effects of VIPs, accelerated ageing experiments are vital for such investigations to be carried out within a limited timeframe. As no standardized methods exist at this time, a variety of ageing experiments are tested to evaluate their suitability as accelerated ageing methods for VIPs.

The ageing of VIPs depend both on the core material of the panels, and on the materials used for envelope barrier. The most common core material for VIPs are pressed fumed silica or pyrogenic silica (SiO_2), which is a fine powdered, highly porous, silica based material with low solid state conductivity. This low solid state conductivity combined with low gas conduction in the vacuum pores lead to the high thermal performance of VIPs.

As envelope barriers the most common materials are so called multilayer (MF) foils, which consist of several layers of aluminum-metalized polyethylene terephthalate (PET) or polypropylene (PP) sheets sealed on the inside with a polyethylene (PE) layer. This provides sufficient gas and vapour tightness and a minimal thermal bridge at the panel edges. A variety of foil configurations are shown in Figure 1.

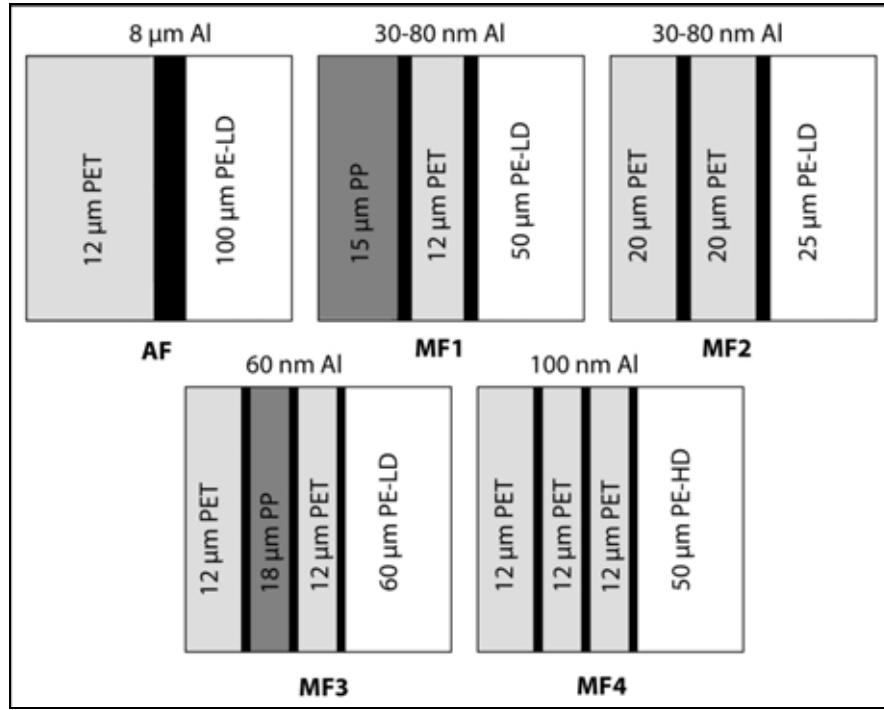


Figure 1 Cross-sections of various envelope solutions for application in VIPs. The drawing are not to scale.

2. BACKGROUND

The ageing of VIPs is dependent upon the gas and vapour diffusion through the envelope barrier into the core. This will only be summarized briefly here. A comprehensive review of most VIP aspects can be found in Baetens *et al.* (2010).

The total center-of-panel thermal conductivity of VIPs (λ_{tot}) is considered as a sum of the contributions from solid conductivity (λ_{cd}), gaseous conductivity (λ_g), radiative thermal conductivity (λ_r), and conduction due to air and moisture convection in the pores (λ_{cv}). In addition a coupling term (λ_{coup}) is added to account for the interaction between the gas molecules and the pore walls (Brodt 1995).

$$\lambda_{tot} = \lambda_r + \lambda_{cd} + \lambda_g + \lambda_{cv} + \lambda_{coup} \quad (1)$$

As gas and water vapour penetrate the barrier foil, the gas pressure and water content of the core increases, leading to an increased gaseous and solid thermal conductivity. The increase in thermal conductivity over time may be calculated as (Tenpierik 2010):

$$\begin{aligned} \Delta\lambda_c &= \frac{\partial\lambda_c}{\partial p_g} \Delta p_g + \frac{\partial\lambda_c}{\partial p_{wv}} \Delta p_{wv} + \frac{\partial\lambda_c}{\partial u} \Delta u \\ &\approx \frac{\partial\lambda_c}{\partial p_g} P_{g;e} (1 - e^{-(t-t_{get})/\tau_g}) + \frac{\partial\lambda_c}{\partial p_{wv}} P_{wv;e} (1 - e^{-(t-t_{des})/\tau_w}) + \frac{\partial\lambda_c}{\partial u} \frac{du}{d\varphi} \varphi_e (1 - e^{-(t-t_{des})/\tau_w}) \end{aligned} \quad (2)$$

where

p_g = Pore gas pressure (Pa)

$p_{g,e}$ = Atmospheric gas pressure (Pa)

$p_{wv,e}$ = Partial water vapour pressure outside the VIP (Pa)

φ_e = Relative humidity of the air outside the VIP (-)

u = Water content of the core material (-)

t = Time (days)

t_{get} and t_{des} = Time shifts due to getters and desiccants (s)

τ_g and τ_w are time constants according to:

$$\tau_g = \frac{\varepsilon V}{GTR(T, \varphi)} \cdot \frac{T_0}{p_o T} \quad (3)$$

$$\tau_w = \frac{\rho_{dry} V}{WVTR(T, \varphi)} \cdot \frac{1}{p_{sat}(T)} \frac{du}{d\varphi} \quad (4)$$

GTR and WVTR are the empirically found *gas transmission rate* and *water vapour transmission rate* for VIPs, respectively. Graphical plots for thermal conductivity for constant climatic conditions up to 100 years can be found in Baetens *et al.* (2010) and Wegger *et al.* (2010).

To be able to accelerate the ageing of VIPs, it is necessary to increase the permeation of water vapour and air gases through the envelope barrier. In Wegger *et al.* (2010) it is found that temperature, moisture and pressure are the external factors contributing most to ageing of VIPs. These external factors are all elements in the thermal conductivity formula in eq. 1.

3. EXPERIMENTAL

Three different ageing methods have been applied in this study, based on existing methods and knowledge on ageing. The ageing procedures are described below.

The VIPs used in the experiments presented in this paper are of the type va-Q-vipB from the producer va-Q-tec (2009). Va-Q-vipB consists of a core of amorphous silicon dioxide and an inorganic opacifier. The panel is sealed with a high barrier film which is again covered on the exterior with a black fire protection fleece. The high barrier film consists of three layers of metalized polyethylene terephthalate (PET) with polyethylene (PE) as a sealing layer on the inside. Total thickness is approximately 100 µm. The panel dimensions are 100 cm x 60 cm x 2 cm. One VIP sample is used for each procedure.

To evaluate the change in thermal conductivity of VIPs, a heat flow meter apparatus (HFM) has been used. All measurements are performed in accordance with current versions of ISO 8301 and NS-EN 12667.

3.1 Temperature Ageing According to CUAP 12.01/30

One method for testing ageing effects on VIPs is suggested in CUAP 12.01/30. The test is based on severe temperature conditions over an extended period of time. The accelerated temperature ageing is supposed to cover a natural ageing time span of 25 years.

3.1.1. Scope

The main scope of the experiment is to verify whether an ageing of 25 years can be achieved by application of this procedure. The procedure has been altered somewhat, to accommodate more measurements than originally specified.

3.1.2 Procedure

- Conditioning at $(23 \pm 2)^\circ\text{C}$ and $(50 \pm 5)\%$ RH for at least 72 hours.
- Determination of initial thermal conductivity
- Cycling in alternating climate (8 cycles), where one cycle consists of:
 - 8 hours at $(80 \pm 3)^\circ\text{C}$
 - 16 hours at $(-15 \pm 3)^\circ\text{C}$
- Determination of thermal conductivity
- Temperature ageing for 90 days at $(80 \pm 3)^\circ\text{C}$
- Determination of thermal conductivity
- Temperature ageing continued for another 90 days at $(80 \pm 3)^\circ\text{C}$
- Final determination of thermal conductivity

Additional measurements of thermal conductivity were conducted when considered required. Alternating climate was achieved by manually transferring the VIP between a heating cabinet and a freezer at the end of each period.

3.2 Cyclic Climate Ageing According to NT Build 495

The Nordtest Method NT Build 495 is a test method exposing materials in the vertical position to accelerated climate strains.

3.2.1. Scope

The scope of this experiment is to evaluate the resistance of VIPs to varying climate strains. This involves the integrity of the panels in addition to the thermal properties. By using two samples, one exposed and one protected by a timber-frame, the durability and robustness of exposed VIPs can be evaluated and compared to that of protected VIPs. The testing of the exposed VIP would especially be interesting for storage and handling of VIPs during the construction phase.

3.2.2 Procedure

The test rig consists of the following successive climate strains:

- UV-radiation ($\text{UVA} = 33 \text{ W/m}^2$, $\text{UVB} = 2.4 \text{ W/m}^2$) and IR-radiation giving a black panel temperature of $(63 \pm 5)^\circ\text{C}$
- Wetting with a spray of water
- Freezing at $-20 \pm 5^\circ\text{C}$
- Thawing at laboratory climate

The time interval in each of the climate strain positions is one hour. The setup of the test rig is shown in Figure 2.

The test consists of two different specimens. One is a VIP that is directly exposed to the climatic strains. The other specimen is a VIP built into a ventilated timber frame wall. Wall construction details are shown in Figure 3.

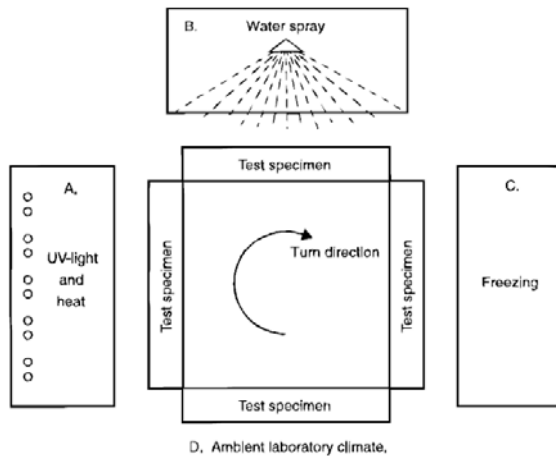


Figure 2 Test rig for accelerated climate exposure according to NT Build 495 (2000)

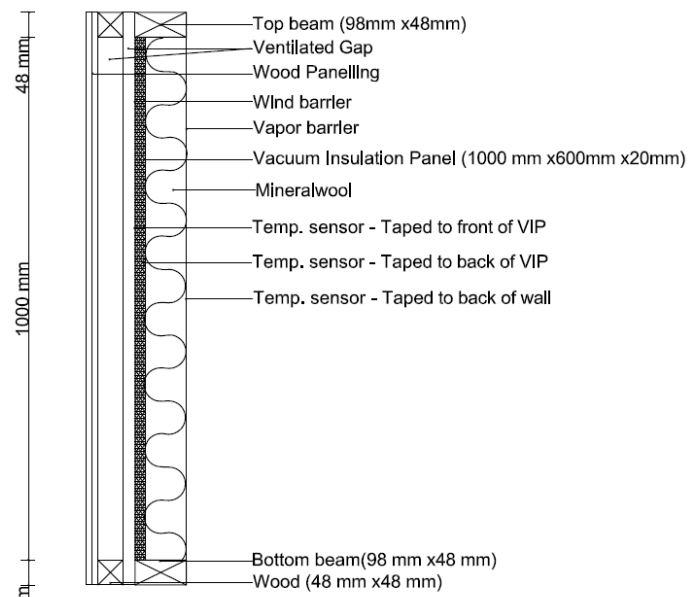


Figure 3 Construction detail for wall exposed to accelerated climate strains.

To be able to evaluate any change in the internal conditions after exposure, the initial VIP weight and thermal conductivity were determined.

3.3 Moisture and Temperature Ageing

To evaluate the effect of severe hygrothermal conditions on VIPs, a test is designed to expose a VIP to high temperature in combination with high moisture pressure.

3.3.1 Scope

The scope of the experiment is to evaluate which ageing effect that can be achieved by exposing a VIP to high relative humidity and high temperature simultaneously. Since saturation vapour pressure show an exponential increase with temperature, a very high external moisture pressure is possible when the temperature is increased.

3.3.2 Experimental Setup

In this preliminary experiment it is desired to maximize the moisture pressure within the specified temperature limits for the VIP. To facilitate this, the VIP is sealed inside a plastic envelope together with a water container. The whole envelope is then placed in a heating cabinet at 70°C, giving a RH of between 90 and 100%.

The following procedure has been employed in the testing:

- Conditioning at $(23 \pm 2)^\circ\text{C}$ and $(50 \pm 5)\%$ RH for at least 72 hours.
- Determination of initial thermal conductivity
- Storage in heating cabinet (with water container) for 30 days at 70°C
- Determination of thermal conductivity
- Storage in heating cabinet (with water container) for 30 days at 70°C
- Determination of thermal conductivity
- Storage in heating cabinet (with water container) for 30 days at 70°C
- Final determination of thermal conductivity

4. RESULTS AND DISCUSSIONS

4.1 Temperature Ageing According to CUAP 12.01/30

The initial thermal conductivity was measured to be $4.6 \pm 0.1 \text{ mW/(mK)}$. The panel was then subjected to freeze/thaw cycles. At the end of these cycles the outer fleece had begun to fray, and the laminate beneath were visible.

The VIP was then stored at 80°C in a heating cabinet. After less than a week, delamination of the outer fleece layer of the VIP was visible. Large areas of the fleece had loosened from the substrate, creating blisters of various shapes and sizes. These blisters became more pronounced over time, which is depicted in Figure 4.



Figure 4 Visible delamination of the fleece cover after exposure at 80°C for approximately 1 month.

When thermal conductivity measurements were performed after approximately 100 days in ageing conditions, it became evident that the panel had swelled approximately 2 mm. This corresponds to 5-10% increase in thickness for the panel. Thermal conductivity measurements for the temperature ageing are summarized in Figure 6 and 7.

4.2 Cyclic Climate Ageing According to NT Build 495

After less than a day in the vertical climate simulator, the outer fleece layer on the exposed panel began blistering from the substrate, similar to the panel in the heating cabinet. The

delamination did not, however, sustain, and only relatively small areas blistered. Another effect on the exposed panel was that it curved slightly towards the exposed side, as can be seen in Figure 5. For the protected VIP, no such effects was observed.

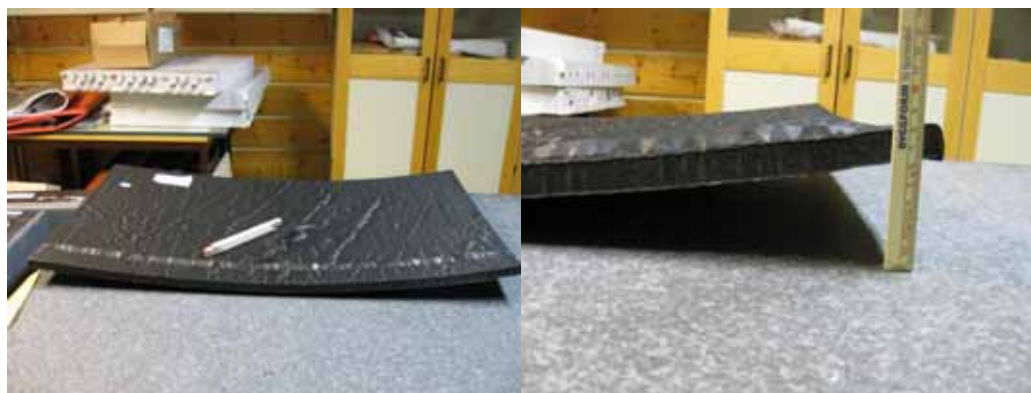


Figure 5 Uncovered panel after exposure to cyclic climate strains in vertical climate simulator for approximately one month. Some delamination of the fleece cover is visible. The panel had curved during exposure.

Thermal conductivity measurements for the cyclic climate ageing are summarized in Figure 6 and 7.

4.3 Moisture and Temperature Ageing

When the VIP was tested after 60 days in ageing conditions, its thermal conductivity had increased drastically to 17.9 mW/(mK) . This might be best explained by failure of the VIP due to some external source, such as mechanical damage. The experiment was then discontinued. Thermal conductivity measurements for the moisture and temperature ageing are summarized in Figure 6 and 7.

4.4 Thermal Conductivity for VIPs exposed to Ageing Experiments

Results from the thermal conductivity measurements are summarized below in Figure 6 and 7. Figure 6 show the changes of thermal conductivity for the various VIPs over time. The test periods vary somewhat. Figure 7 show the thermal resistance for all VIPs. Since some panels experienced physical changes like swelling, the thermal resistance might give a more appropriate measure of the acceleration effect of the various methods.

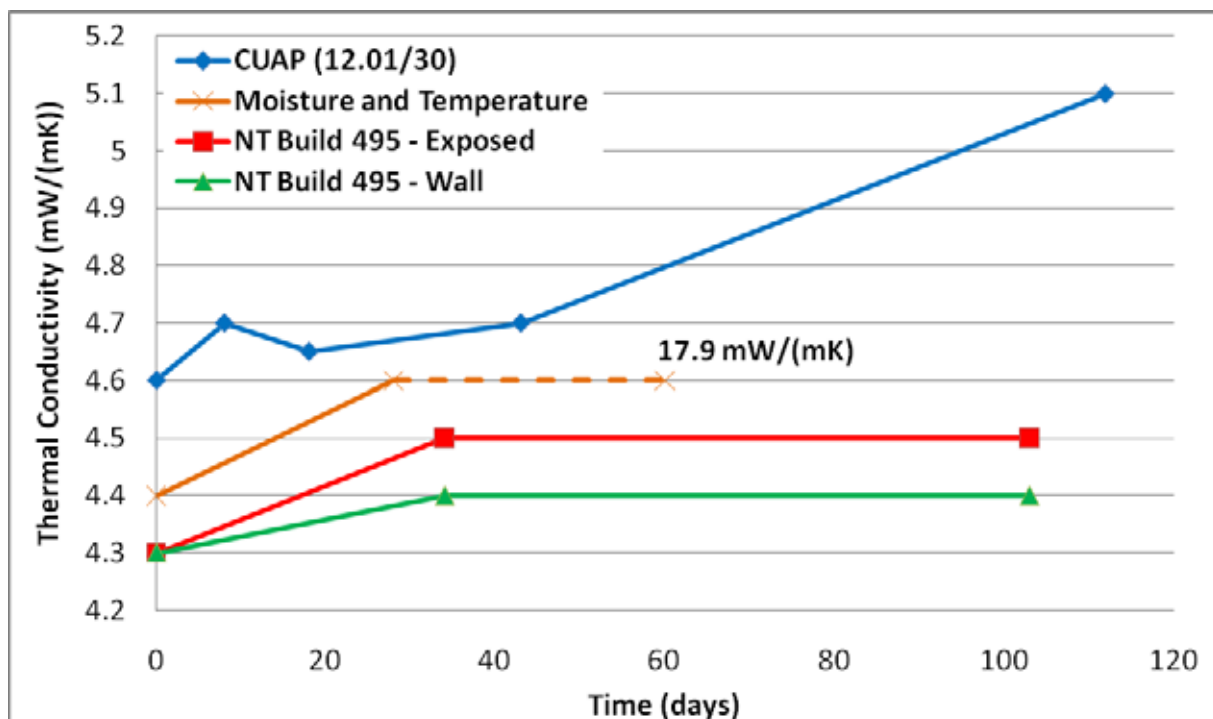


Figure 6 Thermal conductivity versus time for VIPs exposed to various acceleration procedures

Note that the initial non-aged thermal conductivity of the VIPs vary by 0.3 mW/(mK) which is approximately 7% of the total conductivity. Due to the relatively low rise in thermal conductivity for the VIPs exposed to ageing procedures, the variation in initial thermal conductivity might have as large or larger impact on thermal performance as the ageing effects. This variation also makes it necessary to confirm results with more extensive testing on several VIP samples.

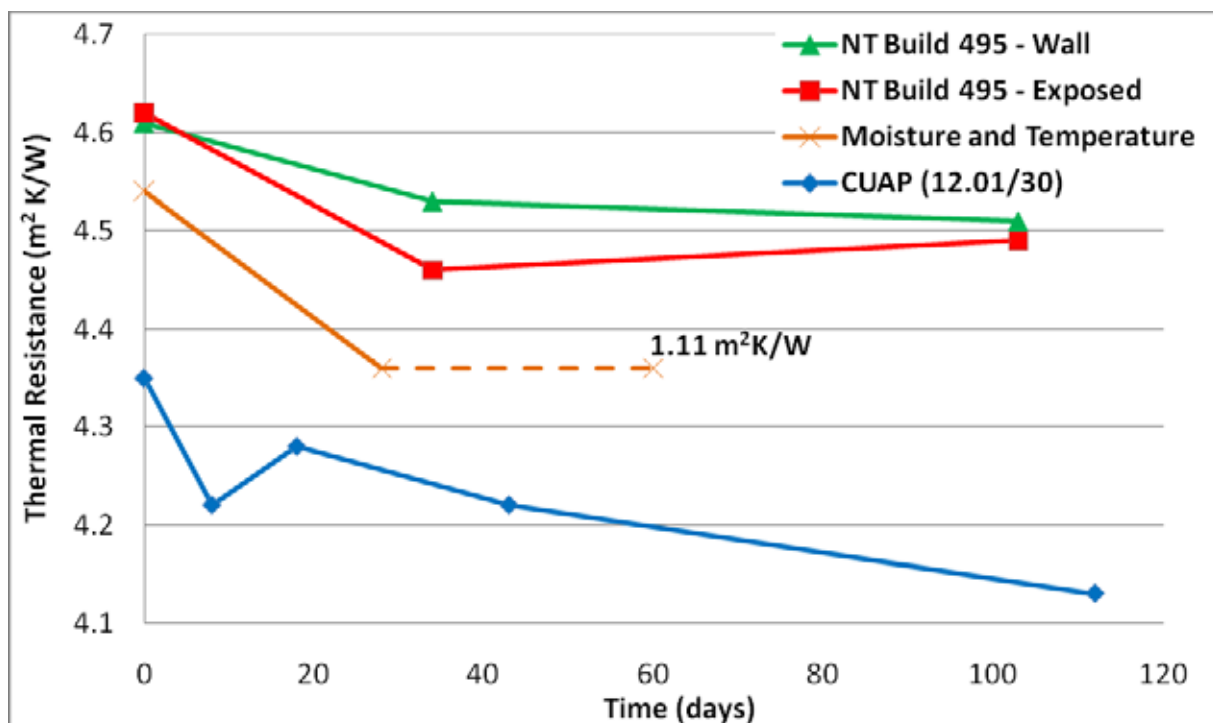


Figure 7 Thermal resistance versus time for VIPs exposed to various acceleration procedures

For all ageing procedures the changes in thermal conductivity and resistance are small, compared to the overall performance of VIPs. This shows that the VIPs have a relatively high robustness to severe climatic loads. This is in agreement with prediction curves for the ageing of VIPs under constant climatic conditions. For a VIP with MF2 foil and size 100 cm x 100 cm x 2 cm, the predicted thermal conductivity after 100 years is ≈ 8.5 mW/(mK). This represents a total increase of 4.5 mW/(m K), or less than 0.05 mW/(mK) each year. In other words, a relatively low increase in thermal conductivity should be expected if the predictions are correct.

One of the most interesting result of these experiments are the physical alterations experienced by the panel at 80°C in heating cabinet (CUAP 12.01/30), and the exposed panel in the vertical climate simulator. The swelling of the panel in the heating cabinet, approximately 10% of panel thickness, is most likely a result of physical changes in the panel core. Seemingly this has no significant effect on the thermal performance. It should also be noted that 80°C is the maximum upper limit of the temperature range specified by the producer for these panels, and will not normally be encountered during the application of VIPs in buildings. It might be experienced for shorter time interval though e.g. on roofs. The temperature is also higher than the temperatures usually applied for ageing of polymers and other plastic materials that might be similar to the VIP envelope. The curvature on the exposed panel in the climate simulator is relevant for interim storage or exposed condicions of VIPs at construction sites. Exposure of VIPs to extreme temperatures and UV-radiation on building sites should therefore be avoided.

Note that most of the physical changes of the VIPs in this study might be an effect of the severe climatic strains they are exposed to. Too much emphasis on these changes should therefore be avoided. However, for the design of future ageing experiments, it will be of interest to be aware of such changes occurring.

The temperature and moisture experiment showed potential to give the highest acceleration effect, but was discontinued when the VIP was punctured. The few results found prior to this are inconclusive as to the acceleration effect of the procedure. From theoretical relationships it seems likely that this method will provide at least as high acceleration effect as the CUAP method, as moisture permeates more easily through the envelope than air gases, and since moisture can potentially contribute greatly to the thermal conductivity. However, results from other studies suggest that such high moisture contents and temperatures will lead to failure of the VIP within 2 years (Brunner et al. 2008).

Of the acceleration methods conducted, only the protected VIP in the climate simulator is considered to receive realistic ageing conditions. Also the CUAP experiment is considered giving a realistic load, although the duration of testing might be discussed. Despite this, all procedures are considered important for the design of future ageing experiments.

5. CONCLUSIONS

Miscellaneous ways to perform accelerated climate ageing of vacuum insulation panels (VIP) have been investigated. The changes in thermal conductivity were relatively small compared to the initial thermal conductivity of the VIPs. This is in agreement with the theoretical predictions. The temperature and moisture experiment seemed to achieve a quite high acceleration effect. Evidence from literature suggests that the climatic loads in this test might be too severe to serve the purpose of accelerated ageing.

Some physical changes were observed on the VIPs. On the panels subjected to thermal ageing the outer fleece layer lifted from its substrate after less than a week, and after approximately 100 days the panel had swelled 10%. The exposed panel in the climate simulator experienced a similar effect as the thermally aged panel, with the protection fleece lifting from the substrate. In addition this panel curved permanently during exposure. Too much emphasis should not be given to this, as they might be an effect of the extreme climatic conditions.

ACKNOWLEDGEMENTS

This work has been supported by the Research Council of Norway and several partners through the SINTEF/NTNU research project "*Robust Envelope Construction Details for Buildings of the 21st Century*" (ROBUST) and "*The Research Centre on Zero Emission Buildings*" (ZEB). The company va-Q-tec, by Roland Caps, is acknowledged for supplying the vacuum insulation panel test samples. Ole Aunrønning (NTNU), Per Christian Moe (SINTEF) and Egil Rognvik (SINTEF) provided valuable help during various experimental tasks.

REFERENCES

- Baetens R., Jelle B.P., Thue J.V., Tenpierik M.J., Grynning S., Uvsløkk S., Gustavsen A., 2010, Vacuum Insulation Panels for Building Applications: A Review and Beyond, *Energy and Buildings*, vol. 42, p. 147-172, 2010
- Brodt K., 1995, *Thermal insulations: cfc-alternatives and vacuum insulation*, PhD thesis, Delft University of Technology, Delft, 1995.
- Brunner S., Tharian P.J., Simmler H., Ghazi Wakili K., 2008, Focused Ion Beam (FIB) Etching to Investigate Aluminum-coated Polymer Laminates Subjected to Heat and Moisture Loads, *Surface & Coatings Technology*, vol. 202, p.6054-6063, 2008
- CUAP 12.01/30, 2009, *Factory made vacuum insulation panels*
- Nordtest Method, NT Build 495, 2000, *Building Materials and Components in the Vertical Position: Exposure to Accelerated Climatic Strains*, Nordtest
<http://www.nordicinnovation.net/nordtestfiler/build495.pdf> (Downloaded: 07.12.2009)
- Tenpierik M., 2009, *Vacuum Insulation Panels Applied in Building Constructions*, PhD thesis, Technische Universiteit Delft, Delft, 2009
- Wegger E., Jelle B.P., Sveipe E., Grynning S., Baetens R., Thue J.V., 2010, Ageing Effects on Thermal Properties ans Service Life of Vacuum Insulation Panels, Submitted for publication in *Journal of Building Physics*, 2010
- Willems M.K., Schild K., Hellinger G., 2005, Numerical investigation on thermal bridge effects in vacuum insulating elements, In: M. Zimmerman (Ed.), Proceedings of the *7th International Vacuum Insulation Symposium*, EMPA, p. 145–152, 2005

Towards a zero emission built environment – M.Sc. programme in sustainable architecture

A. Wyckmans
NTNU Norwegian University of Science and Technology

ABSTRACT

At the Norwegian University of Science and Technology (NTNU) in Trondheim, an international interdisciplinary M.Sc. programme in Sustainable Architecture starts in autumn 2010. The curriculum is based on long experience with graduate and post-graduate courses in the field, which are now being bundled into one holistic education.

The M.Sc. programme aims to educate building professionals in the use and development of competitive methods and solutions for existing and new buildings that will contribute to lowering greenhouse gas (GHG) emissions related to the production, use, management, and demolition of architecture in a life-cycle perspective.

Throughout the two years of the M.Sc. programme, a holistic perspective stresses the many architectural expressions and possibilities encompassed within a zero emission built environment. Within each of the theory and project courses, high demands are made towards integrated design strategies to ensure usability and synergy of the design with its surroundings and users. The students are continuously trained in interdisciplinary co-operation enabling them to integrate these routines in their professional practice.

The paper describes the learning aims, course structures and pedagogical methods of the M.Sc. programme. In addition, it focuses on the strong link with the Research Centre on Zero Emission Buildings at NTNU, ensuring immediate contact with and transfer of high-quality research and practice experiences in Norway and abroad: education and research institutions; producers of materials and products for the building industry; contractors, consultants, architects; trade organisations; public administration; public and private construction and property management; and users.

Keywords: interdisciplinary, architectural design, professional role, lifecycle perspective, zero emission

1. EDUCATION TOWARDS A ZERO EMISSION BUILT ENVIRONMENT

In 2008, the main political parties in Norway reached a Climate Agreement stating that Norway will be carbon-neutral by 2030; only one-third of the emission reductions can be achieved through international measures (Norwegian Ministry of the Environment 2008). Along with the European Union, Norway has committed itself to limit a global increase in temperature to 2°C by 2050. On a global scale, the ambition is to reduce GHG emissions by 2050 to two tonnes CO₂-equivalents per capita and year if the concentration in the atmosphere is to be stabilized at 400-450 ppm CO₂-equivalents by the year 2100. The current Norwegian average is 12 tonnes CO₂-equivalents per capita per year (Randers *et al.* 2006).

The development of a well-functioning society that provides a high quality of life for all citizens but only emits an average of two tons of CO₂-equivalents per capita per year forms a huge challenge for all professions, not in the least the construction sector. In a global and European perspective, buildings are accountable for about 40 % of all GHG emissions (Cheng *et al.* 2008). IPCC (2007) and McKinsey (Enkvist *et al.* 2007) reports point to measures in the building sector as being the most economical, when compared to other important sectors. Sadly, this reduction potential is “spread over hundreds of millions of individual buildings, each one presenting multiple and very diverse types of interventions” (Cheng *et al.* 2008:1). In addition, energy use in Norwegian buildings contributes little to global GHG emissions due to extensive use of hydropower electricity (Jones *et al.* 2009). However, architecture and the built environment exert a large influence on GHG emissions by means of transportation and land use planning, lifestyle and consumption, development of better materials and components, and life-cycle management of natural resources. Therefore, there is need for a development of holistic architectural policies that can lead society to a more sustainable use of resources and adapt to future climate challenges. This requires for the building profession to act as change agents to improve the manner in which society defines quality in the built environment.

How should educational institutions prepare their students for this reality? How should we educate architects, engineers and other building professionals to be able to contribute to this political goal in an optimal manner?

NTNU has taken an important step in this direction with a new international interdisciplinary M.Sc. curriculum in Sustainable Architecture: Towards a zero emission built environment starting in autumn 2010. The main scope of the programme is related to the environmental performance of buildings and the built environment, made explicit by their greenhouse gas emissions. However, these issues cannot be seen in isolation from the more general issue of sustainability including environmental as well as economic and social focus. The programme is based on long experience with graduate and post-graduate courses in the field, which are now being bundled into one holistic education. Close co-operation with the newly formed Research Centre on Zero Emission Buildings ensures a highly-engaged teaching staff in close connection to innovative research and practice.

2. PROFESSIONAL PERSPECTIVES

Each year, an international mix of 16 to 20 students is admitted to the programme, with an equal distribution between students with an architectural background and those with a bachelor or equal in engineering. In order to provide them with the optimal learning environment, the following three issues are stressed during the entire curriculum: (1) interdisciplinary students and staff; (2) from theory to design routines; (3) redefining the role of building professionals in society.

2.1 Interdisciplinary Students and Staff

In order to co-ordinate professions, we need to co-ordinate education. Therefore, within each course, the students are trained in interdisciplinary teams and by an interdisciplinary teaching staff. In this manner, the students get to know various distributions in responsibilities and tasks throughout the design process and learn in practice the integrated

design strategies that can ensure usability and synergy of their design project with its surroundings and users.

The teaching staff consists of a mixture of professionals from building practice and research to provide the students with professional perspectives from a wide variety of actors ranging from the latest scientific discoveries to concrete building experiences. The fixed core of teachers, extended by invited guest teachers, present the students with a curriculum that aims at making maximum connections among the different institutions and professions.

One of the most important insights the students learn is the importance of building teams. Given the complexity of modern-day architectural projects, it is an absolute necessity to complement one's own expertise with others' into a constructive co-operation. While architecture and engineering students on occasion still consider interdisciplinary co-operation as unnecessarily time-consuming and frustratingly reducing their own chance at achieving a high grade, the best manner in which to counteract these prejudices is to guide the students towards a positive experience and give them time to recognize and respect the contribution the other profession's expertise can make to create a high-quality design project.

2.2 From Theory to Design Routines

In order for future building professionals to be able to translate the climate and resource challenges in society into a fitting architectural form, they need to not only know about the use and development of sustainable building methods and solutions, but, above all, to be able to integrate this knowledge into their every-day design routines. The students need to become creative, active professionals who are able to keep themselves updated on relevant theories, understand how they interact, and currently update their design routines according to this new knowledge.

The course structure is allowing for different types of research and experiments in theory and design. Regular interactive workshops with discussions among peers and with the teaching staff help the students become more conscious of their own knowledge and beliefs. An individual research essay each semester allows the students to develop their own scientific potential. In the design studio, interdisciplinary design teams give the students the opportunity to continually test their own ideas in co-operation with others, and explore their professional, social and cultural behaviour (Nicol and Pilling 2000). In this manner, the students get familiar with different ways in which to work professionally with the built environment, and get a good foundation to mix and recombine the different elements into a meaningful whole.

In addition to design experience and theory, evaluation and reflection form an important part of the students' learning environment. In order to create well-functioning architecture, the students need to be able to build a thorough knowledge of a project's local climate and site as well as its cultural history and recognize the consequences of the existing structures and dynamics for the design of their project. They need to know how to start a project with specifying well-defined performance goals, not by choosing a particular type of technology as the core solution. The students also need to be able to analyse the performance of building projects in reality, such as the measured energy efficiency of a project, and the patterns of use in and around buildings. Case studies, discussions of different environmental modelling schemes and methods of analysis therefore form an integrated part of each semester.

2.3 Redefining the Role of Building Professionals in Society

All building professionals need to be able to handle challenges related to climate change and resource scarcity, and realise that this reality affects professional ethics, regulations and skills required in practice and research. Ever more strict building regulations require for even ‘ordinary’ building projects to stress low carbon emissions and high energy efficiency, not only one-off signature buildings. As professionals, the students will be expected to not only build projects with a set of measures and targets that put energy and greenhouse gas emissions at the heart of their performance, but also be able to negotiate the performance targets of the project with the building owner and building team while thinking about the long-term transformation of society and the development of innovative strategies.

The curriculum stresses the importance of the questions a building professional should ask at the start of, during and after having finished a design project, in order to affect the building and environmental programme and the project’s consequential performance. It also teaches the students how to assess which measures work best under given circumstances within a given budget, the different outcomes of various contracting frameworks and the negative consequences of particular types of actors not being engaged in the project from day zero.

3. COURSE STRUCTURE

The curriculum consists of three consecutive semesters with theory and project courses, and a fourth semester during which the participants write their M.Sc. thesis. Throughout the two-year curriculum, a holistic perspective stresses the many architectural expressions and possibilities encompassed within a zero emission built environment. For each consecutive semester, a specific area of focus is selected:

- Semester 1: Climate and built form (project); Climate and built form (theory); Concepts and strategies related to energy efficient, sustainable and zero emission buildings and built environment (theory);
- Semester 2: Integrated energy design (project); Energy systems and services and their integration in architectural design (theory); Sustainable building materials and components (theory);
- Semester 3: Design of zero emission buildings (project); Use and operation of zero emission buildings (theory); Elective Course (theory – to be agreed upon with supervisor and course coordinator);
- Semester 4: Master thesis

3.1 Semester 1: Climate and Built Form

The first semester starts off with a 7.5 credits theory course on concepts and strategies in sustainable architecture, in which the students learn to identify, understand and analyse terminology, principles and challenges related to sustainable architecture. The course provides a broad scope of issues ranging from insight in the history of sustainable architecture to a discussion of the most up-to-date concepts of zero-emission buildings and built environment. Different levels ranging from building to community and urban areas are discussed, including an introduction to issues such as land use, green infrastructure, traffic, and urban storm-water management and the corresponding challenges and strategies related

to mitigation and adaptation to climate change and resource scarcity. Also policy and economic challenges posed by innovative building strategies in society are included. After an intensive series of lectures and workshop discussions, the students pick a topic for their individual research essay, which they defend orally at the end of the semester.

Climate and built form is a combined design and theory course of 22.5 credits in which the students learn to design a range of projects in accordance with the resources and limitations posed by local site conditions, indoor and outdoor climate. To this purpose, the students learn to analyse local site and climate and their consequences for built form, along with an in-depth study of building physics and human comfort requirements. Particular attention is given to the importance of daylight, solar access and shading, ventilation, heating and cooling heating strategies, wind and precipitation. Different building shapes, functional programmes and site types are addressed, with focus on indoor as well as outdoor areas. The students' grades are based on their project work as well as a written theory exam.

3.2 Semester 2: Integrated Energy Design

The second semester has a structure similar to the first, with a 22.5 credits combined design and theory course on integrated energy design, and an additional 7.5 credits theory course on sustainable building materials and components.

The integrated energy design courses aim to teach the students how to integrate energy systems in architectural design, and to practice the interdisciplinary procedures necessary to ensure a successful functioning of these systems in architecture. A mixture of lectures, exercises and workshops provides theoretical background in building systems and services and their integration in architecture to provide a good indoor climate in a resource-efficient manner. Also integrated design methodology, evaluation tools and user behaviour are discussed. A particular point of focus is formed by challenges related to the renovation of existing buildings and cultural heritage sites. Based on these theoretical insights, the students design a range of projects with focus on integrated energy design and interdisciplinary co-operation between building professionals. The projects address domestic and non-domestic buildings, as well as new and existing building structures. The courses are taught in co-operation with the Faculty of Engineering Sciences and Technology at NTNU. The students' grades are based on their project work as well as a written theory exam.

A theory course on sustainable building materials and components, arranged as a series of lectures and workshops, provides the students with in-depth knowledge of a wide range of building materials and their correspondent construction methods, and the consequences they have on GHG emissions during the building's life cycle: production, transportation, construction, waste, operation, maintenance and cleaning, renovation, reuse, recycling and demolition. The students learn how to specify construction materials in a brief, how to compare materials' performance using different criteria, and how to critically analyse product information. The students also receive an introduction to environmental labelling of building materials and components and their effect on the building users' health and indoor climate, and learn how to use these criteria to select the appropriate materials for their project. The students are introduced to a wide selection of materials ranging from vernacular building materials to innovative nano-materials, and their corresponding consequences on building detailing and budget. Within the course theme, the students are free to choose the topic of their research essay, which they have to submit and defend at the end of the semester. The

course is taught in co-operation with the Industrial Ecology Programme and the Faculty of Natural Sciences and Technology.

3.3 Semester 3: Zero Emission Building

During the third semester, the students are offered a combined theory and design course on the design, use and management of zero emission buildings throughout the entire life cycle of the project. The course is provided in co-operation with the Faculties of Arts and Humanities, and Engineering Science and Technology. The students learn about environmental management, planning and procurement of the construction site and building project, as well as user participation in the design and operation of low-energy architecture. The various evaluation criteria of environmental classification tools are discussed along with specific quality control and documentation methodology. Contracting alternatives are investigated for their effect on the overall environmental and economic performance of the project. In addition, the students are asked to design a project that integrates strategies for energy, emissions, materials and users into high-quality architecture.

During the third semester, the students need to choose one elective course at other faculties at NTNU or another educational institution, in order to prepare themselves in the best possible manner for their thesis work. The elective course may for example be related to environmental policy, economics, project management, or user participation.

3.4 Semester 4: The M.Sc. Thesis

During the final semester of the curriculum, the students work on their thesis project, based on their individual professional interest and the elective course they have taken earlier. The scope and topic of the thesis is adapted to the particular professional background of each of the students.

4. IN THE FOREFRONT OF ARCHITECTURAL PRACTICE AND RESEARCH

The M.Sc. programme in Sustainable Architecture lies in the forefront of research, innovation and implementation related to reducing GHG emissions in architecture which the students will be able to transfer into their practice as building professionals. The continuous focus on integrated design methodology will enable the students to perform in any building design team, both as co-worker and leader.

A strong link with the Research Centre on Zero Emission Buildings at NTNU ensures immediate contact with and transfer of high-quality research and practice experiences in Norway and abroad: education and research institutions; producers of materials and products for the building industry; contractors, consultants, architects; trade organisations; public administration; public and private construction and property management; and users. In addition, several of the teaching staff are involved in the Norwegian “Cities of the Future” programme, a collaboration between the Government and the 13 largest cities in Norway to reduce greenhouse gas emissions and make the cities better places to live. Within this programme, the Brøset planning and research project is developed to become a carbon neutral suburban area in Trondheim, in close co-operation between Trondheim municipality and NTNU. On a regular basis, student projects will be linked to the ZEB and Brøset projects to develop a platform for developing and implementing new approaches.

5. CONCLUSIONS

The M.Sc. in Sustainable Architecture equips the students with extensive knowledge and experience that prepare them for a challenging, rapidly changing profession. There is a dire need for an architectural policy that encompasses the new technological opportunities while improving quality of life and reducing environmental impact. The development of a zero-emission built environment creates a new physical framework for large parts of society, reflecting cultural values, existing structures and the new layers of the future. An architecture that does not look for definitive solutions and permanent projects, but for structures that can continue to adapt to the need of society and citizens. More architecture for less CO₂.

REFERENCES

- Cheng, C. et al., 2008, *The Kyoto Protocol, The Clean Development Mechanism and the Building and Construction Sector*. A Report for the UNEP Sustainable Buildings and Construction Initiative, United Nations Environment Programme, Paris, France, 88 p.
- Enkvist, P.-A. et al., 2007, A cost curve for greenhouse gas reduction, *The McKinsey Quarterly*, no.1, p. 35-45.
- IPCC, 2007, *Climate change 2007: Contribution of working group III to the Fourth Assessment report of the intergovernmental Panel on Climate Change*, Cambridge University Press, Cambridge, p. 746-807.
- Jones, P. et al. (eds), 2009, *European Carbon Atlas. Low Carbon Urban Built Environment*, The Welsh School of Architecture, Cardiff, 220 p.
- Nicol, D., Pilling, S., 2000, Architectural education and the profession. Preparing for the future, In: Nicol, D., Pilling, S. (eds), *Changing architectural education. Towards a new professionalism*, Spon Press, London, p. 1-26.
- Norwegian Ministry of the Environment, 2008, Enighet om nasjonal klimadugnad
(translated:
National climate agreement), <http://www.regjeringen.no>, in Norwegian, last accessed 30 April 2010.
- Randers, J., 2006, Et klimavennlig Norge (translated: A Climate-Friendly Norway), NOU2006:18 (Norwegian Government White Book no.18, 2006), Oslo, 144 p.
- <http://www.broset.com>
<http://www.ntnu.no/studies/sustainablearchitecture>
<http://www.regjeringen.no/en/sub/framtidensbyer/cities-of-the-future.html?id=548028>
<http://www.zeb.no>